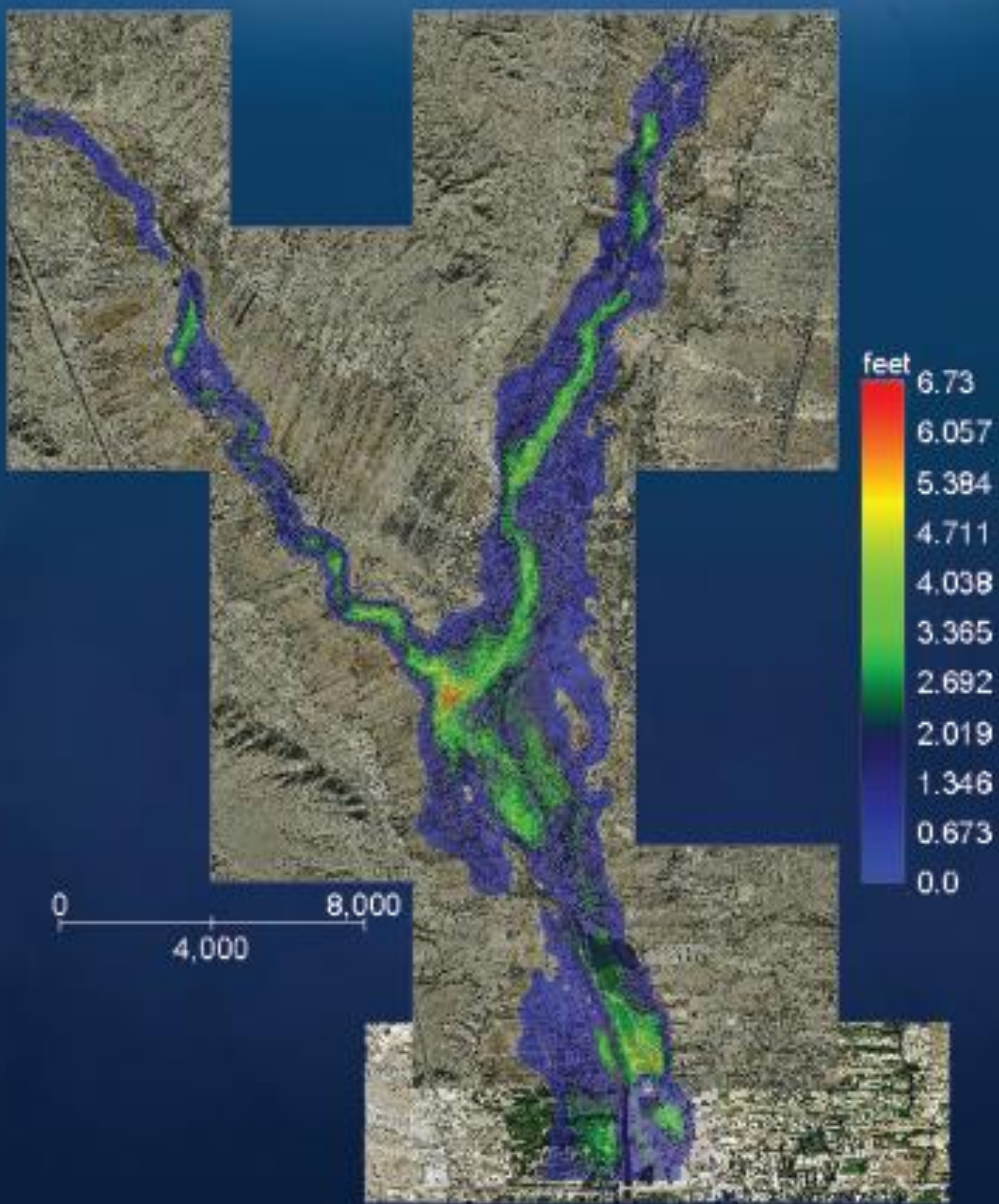


# FLO-2D

## REFERENCE MANUAL









### *A few comments on modeling free surface flows...*

Flood routing models are becoming very detailed. While models have become larger and faster with higher resolution (smaller elements) and expanding GIS and digital terrain model (DTM) resources, the accuracy of flood hazard delineation is still limited by hydrologic data bases (rainfall and flood inflow hydrographs). When adding complex urban detail to a two-dimensional flood routing model, the user should try to find a balance between the data base, model resolution, computer resources and budget. Reliable flood hazard delineation also requires a critical review of model component applicability and modeling assumptions. Digital terrain models are becoming the foundation of high resolution flood mapping, but post-flood event surveys of high water marks and aerial photography of the area of inundation for model calibration are often either unavailable or were collected long after the flood waters have receded. Correlating the area of inundation with flood peak discharge can lead to the harsh realization that even the best gaging data has limited accuracy at high flows.

With the advances in flood simulation, it may appear that model complexity is becoming overwhelming. Please take heart in the comments of Cunge et al. (1980):

*"The modeler must resist the temptation to go back to one-dimensional schematization because of lack of data otherwise necessary for an accurate two-dimensional model calibration. If the flow pattern is truly two-dimensional, a one-dimensional schematization will be useless as a predictive tool..." "It is better to have a two-dimensional model partially calibrated in such situations than a one-dimensional one which is unable to predict unobserved events. Indeed, the latter is of very little use while the former is an approximation which may always be improved by complimentary survey."*

As a final word, please note that all software programs have bugs that are inherent part of the process of implementing model enhancements for detail, speed and accuracy. Even when a model engine is well tuned, adding components may introduce conflicts or perhaps uncover bugs that were previously undetected. FLO-2D is certainly no exception. The model is continually evolving and when comparing results with previous versions, you may note some differences. While the current model results should be more accurate, we will address all questions and concerns over model application and accuracy. On occasion a project application pushes the model to new limits which can lead to new developments that benefit all users. The modeler is encouraged to share interesting projects with us and we will aspire to make the FLO-2D model a comprehensive, affordable and flexible tool.

## BRIEF OVERVIEW

FLO-2D is a finite volume conservation flood routing model. It is a valuable tool for delineating flood hazards, regulating floodplain zoning or designing flood mitigation. The model will simulate river overbank flows, but it can also be used on unconventional flooding problems such as unconfined flows over complex alluvial fan topography and roughness, split channel flows, mud/debris flows and urban flooding. Its primary application is for urban flood simulation with buildings, streets, walls and storm drains. FLO-2D is listed as FEMA approved hydrologic/hydraulic model. Contact us for help with getting the model approved for local FIS studies in your community.

The FLO-2D software package includes a, QGIS Plugin Tool, a grid developer system (GDS), a MAPPER Pro program that automates flood hazard delineation, and three other processor programs; HYDROG, PROFILES and MAXPLOT. The QGIS plugin tool will provide complete GIS integration for generating the FLO-2D data files and mapping the model results. The older GDS program will interpolate the DTM data, assign elevations to an assigned grid system and provide graphical interface to generate and edit model component data. The MAPPER Pro program automates flood hazard map delineation. MAPPER Pro will generate very detailed flood inundation color contour maps and shape files. It will also replay flood animations.

The FLO-2D Reference Manual is devoted to model description, theory and components. The user is encouraged to read this manual to become familiar with the overall modeling approach, theory and background. The Data Input Manual is a separate manual subdivided into a series of data files with variable descriptions and comments. There is a Data Input Manual appendix with White Papers that discuss specific component development guidelines. There is also a separate Storm Drain Manual because of the detail and complexity of modeling the storm drain system. Individual manuals are devoted to the application of the GDS, MAPPER Pro and the QGIS Plug-in Tool.

The user can keep current on the FLO-2D model and processor program updates, training and other modeling news at the website: [www.flo-2d.com](http://www.flo-2d.com).

*FLO-2D Software, Inc.*

*P.O. Box 66*

*Nutrioso, AZ 85932*

*Phone: (928) 339-1935*

*Email: [contact@flo-2d.com](mailto:contact@flo-2d.com)*

## Table of Contents

<b>BRIEF OVERVIEW .....</b>	<b>II</b>
<b>TABLE OF CONTENTS.....</b>	<b>I</b>
<b>LIST OF FIGURES .....</b>	<b>II</b>
<b>LIST OF TABLES .....</b>	<b>V</b>
<b>CHAPTER 1. INTRODUCTION .....</b>	<b>1</b>
1.1 <i>Evolution of the FLO-2D Model.....</i>	<i>1</i>
1.2 <i>Modeling the Hydrologic System with FLO-2D.....</i>	<i>2</i>
1.3 <i>Getting Started on a Project – A Brief Overview.....</i>	<i>5</i>
<b>CHAPTER 2. FLO-2D MODEL THEORY.....</b>	<b>7</b>
2.1 <i>Governing Equations.....</i>	<i>7</i>
2.2 <i>Solution Algorithm - How the Model Works .....</i>	<i>8</i>
2.3 <i>The Importance of Volume Conservation.....</i>	<i>15</i>
2.4 <i>Courant Number Variability for Numerical Stability .....</i>	<i>16</i>
2.5 <i>Volume Evacuation from Small Grid Elements.....</i>	<i>19</i>
2.6 <i>Limiting Froude Number .....</i>	<i>22</i>
2.7 <i>Shallow Flow Roughness and TOL.....</i>	<i>23</i>
<b>CHAPTER 3. FLO-2D MODEL SYSTEM .....</b>	<b>25</b>
3.1 <i>Assumptions and Special Conditions.....</i>	<i>25</i>
3.2 <i>Roughness Parameter Variability .....</i>	<i>27</i>
3.3 <i>Inflow and Outflow Control.....</i>	<i>35</i>
3.4 <i>Floodplain Cross Sections.....</i>	<i>36</i>
3.5 <i>Grid Developer System (GDS).....</i>	<i>36</i>
3.6 <i>QGIS Plug-in .....</i>	<i>36</i>
3.7 <i>Graphical Output Options .....</i>	<i>40</i>
3.8 <i>Data Output Options.....</i>	<i>45</i>
<b>CHAPTER 4. MODEL COMPONENTS.....</b>	<b>47</b>
4.1 <i>Model Features .....</i>	<i>47</i>
4.2 <i>Overland Flow .....</i>	<i>48</i>
4.3 <i>Channel Flow.....</i>	<i>52</i>
4.4 <i>Channel-Floodplain Interface.....</i>	<i>54</i>
4.5 <i>Levees .....</i>	<i>54</i>
4.6 <i>Levee and Dam Breach Failures .....</i>	<i>56</i>
4.7 <i>Hydraulic Structures.....</i>	<i>60</i>
4.8 <i>Storm Drain Modeling.....</i>	<i>62</i>
4.9 <i>Street Flow .....</i>	<i>63</i>
4.10 <i>Floodplain Storage Modification and Flow Obstruction .....</i>	<i>63</i>
4.11 <i>Rainfall Runoff .....</i>	<i>67</i>
4.12 <i>Infiltration and Abstraction.....</i>	<i>69</i>
4.13 <i>Evaporation.....</i>	<i>74</i>
4.14 <i>Overland Multiple Channel Flow.....</i>	<i>74</i>
4.15 <i>Sediment Transport – Total Load.....</i>	<i>76</i>
4.16 <i>Mud and Debris Flow Simulation .....</i>	<i>83</i>
4.17 <i>Specific Energy, Impact and Static Pressure .....</i>	<i>93</i>

4.18	<i>Floodway Delineation</i> .....	93
4.19	<i>Groundwater – Surface Water Modeling</i> .....	98
4.20	<i>Building Collapse</i> .....	99
4.21	<i>Predicting Alluvial Fan Channel Avulsion</i> .....	104
4.22	<i>Low Impact Development (LID) Modeling</i> .....	109
4.23	<i>Building Rainfall Runoff</i> .....	114
4.24	<i>Gutter Tool</i> .....	132
4.25	<i>Bridge Routine</i> .....	136
<b>CHAPTER 5.</b>	<b><i>FLO-2D PROJECT APPLICATIONS</i></b> .....	<b>165</b>
5.1	<i>River Applications</i> .....	165
5.2	<i>Unconfined Floodplain and Alluvial Fan Flooding</i> .....	166
5.3	<i>Watershed Rainfall Runoff Simulation</i> .....	167
5.4	<i>Urban Flooding</i> .....	168
5.5	<i>Coastal Flooding</i> .....	170
5.6	<i>Model Results – What Constitutes a Successful Flood Simulation?</i> .....	171
5.7	<i>FLO-2D Bridge Routine Comparison with HEC-RAS</i> .....	172
<b>REFERENCES</b>	.....	<b>185</b>

## List of Figures

Figure 1.	Physical Processes Simulated by FLO-2D. ....	3
Figure 2.	Channel – Floodplain Interface. ....	4
Figure 3.	FLO-2D Flow Chart. ....	6
Figure 4.	Flow Direction.....	9
Figure 5.	Discharge Flux across Grid Element Boundaries.....	11
Figure 6.	FLO-2D Stability Criteria Flow Chart. ....	13
Figure 7.	Numerical Surging in a Channel Element Hydrograph. ....	17
Figure 8.	File Sample VELTIMFP.OUT. ....	17
Figure 9.	TOL Definition.....	20
Figure 10.	Vertical Velocity Profiles. ....	26
Figure 11.	Tsunami Wave Progression Overland in an Urban Area (Waikiki Beach, Hawaii). ....	35
Figure 12.	FLO-2D QGIS Plugin Tool Working Environment. ....	37
Figure 13.	Toolbar FLO-2D Plugin. ....	37
Figure 14.	User and Schematic Layer Structure. ....	39
Figure 15.	FLO-2D Table Editor. ....	39
Figure 16.	Control Panel for Various FLO-2D Components. ....	40
Figure 17.	QGIS Plug-in Tool for FLO-2D Model Development and Displaying Results. ....	41
Figure 18.	MAXPLOT Mapping Controls.....	42
Figure 19.	MAXPLOT Floodplain Maximum Flow Depths (Based on Grid Element).....	43
Figure 20.	MAXPLOT Maximum Scour Depths (Based on Grid Element).....	43
Figure 21.	MAPPER PRO Plot of Maximum Depths.....	44
Figure 22.	Overland Flow Routing Subroutine Flow Chart.....	49
Figure 23.	Editing Grid Elements to Represent Streets. ....	50
Figure 24.	Stage-Volume Rating Table for Assigning Flow Depths. ....	51
Figure 25.	Channel Extension Over Several Grid Elements.....	52
Figure 26.	Levees are Depicted in Red and the River in Blue in the GDS Program. ....	55

Figure 27. Levee Freeboard Deficit Plot Using MAXPLOT.....	55
Figure 28. Example of Levee Breach Urban Flooding.....	56
Figure 29. Example of a Proposed Domestic Water Supply Reservoir Breach Failure.....	57
Figure 30. Dam Breach Piping Failure.....	59
Figure 31. Dam Breach Channel Development.....	59
Figure 32. Breach Failure Geometry. (Teton Dam Failure 1976 USBR). .....	60
Figure 33. Storm Drain Layout in the GDS with a Background Image.....	62
Figure 34. Streets Depicted in Green in the GDS Program.....	63
Figure 35. ARF Assignments for Buildings with Walls, Storm Drain and Background Image.....	65
Figure 36. Color Depiction of ARF and WRF Factors.....	65
Figure 37. Roof Rainfall Runoff Routed to a Downspout.....	66
Figure 38. Roof Downspout and Parapet Walls for Roof Storage.....	66
Figure 39. Building Collapse Vulnerability Curves.....	67
Figure 40. Flooding Replicated from NEXRAD Data near Tucson, Arizona.....	68
Figure 41. Gully on an Alluvial Fan where Overland Sheet Flow is Minimal.....	75
Figure 42. Maximum Flow Depth with Multiple Channel Flow Shown as Dark Blue and Red.....	76
Figure 43. Sediment Transport Bed Exchange Layer.....	78
Figure 44. Inflow Node Locations.....	79
Figure 45. Classification of Hyperconcentrated Sediment Flows.....	84
Figure 46. Shear Stress as a Function of Shear Rate for Fluid Deformation Models.....	88
Figure 47. Dynamic Viscosity of Mudflow Samples versus Volumetric Concentration.....	91
Figure 48. Yield Stress of Mudflow Samples versus Volumetric Concentration.....	91
Figure 49. Floodway Schematic Flow Chart.....	96
Figure 50. Base Flood. ....	97
Figure 51. Floodway Delineation No Floodway.....	97
Figure 52. Floodway Delineation.....	97
Figure 53. GDS Data Entry for a MODFLOW Groundwater Simulation.....	98
Figure 54. Buildings with a FLO-2D Grid System and ARF Values Representing Buildings.....	99
Figure 55. Vulnerability Curves. (Pilotti et al., 2016). .....	100
Figure 56. Vulnerability Curve for Mobile Homes (BOR, 1988).....	100
Figure 57. Vulnerability Curves for Buildings with a Foundation (BOR, 1988).....	101
Figure 58. Vulnerability Curve for a Masonry Building (Pilotti et al., 2016). .....	101
Figure 59. Vulnerability Curves for Building Subject to Collapse.....	102
Figure 60. Building (red square) is Flooded from the North Direction.....	104
Figure 61. Alluvial Fan Distributary Channel Definition for Avulsion Analysis (from FCDMC, 2014).....	106
Figure 62. Channel Forming Depth versus Channel Forming Discharge (from USACE, 1994).....	107
Figure 63. Channel Forming or Bank Full Discharge (from USACE, 1994).....	107
Figure 64. Low Impact Development Water Retention.....	110
Figure 65. FLO-2D Grid Element LID Concept – Spatially Variable TOL Elements (brown).....	110
Figure 66. Global TOL.....	111
Figure 67. Spatially Variable TOL Value Format in TOLSPATIAL.DAT.....	111
Figure 68. MAXPLOT Difference Analysis of the FINALDEP.OUT Files (Spatially Variable – Base Run).....	112
Figure 69. SUMMARY.OUT Comparison.....	113
Figure 70. MAXPLOT Difference Analysis of the FINALDEP.OUT Files (Spatially Variable – Infiltration).....	113
Figure 71. SUMMARY.OUT File for the Spatially Variable TOL Value and Infiltration.....	114
Figure 72. Buildings on a 25 ft Grid System (red lines indicate walls represented as levees).....	115
Figure 73. Assigned ARF Values to the Buildings.....	116
Figure 74. Location of a Large Building.....	117
Figure 75. Maximum Flow Depths Inside the Building.....	118

Figure 76. Maximum Flow Velocities on the Alluvial Fan.....	119
Figure 77. Maximum Flow Velocities.....	119
Figure 78. Project Building Location (in blue oval).....	120
Figure 79. Building Roof Element Elevation Editing.....	121
Figure 80. Grid Element Levee Crest Elevation Editing.....	121
Figure 81. Grid Element Elevation Editing.....	122
Figure 82. Roof Element Elevation Editing Command.....	122
Figure 83. Roof Element Elevation Editing Tab.....	123
Figure 84. Selecting the Two Cornerstone Grid Elements to Interpolate the Roof Slope.....	123
Figure 85. Graphic Display of the Roof Element Elevations Between the Two Cornerstone Cells.....	124
Figure 86. Completed Roof Element Elevation Slope Interpolation.....	124
Figure 87. Downspout Hydraulic Structure as Brown Elements in the Upper Right Corner.....	125
Figure 88. Hydraulic Structure Dialog Box with Entered Downspout Data.....	126
Figure 89. Total Rainfall (3 inches) Accumulated on a Flat Roof.....	127
Figure 90. Maximum Flow Depth and Water Surface Elevation on a Sloped Roof.....	128
Figure 91. Maximum Flow Depth (Sloped Roof with Parapet wall Being Overtopped).....	128
Figure 92. Maximum Flow Depth and Water Surface Elevation. (Sloped Roof with a Downspout).....	130
Figure 93. Gutter Diagram.....	133
Figure 94. Street and Gutter Flow Diagram.....	133
Figure 95. Flow Distribution Street to Sidewalk.....	134
Figure 96. Flow Distribution Sidewalk to Street.....	134
Figure 97. Gutter Elements with Storm Drain.....	135
Figure 98. Flow Depth without Gutter.....	135
Figure 99. Flow Depth with Gutter.....	136
Figure 100. Constricted Flow through a Bridge (Tom Imbrigiotta, USGS).....	137
Figure 101. Unsteady Non-Uniform Flow through a Bridge Constriction.....	138
Figure 102. Type 1 Flow: Free surface, subcritical flow ( $Z > Y_u > Y_d$ ).....	139
Figure 103. Type 2 Flow: Inlet submerged, outlet free surface, partially full, sluice gate flow ( $Y_u > Z > Y_d$ ).....	140
Figure 104. Type 3 Flow: Inlet submerged, outlet submerged, opening full, sluice gate-orifice transition flow .....	141
Figure 105. Type 4 Flow: Inlet submerged, outlet submerged, orifice flow ( $Y_u > Y_d > Z$ ).....	141
Figure 106. Type 5 Flow: Inlet submerged, outlet submerged, deck overflow ( $Y_u > Y_d > Z$ ).....	142
Figure 107. Pressure Flow with the Water Surface above the Low Chord Elevation (M. Huard, USGS).....	143
Figure 108. Bridge Deck Overflow with Guardrail (Llano River Bridge Collapse, CBS Austin).....	144
Figure 109. FLO-2D Model Bridge Inflow and Outflow Elements Separated by a Number of Grid Elements.....	145
Figure 110. Conceptual Bridge Plan and Profile with River Cross Sections.....	147
Figure 111. Stage-Discharge Variation between Free Surface Flow and Bridge Flow (Hamill, 1999; p. 53).....	151
Figure 112. Sluice Gate Discharge Coefficient as Function of the Low Chord Submergence (FHA, 2012).....	152
Figure 113. Orifice Coefficient of Discharge as Function of Low Chord Submergence (Hamill, 1999).....	153
Figure 114. Middle Rio Grande and Rio Chama Confluence Model.....	166
Figure 115. Unconfined Alluvial Fan Flooding.....	167
Figure 116. Urban flooding with Street Flow and Building Obstruction (1 million 10 ft elements).....	168
Figure 117. Urban Model with Streets, Buildings and Storm Drains .....	169
Figure 118. Urban Model Results with Storm Drains .....	169
Figure 119. Hurricane Wilma 2005 Predicted Storm Surge in the Florida Keys.....	171
Figure 120. Plan View of the Los Lunas Bridge.....	175
Figure 121. View Downstream through Los Lunas Bridge (Wolf Engineering).....	175
Figure 122. HEC-RAS Cross Sections and Stationing (Wolf Engineering).....	176
Figure 123. Los Lunas HEC-RAS Bridge .....	177

Figure 124. Los Lunas Bridge HEC-RAS Water Surface Elevations.....	178
Figure 125. Los Lunas Bridge Stage-Discharge Relationship Cross Section 1 .....	180
Figure 126. Los Lunas Bridge Stage-Discharge Relationship Cross Section 2 .....	180
Figure 127. Los Lunas Bridge Stage-Discharge Relationship Cross Section 3 .....	181
Figure 128. Los Lunas Bridge Stage-Discharge Relationship Cross Section 4 .....	181
Figure 129. Los Lunas Bridge Stage-Discharge Relationship Cross Section 5 .....	182
Figure 130. FLO-2D Maximum Depth for a Discharge of 45,000 cfs.....	183

## List of Tables

Table 1. Range of Values Limiting Froude. ....	22
Table 2. QGIS Plugin Tools. ....	37
Table 3. Overland Flow Manning's n Roughness Values. <sup>1</sup> .....	48
Table 4. Maximum Allowable ARF Values. ....	64
Table 6. Green-Ampt Infiltration - Hydraulic Conductivity and Porosity.....	70
Table 7. Green-Ampt Infiltration - Soil Suction.....	70
Table 8. Green-Ampt Infiltration.....	71
Table 10. Mudflow Behavior as a Function of Sediment Concentration.....	85
Table 11. Resistance Parameters for Laminar Flow. <sup>1</sup> .....	89
Table 12. Yield Stress and Viscosity as a Function of Sediment Concentration.....	90
Table 13. Bridge Parameters (B-Lines in HYSTRU.C.DAT) .....	158
Table 14. Stage Time Relationship.....	170



## **Chapter 1. INTRODUCTION**

This Reference Manual discusses the physical processes of flooding. It is designed to acquaint the user with the model theory, finite difference algorithms, model components, modeling assumptions and limitations, and potential flood scenarios. A reference list is provided for further reading.

### **1.1    *Evolution of the FLO-2D Model***

The first version of the FLO-2D model was called MUDFLOW. It was initiated in 1988 to conduct a Federal Emergency Management Agency (FEMA) flood insurance study (FIS) of an urbanized alluvial fan in Colorado. FEMA had requested the investigation of flood routing models that might be suitable for simulating mudflows. The Diffusive Hydrodynamic Model (DHM) created by Hromadka and Yen (1987) and distributed by the USGS was considered as a template to develop a more sophisticated hydraulic model for mudflows. The selection of the DHM model as a guide for the MUDFLOW model was based on its availability in the public domain, its simple numerical approach and a finite difference scheme that permitted modification of the grid element attributes.

The original MUDFLOW model was only a few hundred lines of FORTRAN code and was limited to 250 grid elements. A six-hour hydrograph took over 12 hours to run on an XT computer. After 28 years of development, the program code has grown to be more than 50,000 lines of code, over 90 subroutines and a number of processor programs. Virtually none of the original simplistic DHM concept remains in the current FLO-2D model. FLO-2D computes overland flow in 8-directions, reports on mass conservation, utilizes a variable timestep incrementing and decrementing scheme, incorporates efficient numerical stability criteria, has unlimited array allocation (unlimited grid elements), includes graphical editing, and has output display processor programs.

FLO-2D is a physical process model that routes rainfall-runoff and flood hydrographs over unconfined flow surfaces or in channels using the dynamic wave approximation to the momentum equation. It has many components to simulate street flow, buildings and obstructions, sediment transport, spatially variable rainfall and infiltration, floodways, storm drains and many other flooding details. Predicted flow depth and velocity between the grid elements represent average hydraulic flow conditions computed for a small timestep (on the order of seconds). Typical applications have grid elements that range from 10 ft (3 m) to 500 ft (130 m) on a side and the number of grid elements is limited only by the computer resources and runtime.

## **1.2 Modeling the Hydrologic System with FLO-2D**

The FLO-2D model has components for rainfall, channel flow, overland flow, street flow, infiltration, levees, sediment transport, storm drain and other features. The model utility is experienced through its application to diverse flooding problems. Starting with a basic overland flood scenario, details can be added to the simulation by simply turning ‘on’ or ‘off’ switches for the various components shown in Figure 1. Multiple flood hydrographs can be introduced to the system either as a floodplain or channel inflow. As the floodwave moves over the floodplain or down channels or streets, flow over adverse slopes, floodwave attenuation, ponding and backwater effects can be simulated. In urban areas, buildings and flow obstructions can be simulated to account for the loss of storage and redirection of the flow path. The levee component can be used to simulate walls or berms that confine the flow.

Channel flow is one-dimensional with the channel geometry represented by either by natural, rectangular or trapezoidal cross sections. Street flow is modeled as a rectangular channel. Overland flow is modeled two-dimensionally as either sheet flow or flow in multiple channels (rills and gullies). Channel overbank flow is computed when the channel capacity is exceeded. An interface routine calculates the channel to floodplain flow exchange including return flow to the channel. Similarly, the interface routine also calculates flow exchange between the streets and overland areas within a grid element (Figure 2). Once the flow overtops the channel, it will disperse to other overland grid elements based on topography, roughness and obstructions. There are sediment transport and mud and debris flow and components to address mobile bed and hyperconcentrated sediment flows. The user is encouraged to apply these components while understanding the contribution of each component to the overall flood distribution.

It is important to assess the level of detail required on a given project. FLO-2D users tend to put more detail into their models than is necessary for a large flood event. Preparation of channel flow, street flow, buildings and flow obstructions data files can be time consuming and should be tailored to meet the project needs. The desired accuracy of predicted water surface elevations should be consistent with the resolution of the mapping, survey and hydrologic data bases. Simulating large floods requires less detail than shallow flood or mitigation design models. Grid element sizes ranging from 20 ft (8 m) to 500 ft (130 m) is practical for most flood inundation projects.

The accuracy of a FLO-2D flood simulation is dependent on the volume of water introduced to the model either in the form of rainfall and inflow flood hydrographs. FLO-2D reports on volume conservation both during and after the simulation. This reveals the ultimate disposition of inflow volume either as a loss to the system (abstraction, infiltration, or evaporation), as floodplain or channel storage, or as outflow off the grid system. The inflow volume dictates the area of inundation and will control model calibration to available post flood data if replicating an historical storm.

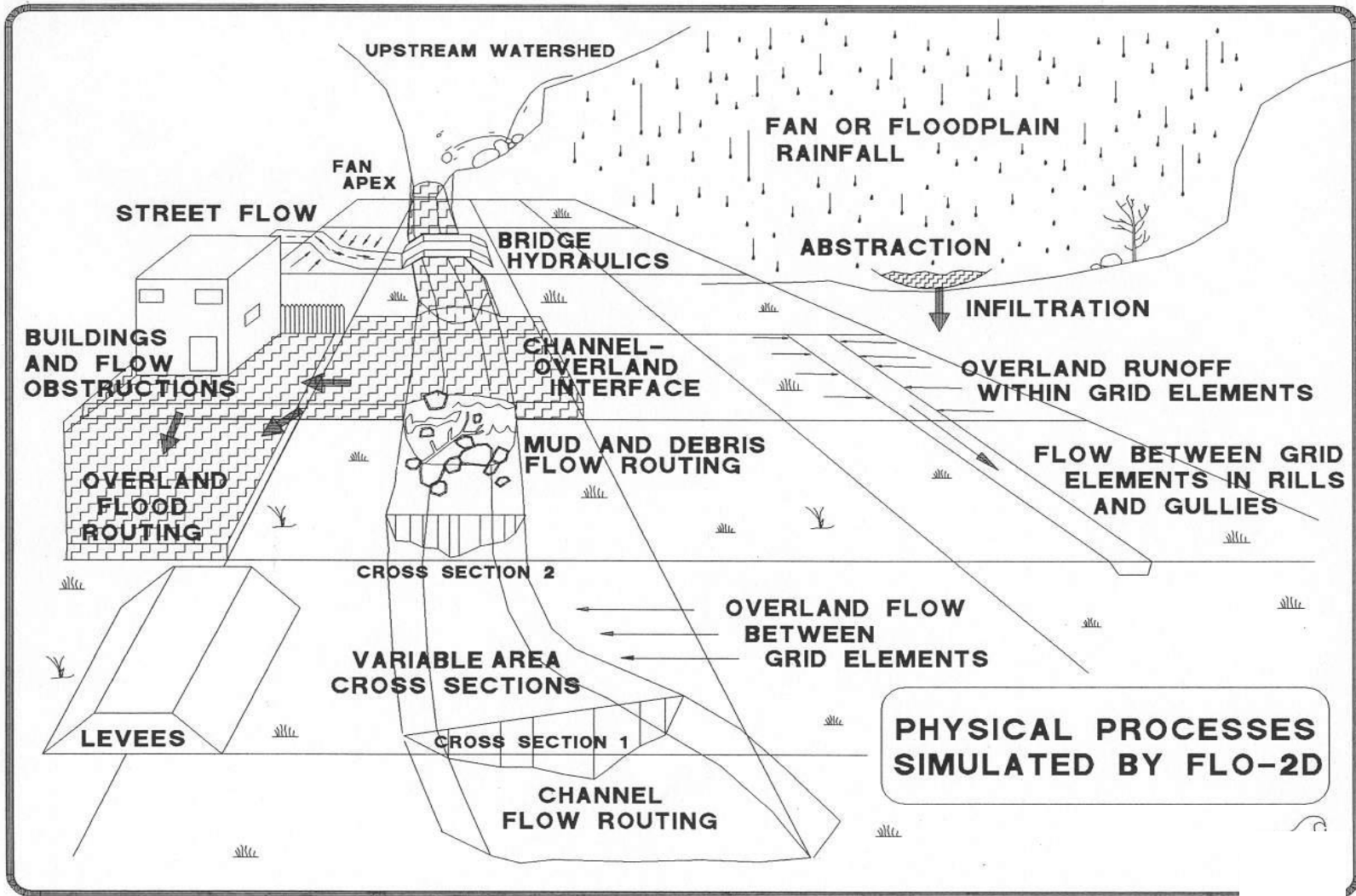


Figure 1. Physical Processes Simulated by FLO-2D.

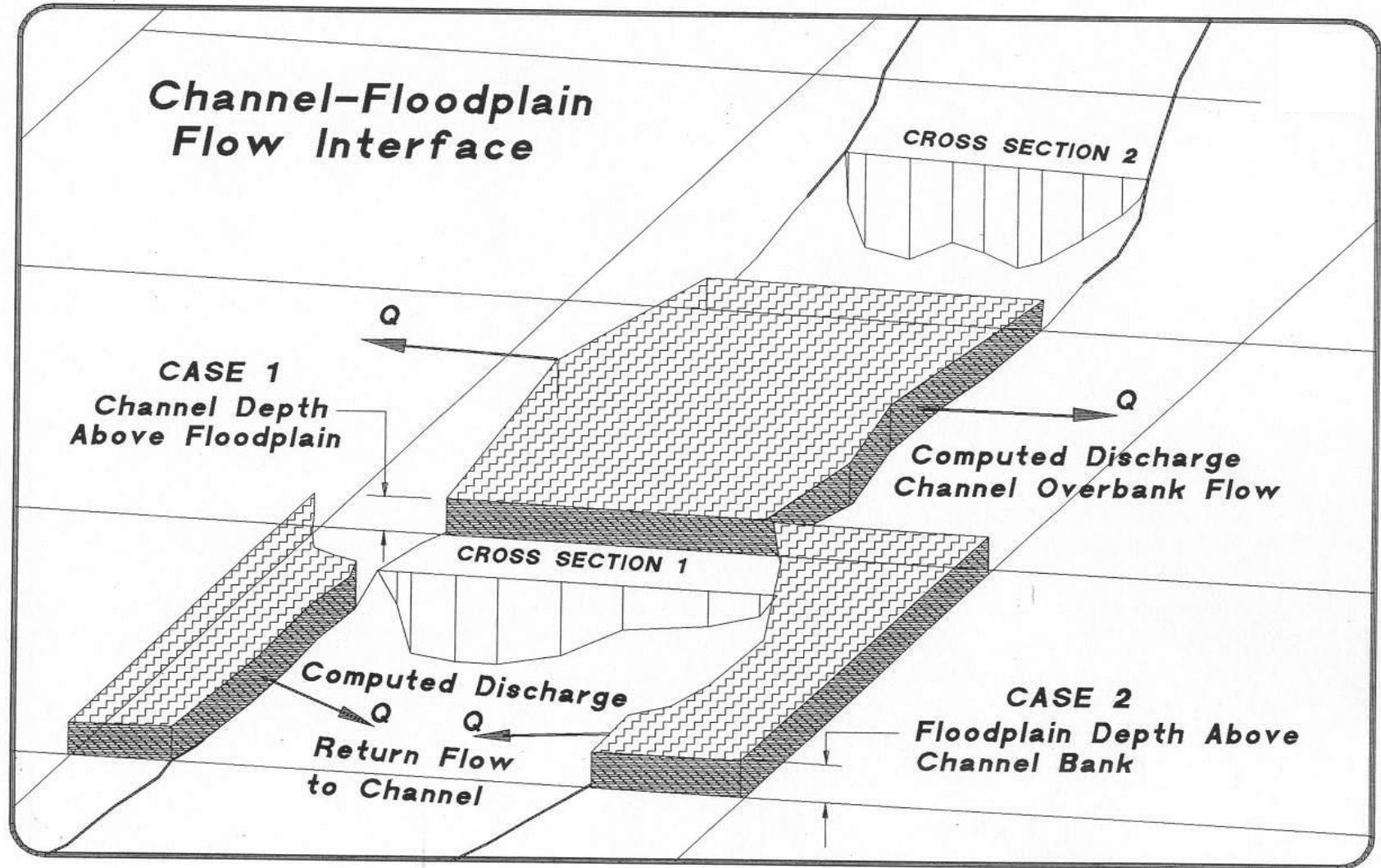


Figure 2. Channel – Floodplain Interface.

### **1.3     *Getting Started on a Project – A Brief Overview***

There are two steps to starting a flood simulation, obtaining the topographic data base and developing the flood hydrology. For the first step, a digital terrain model (DTM) must be overlaid with a grid system. Either the QGIS plug-in tool or the Grid Developer System (GDS) processor program will generate a grid system on a DTM data base and assign elevations to the grid elements. Shape files, aerial photography, detailed topographic maps, orthographic photos and digitized mapping can be used to locate key features with respect to the grid system such as streets, buildings, bridges, culverts or other flood conveyance or containment structures. Figure 3 is a flow chart that outlines how the various components interface with each other.

Each flood simulation requires some water either as an inflow flood hydrograph or as rainfall. The discharge inflow points might include the alluvial fan apex or a known discharge location in a river system. FLO-2D can be used to generate the flood hydrograph at a specific location by modeling the rainfall-runoff in the upstream watershed. Another approach is to use an external hydrologic model to generate an inflow hydrograph for the FLO-2D model. Any number of spatially variable inflow hydrographs can be input to the model. Rainfall can also be simulated on the water surface as the flood progresses over the grid system. Rainfall can be uniformly distributed or spatially variable using either depth area reduction values or grid element interpolated rainfall radar data bases (NEXRAD). The inflow flood volume is the primary factor that determines the predicted area of inundation. For that reason, it is suggested that an appropriate effort be spent on the hydrologic analysis to support the accuracy of the flood routing simulation.

Results from a FLO-2D flood simulation may include: outflow hydrographs from flow off the grid system; hydrographs and flow hydraulics for each channel element; flood hydrographs and hydraulics for designated floodplain cross sections; maximum flow depths and velocities for all grid elements; changes in bed elevation; impact force and number of other specific hydraulic variables, and a summary of the inflow, outflow, storage and volume losses in the system. The user can specify the temporal and spatial output detail including the outflow hydrograph locations, the output time intervals and the graphical display of the flood progression over the grid system. After the preliminary FLO-2D runs, the user can apply the output options to determine required level of output detail.

## FLO-2D Flow Chart

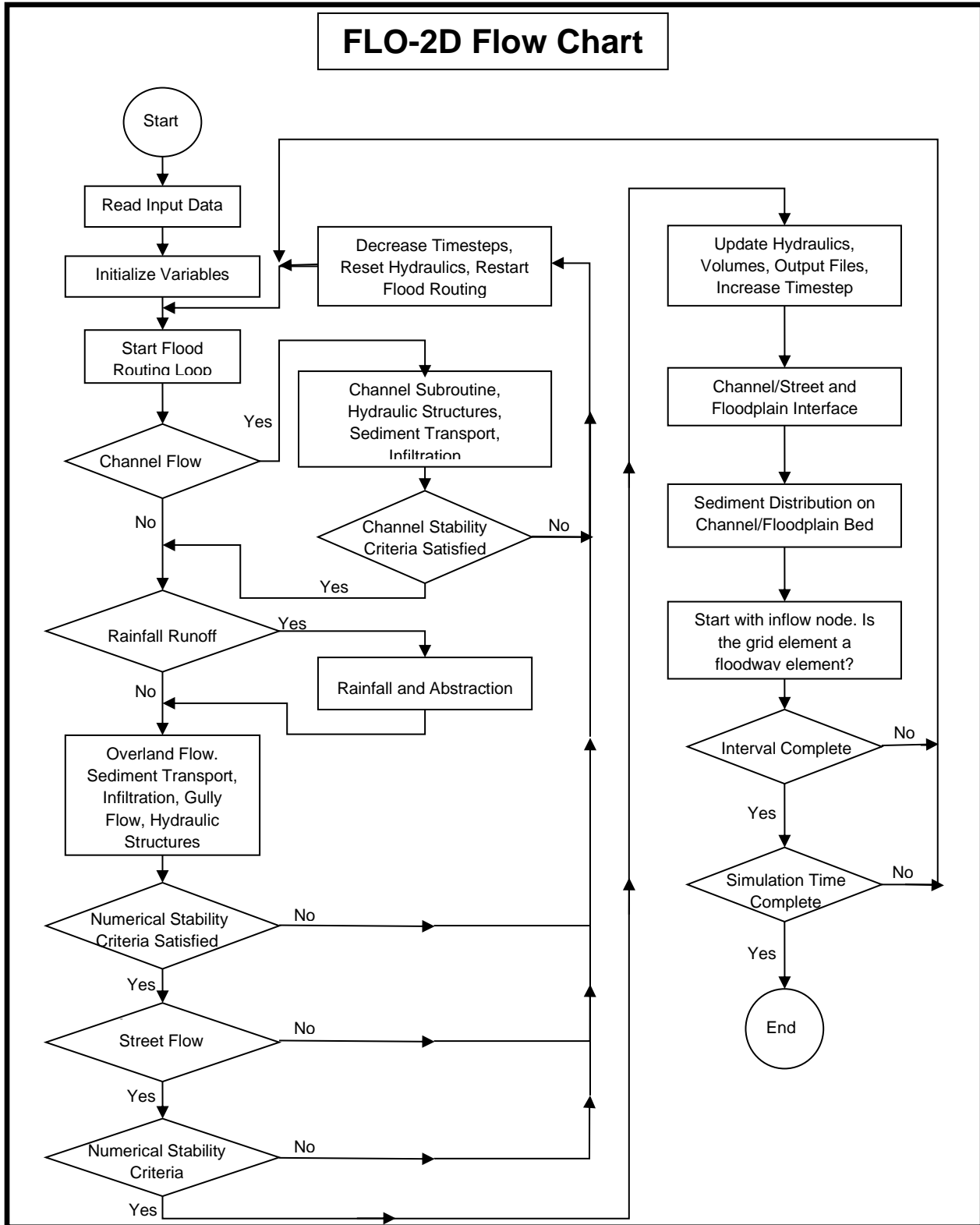


Figure 3. FLO-2D Flow Chart.

## Chapter 2. FLO-2D MODEL THEORY

FLO-2D is a simple volume conservation model. It moves the flood volume around on a series of tiles for overland flow or through stream segments for channel routing. Floodwave progression over the flow domain is controlled by topography and resistance to flow. Flood routing in two dimensions is accomplished through a numerical integration of the equations of motion and the conservation of fluid volume for either a water flood or a hyperconcentrated sediment flow. A discussion of the governing equations follows.

### 2.1 Governing Equations

The constitutive fluid motion equations include the continuity equation and the momentum equation:

$$\frac{\partial h}{\partial t} + \frac{\partial h V}{\partial x} = i$$
$$S_f = S_o - \frac{\partial h}{\partial x} - \frac{V}{g} \frac{\partial V}{\partial x} - \frac{I}{g} \frac{\partial V}{\partial t}$$

where  $h$  is the flow depth and  $V$  is the depth-averaged velocity in one of the eight flow directions  $x$ . The excess rainfall intensity ( $i$ ) may be nonzero on the flow surface. The friction slope component  $S_f$  is based on Manning's equation. The other terms include the bed slope ( $S_o$ ) pressure gradient and convective and local acceleration terms. This equation represents the one-dimensional depth averaged channel flow. For the floodplain, while FLO-2D is multi-direction flow model, the equations of motion in FLO-2D are applied by computing the average flow velocity across a grid element boundary one direction at time. There are eight potential flow directions, the four compass directions (north, east, south and west) and the four diagonal directions (northeast, southeast, southwest and northwest). Each velocity computation is one-dimensional and is solved independently of the other seven directions. Since the flow is being shared with all of a given grid element neighbors, resolution of the velocity vectors is not required. The stability of this explicit numerical scheme is based on strict criteria to control the magnitude of the variable computational timestep. The equations representing hyperconcentrated sediment flow are discussed later in the manual.

Understanding the relative magnitude of the acceleration components to the bed slope and pressure terms is important. Henderson (1966) computed the relative magnitude of momentum equation terms for a moderately steep alluvial channel and a fast rising hydrograph as follows:

	Bed Slope	Pressure Gradient	Convective Acceleration	Local Acceleration
Momentum Equation Term:	$S_o$	$\partial h / \partial x$	$V \partial V / g \partial x$	$\partial V / g \partial t$
Magnitude (ft/mi)	26	0.5	0.12 - 0.25	0.05

This illustrates that the application of the kinematic wave ( $S_o = S_f$ ) on moderately steep slopes with relatively steady, uniform flow is sufficient to model floodwave progression and the contribution of the pressure gradient and the acceleration terms can be neglected. The addition of the pressure gradient term to create the diffusive wave equation will enhance overland flow simulation with complex topography. The diffusive wave equation with the pressure gradient is required to predict floodwave attenuation and the change in storage on the floodplain. The local and convective acceleration terms in the full dynamic wave equation are important to the flood routing for flat or adverse slopes or very steep slopes or unsteady flow conditions. Only the full dynamic wave equation is applied in FLO-2D model and the contribution of each term in the equation is computed regardless of an assumption of negligibility.

## **2.2    *Solution Algorithm - How the Model Works***

The differential form of the continuity and momentum equations in the FLO-2D model is solved with a central, finite difference numerical scheme. This explicit algorithm solves the momentum equation for the flow velocity across the grid element boundary one element at a time. The solution to the differential form of the continuity and momentum equations results from a discrete representation of the equation when applied at a single point. Explicit schemes are simple to formulate but usually are limited to small timesteps by strict numerical stability criteria. Finite difference schemes can require lengthy computer runs to simulate steep rising or very slow rising floodwaves, channels with highly variable cross sections, abrupt changes in slope, split flow and ponded flow areas.

The FLO-2D computational domain is discretized into uniform, square grid elements. The computational procedure for overland flow involves calculating the discharge across each of the boundaries in the eight potential flow directions (Figure 4) and begins with a linear estimate of the flow depth at the grid element boundary. The estimated boundary flow depth is an average of the flow depths in the two grid elements that will be sharing discharge in one of the eight directions. Non-linear estimates of the boundary depth were attempted in previous versions of the model, but they did not significantly improve the results. Other hydraulic parameters are also averaged between the two grid elements to compute the flow velocity including flow resistance (Manning's n-value), flow area, slope, water surface elevation and wetted perimeter. The flow velocity (dependent variable) across the boundary is computed from the solution of the momentum equation (discussed below). Using the average flow area between two elements, the discharge for each timestep is determined by multiplying the velocity times flow area.

The full dynamic wave equation is a second order, non-linear, partial differential equation. To solve the equation for the flow velocity at a grid element boundary, initially the flow velocity is calculated with the diffusive wave equation using the average water surface slope (bed slope plus pressure head gradient). This velocity is then used as a first estimate (or a seed) in the second order Newton-Raphson tangent method to determine the roots of the full dynamic wave equation (James, et. al., 1977). Manning's equation is applied to compute the friction slope. If the Newton-Raphson solution fails to converge after 3 iterations, the algorithm defaults to the diffusive wave solution.

In the full dynamic wave momentum equation, the local acceleration term is the difference in the velocity for the given flow direction over the previous timestep. The convective acceleration term is evaluated as the difference in the flow velocity across the grid element from the previous timestep. For example, the local acceleration term ( $1/g * \partial V / \partial t$ ) for grid element 251 in the east (2) direction converts to:

$$\Delta(V_t - V_{t-1})_{251} / (g * \Delta t)$$

where  $V_t$  is the velocity in the east direction for grid element 251 at time  $t$ ,  $V_{t-1}$  is the velocity at the previous timestep ( $t-1$ ) in the east direction,  $\Delta t$  is the timestep in seconds, and  $g$  is the acceleration due to gravity. A similar construct for the convective acceleration term ( $(V_2 * g * \partial V / \partial x)$ ) can be made where  $V_2$  is the velocity in the east direction and  $V_4$  is the velocity in the west direction for grid element 251:

$$V_2 * \Delta(V_2 - V_4)_{251} / (g * \Delta x)$$

The discharge across the grid element boundary is computed by multiplying the velocity times the cross sectional flow area. After the discharge is computed for all eight directions, the net change in discharge (sum of the discharge in the eight flow directions) in or out of the grid element is multiplied by the timestep to determine the net change in the grid element water volume. This net change in volume is then divided by the available surface area ( $A_{surf}$  = storage area) on the grid element to obtain the increase or decrease in flow depth  $\Delta h$  for the timestep.

$$\sum Q_x^{i+1} = Q_n + Q_e + Q_s + Q_w + Q_{ne} + Q_{se} + Q_{sw} + Q_{nw} = A_{surf} \Delta h / \Delta t$$

where:

$Q_x$  = discharge across one boundary

$A_{surf}$  = surface area of one grid element

$\Delta h / \Delta t$  = change in flow depth in a grid element during one timestep

The channel routing integration is performed in essentially the same manner except that the flow depth is a function of the channel cross section geometry and there are usually only one upstream and one downstream channel grid element for sharing discharge. The computational index is the flow direction (1 of 8 directions) not the grid element. This simplifies and reduces the number of steps in the solution algorithm. Each direction is visited only once during a sweep of the grid system domain and involves two grid elements whereas a grid element index requires each grid element to be visited (Figure 4).

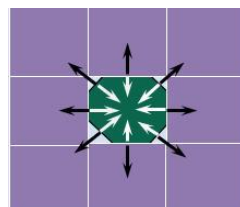


Figure 4. Flow Direction.

Flow Direction is the Computational Index not the Grid Element Number. To summarize, the solution algorithm incorporates the following steps:

1. For a given flow direction location in the grid system, the average flow geometry, roughness and slope between two grid elements are computed.
2. The flow depth  $d_x$  for computing the velocity across a grid boundary for the next timestep ( $i+1$ ) is estimated from the previous timestep  $i$  using a linear estimate (the average depth between two elements).

$$d_x^{i+1} = d_x^i + d_{x+1}^i$$

3. The flow direction first velocity overland, 1-D channel or street estimate is computed using the diffusive wave equation. The only unknown diffusive wave equation variable is the velocity.
4. The predicted diffusive wave velocity for the current timestep is used as a seed in the Newton-Raphson method to solve the full dynamic wave equation for the velocity. It should be noted that for hyperconcentrated sediment flows such as mud and debris flows, the velocity calculations include the additional viscous and yield stress terms.
5. The discharge  $Q$  across the boundary is computed by multiplying the velocity by the cross sectional flow area. For overland flow, the flow width is adjusted by the width reduction factors (WRFs).

The incremental discharge for the timestep across the eight boundaries (or upstream and downstream channel elements) are summed:

$$\Delta Q_x^{i+1} = Q_n + Q_e + Q_s + Q_w + Q_{ne} + Q_{se} + Q_{sw} + Q_{nw}$$

and the change in volume (net discharge  $\times$  timestep) is distributed over the available storage area within the grid or channel element to determine an incremental increase in the flow depth.

$$\Delta d_x^{i+1} = \Delta Q_x^{i+1} \Delta t / A_{surf}$$

where  $\Delta Q_x$  is the net change in discharge in the eight floodplain directions for the grid element for the timestep  $\Delta t$  between time  $i$  and  $i + 1$ . See Figure 5.

6. The numerical stability criteria are then checked for the new flow depth. If the Courant number stability criteria is exceeded, the timestep is reduced to the Courant number computed timestep, all the previous timestep computations are discarded and the velocity computations begin again with the first computational flow direction.
7. The simulation progresses with increasing timesteps using a timestep algorithm until the stability criteria are exceeded again.

+ 38	39	40	41
0.15	0.15	0.15	0.15
+ 1280.0 + 1263.7 + 1271.3 + 1278.8			
0.15			
25	26	27	28
0.15	0.15	0.15	0.15
+ 1272.4 + 1274.3 + 1278.6 + 1280.0			
0.15			
12	13	14	15
0.15	0.15	0.15	0.15
+ 1320.0 + 1322.6 + 1320.0 + 1317.9			
0.15			
5	6	7	
0.15	0.15	0.15	
+ 1305.4 + 1320.0 + 1320.0			
0.15			
2	3	4	
0.15	0.15	0.15	
+ 1320.0 + 1320.0 + 1309.4			
0.15			
	1300		

## Overland Flow

Grid Element

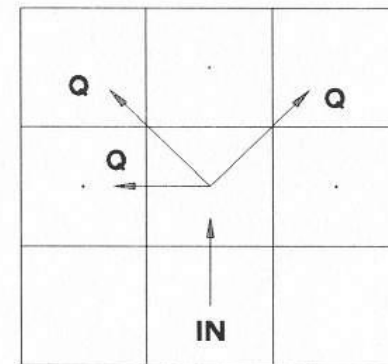
Elevation

Manning's n

13	14	15
+ 1282.6 + 1320.0 + 1317.9		
0.15	0.15	0.15
5	6	7
0.15	0.15	0.15
+ 1306.4 + 1320.0 + 1320.0		
0.15		
2	3	4
0.15	0.15	0.15
+ 1320.0 + 1320.0 + 1309.4		
0.15		

150'

## 8 Flow Directions



$$- Q_{14} - Q_{15} + Q_7 - Q_4 + Q_3 + Q_2 - Q_5 - Q_{13} = A_6 \frac{\Delta h}{\Delta t}$$

Discharge Flux Across Grid Boundaries



Figure 5. Discharge Flux across Grid Element Boundaries.

To accomplish the discharge exchange between grid elements based on the flow direction, the model sets up an array of side connections at runtime as shown in Figure 6. These flow directions are only accessed once during a timestep instead of the dual visitation required by searching for contiguous elements. This approach facilitates additional parallel processing for model speedup and has the additional benefits of:

- Reducing the required discharge computations by about 40% increasing model speed.
- Ignoring completely blocked sides.
- Eliminating NOFLOC assignment for channels.

In this computation sequence, the grid system inflow discharge and rainfall are computed first, and then the channel flow is computed. Next, if streets are being simulated, the street discharge is computed and finally, overland flow in 8-directions is determined (Figure 6). After all the flow routing for these components has been completed, the numerical stability criteria are tested for every floodplain, channel or street element. If stability criteria of any element are exceeded, the timestep is reduced by various functions depending on the previous history of stability success and the computation sequence is restarted. If all the numerical stability criteria are successfully met, the timestep is increased for the next grid system computational sweep. During a sweep of the grid system for a timestep, discharge flux is added to the inflow elements, flow velocity and discharge between grid elements are computed and the change in storage volume in each grid element for both water and sediment are determined. All the inflow volume, outflow volume, change in storage or loss from the grid system area are summed at the end of each time step and the volume conservation is computed. Results are written to the output files or to the screen at user specified output time intervals.

## FLO-2D Timestep Incrementing and Decrementing Scheme

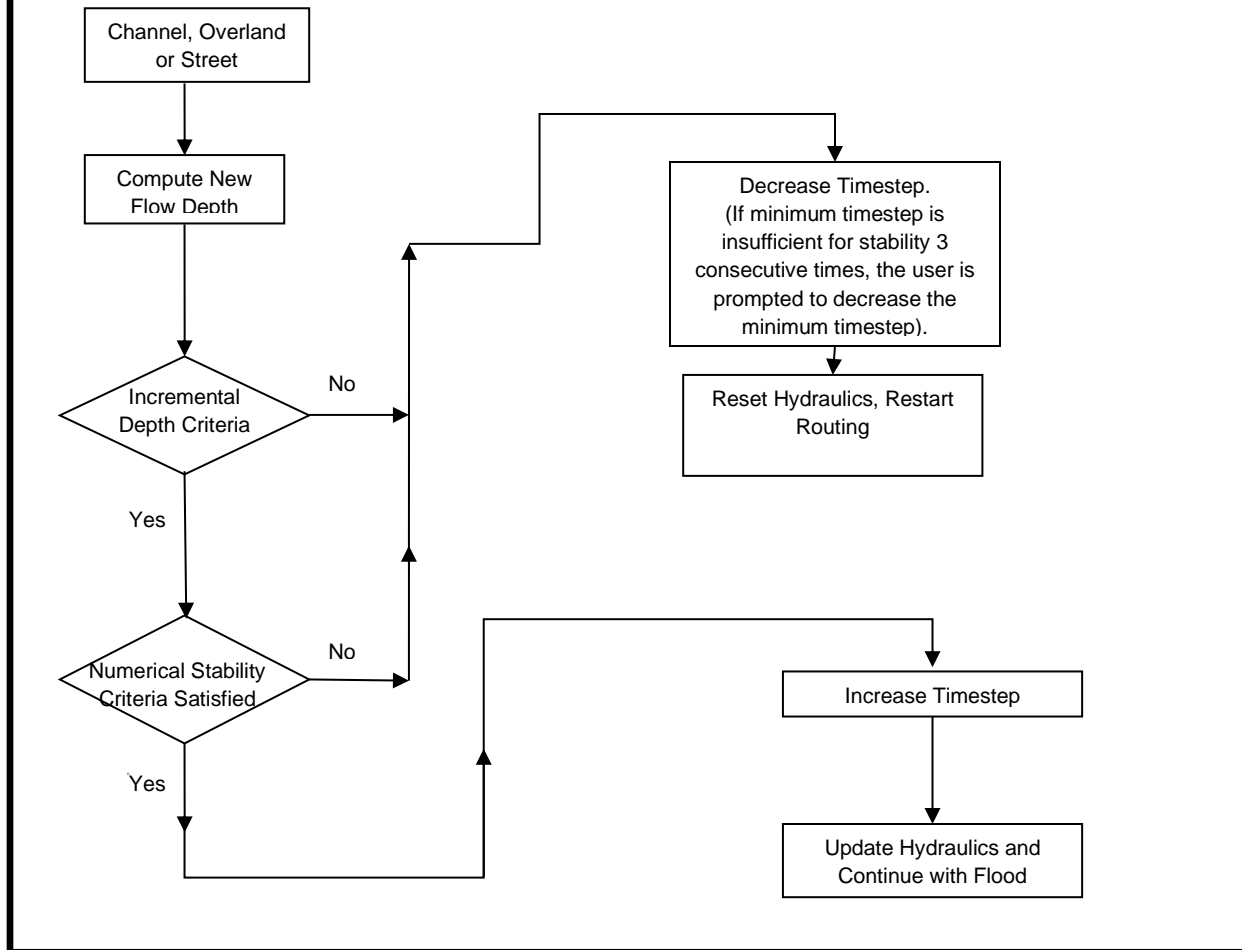


*Figure 6. FLO-2D Stability Criteria Flow Chart.*

The FLO-2D flood routing scheme proceeds on the basis that the timestep is sufficiently small to insure numerical stability (i.e. no numerical surging). The key to efficient finite difference flood routing is that numerical stability criteria limits the timestep to avoid numerical surging and yet allows large enough timesteps to complete the simulation in a reasonable time. FLO-2D has a variable timestep depending on whether the numerical stability criteria are not exceeded. The numerical stability criteria are checked for every grid element on every timestep to ensure that the solution is stable. If the numerical stability criteria are exceeded, the timestep is decreased and all the previous hydraulic computations for that timestep are discarded. Most explicit schemes are subject to the Courant-Friedrich-Lowy (CFL)

condition for numerical stability (Jin and Fread, 1997). The CFL condition relates the floodwave celerity to the model time and spatial increments. The physical interpretation of the CFL condition is that a particle of fluid should not travel more than one spatial increment  $\Delta x$  (grid element side) in one timestep  $\Delta t$  (Fletcher, 1990). FLO-2D uses the CFL condition for the floodplain, channel and street routing. The timestep  $\Delta t$  is limited by:

$$\Delta t = C \Delta x / (\beta V + c)$$

where:

C is the Courant number ( $C \leq 1.0$ )

$\Delta x$  is the square grid element width or channel length

V is the computed average cross section velocity

$\beta$  is a coefficient (5/3 for a wide channel)

c is the computed wave celerity

While the coefficient C can vary from 0.2 to 1.0 depending on the type of explicit routing algorithm, a default value of 0.6 is recommended in the FLO-2D model. When C is set to 1.0, artificial or numerical diffusivity is theoretically zero for a linear convective equation (Fletcher, 1990). If the simulation has some numerical surging identified by unreasonably high velocities or spikes in an outflow discharge hydrograph, the Courant number should be reduced by 0.1 until a value of 0.2 or 0.3 is reached. The Courant number is spatially variable by grid element within a small range. With a successful completion the cell Courant number is permitted to increase by 0.0001 up to a value 0.05 greater than the assigned value. If the Courant number is exceeded, the value is decrease by 0.002 until the assigned value is reached. The assigned Courant is the minimum value allowed.

It may not be possible to completely avoid the artificial diffusivity or numerical dispersion using the Courant number to limit the timestep (Fletcher, 1990). Timesteps generally range from 0.1 second to 30 seconds with a typically timestep on the order of 1 second during the highest discharge flux. The model starts with the a minimum timestep equal to 5 seconds and increases it until the numerical stability criteria exceeded, then the timestep is reset to the computed Courant number timestep. If the stability criteria continue to be exceeded, and the minimum timestep is not small enough to conserve volume or maintain numerical stability, then the input data must be modified. The timesteps are a function of the discharge flux for a given grid element and its size. Small grid elements with a steep rising hydrograph and large peak discharge require small timesteps. Accuracy is not compromised if small timesteps are used, but the runtime time can be long if the grid system is large.

The timestep incrementing and decrementing functions were designed to support the role of the Courant number in the model stability. It was determined that varying the Courant number within a certain range of the original value reduced the number of ineffective timestep decreases. In addition, the timestep increments and decrements were reduced to enable the computational timestep to more gradually adjust to numerical stability criteria. This replaced the method of a large timestep decrease

followed by more numerous small timestep increases. Results show there was a significant increase in runtime model speed up from 15 to 40%. The stability criteria are applied as follows:

- Separate Courant number assignment for floodplain, channel and street flow.
- Automated spatial variation in the floodplain, channel or street Courant number within a specified range depending on the whether the Courant number criteria was exceeded or not exceeded.

It should be noted that the obsolete stability parameters DEPTOL (% change in flow depth) and WAVEMAX (dynamic wave) stability criteria has been eliminated.

A timestep accelerator parameter (TIME\_ACCEL) was coded into the model. Several adjustments of this variable have been made over the years. The default value was changed from 0.1 to 1.0. A higher value of TIME\_ACCEL will result in larger timestep increments. When the computational timestep is less than 1.0 second and a simulation timestep loop was successfully completed without exceeding the stability criteria, the timestep is incremented by the TIME\_ACCEL (default 1.0) + 0.001. So if the timestep was 0.5, then the next timestep would be increased to 0.501 seconds. If the timestep is greater than 1 second, then the timestep increment is:

$$DSEC = DSEC + TIME\_ACCEL * 0.0085 / XFAST$$

where:

DSEC = computational timestep in seconds

TIME\_ACCEL = user defined parameter ranging from 0.1 to 10.0 with a default value of 1.0

XFAST = XFAST + 0.001 for each successfully completed timestep loop when DSEC > 1.0 second.

XFAST resets to 1.0 each time the DSEC timestep is decremented.

This algorithm increases the timestep uniformly until the timestep DSEC is greater than 1 second. When DSEC > 1.0, successive increases in DSEC result in a larger value of XFAST which begins to slow down the timestep rate of change. The maximum timestep is limited to 30 seconds.

### **2.3    *The Importance of Volume Conservation***

A review of any flood model simulation results begins with volume conservation. Volume conservation indicates accuracy and numerical stability. The inflow volume, outflow volume, changes in storage and losses (infiltration) are summed at the end of each time step. FLO-2D volume conservation results are written to the output files or to the screen at user specified output time intervals. Data errors, numerical instability, or poorly integrated components may cause a loss of volume conservation. Any simulation not conserving volume should be revised. It should be noted that volume conservation in any flood simulation is not exact. While some numerical error is introduced by rounding numbers, approximations or interpolations (such as with rating tables), volume should be conserved within a fraction of a percent of the inflow volume. The user must decide on an acceptable level of error in the volume conservation. While volume conservation with 0.001 percent is considered very accurate, most FLO-2D simulations have a volume conservation accuracy within a few millionths of one percent.

## 2.4 Courant Number Variability for Numerical Stability

The key to efficient FLO-2D flood routing is assigning numerical stability criteria that limits the timestep to avoid surging and yet allows large enough timesteps for a fast simulation. FLO-2D has a variable timestep that is a function of the numerical stability criteria. The numerical stability criteria are checked for every grid element flow direction for each timestep. If any of the numerical stability criteria are exceeded, the timestep is decreased and all the previous hydraulic computations for that timestep are discarded.

The FLO-2D computation routing algorithm is an explicit scheme that is subject to the Courant-Friedrich-Lowy (CFL or Courant number) condition for numerical stability. The Courant number relates the floodwave movement to the model discretization in time and space. The concept of the Courant number is that a particle of fluid should not travel more than one spatial increment  $\Delta x$  (between the center of cells) in one timestep  $\Delta t$ . If the model computational timestep exceeds the Courant relationship timestep, the stability criteria is exceeded and a timestep decrement occurs.

Mathematically the Courant relationship is given by:

$$V + c = C \Delta x / \Delta t$$

where:

$C$  = Courant Number ( $C \leq 1.0$ )

$\Delta x$  = FLO-2D square grid element width (distance between node centers)

$V$  = depth averaged velocity

$c$  = floodwave celerity =  $(gd)^{0.5}$  where  $g$  is gravitation acceleration and  $d$  is the flow depth above the thalweg.

This equation relates the progression of the floodwave ( $V + c$ ) to the discretized model in space and time. The Courant number  $C$  can vary from 0.1 to 1.0, and a value of 1.0 will enable the model to have the largest possible timestep. When  $C$  is set to 1.0, artificial or numerical diffusivity is theoretically zero for a linear convective equation. Testing has shown that the FLO-2D model can run faster (more consistent higher timesteps) with greater stability if the Courant number is set to values less than 1.0. The FLO-2D default Courant number is 0.6 which will provide a numerically stable model for most applications. Rearranging the CFL relationship, the model computes the Courant timestep  $\Delta t$  as:

$$\Delta t = C \Delta x / (V + c)$$

Numerical instability occurs when the computational timestep is too large or the rate of change in the timestep is too large and too much volume enters or leaves a grid element (discharge flux). The corresponding change in flow depth can result in a high velocity (or Froude number) with the discharge causing a rapid fluctuation in the grid element water surface elevation (surging). Numerical surging may cause spikes in the discharge hydrograph (Figure 7), adverse water surface slope in the downstream direction or unreasonable maximum velocities (VELTIMEFP.OUT (Figure 8) for the floodplain or VELTIMC.OUT for channels) or Froude numbers (SUPER.OUT). Unreasonable maximum velocities are

easy to identify because the VELTIM\_x.OUT files are sorted in descending order. The first several reported maximum velocities should not be significantly greater than the rest of the file as in the case of node 4887 in the VELTIMFP.OUT file below.

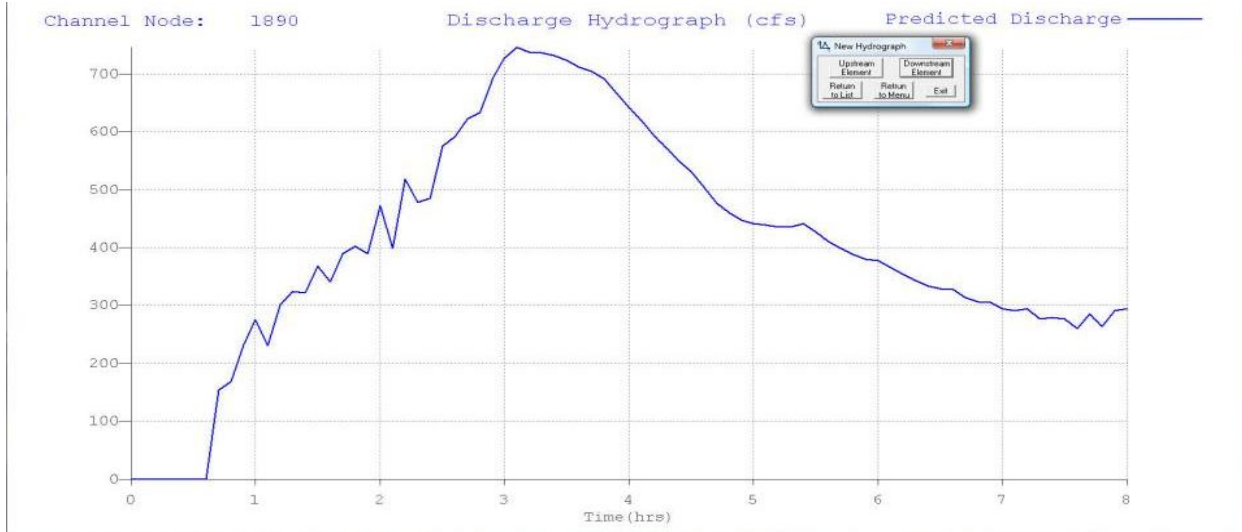


*Figure 7. Numerical Surging in a Channel Element Hydrograph.*

TOP 100 CELLS MAXIMUM FLOODPLAIN VELOCITIES LISTED IN DESCENDING ORDER

NODE	MAXIMUM VELOCITY (FPS OR MPS)	DEPTH AT MAX. VELOCITY (FT OR M)	TIME OF OCCURRENCE (HRS)
4887	10.69	4.73	2.29
4834	7.12	4.93	2.04
1781	6.24	1.26	2.87
4833	6.16	3.55	2.11
1843	6.00	1.12	2.89
4832	5.97	3.77	2.52
4781	5.96	3.74	2.04
1907	5.93	0.54	2.60
1811	5.90	1.27	2.88
1455	5.72	2.60	2.81
4452	5.62	2.19	2.93
1875	5.58	1.10	2.89
4387	5.58	3.30	3.06
1939	5.57	0.49	3.64
1971	5.45	0.49	2.80
1146	5.30	2.40	2.76
3268	5.25	1.34	2.99
3974	5.23	1.66	2.93
1426	5.23	3.77	2.81
4230	5.10	0.50	2.95
2690	5.09	1.59	2.96
3816	5.08	2.94	2.92
3765	4.99	2.74	2.92
3267	4.97	1.33	3.05
4779	4.93	2.21	2.12

*Figure 8. File Sample VELTIMFP.OUT.*

## Using the Courant Number and Timestep Accelerator Parameter

The global Courant Number is assigned in the TOLER.DAT file line 2 as follows:

Line 1.	0.1	0.0	(TOL; the DEPTOL parameter is not required)
Line 2.	C	0.6	0.5    0.5 (floodplain, channel and street COURANT numbers)
Line 3.	T	0.1	(TIME_ACCEL; referred to as ‘timestep accelerator’)

where C is a line character identifier and the Courant number for floodplain, channel and street are entered. The Courant number should only be assigned for those components that are used. The channel and street components may not be used in a given project.

The typical range of the Courant number is from 0.2 (slower more stable model) to 0.9 (faster less stable model). The default of 0.6 is recommended as a starting value. For models that appear to be unstable, reducing the Courant Number to a lower value in decrements of 0.1 (from 0.6 to 0.5 down to 0.2) should control any numerical surging. Lower Courant numbers should be assigned for steep rising hydrographs, high velocity conditions or high flow depths as in the case of a reservoir or large detention basin filling.

Courant numbers are slightly spatially variable during runtime. When the flood routing algorithm for a given grid element is completed successfully without a timestep decrement, the Courant number is increased by 0.0001 for the next timestep. The increase in the Courant number is limited to 0.05 greater than the original global Courant number. The Courant number cannot exceed 1.0 for any condition. When the Courant number timestep is exceeded, then the Courant number is reduced by 0.002 and the model computational timestep is decremented by a small percentage. Consecutive timestep decrements force a larger percent reduction and after several successive decrements by the same grid element, the computational timestep is set to the Courant number timestep. In this manner, an initial small reduction in the computational timestep may allow the model to proceed with further exceeding the Courant timestep.

While the Courant number defines the base timestep, the TIME\_ACCEL parameter controls the rate of increase of the timestep after a successful routing loop is completed for a computational timestep. The practical range of the TIME\_ACCEL parameter is 0.1 to 1.0. Values outside this range, although possible, would not improve the simulation. If TIME\_ACCEL = 0.1, a small rate of increase of the timestep occurs. This reduces the number of total timestep decrements. A large rate of change in the computational timestep for TIME\_ACCEL = 1.0 will have a corresponding increase in the number of timestep decrements and more opportunity for numerical instability.

The model speed tends to be the faster when there is balance between the number of timestep decreases and a gradual rate of climb or increase in the computational timestep. It is possible to limit the number of timestep decrements as reported to the TIME.OUT file, but this corresponds to a slow rate of increase in the timestep. A large rate of timestep increase (higher TIME\_ACCEL) will result in higher average timesteps and more timestep decrements, but overall the model speed may be faster and the runtime shorter.

### **Suggested Approach:**

Use the default Courant number (0.6) and TIME\_ACCEL (0.1) for the initial simulation. Then review the VELTIMEFP.OUT file (and VELTIMEC.OUT file for the channel) files that report the maximum velocities in descending order to determine if there are any unreasonable velocities. Verify the adequacy of the results by reviewing the SUPER.OUT file for high maximum Froude numbers. Post-processor program review of the graphical display of the channel hydrographs in the HYDROG or the PROFILES plot of the maximum channel water surface elevation profile might also reveal numerical surging. The following approach is suggested for making adjustments to speed up the model or slow down the model to eliminate numerical instability:

1. If the model has no numerical surging or unreasonable maximum velocities and it is desired to have the model run faster, increase the TIME\_ACCEL parameter from 0.1 to 0.25 and run the model again. If the model runs faster and the results still don't indicate any numerical instability, then increase TIME\_ACCEL to 0.3 or 0.4. Some numerical instability may begin to appear in VELTIMFP.OUT when TIME\_ACCEL is 0.4 - 0.5 or higher.
2. Once unreasonable velocities or Froude numbers are noted, decrease the TIME\_ACCEL by 0.05. Review the mode runtime at the end of the SUMMARY.OUT file and do the various numerical instability checks. At this point, a pattern will probably be apparent and the optimum Courant number and TIME\_ACCEL parameter can be achieved. If the model becomes numerically stable with the decreased TIME\_ACCEL, it may be possible to increase the Courant number to achieve a slightly faster model.
3. If the model has some initial numerical instability, leave the TIME\_ACCEL at the default value of 0.1 and decrease the Courant Number from 0.6 to 0.5 to 0.4 over several runs until the numerical instability is eliminated. Data adjustments to eliminate numerical surging might include increasing n-values using the limiting Froude number and the ROUGH.OUT file. Depressed grid elements, hydraulic structure rating tables, deep ponded water or steep slopes may also contribute to unreasonable high maximum velocities.

Following each flood simulation, the TIME.OUT file should be reviewed to determine which of the grid elements are frequently exceeding the Courant timestep and contributing to a slow model speed. For those grid elements with excessive timestep decrements, adjustments can be made to the node attributes such as topography, roughness, available surface area (area reduction values ARFs) or width reduction values (WRFs).

## **2.5 Volume Evacuation from Small Grid Elements**

Potential negative storage with very shallow flows was not a significant issue when the original TOL (depression storage TOL value) was typically assigned a value of 0.1 ft. Very low spatially variable TOL values are now being assigned for urban rainfall models to maximize runoff. With the opportunity for faster FLO-2D simulations, several factors can contribute to the evacuation of volume from floodplain and channel elements with shallow flow (negative storage volume). Faster simulations and more parallel processing code have resulted in larger project grid systems with smaller grid elements. Smaller elements combined with small assigned depression storage tolerance values ( $TOL \sim 0.004$  ft or 0.001 m) results less volume on a cell for shallow flows than for previous model versions (Figure 9). The FLO-2D model has an explicit numerical scheme that exchanges flow with contiguous elements in eight

directions, so it is possible with very shallow flows to completely drain an element of volume if the outflow exceeds the inflow plus storage. This may occur more frequently with hydraulic structure inflow nodes.

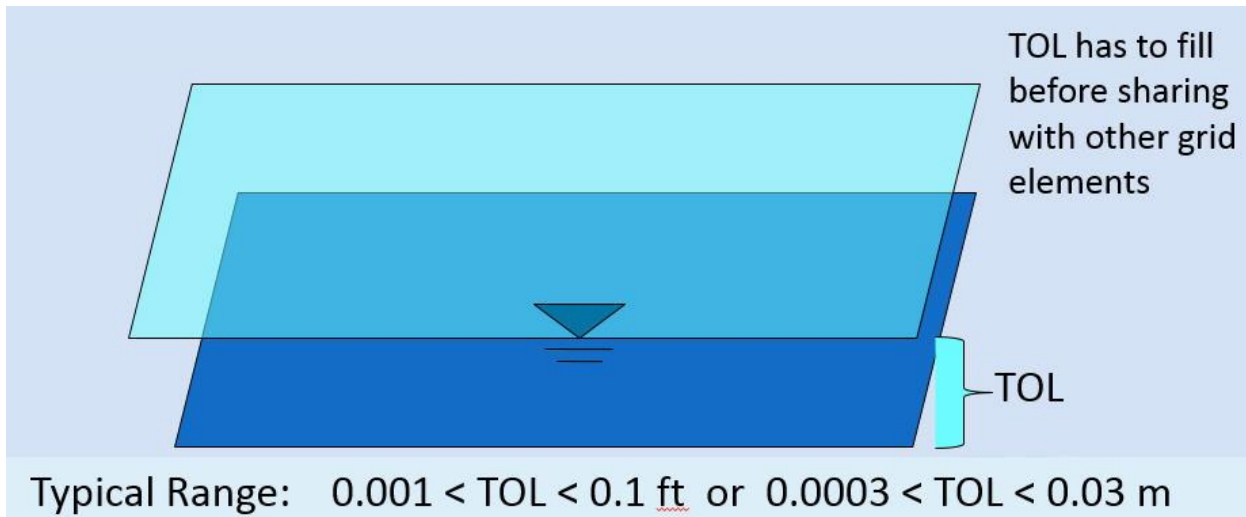


Figure 9. TOL Definition.

Grid Element Depression Storage that Must Be Filled Before Volume is Exchanged with Another Element

#### Previous Methods for Addressing Volume Evacuation

Any negative volume in floodplain or channel elements after the computational loop was previously redistributed to the other neighbor elements and the volume in the given cell was set to zero. This necessitated an extra computation loop for all the elements to re-sum all the volumes after the redistribution, but the timestep was not decremented. Instead, the normal computational routine continued uninterrupted but with an extra computational loop for all the grid elements for all timesteps. This was a computationally expensive approach. Addressing the volume evacuation issues required a review of the cells listed in the EVACUATEDFP.OUT and EVACUATEDCH.OUT files and adjusting cell attributes such as n-values, elevation, surface area or other features or components. Narrow inset low flow triangular channels were typically a problem and needed to be revised to a U-shaped channel that holds more volume at low flow depths. Correlating the grid elements listed in these files with those listed TIME.OUT enabled the most critical cells slowing down the model to be addressed first.

In addition, if the number of times evacuated elements on the floodplain reached 1,000, this caused the model to stop; presuming that this number of incidents of evacuated cells needed to be corrected. Often evacuated cells may be associated with discharge or water surface controls such as hydraulic structure or other components. The concept was to review the EVACUATEDxx.OUT files and adjust those evacuated element attributes before the final model product was completed.

## **Evacuated Element Revisions**

Several codes revisions were made to simplify and automate the model response to evacuated elements including:

- The separate computational loop for evaluating the evacuated cells was eliminated.
- The limitation on the number of times (1,000) that evacuated elements were encountered was eliminated. The number of times each floodplain or channel element is now evacuated is listed in the EVACUATEDxx.OUT files.
- Evacuated element n-values are increased by 0.001 to a limit of 0.250 for both the floodplain and channel.
- The model terminates the current timestep loop and reduces the timestep by 1 percent.
- The evacuated channel element TOL value is increased to 0.2 ft (0.067) if TOL is less than 0.2 ft (0.067 m) and increases the TOL by 0.02 ft (0.006 m) if greater than 0.2 up to a maximum value of 0.4 ft (0.122 m).
- The floodplain evacuated element TOL value is increased to 0.1 ft (0.03) if TOL is less than 0.1 ft (0.03 m) and increases the TOL to 0.25 ft (0.076 m) if greater than 0.1 ft (0.03 m).

The focus is to adjust the flood hydraulics and the depression storage rather than the timestep for evacuated elements at shallow flows.

## **Reviewing the Evacuated Element Results**

First review the SUMMARY.OUT and CHVOLUME.OUT file to see if there is any volume conservation error. Volume conservation error is not always related to evacuated elements, but it could be.

Reviewing the EVACUATEDFP.OUT and EVACUATEDCH>OUT files and the TIME.OUT file will further help to identify if the model is not conserving volume in response to the evacuated elements. If EVACUATEDxx.OUT are empty or non-existent, the volume conservation error is being cause by some other component of the model. If the grid elements in these files are correlated, then review the ROUGH.OUT file to see if the same elements have increased n-values. When it appears that there are evacuated elements that are impacting the model performance, then it is necessary to review these elements in detail in terms of their attributes (n-values, elevations) or components (ARF-values, streets, infiltration, etc.) and make some adjustments. For these projects, only run the simulation until the model begins to slow down (a timestep less than 0.1 second or lower) and continue to adjust the evacuated elements until these no longer appear in the output files.

## 2.6 Limiting Froude Number

Using the Froude number in flood routing models is an important to both the understanding of the floodwave movement and the numerical stability of the model. It is even more important when considering mobile bed channels such as alluvial fans or high bedload rivers. The dimensionless Froude number  $Fr$  is given by:

$$Fr = \alpha^{0.5} V/(gd)^{0.5}$$

Where:

$V$  = depth averaged flow velocity

$G$  = acceleration due to gravity

$d$  = depth of flow above the thalweg

$\alpha$  = kinetic energy correction factor (involving the fluid density and specific weight). Typically  $\alpha$  is assumed to be 1.

The Froude number helps to define the influence of gravity on the flow pattern. A low wave will propagate in free surface flow (open channel) depending only on the gravitational acceleration and the flow depth. The movement (speed) of the shallow wave, known as the wave celerity  $c = \sqrt{gd}$ , is related to average flow velocity through the Froude number. By accepting reasonable limitations of the overland (or channel) flow velocity and floodwave movement, the Froude number can be used to further define the relationship between the velocity and flow depth.

For essentially steady and uniform flow, the Manning's  $n$  value is defined would be defined by:

$$n = (0.262/F_r) d^{0.17} S^{0.5}$$

indicating that the flow roughness is inversely proportional the Froude number. By assuming a reasonable limiting Froude number, the  $n$  value can be estimated from the normal depth and slope for a given flow discharge.

In the FLO-2D model, the suggested  $n$ -value is based on either bankfull discharge for channel flow or 1 meter (3 ft) flow depth for overland flow (roughness is fully submerged). Suggested typical limiting Froude numbers are defined in Table 1.

**Table 1. Range of Values Limiting Froude.**

Tool	Flat or Mild Slope (large rivers and floodplains)	Steep Slope (alluvial fans and watersheds)
Channels	0.4 – 0.6	0.7 – 1.05
Overland flow	0.5 – 0.8	0.7 – 0.95
Streets	0.9 – 1.2	1.1 – 1.5

Similar values are also reported in the CVFED FLO-2D Application Guide. If the limiting Froude number is exceeded, the grid element n-value increases by 0.001 for the next timestep. When limiting Fr is no longer exceeded, the n-value decreases by 0.0005 if it's greater than the original n-value. The changes in n-value reported in ROUGH.OUT, FPLAIN.RGH, CHAN.RGH and STREET.RGH files. The use of limiting Froude number in the FLO-2D model is documented in the FLO-2D Pocket Guide, the FLO-2D Reference Manual, and the CVFED FLO-2D Application Guide.

The maximum n-values for discretized models will be greater than typical n-values for HEC-RAS cross sections (both channel and overbank areas). This is because of the unsteady and non-uniform flow contribution between elements and the flow not being parallel to the cross section.

For flows over mobile bed conditions (supply unlimited), critical flows are approached asymptotically (Grant, 1997). A relatively steep slope is required for flow with sediment transport to achieve critical flow because the flow hydraulics oscillate. For  $Fr > 1$ , flow instability leads to rapid energy dissipation and bed erosion. Flow is forced to stay around critical by incipient motion thresholds. The equilibrium sand bed morphology tends to minimize the Froude number (Jia, 1990).

The limiting Froude number for mobile bed conditions can be approximated by (Grant, 1997):

$$Fr = 3.85 S^{0.33} \text{ gravel bed } (\tau^*_{cr} = 0.03)$$

$$Fr = 5.18 S^{0.11} \text{ sand bed } (\tau^*_{cr} = 0.06)$$

Roughness n-values include many factors:  $n = n_1 + n_2 + n_3 + n_4 + \dots$  such as friction drag, vegetation, expansion/contraction, bed forms, flow in bends, unsteady and non-uniform flow.

## **2.7 Shallow Flow Roughness and TOL**

Open channel (or floodplain) uniform flow is characterized by a constant depth, velocity, flow area and discharge such that the bed slope, water surface slope and energy grade line are all parallel. Generally, uniform flow dictates that the flow is also steady. Unsteady, uniform flow would not occur naturally. For practical purposes natural uniform flow is also turbulent implying that a stable velocity distribution has been attained and the turbulent boundary layer is fully developed. There are a number of uniform flow mean velocity equations for open channels and Manning's equation is the best known of these:

$$V = 1.486/n R^{2/3} S^{1/2}$$

where  $V$  = velocity,  $R$  = hydraulic radius,  $S$  = friction slope,  $n$  = Manning's roughness coefficient.

The hydraulic radius exponent value (0.667) has been known to vary over a range from about 0.59 to 0.85 depending primarily on channel geometry and roughness (Chow, 1959). The roughness coefficient or Manning's n-value varies with a number of factors including but not limited to bed friction, bed form, expansion/contraction, vegetation, obstructions, and flow depth.

Manning's n-value is known to increase with decreasing flow depth. Manning's equation can be assumed to apply within and above the turbulent boundary layer. By definition, the turbulent boundary

terminates at depth where the vertical velocity distribution for uniform steady flow in a rough wide channel has attained a value of 99% of the free stream flow. At the lower depth, this flow regime extends from the height of the displacement thickness near the laminar boundary layer and varies as a function of the Reynolds number. The displacement thickness is generally 1/8 (rough) to 1/10 (smooth) of the turbulent boundary layer. If the flow is very shallow roughness elements may protrude through the laminar sublayer and into the flow. Flows are considered hydraulically rough if the grain size or roughness element is greater than 6 times the laminar boundary layer:

$$\delta = 11.6 v/u^*$$

where  $v$  = kinematic viscosity and  $u^*$  = shear velocity

The applicability of Manning's equation to a given flow condition depends on the relative submergence of the roughness elements ( $R/k_s$ ) where  $k_s$  is the effective roughness height. In general, Manning's equation is appropriate for a relative submergence (Julien, 1995):

$$R/k_s > 100$$

which will correspond to the Manning-Stickler fixed bed roughness as function of sediment size D relationship (Simons and Senturk, 1976):

$$n = D^{1/6}/21.1$$

For lower a submergence value ( $R/k_s < 100$ ), the logarithmic form of the resistance equation should be used (Julien, 1995). For flow transporting sediment in suspension, the flow will be primarily turbulent if

$$R/k_s > 70$$

Typical roughness height for grain size bed material can range from 0.0015 ft for rough concrete to 0.01 ft for coarse sand or uniform earth channels. In this case Manning's equation for a coarse sand plane bed would be applicable to about 0.7 ft. Julien (1995) plotted the logarithmic velocity equation solution for turbulent flow over rough plane boundaries and it is noted that Manning's equation can still provide a reasonable approximation as low as about  $R/k_s \sim 25$ . Taking this as a less conservative approach for a rough surface where the roughness height is sand size or smaller, Manning's equation should apply if the flow depth is roughly 25 times the relative roughness. For coarse sand this would be a flow depth of about 0.25 ft.

Manning's equation will overpredict the velocity for shallow flow if typical low n-values assigned to deeper flows are applied. Manning's equation was an empirical equation that relates the velocity to several parameters using a coefficient (n-value) for flow depths generally greater than 0.5 ft. When computing velocity for shallow flow depths near the FLO-2D tolerance value TOL on the order of 0.1 ft or smaller, it is unlikely that the flow will be fully developed turbulent flow. In lieu of using multiple mean velocity equations, one for deeper flow and one for shallow flow, it is necessary to compensate for overpredicting the velocity using Manning's equation by assigning higher shallow n-values or using depth variable n-values or both.

## **Chapter 3. FLO-2D MODEL SYSTEM**

### **3.1    *Assumptions and Special Conditions***

#### **Conceptualization**

FLO-2D flood routing scheme moves around blocks of fluid on a discretized flow domain consisting of a system of square tiles. FLO-2D numerically distributes the volume in finite fluid blocks to mimic the floodwave progression and timing over the discretized surface. Conceptually FLO-2D is not a Lagrangian particle dynamics model but rather a finite volume model that moves discrete parcels of fluid around on the grid system in eight directions with realistic flow velocities.

#### **Spatial Resolution**

The spatial and temporal resolution of the FLO-2D model is dependent on the size of the grid elements and rate of rise in the hydrograph (discharge flux). The rate of change in flood discharge results in an incremental change in the flow depth when distributed over the available grid element surface area for a given timestep. Smaller grid elements may improve the resolution of the flood distribution at the cost of increased computational time, more extensive data files and boundary conditions. A balance must be achieved between the number of grid elements and an acceptable computational time. A grid size of 20 ft (8 m) to 500 ft (130 m) is usually appropriate for most simulations. Smaller grid elements will not only significantly increase the number of grid elements (the number of grid elements is quadrupled each time the grid element size is divided by two), but the rate of discharge flux per unit area of the grid element also increases.

FLO-2D was developed to simulate large flood events on unconfined surfaces. The discretization of the floodplain topography into a system of square grid elements to accommodate large discharges can obscure some topographic features such as mounds and depressions. This topographic variability will not affect the water surface when the entire valley is flooded, however, when simulating shallow flow, smaller grid elements should be used. Grid element rating tables can also be applied to reflect the variable topography within the grid element. Map resolution and accuracy should be considered when selecting the grid element size. Topographic contour resolution of plus or minus 1 ft (0.3 m) may not support grid elements less than 30 ft (10 m).

For one-dimensional channel flow, the spatial representation and variation in channel geometry is usually limited by the number of cross sections that are surveyed or cut from a DTM data base. Generally, one cross section represents 5 to 10 grid elements. The relationship between flow area, slope and roughness can be distorted by having an insufficient number of surveyed cross sections. Abrupt channel transitions can result in numerical surges if the choice of the roughness values is representative. The objective is to eliminate any discharge surges without substantially reducing the timestep so that the model runs as fast as possible. This can be accomplished by having gradual transitions between wide and narrow reaches.

## Floodwave Attenuation and Discontinuities

Floodwave attenuation occurs in response to flood storage (both channel and overbank). Infiltration and evaporation losses can also contribute to floodwave attenuation. Floodwave attenuation represents the interaction of the friction and bed slope terms with the diffusive pressure gradient. While the application of the dynamic wave equation can reduce instabilities in the flood routing computations, simulating rapidly varying flow is still limited by the grid element size. The model does not have the ability to simulate the water surface profile of shock waves, rapidly varying flow (roll waves) or hydraulic jumps because of temporal and spatial discretization. These discontinuities in the flow profile are smoothed out in the model's calculations. Subcritical and supercritical flow transitions are assimilated into the average hydraulic conditions (flow depth and velocity) between two grid elements, however, sequent depths of sustained hydraulics are computed.

## Simulating Ponded Water Conditions

Ponded water conditions (>10 ft or 3 m with low velocities) in a flood simulation may require extra review. FLO-2D uses Manning's equation to assess hydraulic roughness and it is based on uniform, fully developed turbulent flow. In a ponded water condition, Manning's equation for channel flow does not apply. The velocity profile may not represent uniform flow with a vertical logarithm distribution. Flow near the bed could be in one-direction and flow near the surface in another direction (Figure 10). A ponded water surface might have a very mild, but using Manning's equation, high average velocities could still be computed because the velocity is a power function of the depth. It is possible to compute reasonable or accurate water surface elevations in a ponded water condition with FLO-2D, but high Manning's n-values should be applied to keep the depth integrated flow velocity below 1 fps (0.33 mps).

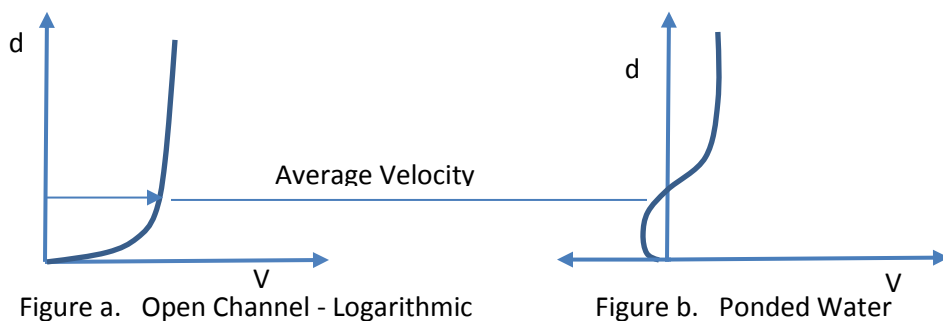


Figure 10. Vertical Velocity Profiles.

## Basic Assumptions

The inherent assumptions in a FLO-2D simulation are:

- Steady flow for the duration of the timestep;
- Hydrostatic pressure distribution;
- Hydraulic roughness is based on steady, uniform turbulent flow resistance;
- A channel element is represented by uniform channel geometry and roughness.

These assumptions are self-explanatory but they remind us that the flow conditions between grid elements are being averaged. For more information on reservoir routing and ponded flow, look at the Levee, Dam, and Wall Breach Guidelines.

### Rigid Bed versus Mobile Bed

When sediment transport is not simulated, a rigid bed is presumed for the flood simulation. Rigid boundary conditions are appropriate for flow over steep slopes, urban flooding and mudflow events. This is because the amount of storage change associated with scour holes or deposition is generally negligible compared with the flood volume. The area of inundation associated with large flood events is unaffected by bed changes. Channel bed changes generally deviate about a mean condition, and the portion of the flood volume stored in the channel can be small relative to the volume stored on the floodplain during a large event. It is assumed in rigid bed simulations that the average flow hydraulics and water surface are not appreciably affected by the scour and deposition that might occur in an individual grid element. Entire channel reaches must aggrade or degrade to significantly affect the area of inundation. This is the reason that FEMA FIS river studies typically do not require sediment transport analyses. Simulating a mobile bed can be more important for smaller floods, for alluvial fan flows and where channel avulsion or sediment deposition might change the flow path.

### **3.2 Roughness Parameter Variability**

The constitutive fluid motion equations in the FLO-2D are the continuity equation and the momentum equation:

$$\frac{\partial h}{\partial t} + \frac{\partial h V}{\partial x} = i$$

$$S_f = S_o - \frac{\partial h}{\partial x} - \frac{V}{g} \frac{\partial V}{\partial x} - \frac{I}{g} \frac{\partial V}{\partial t}$$

where  $h$  is the flow depth and  $V$  is the depth-averaged velocity in one of the eight flow directions  $x$  for a computational timestep  $\partial t$  and  $g$  is the gravitational acceleration. The excess rainfall intensity ( $i$ ) may be nonzero on the flow surface. The friction slope component  $S_f$  is based on Manning's equation. The other terms include the bed slope ( $S_o$ ) pressure gradient and convective and local acceleration terms. The two unknown variables are velocity and flow depth. The discharge  $Q$  is given by  $Q = VA$  where  $A$  is the cross section flow area.

Open channel (or floodplain) uniform flow is characterized by a constant depth, velocity, flow area and discharge such that the bed slope, water surface slope and energy grade line are all parallel (i.e.  $S_f = S_o$  for uniform flow). Often uniform flow accompanied by a steady flow condition (such as flume flow). Unsteady, uniform flow would not occur naturally. For practical purposes natural uniform flow is almost always turbulent implying that a stable velocity distribution has been attained and the turbulent boundary layer is fully developed. There a number of uniform flow mean velocity equations for open channels and Manning's equation is the best known of these:

$$V = 1.486/n R^{2/3} S_f^{1/2}$$

where  $R$  = hydraulic radius,  $S_f$  = friction slope,  $n$  = Manning's roughness coefficient. For wide cross section flow the hydraulic radius approaches the flow depth and the flow area can be expressed as a power function of the flow depth:

$$A = a h^b$$

where  $a$  and  $b$  are a regressed coefficient and exponent respectively. The hydraulic radius exponent value (0.667) in Manning's equation has been known to vary over a range from about 0.59 to 0.85 depending primarily on cross section geometry and roughness (Chow, 1959). The roughness coefficient or Manning's  $n$ -value varies with a number of factors including but not limited to bed friction, bed form, expansion/contraction, vegetation, obstructions, and flow depth.

The discharge  $Q$  is a function of three variables, flow area slope and roughness when computing a solution to the equations of motion:

$$Q = f(A^{2.0}, S_o^{0.5}, 1/n)$$

Since the discharge is function of the square root of the slope, the rate of change in the discharge is not overly sensitive to change in slope. Similarly, the discharge is only inversely proportional to the roughness coefficient. The discharge, however, is very sensitive to small changes in the flow area to the second power. An  $n$ -value is selected to balance the relationship between the discharge, slope and flow area for steady, uniform flow, but since overland is neither steady nor uniform the variation in the roughness coefficient should be dynamic during a flood. The hydraulic radius exponent can also vary but is held constant in the FLO-2D model and the  $n$ -value coefficient is further adjusted to compensate for the constant exponent. The  $n$ -value adjustments eliminate the need for a Boussinesq coefficient for the convective acceleration term and a velocity distribution coefficient for the local acceleration term.

The FLO-2D computation routing algorithm is an explicit scheme that is subject to the Courant-Friedrich-Lowy (CFL or Courant number) condition for numerical stability. The Courant number relates the floodwave movement to the model discretization in time and space. The concept of the Courant number is that a particle of fluid should not travel more than one spatial increment  $\Delta x$  (between the center of cells) in one timestep  $\Delta t$ . If the model computational timestep exceeds the Courant relationship timestep, the stability criteria is exceeded and a model computational timestep decrement occurs. Mathematically the Courant relationship is given by:

$$V + c = C \Delta x / \Delta t$$

Where  $C$  = Courant Number ( $C \leq 1.0$ );  $\Delta x$  = FLO-2D square grid element width (distance between node centers);  $V$  = depth averaged velocity; and  $c$  = floodwave celerity =  $(gd)^{0.5}$  where  $g$  is gravitation acceleration and  $d$  is the flow depth above the thalweg.

This equation relates the progression of the floodwave ( $V + c$ ) to the discretized model in space and time. The Courant number  $C$  can vary from 0.1 to 1.0, and a value of 1.0 will enable the model to have the largest possible timestep. When  $C$  is set to 1.0, artificial or numerical diffusivity is theoretically zero

for a linear convective equation. Testing has shown that the FLO-2D model can run faster (more consistent higher timesteps) with greater stability if the Courant number is set to values less than 1.0. The FLO-2D default Courant number is 0.6 which will provide a numerically stable model for most applications. Rearranging the CFL relationship, the model computes the Courant timestep  $\Delta t$  as:

$$\Delta t = C \Delta x / (V + c)$$

Numerical instability occurs when the computational timestep is too large or the rate of change in the timestep is too large and too much volume enters or leaves a grid element (discharge flux). The corresponding change in flow depth can result in a high velocity (or Froude number) with the discharge causing a rapid fluctuation in the grid element water surface elevation (surging). Numerical surging may cause spikes in the discharge hydrograph, adverse water surface slope in the downstream direction or unreasonable maximum velocities or Froude numbers [ $F_r = V/(gh)^{1/2}$ ]. Substituting the Froude number  $F_r$  for the velocity, the relationship between the Courant number and the Froude number is:

$$C = c (F_r + 1) / \Delta x / \Delta t$$

It is demonstrated with these equations that there is a unique relationship between discharge, n-value, Froude number and numerical stability (Courant number) with varying flow depths. Selecting one steady, uniform flow n-value for a full range of flood flow conditions on a cell is not realistic and can lead to numerical instability and unreasonable Froude numbers.

### Manning's n-value Variation with Flow Depth

Typically, Manning's n-values are assigned based on bed friction, form drag or vegetation and one value is assigned for all flow conditions. For FLO-2D simulations, it is recommended that the n-value be assigned to represent channel bankfull conditions or for overland flow a depth of roughly 1 m (3 ft) deep. Roughness is known to increase with decreasing flow depth and can vary with accelerating and decelerating flows (any departure from a steady and uniform flow condition).

Manning's equation can be assumed to apply above the turbulent boundary layer. By definition the turbulent boundary terminates at depth where the vertical velocity distribution for uniform steady flow in a rough wide channel has attained a value of 99% of the free stream flow. At the lower depth, this flow regime extends from the height of the displacement thickness near the laminar boundary layer and varies as a function of the Reynolds number. The displacement thickness is generally 1/8 (rough) to 1/10 (smooth) of the turbulent boundary layer. If the flow is very shallow, roughness elements may protrude through the laminar sublayer and into the flow. Flows are considered hydraulically rough if the grain size or roughness element is greater than 6 times the laminar boundary layer:

$$\delta = 11.6 v/u^*$$

where  $v$  = kinematic viscosity and  $u^*$  = shear velocity

The applicability of Manning's equation to a given flow condition depends on the relative submergence of the roughness elements ( $R/k_s$ ) where  $k_s$  is the effective roughness height. In general, Manning's equation is appropriate for a relative submergence (Julien, 1995):

$$R/k_s > 100$$

which will correspond to the Manning-Stickler fixed bed roughness as function of sediment size D relationship (Simons and Senturk, 1976):

$$n = D^{1/6}/21.1$$

For lower a submergence value ( $R/k_s < 100$ ), the logarithmic form of the resistance equation should be used (Julien, 1995). For flow transporting sediment in suspension, the flow will be primarily turbulent if

$$R/k_s > 70$$

Typical roughness height for grain size bed material can range from 0.0015 ft for rough concrete to 0.01 ft for coarse sand or uniform earth channels. In this case Manning's equation for a coarse sand plane bed would be applicable to about 0.7 ft. Julien (1995) plotted the logarithmic velocity equation solution for turbulent flow over rough plane boundaries and it is noted that Manning's equation can still provide a reasonable approximation as low as about  $R/k_s \sim 25$ . Taking this as a less conservative approach for a rough surface where the roughness height is sand size or smaller, Manning's equation should apply if the flow depth is roughly 25 times the relative roughness. For coarse sand this would be a flow depth of about 0.25 ft.

Manning's equation will overpredict the velocity for shallow flow if typical low n-values assigned to deeper flows are applied. Manning's equation was an empirical equation that relates the velocity to several parameters using a coefficient (n-value) for flow depths generally greater than 0.5 ft. When computing velocity for shallow flow depths near the FLO-2D tolerance value TOL on the order of 0.1 ft or smaller, it is unlikely that the flow will be fully developed turbulent flow. In lieu of using multiple mean velocity equations, one for deeper flow and one for shallow flow, it is necessary to compensate for overpredicting the velocity using Manning's equation by assigning higher shallow n-values or using FLO-2D depth variable n-values or both. Overpredicting the velocity may result in unreasonable Froude numbers or exceeding the Courant condition for model numerical stability.

### FLO-2D n-values Adjustments

The FLO-2D model has the ability to adjust n-values during a simulation to maintain a reasonable maximum Froude and improve numerical stability. There are four n-value adjustment tools:

1. Global and spatially variable shallow n-value;
2. Depth integrated n-value;
3. Courant number n-value adjustments;
4. Limiting Froude number n-value adjustments.

**SHALLOW n-values:** If shallow flow has low n-values that result in unreasonably high velocities, the existing water volume stored on the grid element can be evacuated in one timestep. This results in a wetting and drying response and the possible cascading numerical instability that plagues many 2-D flood routing models. To avoid very shallow flow instability issues, set a reasonable TOL value and set

the global shallow n-value (SHALLOWN) to 0.1 or 0.2. This will ensure enough volume is left on the grid element and the velocities will be realistically slow enough to avoid evacuating the grid element. The SHALLOWN default value of 0.2 is recommended and the model has rules set up to allow the SHALLOWN value to interact with the depth averaged flow n-values. Individual grid element SHALLOWN(i) values can be assigned in SHALLOWN\_SPATIAL.DAT to create spatial variability to delineate between street flow and flow in fields.

**Depth Integrated n-values:** To improve the timing of the floodwave progression through the grid system, a depth variable roughness can be assigned. The equation for the grid element roughness  $n_d$  as function of flow depth is:

$$n_d = n_b * 1.5 * e^{-(0.4 \text{ depth/dmax})}$$

$n_b$  = bankfull discharge roughness

depth = computed model flow depth

dmax = flow depth for drowning the roughness elements and vegetation (hardwired 3 ft or 1 m)

This equation prescribes that the variable depth floodplain roughness is equal to the assigned flow roughness for the complete submergence of all roughness (assumed to be 3 ft or 1 m) and it is applied by the model as a default condition. The user can turn ‘off’ the depth roughness adjustment coefficient for all grid elements by assigning AMANN = -99 in CONT.DAT. For channel flow, the depth integrated roughness computation is turn ‘on’ by assigning a ROUGHADJ value in the first line of data of each channel segment in CHAN.DAT

This depth integrated roughness adjustment will slow the downstream progression of the floodwave. It is applied valid for flow depths ranging from 0.5 ft (0.15 m) to 3 ft (1 m). For example, at 1 ft (0.3 m), the computed roughness will be approximately 1.3 times the assigned roughness for a flow depth of 3 ft. Using the depth integrated roughness may reduce unexpected high Froude numbers. As the flow depth increases from a dry bed condition, the following rules apply:

0.0 < SHALLOWN < 0.1	SHALLOWN = 0.1
0.0 < flow depth < 0.2 ft (0.06 m)	$n = \text{SHALLOWN value}$
0.2 ft (0.06 m) < flow depth < 0.5 ft (0.15 m)	$n = \text{SHALLOWN}/2.$
0.5 ft (0.15 m) < flow depth < 3 ft (1 m)	$n = n_b * 1.5 * e^{-(0.4 \text{ depth/dmax})}$
3 ft (1 m) < flow depth	$n = \text{assigned value in MANNINGS\_N.DAT}$

**Courant Number n-value Adjustments:** When the Courant number timestep is exceeded for a given cell, the model makes an n-value adjustment for the next computation routing loop through grid system. This is an artificial intelligence approach to enable the model to avoid numerical instability at sensitive grid elements as the floodwave progression continues downstream. The Courant number n-value adjustments are based on the number of times (N) that a specific grid element has consecutive timestep decrements as follows:

$3 < N \leq 5$	n-value increased by 0.005
$6 < N \leq 10$	n-value increased by 0.002
$11 < N$	n-value increased by 0.001
If n-value > 0.2	n-value = 0.2

The n-value adjustments based on exceeding the Courant number timestep are turned ‘off’ or not applied during a model simulation if AMANN = -99 in CONT.DAT. The maximum n-values are reported in ROUGH.OUT if a given n-value is greater than the originally assigned n-value.

**Limiting Froude Number n-value Adjustments:** The Froude number provides a non-dimensional relationship between the velocity and depth that defines the transition between subcritical and supercritical flow. It is the ratio of flow velocity to the floodwave celerity and also relates the flow kinematic forces to the gravitational forces. There is an upper limit to the Froude number for both channel and overland flow for various conditions that should not be exceeded. Typical upper limits for Froude numbers include:

Major rivers:	0.3 – 0.6	(not a steep watershed river)
Floodplain:	0.5 – 0.8	(grasslands, fields, not a urban environment)
Alluvial fans:	0.9 – 1.1	(steep slope, sediment transport mobile bed)
Street flow:	1.1 – 1.5	(uniform slope and pavement conditions)

There are exceptions to this general range of limiting Froude numbers, but the user has the option of assigning a global overland limiting Froude number (FROUDL in CONT.DAT), a channel limiting Froude number by reach, or a spatially variable floodplain limiting Froude number (FPFROUDE.DAT).

For mobile bed conditions on alluvial fans, as the slope increases, competent flow for sediment transport asymptotically approaches critical flow. As the flow accelerates to critical depth, more sediment is entrained and the hydraulic oscillate with rapid energy dissipation and severe bed erosion. The flow is forced to stay around critical flow conditions by incipient motion thresholds which define the limiting Froude (Grant, 1997):

$$F_r = 3.85 S_o^{0.33} \quad \text{gravel bed } (\tau_{cr}^* = 0.03)$$

$$F_r = 5.18 S_o^{0.11} \quad \text{sand bed } (\tau_{cr}^* = 0.06)$$

where:  $\tau_{cr}^*$  is the critical shear stress for incipient motion for different size bed material.

While most flood routing models report the flow Froude number, none of them use the Froude number to adjust the model parameters. In some cases, the reported Froude number may indicate supercritical flow for a clearly subcritical flow regime. In FLO-2D model, the user assigns a limiting maximum Froude number that should not be reached for the local condition and the model automatically adjusts the n-value to sustain a reasonable Froude number on a grid element basis. When the limiting Froude number for a given grid element is exceeded, the n-value is increased according to the following criteria:

Percent increase over the original n-value	incremental increase in n-value (additive)
--	--

0.2 > % increase	0.0005
0.2 < % increase < 0.5	0.0002
0.5 < % increase < 1.0	0.0001
1.0 < % increase < 2.0	0.00005

When the limiting Froude number is no longer exceeded the n-value is reduced by -0.0002 until the initially assigned n-value is reached. The maximum n-values (if different from the originally assigned n-value) are reported to the ROUGH.OUT file.

### Applying the n-value Adjustments

To use the limiting Froude number to control numerical instability, the data files have to be adjusted to accommodate n-value changes and essentially empty the ROUGH.OUT file. First select reasonable n-values that account for all the flow resistance including vegetation, bed forms, bed friction, contraction and expansion, flow in bends, adverse slope, etc. Then apply the depth variable n-value adjustment (AMANN = 0 in CONT.DAT). Finally assign limiting Froude number to calibrate the n-values. After a simulation is complete, review ROUGH.OUT to determine if any of the maximum n-value appear to be too large. Revise the unreasonable n-values in MANNINGS\_N.RGH and then delete FPLAIN.DAT and MANNINGS\_N.DAT and rename MANNINGS\_N.RGH to MANNINGS\_N.DAT for the next simulation.

If the global limiting Froude number is zero (FROUDL = 0.0), then the limiting Froude number n-value adjustment is not used by the FLO-2D model. In versions 2017 and earlier, instead of the global limiting Froude number equal to zero, assigning AMANN = -99 in CONT.DAT turned ‘off’ the n-value adjustment for the limiting Froude number.

The limits of the FLO-2D model can be tested by turning off the depth integrated floodplain n-values (AMANN = -99), by setting shallow n-value to zero (SHALLOWN = 0, and by having no global limiting Froude number assignment (FROUDL = 0). This combination of data parameters means that the n-value assigned for the depth of 3 ft is also being applied for the very shallow flows.

To summarize, assigning conventional steady, uniform flow Manning’s n-values are not equivalent to unsteady, non-uniform grid element n-values in a discretized flood routing model. Spatially variable and depth variable n-values are key to achieving FLO-2D numerical stability which is inherently linked to the Courant number and reasonable local Froude numbers.

## Flood Component Impact

FLO-2D can simulate essentially the entire hydrologic and hydraulic flood movement system through many detail components including rainfall, infiltration, channel and street flow, flow around buildings, levee failure, flow through hydraulic structures, storm drains, and numerous other components. This level of detail requires a large number of variables. The components having the greatest effect on the area of inundation are as follows:

**Flood Inflow Volume:** Rainfall and inflow hydrograph and losses directly affect the area of inundation.

**Topography:** The overland flow path is primarily a function of the cell topography.

**Roughness:** The floodplain roughness n-values control the overland floodwave speed. River channel n-values can force more water overbank.

**Flow Area:** The relationship between the channel cross section flow area, bed slope and roughness control the floodwave routing, attenuation and numerical stability. Flow area has the most important effect on channel routing stability. Changes in the cross section flow area between channel elements should be limited to 25% or less. More cross section surveys may be necessary to simulate rapidly changing flow geometry. Constructed rapid transitions in channel geometry (such as concrete lined channels) can be modeled but will require smaller timesteps and more channel detail.

**Floodplain Storage Loss:** Buildings and other loss of storage represented by the Area Reduction Factors (ARF) can significantly impact the local flood distribution.

**Flow Path Obstruction:** Levees, buildings, walls, berms and embankments (railroad or highway) can contain flooding or completely obstruct the flow progression over the floodplain. Levees and walls can also overtop or fail in the model and send floodwaves over floodplain dry areas. Hydraulic structures can also control water surface elevations and limit downstream discharge.

**Flood Redistribution:** Channels, streets and storm drains can redistribute the flood from one area of the model to another. Storm drains will also significant impact more frequent flood events by removing surface water volume and debouching it off the project area.

**Sediment Loading:** Most watershed and alluvial fan flooding should be bulked for sediment loading. Typically, sediment volume will have a greater impact on the area of inundation than local scour or deposition. If the sediment loading will be relatively minor, the XCONC factor in the CONT.DAT file can be used to uniformly bulk all the inflow hydrograph volumes. Typically, watershed flooding that will not generate mudflows can be conservatively bulked using an XCONC value of 10% to 15% by volume. River flood sediment concentration will rarely exceed 5% by volume and setting XCONC = 5% will conservatively bulk the inflow hydrograph volume by 1.05. Mudflow should be simulated by assigning concentrations by volume to the inflow hydrographs and the XCONC factor should not be used.

### **3.3 Inflow and Outflow Control**

A discretized flood hydrograph from an upstream basin can be inflow either to the floodplain, channel or both. More than one grid element can have an inflow hydrograph. Hydrographs can be assigned as either direct inflow or outflow (diversions) from a channel. This could be a simple constant diversion of 100 cfs or a variable hydrograph over the course of the simulation. If mudflows are being simulated a volumetric sediment concentration or sediment volume must be assigned to each water discharge increment.

For flow out of the grid system, outflow grid elements must be specified for either the floodplain or channel or both. The discharge from outflow elements is equal to sum of the inflows to the outflow cell and a flow depth is then assigned to the outflow element based on a weighted average of the upstream flow depths. In this manner, normal flow is approximated at the outflow element. The outflow discharge is totally removed from the system and is accounted to the outflow volume. It is possible to specify outflow from elements that are not on the boundary of the grid system, but outflow elements should be treated as sinks (all the inflow to them is lost from the flow system). Outflow elements should not be modified with ARF's or WRF's, levees, streets, etc. Channel outflow can also be established by a stage-discharge. This option can be used when channel outflow occurs at a hydraulic structure or when a known discharge relationship is available.

Stage-time relationships can be specified for either the floodplain or channel. These relationships can be assigned for outflow elements or for any elements in the system. When a stage-time relationship is specified, volume conservation is accounted for when the discharge enters or leaves the stage-time designed grid element. Stage-time relationships provide opportunity to simulate coastal flooding related to ocean storm surge, hurricane surges or tsunamis (Figure 11). In addition, the backwater effects of tidal variation on river and estuary flooding can be model.



*Figure 11. Tsunami Wave Progression Overland in an Urban Area (Waikiki Beach, Hawaii).*

### **3.4 Floodplain Cross Sections**

A floodplain cross section analysis can be conducted by specifying grid elements in a cross section in the FPXSEC.DAT file. The grid elements must be contiguous and in a straight line to constitute a cross section on a floodplain or alluvial fan. By designating one or more cross sections, the user can track floodwave attenuation across unconfined surfaces. Both the flood hydrograph and flow hydraulics can be analyzed at cross sections. The average cross section hydraulics as well as the individual grid element hydraulics in the cross section are summarized in cross section output files.

### **3.5 Grid Developer System (GDS)**

The GDS creates and edits the FLO-2D grid system attributes and corresponding data files and provides a platform for running the other pre- and post-processor programs. The GDS is a pre-processor program that will overlay the grid system on the DTM points, interpolate and assign elevations to the grid elements. The GDS will then automatically prepare the basic input files for the FLO-2D model. Geo-referenced aerial photos, shape file images or maps can be imported as background images to support the graphical editing.

In addition to developing the FLO-2D grid system, the GDS also provides important editorial features including the assignment of spatially variable grid element attributes such channels, levees, streets, infiltration, area and width reduction factors, floodplain elevation and roughness, inflow and outflow nodes and rill and gully geometry. It enables the selection of individual elements or large groups of node using the mouse. Rainfall can also be spatially varied. Detailed instructions are presented in the GDS Manual.

### **3.6 QGIS Plug-in**

QGIS is an open source geographical information system that is free to all users. Images and other data can be downloaded from the web or imported from a database. All GIS data formats can be imported into QGIS including rasters, shapefiles, delimited text, SpatiaLite and NETCDF. FLO-2D plugin for QGIS was developed to build and edit FLO-2D data input files and display results. The plug-in is a fully functional digital processing environment that replaces the GDS and MAPPER Pro processor programs and is installed directly onto the QGIS GUI display as shown in Figure 12. It consists of a set of layers that represent the FLO-2D spatial and time variable data. The data is stored in a geopackage in SQLite format.

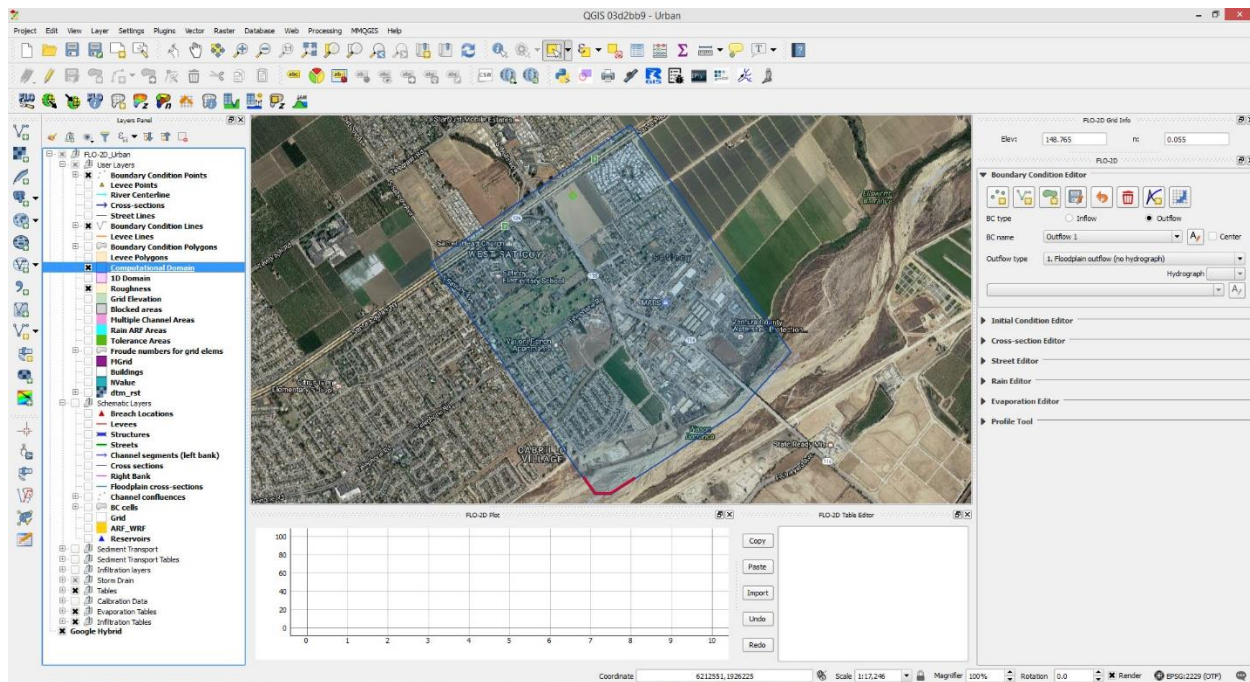


Figure 12. FLO-2D QGIS Plugin Tool Working Environment.

The plug-in package includes a toolbar for building the project geographical system and will have control icons for editing the various FLO-2D component data files. Figure 13 shows toolbar and Table 2 is a list of and description of the tools. The QGIS plug-in tool is continually expanding and will eventually have all the detail editor functions found in the GDS.



Figure 13. Toolbar FLO-2D Plugin.

Table 2. QGIS Plugin Tools.

Tool	Description
	FLO-2D Plugin Settings – Set up the geopackage and project coordinate system. Set grid element size and default Manning's n.
	Import FLO-2D Pro model *.DAT files. Uses CONT.DAT as the pointer file to set the path.
	Exports data files into the FLO-2D *.DAT file format.
	Info tool views information related to a FLO-2D element. This dedicated tool is used to view hydrograph time series and plots, cross section table and plots, etc. The Info Tool works on both User and Schematized Layers.

	Create Grid – this tool builds a grid system from the polygon in the Computational Domain layer and the grid element size set in Settings tool.
	Sampling Grid Elevation – This tool samples an elevation raster to set the grid element elevation.
	Sampling Manning's n – This tool will sample a polygon layer for roughness values and assign that value to the Schematic Layers.
	Evaluate reduction factors (ARF and WRF) – This tool will compute the area and width reduction factors from building polygons.
	Grid info tool – This tool queries spatially variable data assigned to individual grid elements.
	Channel Cross Section Editor – Select and activate a cross section for editing.
	Evaporation Editor – Tool to edit the evaporation table data.
	Assign elevation from polygons – This tool will allow the user to edit the elevation layer with polygons.
	Levee Elevation Tool – This tool eliminate levee and raised topography from the elevation data.
	HAZUS Tool – This tool uses depth and velocity layers to define a hazard for buildings in the flooded area.
	Tailings Dam Tool – This button opens the tailings dam tool.
	Debug Tool – This button imports the debug.out file and opens the component conflict checker.
	Help – This button opens the help manuals in pdf format.

The editable data is accessed via User Layers. The user will import, digitize or compute spatial data through these layers. The User Layers are processed into the schematic system and the data is exported into FLO-2D \*.DAT files that can be utilized by the FLO-2D engine. Figure 14 shows the layout of the User Layers and Schematic Layers. For existing project files, the FLO-2D data files are imported into the Schematic Layers which are regenerated each time the user activates a data processing tool. The Schematic Layers store the data in arrays and process it on the fly so that the user can change any data component without effecting the cell positioning or assignment. This enables the computational domain to be modified at any time and the FLO-2D components like levees, channels and all other data can be then updated automatically.

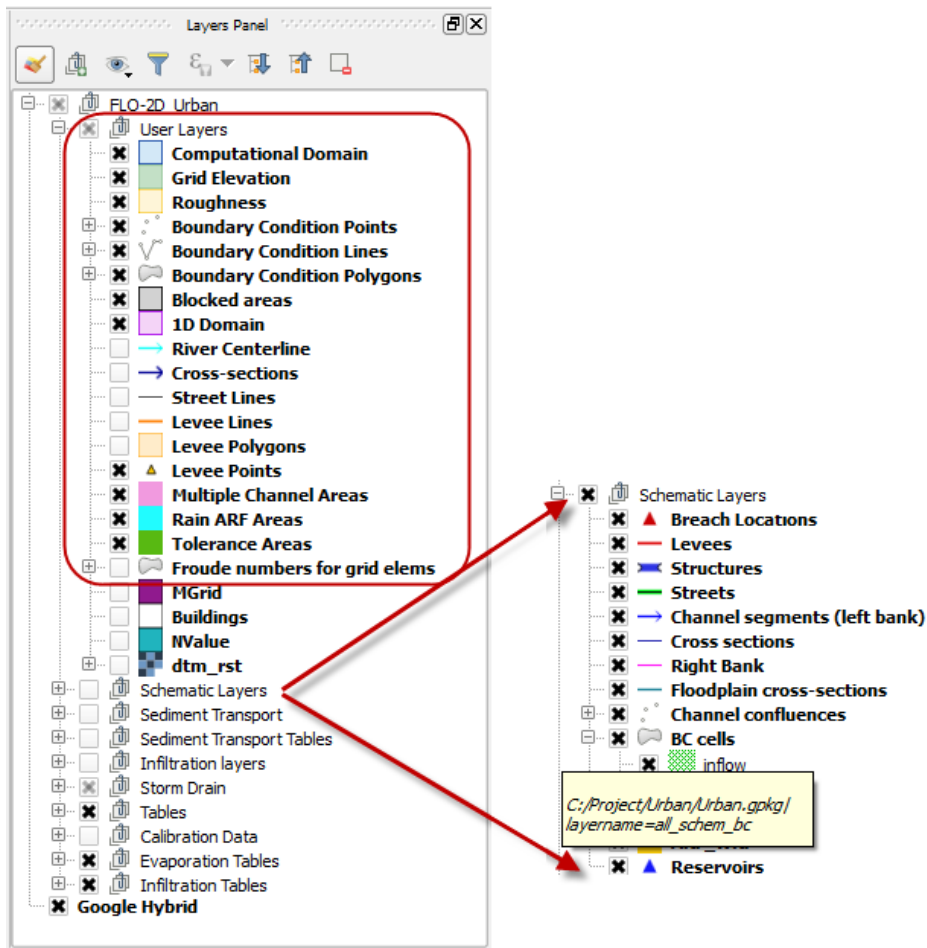


Figure 14. User and Schematic Layer Structure.

A table editor plotting graph is docked to the bottom of the project environment (Figure 15). The data can be editing or replaced as required. These editors have redo functionality and copy paste and import from comma separated values or MS Excel.

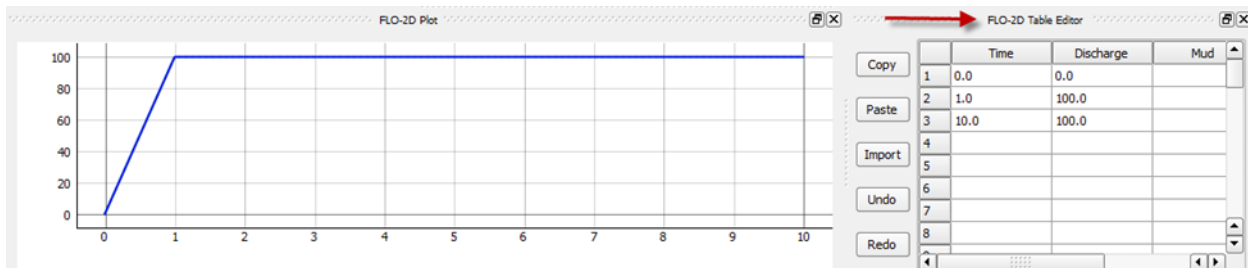
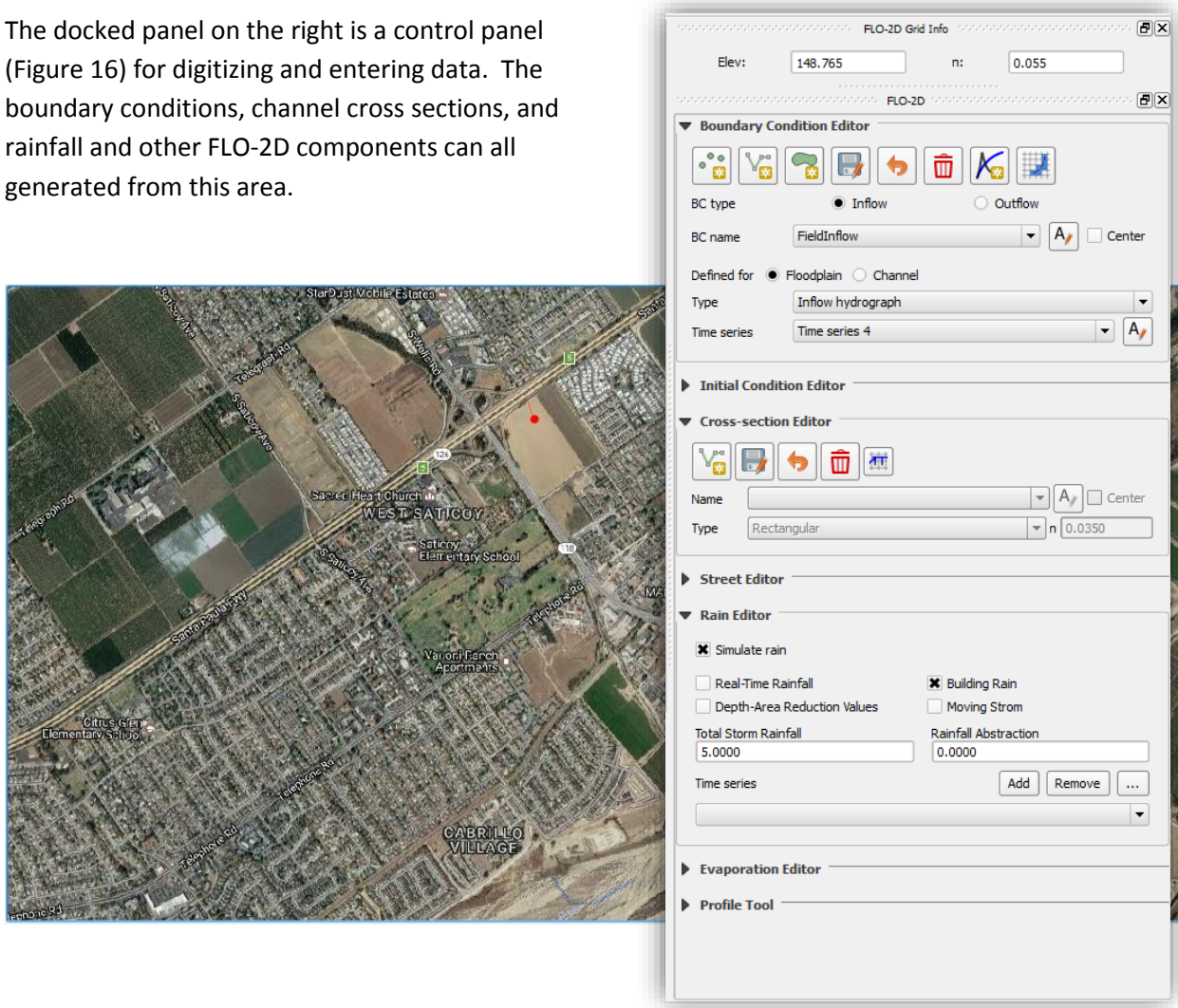


Figure 15. FLO-2D Table Editor.

The docked panel on the right is a control panel (Figure 16) for digitizing and entering data. The boundary conditions, channel cross sections, and rainfall and other FLO-2D components can all generated from this area.



*Figure 16. Control Panel for Various FLO-2D Components.*

### 3.7 Graphical Output Options

A graphical display of the flow depths can be viewed on the screen during a FLO-2D simulation to visualize the progression of the floodwave over the potential flow surface. In addition to the predicted flow depths, an inflow hydrograph will be plotted. For rainfall simulation, the cumulative precipitation can also be plotted. The grid element results for floodplain, channel and street flow can be reviewed in a post-processor program MAXPLOT or flood contours can be generated in MAPPER Pro. Flood mapping can also be generated with the QGIS plug-in tool (Figure 17) and shape files for export can be generated.

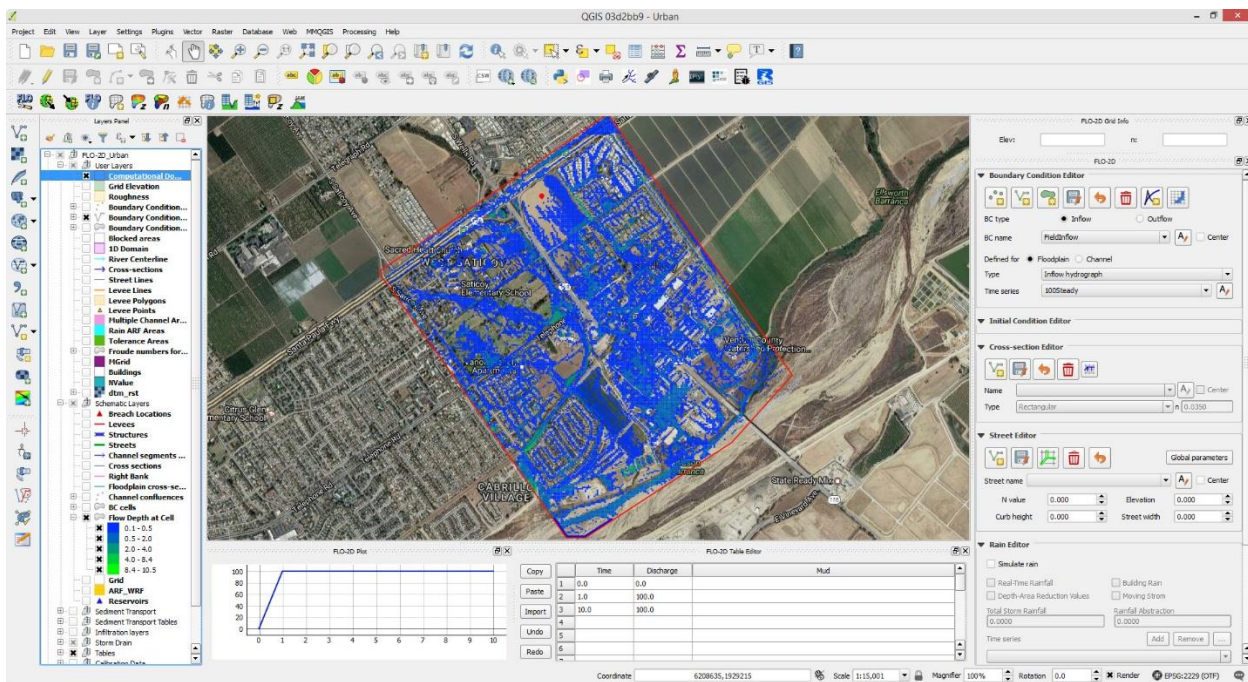


*Figure 17. QGIS Plug-in Tool for FLO-2D Model Development and Displaying Results.*

Graphical displays are provided in the HYDROG, PROFILES, MAXPLOT and MAPPER Pro post-processor programs. HYDROG will plot the hydrograph for every channel element. HYDROG can also be used to evaluate the average channel hydraulics in a given reach. The user can select the upstream and downstream channel elements and the program will compute the average of the hydraulics for all the channel elements in the reach including: velocity, depth, discharge, flow area, hydraulic radius, wetted perimeter, top width, width to depth ratio, energy slope, and bed shear stress. The PROFILES program plots channel water surface and bed slopes. MAXPLOT is a simple, easy to use plotting program on a grid element basis that enables a quick graphical review of the results on a grid element basis. Figure 18 displays a potential list of the plots. A typical maximum depth plot is shown in Figure 19. Even sediment transport results can be plotted as shown in Figure 20. A discussion using MAXPLOT is presented in the Data Input Manual.

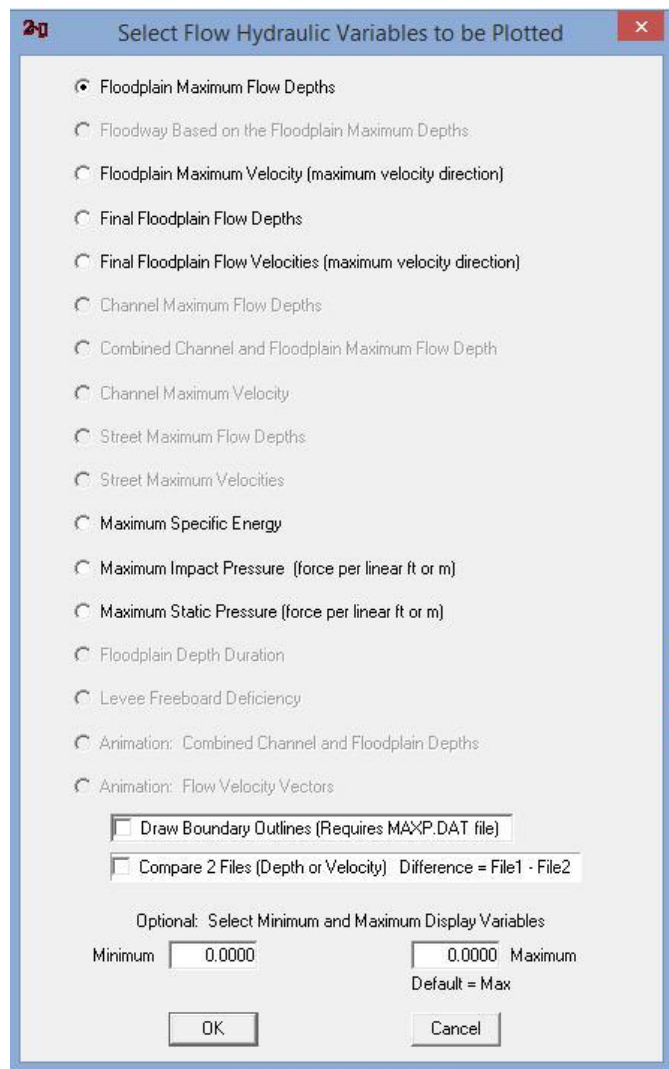


Figure 18. MAXPLOT Mapping Controls.

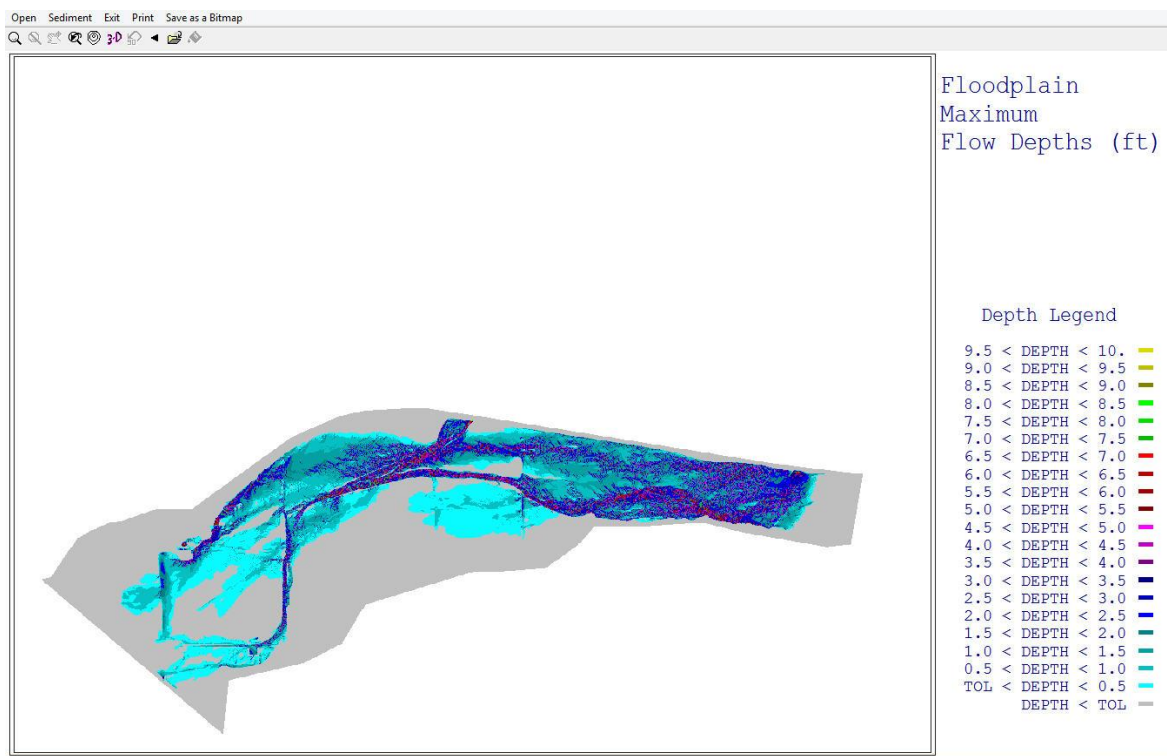


Figure 19. MAXPLOT Floodplain Maximum Flow Depths (Based on Grid Element).

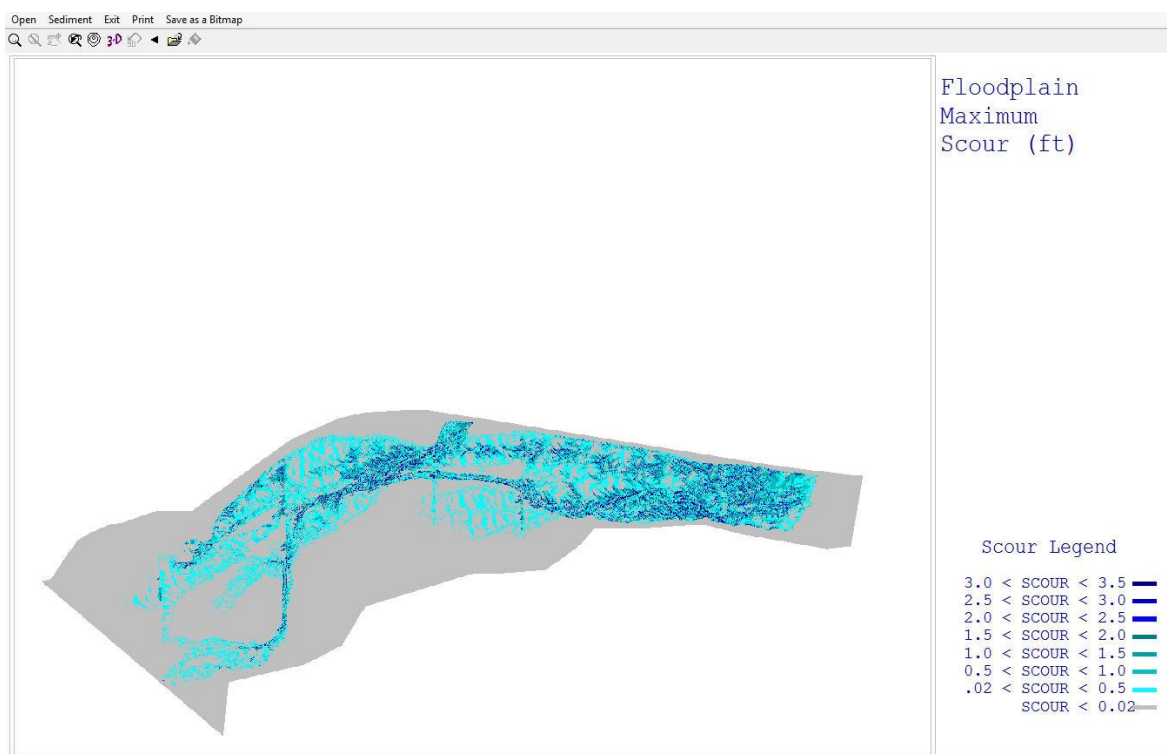


Figure 20. MAXPLOT Maximum Scour Depths (Based on Grid Element).

MAPPER Pro creates high resolution color contour plots. Several map combinations can be created: grid element or DTM point plots, line contour maps and shaded contour maps. Maps can be created for ground surface elevations, maximum water surface elevations, maximum floodplain flow depths, maximum velocities, maximum static and dynamic pressure, specific energy, and floodway delineation. One of the most important features of MAPPER Pro is its capability to create flood depth plots using the DTM topographic points. When the user activates the feature, MAPPER Pro will subtract each DTM ground point elevation from the grid element floodplain water surface elevation. The resultant DTM point flow depths can then be interpolated and plotted as color contours (Figure 21). Some of the MAPPER Pro features include:

- Multiple geo-referenced aerial photos in various graphic formats can be imported such as TIFF, BMP, JPG, etc.
- Multiple layer capability including control of layer properties is available.
- Cut and view flow depth and topography profiles.
- Flood animation. The floodwave progression over the grid system can be viewed.
- Sediment transport maximum deposition and scour can be plotted.
- Maximum flow velocity vectors can be viewed.
- Hazard maps based on flood intensity and frequency can be created.
- GIS shape files (\*.shp) are automatically created with any plotted results. This GIS shape files can be then be imported into ArcView or other GIS programs.

The MAPPER Pro features and functions are described in its own manual.



*Figure 21. MAPPER PRO Plot of Maximum Depths.*

### **3.8     *Data Output Options***

The FLO-2D model has several output files to help the user organize the results. Floodplain, channel and street hydraulic results are written to file. Hydraulic data include water surface elevation, flow depth and velocities in the eight flow directions. Discharge for specified output intervals (hydrographs) are written to various files. A mass conservation summary table comparing the inflow, outflow and storage in the system is presented in the SUMMARY.OUT file. A complete description of all the output files is presented in the Data Input Manual.



## Chapter 4. MODEL COMPONENTS

### 4.1 *Model Features*

The primary FLO-2D flood routing features and attributes are:

- Floodwave attenuation can be analyzed with hydrograph routing.
- Overland flow on unconfined surfaces is modeled in eight directions.
- Floodplain flows can be simulated over complex topography and roughness including split flow, shallow flow and flow in multiple channels.
- Channel, street and overland flow and the flow exchange between them can be simulated.
- Channel flow is routed with either a rectangular, trapezoidal or natural cross section data.
- Streets are modeled as shallow rectangular channels.
- The flow regime can vary between subcritical and supercritical.
- Flow over adverse slopes and backwater effects can be simulated.
- Rainfall, infiltration losses and runoff on the alluvial fan or floodplain can be modeled.
- Bed scour and deposition can be modeled using one of eleven sediment transport equations.
- Viscous mudflows can be simulated.
- The effects of flow obstructions such as buildings, walls and levees that limit storage or modify flow paths can be modeled.
- The outflow from bridges and culverts is estimated by user defined rating curves.
- The number of floodplain and channel elements is unlimited.
- The exchange of surface water and storm drain flows can be simulated.
- The exchange of surface water and groundwater can be simulated using a runtime interface with the MODFLOW groundwater model.
- Dam and levee breach can be simulated with either a prescribe breach rate or breach erosion.

Data file preparation and computer run times vary according to the number and size of the grid elements, the inflow discharge flux and the duration of the inflow flood hydrograph being simulated. Most flood simulations can be accurately performed with square grid elements ranging from 20 ft (8 m) to 500 ft (130 m). Projects have been undertaken with grid elements as small as 10 ft (3 m). It is important to balance the project detail and the number of model components applied with the mapping resolution and anticipated level of accuracy in the results. It is often more valuable from a project perspective to have a model that runs quickly enabling many simulation scenarios to be performed from which the user can learn about how the flood project responds to mitigation or sensitivity. Model component selection should focus on those physical features that will significantly affect the volume distribution and area of inundation. A brief description of the FLO-2D components follows.

## 4.2 Overland Flow

The simplest FLO-2D model is overland flow on an alluvial fan or floodplain. Typical overland flow as reflects the water surface elevation, roughness and 8-direction flow path. The floodplain element attributes can be modified to add detail to the predicted area of inundation. The grid element surface storage area or flow path can be adjusted for buildings or other obstructions. Using the area reduction factors (ARFs), a grid element can be completely removed from receiving any inflow. Any of the eight flow directions can be partially or completely blocked to represent flow obstruction. The area of inundation can also be affected by levees, channel breakout flows, flow constriction at bridges and culverts, or street flow in urban areas. Rainfall and infiltration losses can add or subtract from the flow volume on the floodplain surface. These overland flow components are shown in a computational flow chart in Figure 22.

Overland flow velocities and depths vary with topography and the grid element roughness. Spatial variation in floodplain roughness can be assigned through the GDS pre-processor program. The assignment of overland flow roughness must account for vegetation, surface irregularity, non-uniform and unsteady flow. It is also a function of flow depth. Typical overland flow roughness values (Manning's n coefficients) are shown in Table 3.

**Table 3. Overland Flow Manning's n Roughness Values.<sup>1</sup>**

Surface	n-value
Dense turf	0.17 - 0.80
Bermuda and dense grass, dense vegetation	0.17 - 0.48
Shrubs and forest litter, pasture	0.30 - 0.40
Average grass cover	0.20 - 0.40
Poor grass cover on rough surface	0.20 - 0.30
Short prairie grass	0.10 - 0.20
Sparse vegetation	0.05 - 0.13
Sparse rangeland with debris	
0% cover	0.09 - 0.34
20 % cover	0.05 - 0.25
Plowed or tilled fields	
Fallow - no residue	0.008 - 0.012
Conventional tillage	0.06 - 0.22
Chisel plow	0.06 - 0.16
Fall disking	0.30 - 0.50
No till - no residue	0.04 - 0.10
No till (20 - 40% residue cover)	0.07 - 0.17
No till (60 - 100% residue cover)	0.17 - 0.47
Open ground with debris	0.10 - 0.20
Shallow glow on asphalt or concrete (0.25" to 1.0")	0.10 - 0.15
Fallow fields	0.08 - 0.12
Open ground, no debris	0.04 - 0.10
Asphalt or concrete	0.02 - 0.05

<sup>1</sup>Adapted from COE, HEC-1 Manual, 1990 and the COE, Technical Engineering and Design Guide, No. 19, 1997 with modifications.

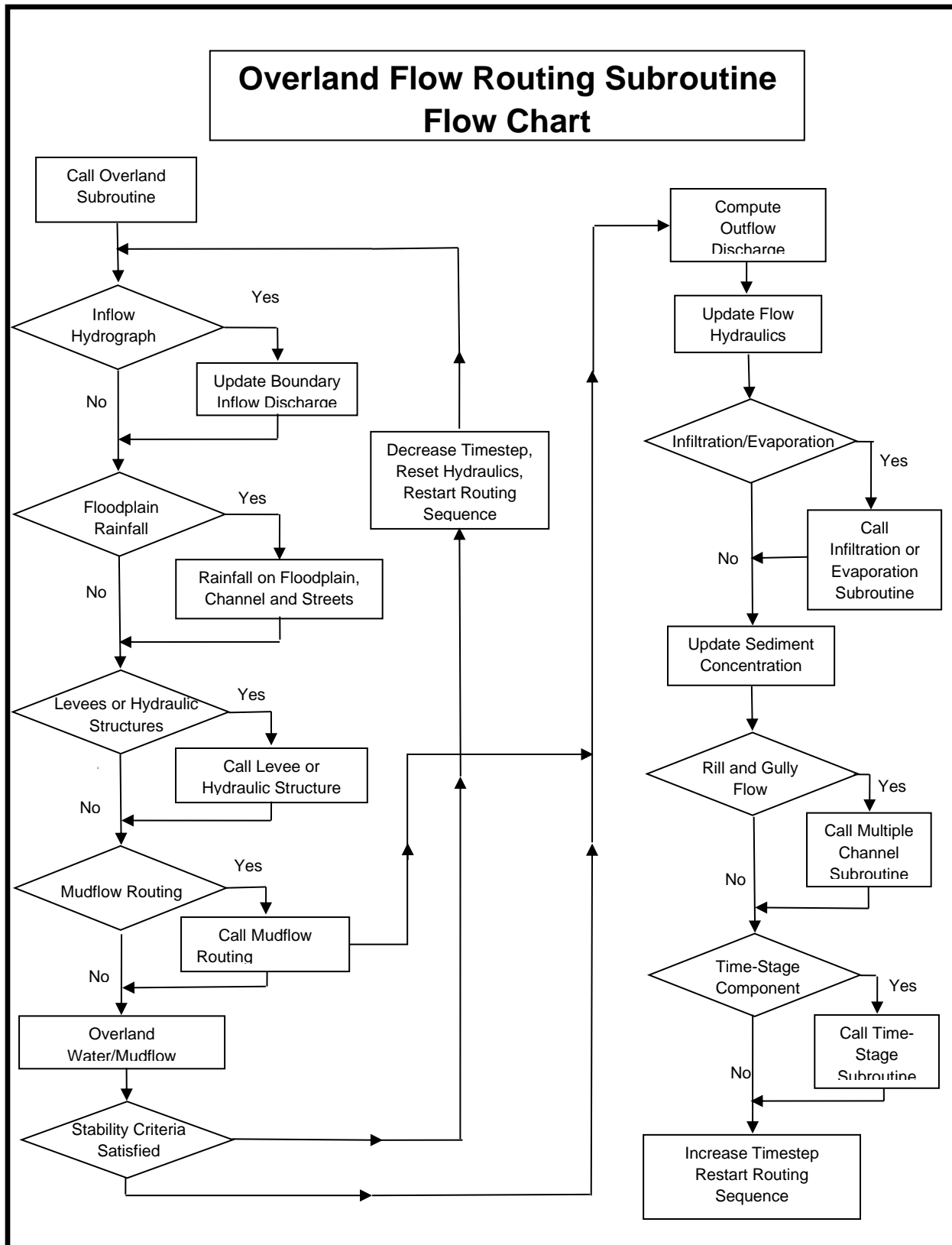


Figure 22. Overland Flow Routing Subroutine Flow Chart.

Streets serving as conveyance features are important for distributing the flow to other project areas. Streets can be modeled either as 1-D rectangular channels or as impervious grid elements with low n-values. If the two or more grid elements fit inside a street because the grid elements are 10 ft square or less, then assigning appropriate elevations and n-values to the grid elements will enable street flow. These street elements can be assigned with shape files either with QGIS plug-in tool or with the GDS (Figure 23). To make the floodplain elements represent the street:

- Assign n-values in an acceptable range for street irregularities, breaks-in-slope, unsteady and non-uniform flow (0.02 to 0.035);
- Select a spatially variable limiting Froude number in the range from 1.5 to 2.5;
- Review and adjust the street profile.

To adjust the street profile, there are two GDS tools: 1) Interpolate elevations downslope and for the street crown. It will also assign minimum curb elevations to the floodplain elevations outside the street. 2) Draw a polyline and interpolate the elevations using the profile tool. For more street editing options and details see the GDS manual or the street editing white paper.

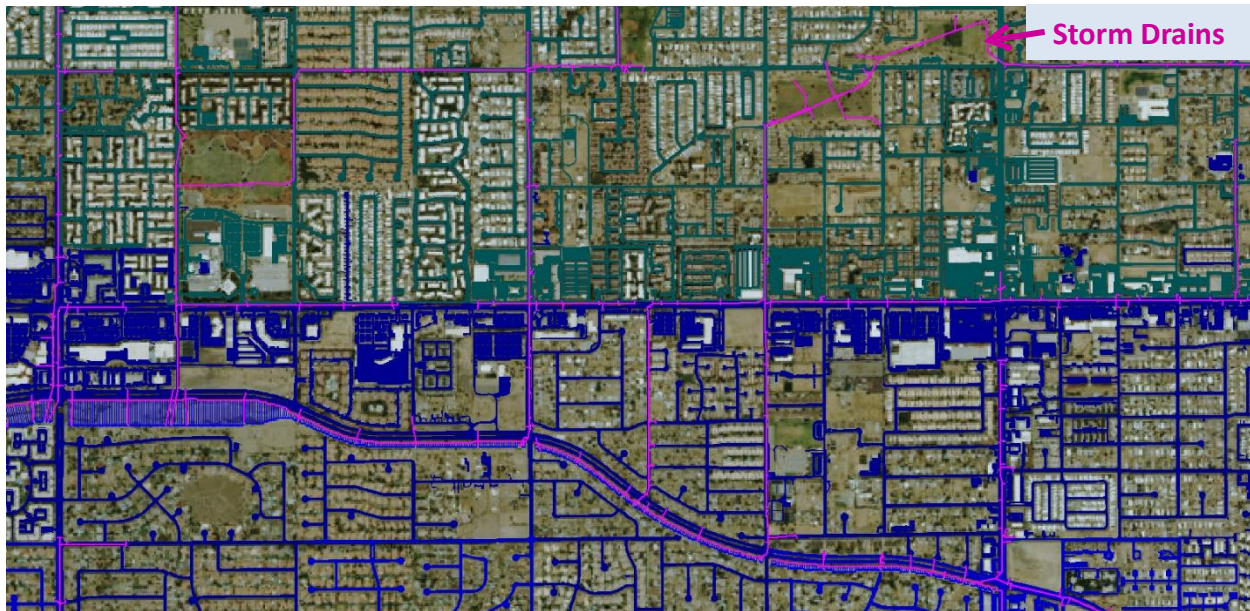


Figure 23. Editing Grid Elements to Represent Streets.

Some of the floodplain or watershed depression storage defined by the DTM point data base is lost in the upscale averaging of the discretized FLO-2D grid surface. This depression storage accuracy can be retained by generating a depth-volume storage rating table for each grid element. The GDS will automatically create the rating table if there are sufficient DTM points for a rating table (e.g. a threshold of 20 points or more are required depending on the topographic setting of the domain). An OUTRC.DAT file lists the potential storage for each cell. The algorithm divides the grid element in subcells where the storage volume is calculated as a function of the stage above the lowest DTM point (Figure 24). At

runtime the FLO-2D model will compute a flow depth based on the storage volume from the rating table. As the cell depression volume fills and eventually spills to other grid elements, the storage retention is infiltrated. The unique attributes of this routine to improve shallow flow runoff are:

- At runtime, the flow depth is based on the stage-volume rating table until the cell is filled.
- A minimum number of DTM points within each grid element are required to assign the storage rating table; otherwise the model uses the TOL value for the depression storage.
- The rating table is created only for those grid cells that do not contain a street or channel or that have an area reduction factor (ARF) less than 0.5.
- If a grid element has a rating table, the cell elevation will be equal to the lowest DTM point used in the calculation of the rating table.

For a complete discussion of this grid element rating table stage-volume tool, refer to the GDS manual.

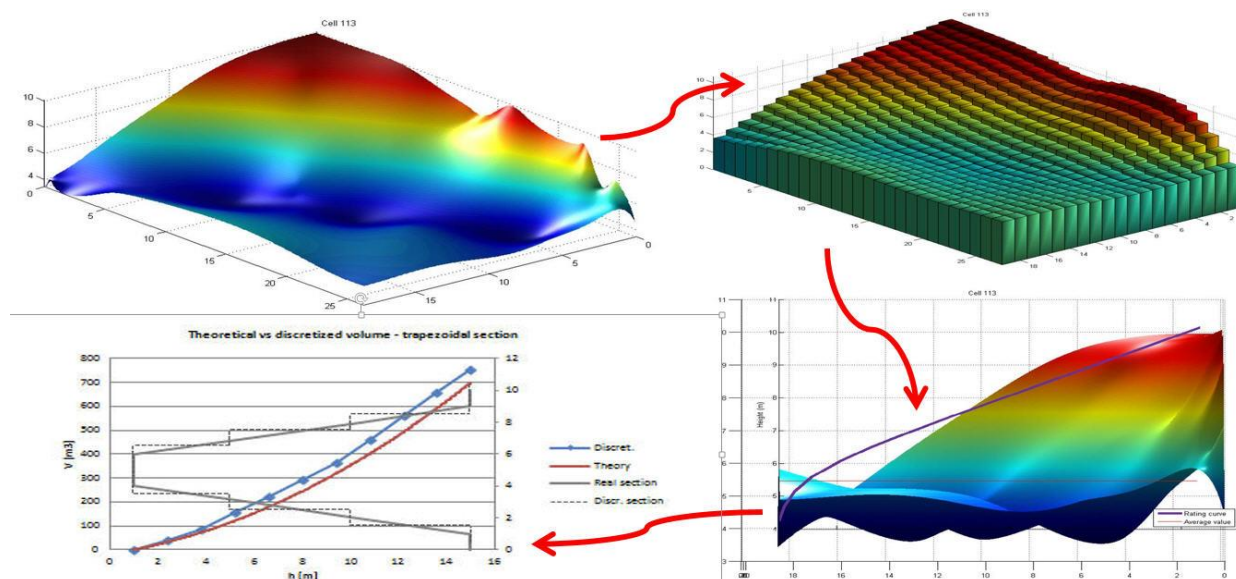


*Figure 24. Stage-Volume Rating Table for Assigning Flow Depths.*

Some FLO-2D projects have been modeled using grid elements inside of the channel. In this case, the channel component is not used and instead the FLO-2D grid system is draped over the channel portion of the topography. While these projects have been conducted with some success, there are several modeling concerns that should be addressed. The FLO-2D model was developed to be able to exchange 1-D channel overbank discharge with the floodplain grid elements. For this reason, the model works well on large flood events and large grid elements. When small grid elements are used inside of a channel with confined flow and large discharges and flow depths, the model may run slow. In addition, there will be zero water surface slope between some grid elements. It should be noted that the application of the Manning's equation for uniform open channel flow to compute the friction slope is no longer valid as the depth average velocity approaches zero (ponded flow condition). The resulting water surface elevations can be accurately predicted but will display some variation across the channel.

### 4.3 Channel Flow

Channel flow is simulated as one-dimensional in the downstream direction. Average flow hydraulics of velocity and depth define the discharge between channel grid elements. Secondary currents, dispersion and super elevation in channel bends are not modeled with the 1-D channel component. The governing equations of continuity and momentum were presented in Section 2.1.

River channel flow is simulated with either rectangular or trapezoidal or surveyed cross sections and is routed with the dynamic wave momentum equation. The channels are represented in the CHAN.DAT by a grid element, cross section geometry that defines the relationship between the thalweg elevation and the bank elevations, average cross section roughness, and the length of channel within the grid element. Channel slope is computed as the difference between the channel element thalweg elevation divided by the half the sum of the channel lengths within the channel elements. Channel elements must be contiguous to be able to share discharge. A tributary confluence is assigned by select the two channel element pairs (tributary and main channel) in the CHAN.DAT file.

The channel width can be larger than the grid element and may encompass several elements (Figure 25). If the channel width is greater than the grid element width, the model extends the channel into neighboring grid elements. A channel may be 1,000 ft (300 m) wide and the grid element only 300 ft (100 m) square. The model also makes sure that there is sufficient floodplain surface area after assigning the right bank. The channel interacts with the bank elements to share discharge to the floodplain. Each bank can have a unique elevation. If the two bank elevations are different in the CHAN.DAT file, the model automatically splits the channel into two elements even if the channel would fit into one grid element.

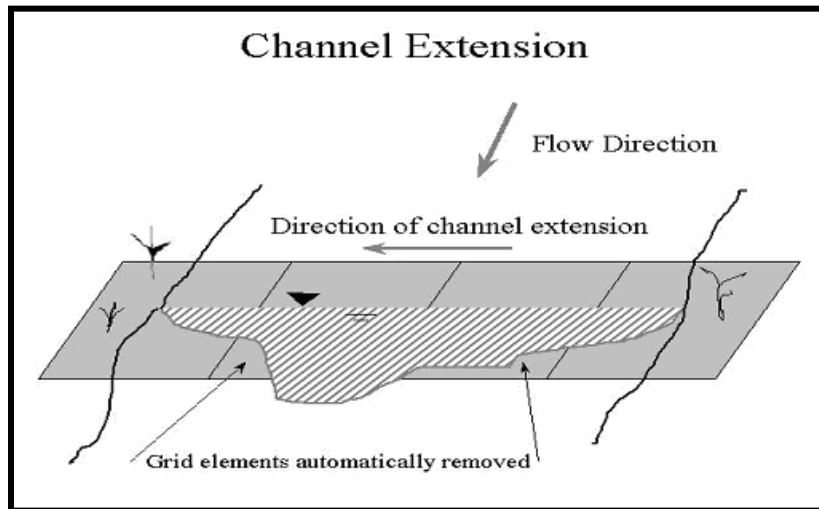


Figure 25. Channel Extension Over Several Grid Elements.

There are three options for establishing the bank elevation in relationship to the channel bed elevation (thalweg) and the floodplain elevation in the CHAN.DAT file:

1. The channel grid element bed elevation is determined by subtracting the assigned channel thalweg depth from the floodplain elevation. This is appropriate for rectangular and trapezoidal cross sections.
2. A bank elevation is assigned in the CHAN.DAT file and the channel bed elevation is computed by subtracting the channel depth from the lowest bank elevation. This is appropriate for rectangular and trapezoidal cross sections.
3. A surveyed cross section data base is assigned in XSEC.DAT and the model automatically assigns the top-of-bank elevation.

When using cross section data for the channel geometry, option 3 should be applied.

In river simulations, the important components include channel routing, the channel-floodplain interaction, hydraulic structures and levees. These components are described in more detail in the following sections. The basic procedure for creating a FLO-2D river simulation is as follows:

*Select Channel Cross Sections.* Surveyed river cross sections should be spaced to represent a uniform river reach that may encompass a number of channel elements, say 5 to 10 elements. Geo-referenced surveyed cross section station and elevation data can be entered directly into the model data files or the data can be defined by setting the highest bank to an arbitrary elevation. For channel design purposes, a rectangular or trapezoidal cross section may be selected. To use surveyed cross section data, an XSEC.DAT file has to be created with all cross section station and elevation data. The cross sections are then assigned to a channel element in the CHAN.DAT. The relationship between the flow depth and channel geometry (flow area and wetted perimeter) is based on an interpolation of depth and flow area between vertical slices that constitute a channel geometry rating table for each cross section. The cross section data in the XSEC.DAT file can be automatically assigned from HEC-RAS file using the GDS.

*Locate the Channel Element with Respect to the Grid System.* Using the GDS and an aerial photo, the channels can be assigned to a grid element. For channel flow to occur through a reach of river, the channel elements must be neighbors.

*Adjust the Channel Bed Slope and Interpolate the Cross Sections.* Each channel element is assigned a cross section in the CHAN.DAT file. Typically, there are only a few cross sections and many channel elements, so each cross section will be assigned to several channel elements. When the cross sections have all been assigned the channel profile looks like a staircase because the channel elements with the same cross section have identical bed elevations. The channel slope and cross section shape can then be interpolated by using a command in the GDS, QGIS Plug-in or in the PROFILES program that adjusts and assigns a cross section with a linear bed slope for each channel element. The cross section interpolation is based a weighted flow area adjustment to achieve a more uniform rate of change in the flow area.

The user has several other options for setting up the channel data file including grouping the channel elements into segments, specifying initial flow depths, identifying contiguous channel elements that do not share discharge, assigning limiting Froude numbers and depth variable n-value adjustments.

#### **4.4 Channel-Floodplain Interface**

Channel flow is exchanged with the floodplain grid elements in a separate routine after the channel, street and floodplain flow subroutines have been completed (see the Flow Chart in Figure 3). When the channel conveyance capacity is exceeded, an overbank discharge is computed. If the channel flow is less than bankfull discharge and there is no flow on the floodplain, then the channel-floodplain interface routine is not called. The channel-floodplain flow exchange is limited by the available exchange volume in the channel or by the available storage volume on the floodplain. The interface routine is internal to the model and there are no data requirements for its application. This subroutine also computes the flow exchange between the street and the floodplain.

The channel-floodplain exchange is computed for each channel bank element and is based on the potential water surface elevation difference between the channel and the floodplain grid element containing either channel bank (Figure 2). The velocity of either the channel overbank or the return flow to the channel is computed using the diffusive wave momentum equation. It is assumed that the overbank flow velocity is relatively small and thus the acceleration terms are negligible. For return flow to the channel, if the channel water surface is less than the bank elevation, the bank elevation is used to compute the return flow velocity. Overbank discharge or return flow to the channel is computed using the floodplain assigned roughness. The overland flow can enter a previously dry channel.

#### **4.5 Levees**

The FLO-2D levee component confines flow on the floodplain surface by blocking one of the eight flow directions. Levees are designated at the grid element boundaries (Figure 26). If a levee runs through the center of a grid element, the model levee position is represented by one or more of the eight grid element boundaries. Levees often follow the boundaries along a series of consecutive elements. A levee crest elevation can be assigned for each of the eight flow directions in a given grid element. The model will predict levee overtopping. When the flow depth exceeds the levee height, the discharge over the levee is computed using the broadcrested weir flow equation. Weir flow occurs until the tailwater depth is 85% of the headwater depth above and then at higher flows, the water is exchanged across the levees using the difference in water surface elevation. Levee overtopping will not cause levee failure unless the failure or breach option is invoked.

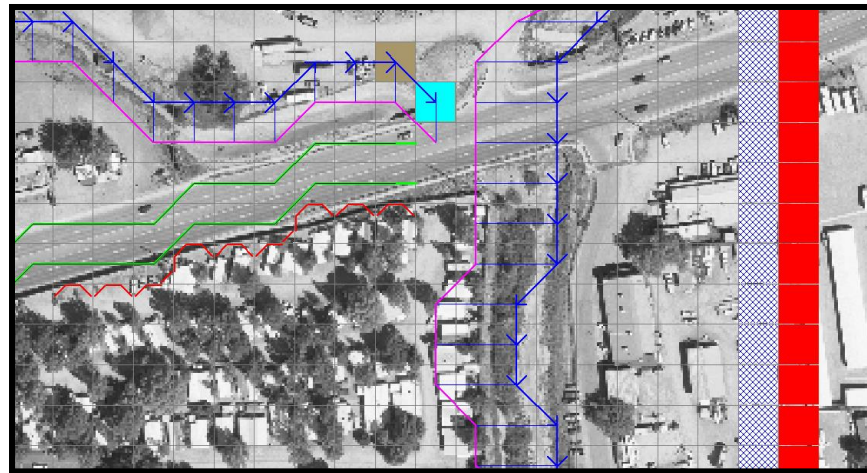


*Figure 26. Levees are Depicted in Red and the River in Blue in the GDS Program.*

The levee output files include LEVEE.OUT, LEOVERTOP.OUT and LEVEEDEFIC.OUT. LEVEE.OUT contains the levee elements that failed. Failure width, failure elevation, discharge from the levee breach and the time of failure occurrence are listed. A discharge hydrograph overtopping the levee element is reported in LEOVERTOP.OUT. The discharge is combined for all the levee directions that are being overtopped. Finally, the LEVEEDEFIC.OUT file lists the levee elements with loss of freeboard during the flood event. Five levels of freeboard deficit are reported:

- 0 = freeboard > 3 ft (0.9 m)
- 1 = 2 ft (0.6 m) < freeboard < 3 ft (0.9 m)
- 2 = 1 ft (0.3 m) < freeboard < 2 ft (0.6 m)
- 3 = freeboard < 1 ft (0.3 m)
- 4 = levee is overtopped by flow.

The levee deficit can be displayed graphically in both MAPPER Pro and MAXPLOT (Figure 27).

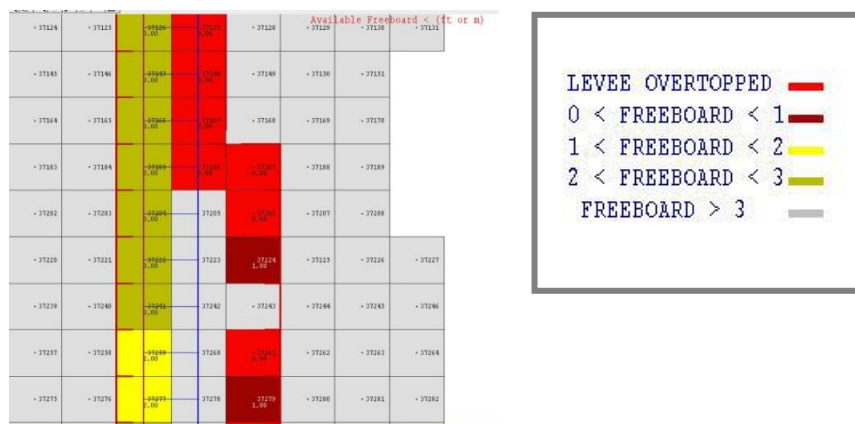


*Figure 27. Levee Freeboard Deficit Plot Using MAXPLOT.*

## 4.6 Levee and Dam Breach Failures

### Breach Options

There are two FLO-2D user defined dam and levee breach options to predict the breach hydrograph: 1) Breach erosion (Figure 28); and 2) Prescribed failure rates (Figure 29). The prescribed breach method uses assigned vertical and horizontal failure rates. The breach erosion option predicts the physical process of sediment scour of the breach opening. In both breach methods, the breach computational timestep is the flood routing timestep. FLO-2D computes the discharge through the breach, the change in upstream storage, the tailwater and backwater effects, and the downstream flood routing. Each failure option generates a series of output files to analyze the dam breach. The model reports of the time of breach or overtopping, the breach hydrograph, peak discharge through the breach, and breach parameters as a function of time. Additional output files to define the dam failure flood hazard include the time-to-flow-depth output files that report the time to the maximum flow depth, the time to one-foot flow depth and time to two-foot flow depth which are useful for delineating evacuation and emergency access routes. The model reports of the time of breach or overtopping, the breach hydrograph, peak discharge through the breach, and breach parameters as a function of time. Additional output files that define the breach hazard include the time-to-flow-depth output files that report the time to the maximum flow depth, the time to one-foot flow depth and time to two-foot flow depth, and deflood time which are useful for delineating evacuation routes.

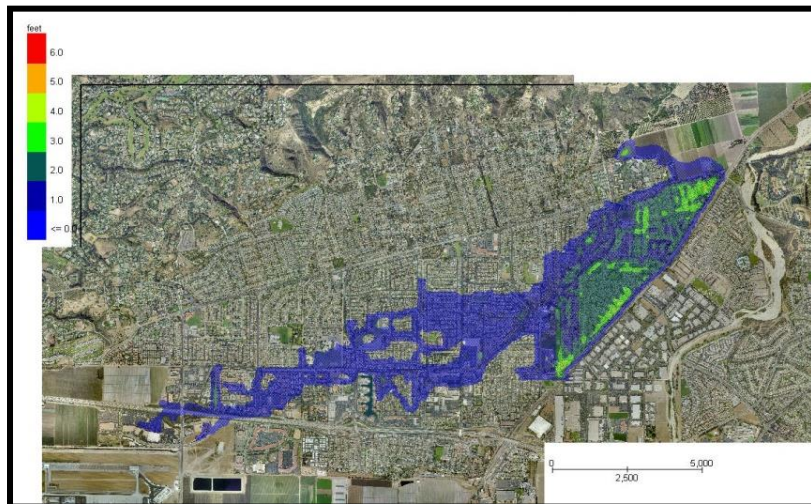
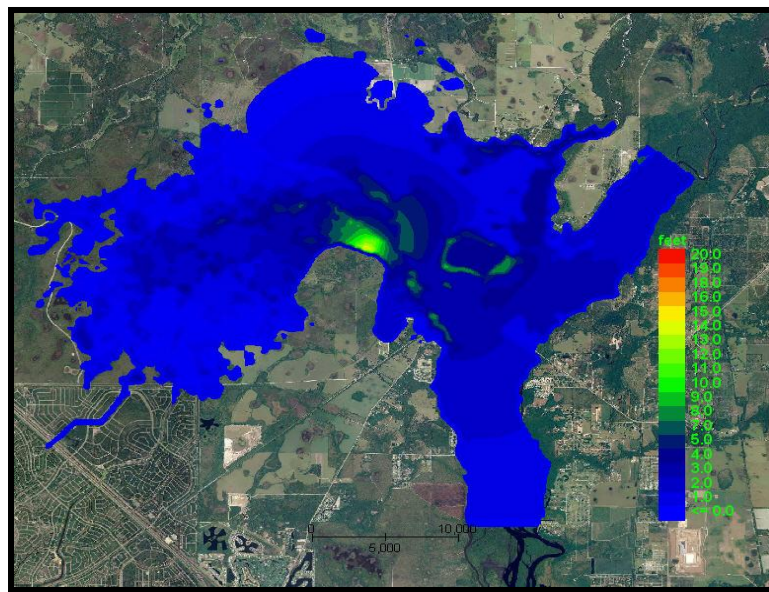


Figure 28. Example of Levee Breach Urban Flooding.



*Figure 29. Example of a Proposed Domestic Water Supply Reservoir Breach Failure.*

### Prescribed Breach

For the prescribed levee failure routine, the breach can enlarge vertically or horizontally. The initial breach width and depth is hardwired as 1 ft (0.3 m). Rates of breach expansion (ft/hr or m/hr) can be specified for both the horizontal and vertical failure modes. Breach discharge is based on the breach width and the difference in water surface elevations on each side of the levee. A final levee base elevation that is higher than the floodplain elevation can also be specified. The levee failure can occur for the entire grid element width for a given flow direction and then the breach can grow to contiguous levee elements. The prescribed levee breach can be assigned to globally predict levee failure anywhere in the grid system based on the computed water surface elevation. Additional breach failure variables such as initial failure elevation if different from overtopping failure and duration of saturation before failure can be assigned to add detail to multiple levee failure locations. For prescribed breaches you can:

- Determine the location of levee failure anywhere in the levee system based on overtopping or based on the water surface elevation reaching a prescribed elevation or distance below the crest elevation for an assigned duration.
- Initiate multiple levee breach failures in various locations that proceed simultaneously.
- Levee failure proceeds with prescribed vertical and horizontal erosion rates that will slow based on the breach shear stress.

### Erosion Breach

The breach erosion component was added to the FLO-2D model to combine the downstream unconfined flood routing with a realistic physical process-based assessment of the dam failure. The basis for the FLO-2D model was National Weather Service BREACH model developed by Fread in 1988.

More information on the breach model development is available in the FLO-2D Reference Manual. In FLO-2D, a dam can fail as follows:

- Overtopping and development of a breach channel;
- Piping failure;
- Piping failure and roof collapse and development into a breach channel;
- Breach channel enlargement through side slope slumping;
- Breach enlargement by wedge collapse.

The user has the option to specify the breach element and breach elevation or to assign global parameters and the model will locate breach failure element based on the water surface elevation and duration of inundation. During an inflow flood simulation, the reservoir fills until the water surface elevation is higher than the crest and overtops it initiating a breach channel. The user can also assign a prescribed breach elevation. If the water elevation exceeds the breach elevation for a given duration, piping is initiated (with or without an inflow flood). Once the pipe roof collapses, then the discharge is computed through the ensuing breach channel.

If the user specifies a breach elevation, then piping will be initiated first. The breach discharge is computed as weir flow with a user specified weir coefficient. The discharge is then used to compute velocity and depth in a rectangular pipe. Using the pipe hydraulics and dam embankment material data, sediment transport capacity is computed using one of nine other sediment transport capacity equations in the FLO-2D model. Sediment is uniformly eroded from the walls, bed and roof of the pipe (Figure 30). When the pipe height is larger than the material remaining in the embankment of above, the roof of the pipe collapses and breach channel flow ensues. The channel discharge is also calculated by the weir equation and like the pipe failure the walls and bed of the rectangular channel are scour. As the channel width and depth increases, the slope stability is checked and if the stability criteria are exceeded, the sides of the channel slump and the rectangular breach transitions to a trapezoidal channel (Figure 31). The scour of the trapezoidal bed and sides can be non-uniform and controlled by user input. The breach continues to widen, and the breach width will expand to other grid elements if necessary.

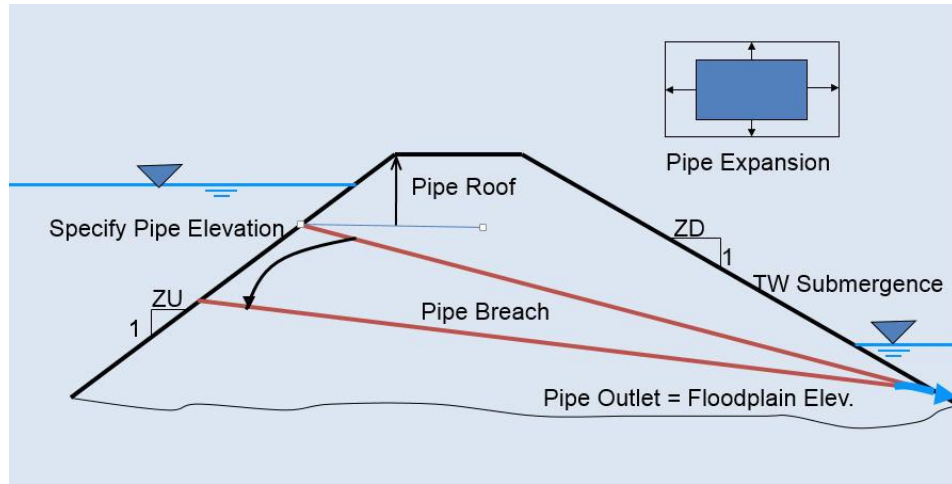


Figure 30. Dam Breach Piping Failure.

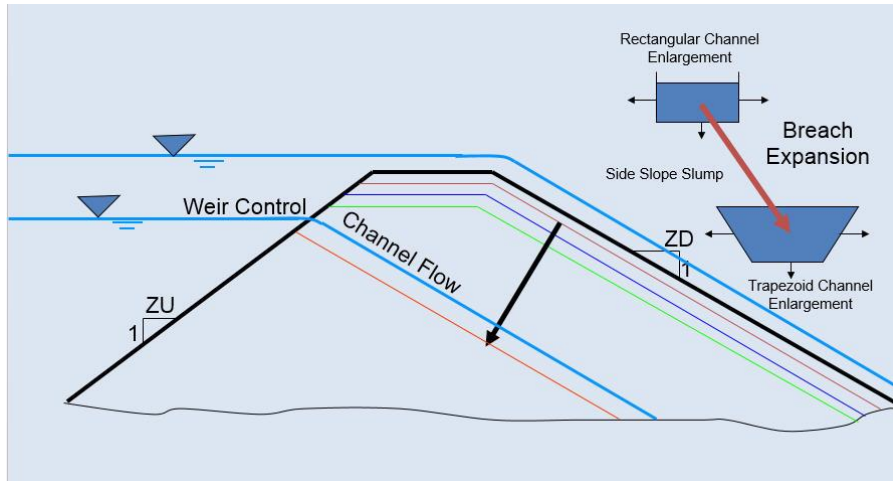


Figure 31. Dam Breach Channel Development.

The dam geometry parameters (Figure 32) associated with a breach erosion failure are:

- Crest Elevation
- Starting Water Surface Elevation (or depth below crest) (ft or m)
- Cumulative Duration of Inundation at Specified Elevation Prior to Breach Initiation (hr)
- Maximum Breach Width (ft or m)
- Prescribed Initial Pipe Elevation (ft or m)
- Tailwater Elevation (ft or m)
- Foundation or Base Elevation for Vertical Breach Cessation (ft or m)

These parameters are defined in Figure 32.

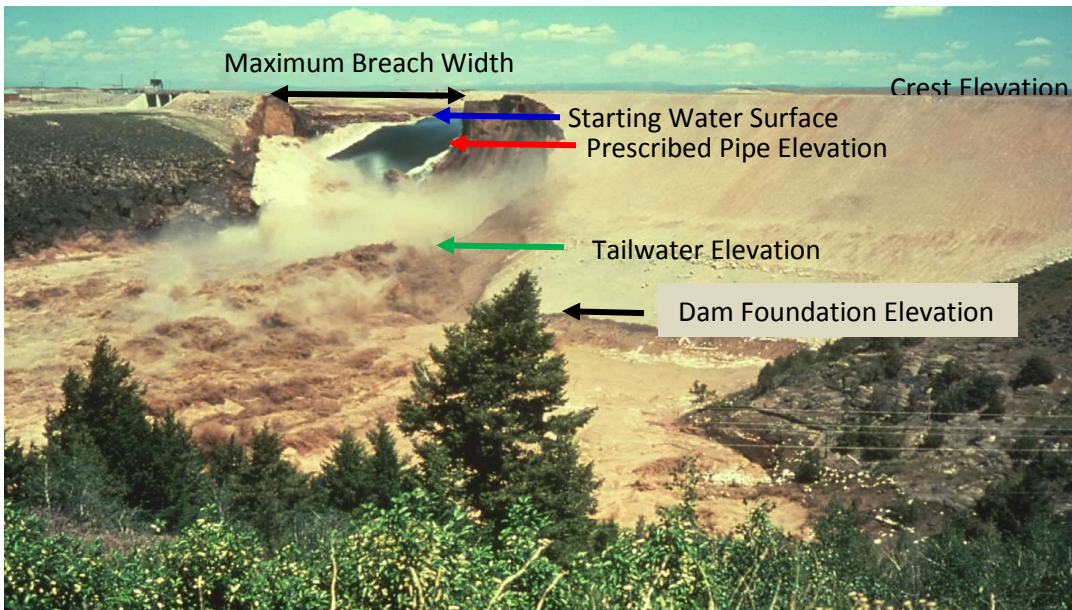


Figure 32. Breach Failure Geometry. (Teton Dam Failure 1976 USBR).

Reservoir water is discharged through the breach and downstream by the FLO-2D routing algorithms using volume conservation that tracks the storage along with the discharge in and out of every grid element based on the computational timesteps. Sediment eroded from the dam is also conserved and matched to the breach hole size conservation and the water discharge through the breach is bulked by the eroded sediment. Routing water through the breach continues until the water surface elevation no longer exceeds the prescribed breach bottom elevation or until all the reservoir water is gone. Tailwater submergence of the weir flow will reduce the breach discharge.

A comprehensive guide to modeling the breach of levees, dams and walls is outlined in the manual Levee, Dam, and Wall Breach Guidelines (FLO-2D, 2018).

#### 4.7 Hydraulic Structures

Hydraulic structures are simulated by specifying either discharge rating curves or rating tables. Hydraulic structures can include bridges, culverts, weirs, spillways or any hydraulic facility that controls conveyance and whose discharge can be specifying by a rating curve or tables. Backwater effects upstream of bridges or culverts as well as blockage of a culvert or overtopping of a bridge can be simulated. A hydraulic structure can control the discharge between channel or floodplain grid elements that do not have to be contiguous but may be separated by several grid elements. For example, a culvert under an interstate highway may span several grid elements.

A hydraulic structure rating curve equation specifies discharge as a function of the headwater depth  $h$ :

$$Q = a h^b$$

where: (a) is a regression coefficient and (b) is a regression exponent. More than one power regression relationship may be used for a hydraulic structure by specifying the maximum depth for which the relationship is valid. For example, one depth relationship can represent culvert inlet control and a second relationship can be used for the outlet control. In the case of bridge flow, blockage can be simulated with a second regression that has a zero coefficient for the height of the bridge low chord.

By specifying a hydraulic structure rating table, the model interpolates between the depth and discharge increments to calculate the discharge. A typical rating curve will start with zero depth and zero discharge and increase in non-uniform increments to the maximum expected discharge or higher. The rating table may be more accurate than the regression relationship if the regression is nonlinear on a log-log plot of the depth and discharge. Flow blockage by debris can be simulated by setting the discharge equal to zero corresponding to a prescribed depth. This blockage option may be useful in simulating worst case mud and debris flow scenarios where bridges or culverts are located on alluvial fans. Simulating blockage of a channel bridge or culvert can force all the discharge to flow overland.

In a simplified storm drain approach, multiple inflow nodes can be assigned to the same outflow element. This will enable the cumulative storm drain discharge at the outlet to be assessed without conduit flow routing. It is possible to assign a limiting conveyance capacity for the outlet node and this will limit the inlet discharge in a successive downstream inflow to the conduit. When the conveyance capacity is exceeded, the discharge in the first inlet to exceed the capacity and the inflow to the remaining downstream inlet nodes is zero. The actual storm drain component engine should be used for a detailed analysis of a storm drain system (see the Storm Drain Section below). Refer to the White Paper Guidelines on Hydraulic Structures for additional details including pump simulation.

Generalized culvert equations for inlet and outlet control are available for the hydraulic structures. Equations to compute culvert discharge for round and rectangular culverts by evaluating inlet and outlet control have been implemented. The culvert discharge will be computed using equations based on experimental and theoretical results from the U.S. Department of Transportation procedures (*Hydraulic Design of Highway Culverts; Publication Number FHWA-NHI-01-0260 revised May 2005*) and these can replace the FLO-2D model rating table or curve methods. The equations include options for box and pipe culverts and will take into account different entrance types for box culverts (wing wall flare 30 to 75 degrees, wing wall flare 90 or 15 degrees and wing wall flare 0 degrees) and three entrance types for pipe culverts (square edge with headwall, socket end with headwall and socket end projecting). The highlights of this component are:

- Computes discharge through box or circular pipe culverts for various entrance conditions.
- Computes both inlet and outlet control and the transition between them.
- No rating curves or tables required.

## **4.8    *Storm Drain Modeling***

The FLO-2D surface water model has a dynamic exchange with the storm drain system. FLO-2D will compute the surface water depth or elevations at storm drain cells and will compute the discharge inflow to the storm drain system based on inlet geometry and water surface head. The storm drain engine will then route the flow in the pipe network and compute potential return flow to the surface water system (Figure 33). Storm drain engine was originally based on the EPA SWMM Model 5.0, but through extensive code enhancements, the FLO-2D storm drain engine represents a completely new model. The general approach to the applying the storm drain component is:

- Storm Drain GUI interface (SWMM GUI) is called by the GDS to locate and develop the storm drain system.
  - GDS automatically develops the required SWMMFLO.DAT based on the SWMM.inp data file.
  - User defines the storm drain geometry in the GDS dialog box.

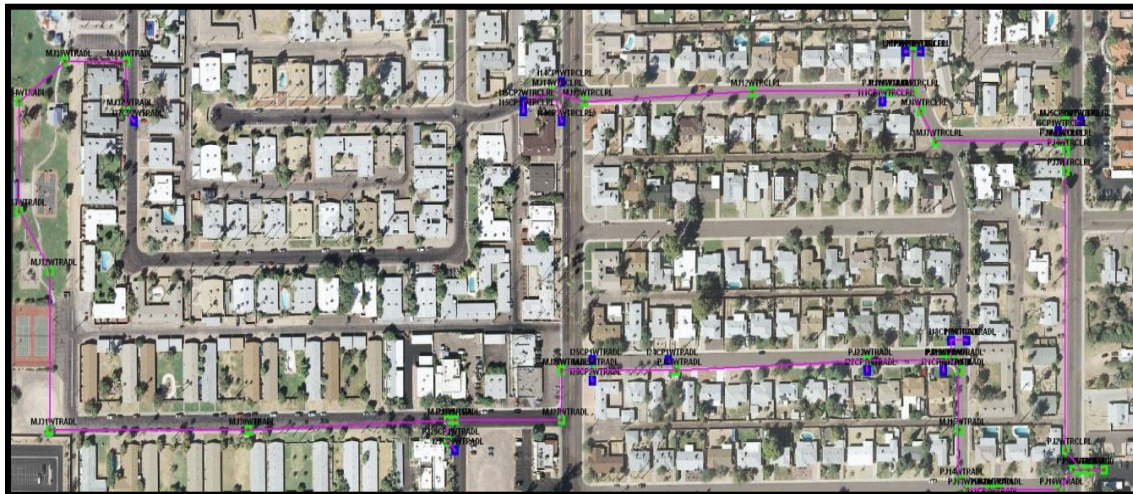


*Figure 33. Storm Drain Layout in the GDS with a Background Image.*

The surface water routing model and storm drain model share the same computational timestep. FLO-2D is the host model, and computes inlet discharge based on the type of inlet and either weir or orifice flow. The storm drain model accepts the inlet discharge and performs the conduit routing and the potential return flow to the surface water through either inlets, outfalls or popped manhole covers.

The FLO-2D Storm Drain Guidelines manual is a companion reference document that describes the model integration and explains the data input. The basic storm drain model development procedure is:

- i. Develop and run a basic FLO-2D overland flow model.
  - ii. Open the GDS and call the Storm Drain model GUI (SWMM GUI).
  - iii. Develop a storm drain network with the provided SWMM GUI or one of any number of other associated external SWMM software GUIs.

- iv. GDS automatically creates the required FLO-2D interface data file when the GUI is closed and sets the storm drain switch to “ON”.
- v. Assign the storm drain inlet geometry and coefficients in the GDS dialog box.
- vi. Run FLO-2D model with the storm drain component.
- vii. Review the results in the SWMM.rpt file and graphically in the SWMM GUI.
- viii. Add other FLO-2D model components and details such as channels, buildings and levees.

#### **4.9 Street Flow**

Street flow as shallow flow in rectangular channels with a curb height using the same routing algorithm as for the 1-D rectangular channels. The flow direction, street width and roughness are specified for each street section within an element. Street and overland flow exchanges are computed in the channel-floodplain flow exchange subroutine. When the curb height is exceeded, the discharge to floodplain portion of the grid element is computed. Return flow to the streets is also simulated.

Streets are assumed to emanate from the center of the grid element to the boundary in the eight flow directions (Figure 34). An east-west street across a grid element would be assigned two street sections. Each section has a length of one-half the grid element side or diagonal. A grid element may contain one or more streets and the streets may intersect. Street roughness values, street widths, elevations and curb heights can be modified on a grid element or street section basis in the GDS program.

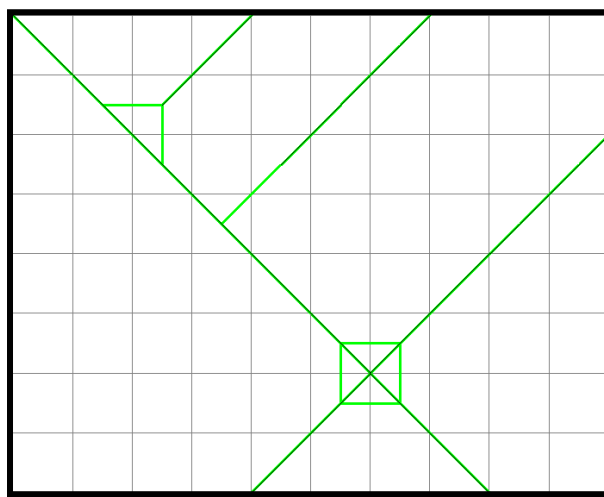


*Figure 34. Streets Depicted in Green in the GDS Program.*

#### **4.10 Floodplain Storage Modification and Flow Obstruction**

One of the unique features the FLO-2D model is its ability to simulate flow conditions associated with flow obstructions or loss of flood storage. Area reduction factors (ARFs) and width reduction factors (WRFs) are coefficients that modify the individual grid element surface area storage and flow width. ARFs can be used to reduce the flood volume storage on grid elements due to buildings or topography.

WRFs can be assigned to any of the eight flow directions in a grid element and can partially or completely obstruct flow paths in all eight directions simulating floodwalls, buildings or berms.

These factors can greatly enhance the detail of the flood simulation through an urban area. Area reduction factors are specified as a percentage of the total grid element surface area (less than or equal to 1.0). Width reduction factors are specified as a percentage of the grid element side (less than or equal to 1.0). For example, a wall might obstruct 40% of the flow width of a grid element side and a building could cover 75% of the same grid element.

It is usually sufficient to estimate the area or width reduction on a map by visual inspection without measurement. Visualizing the area or width reduction can be facilitated by plotting the grid system over an imported image in the GDS to locate the buildings and obstructions with respect to the grid system (Figure 35). The easiest method to assign ARF and WRF factors is to interpolate GIS shapefiles of buildings or other features automatically in the GDS or QGIS. It is possible to specify individual grid elements that are totally blocked from receiving any flow in the ARF.DAT file (gray elements in Figure 36).

It is possible to specify individual grid elements that are totally blocked from receiving any flow in the ARF.DAT file (gray elements in Figure 34). These totally blocked cells do not require any WRF value assignment. To avoid having grid elements with small or negligible surface area (almost totally blocked), any cells with assigned ARF that leave only a small percentage of the grid element are reset at model runtime to ARF = 1 (blocked) according criteria outlined in Table 4.

**Table 4. Maximum Allowable ARF Values.**

<b>Grid Element Size (ft)</b>	<b>Max ARF</b>
Cell Side > 50	0.95
20 < Cell Side < 50	0.90
20 > Cell Side	0.85

A grid element of 10 ft will thereby have at least 15 square ft of surface area.

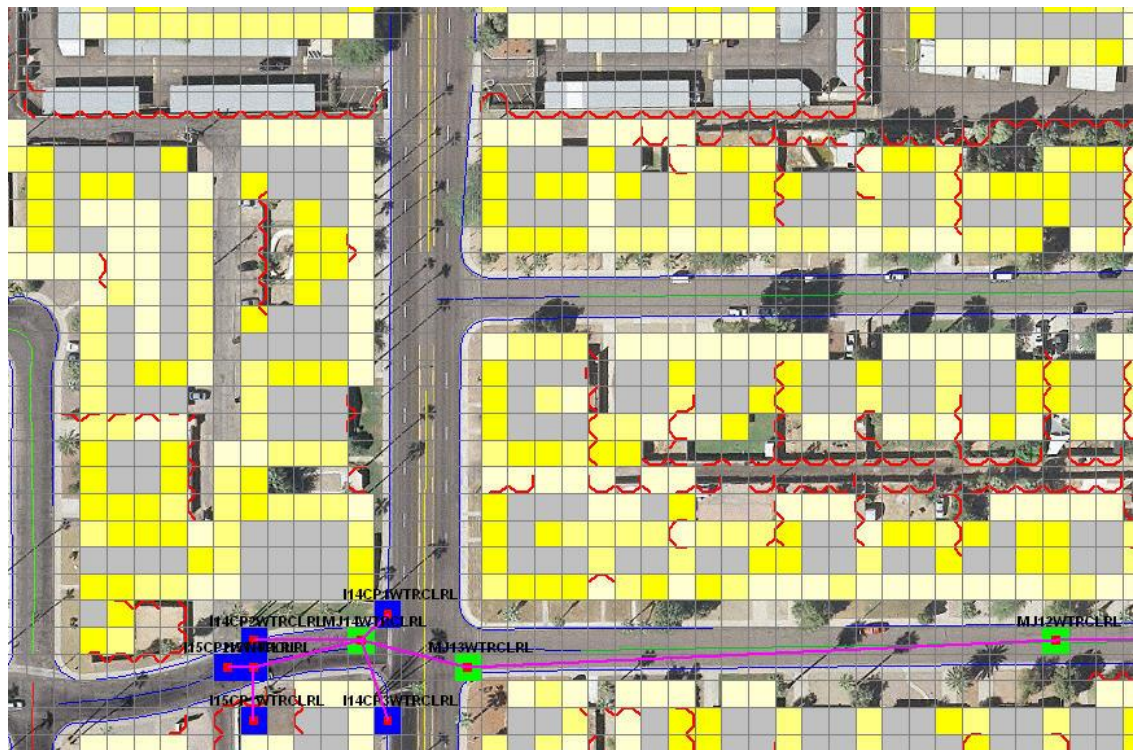


Figure 35. ARF Assignments for Buildings with Walls, Storm Drain and Background Image.

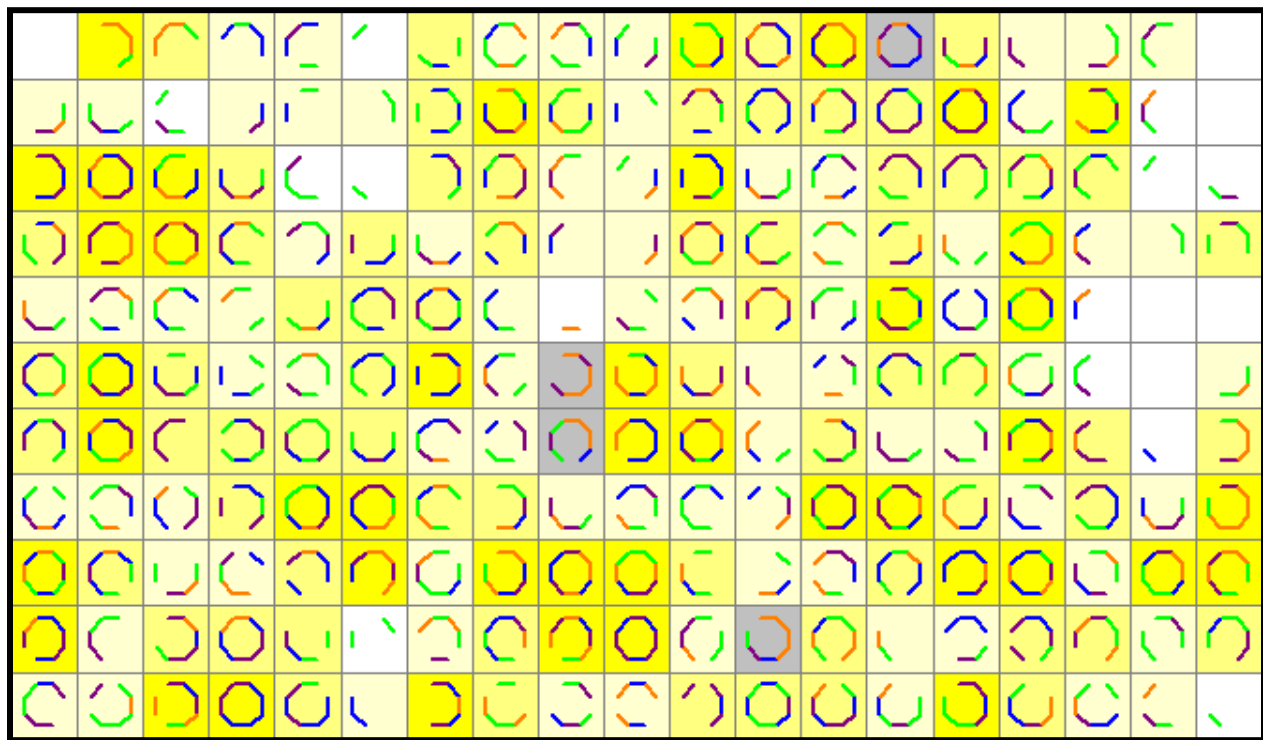


Figure 36. Color Depiction of ARF and WRF Factors.

Two building options are rainfall runoff from building roofs and building collapse. Rainfall can collect on building roofs using levees to represent parapet walls and be routed to downspouts represented by hydraulic structure rating curves (Figure 37 and Figure 38).

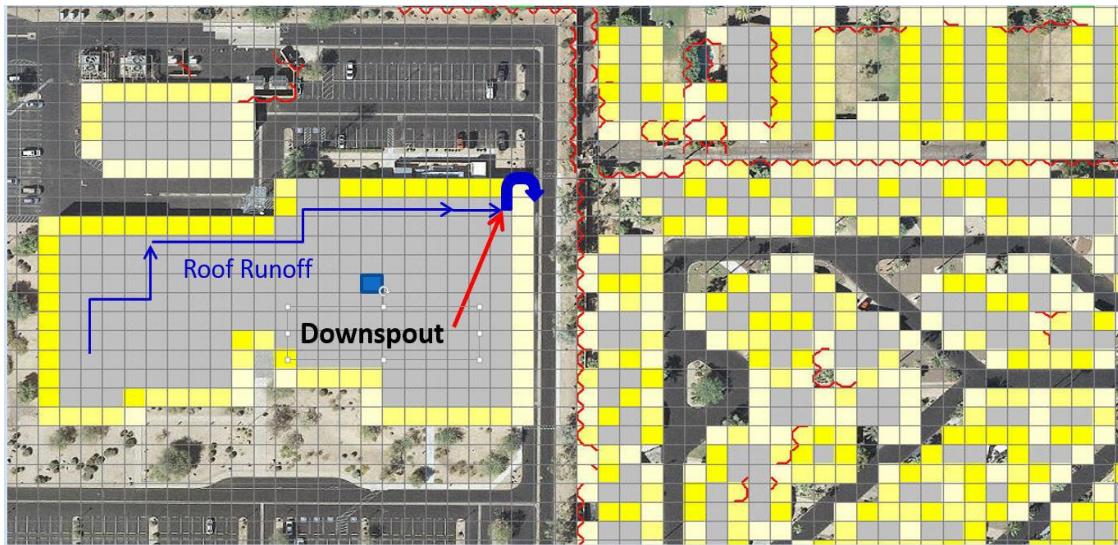


Figure 37. Roof Rainfall Runoff Routed to a Downspout.



Figure 38. Roof Downspout and Parapet Walls for Roof Storage.

A conservative approach is taken to predict the potential collapse of buildings. Based on vulnerability curves of depth versus velocity (Figure 39), when the computed threshold depth is exceeded by flood flow depth associated with a predicted velocity, the building area reduction factor ARF value is reset to zero enabling the flow to go through the grid element and fill it with flood storage. The building collapse routine is triggered by assigning grid element building vulnerability curves in BUILDING\_COLLAPSE.DAT or by assigning a negative ARF values for either a totally blocked or partially blocked grid element.

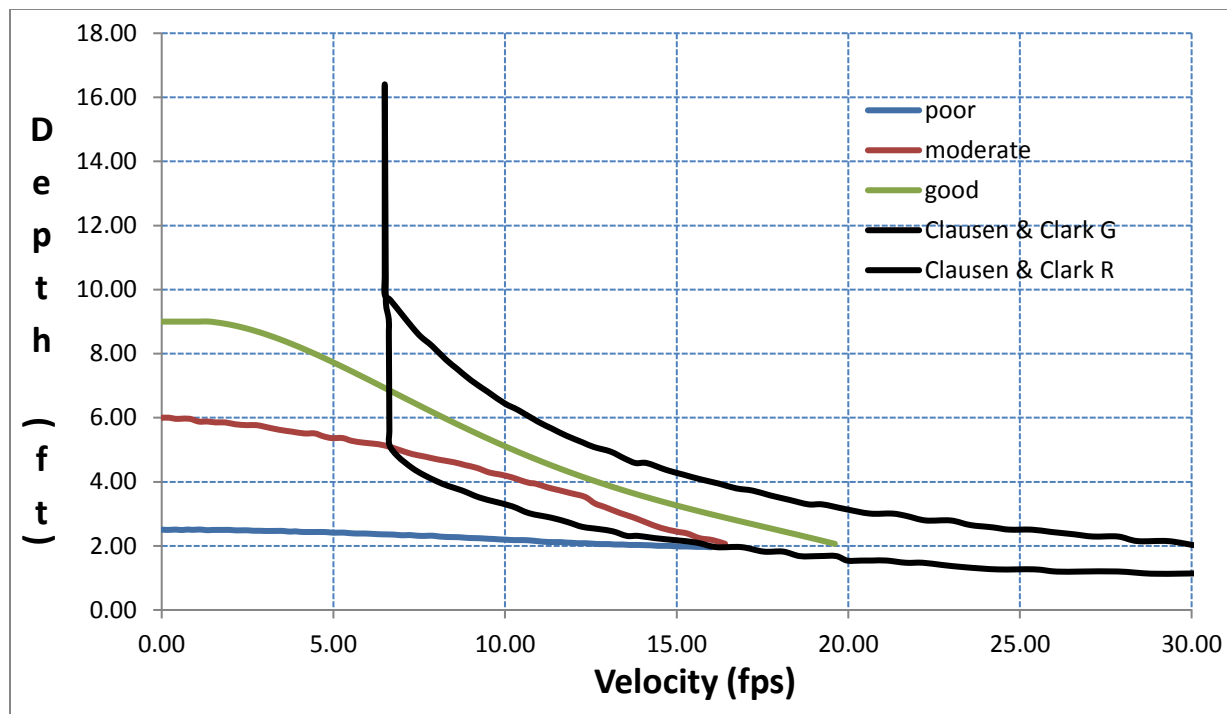


Figure 39. Building Collapse Vulnerability Curves.

#### 4.11 Rainfall Runoff

Rainfall runoff can be routed to the channel system and then the river flood hydraulics can be computed in the same flood simulation. The watershed hydrology and the river routing can also be modeled separately with FLO-2D. Rainfall on the alluvial fan or floodplain can make a significant contribution to the total flood volume. Some fan or floodplain surface areas are similar in size to the upstream watershed areas. In these cases, the excess rainfall may be equivalent to the volume of the inflow hydrograph from the upstream watershed. The fan rainfall/runoff may precede or lag the arrival of the floodwave from the upstream watershed.

The storm rainfall is discretized as a cumulative percent of the total. This discretization of the storm hyetograph is established through local rainfall data, the NOAA Atlas or through regional drainage criteria that defines storm duration, intensity and distribution. The rainfall can be uniform or spatially variable over the grid system. Often in a FLO-2D simulation the first upstream flood inflow hydrograph timestep corresponds to the first rainfall incremental timestep. By altering the storm time distribution on the fan or floodplain, the rainfall can lag or precede the rainfall in the upstream basin depending on the direction of the storm movement over the basin. The storm can also have a different total rainfall than that occurring in the upstream basin.

There are a number of options to simulate variable rainfall including a moving storm, spatially variable depth area reduction assignment, or even grid-based rain gage data from an actual storm event. Storms can be spatially varied over the grid system with areas of intense or light rainfall. Storms can also move

over the grid system by assigning storm speed and direction. A rainfall distribution can be selected from several predefined distributions.

Historical storms can be assigned to the entire grid system. If calibrated or adjusted Next-Generation Radar (NEXRAD) data is available, the NEXRAD pixel rainfall for a given time interval can be automatically interpolated to the FLO-2D grid system using the GDS. Each grid element will be assigned a rainfall total for the NEXRAD time interval and the rainfall is then interpolated by the model for each computational timestep. The result is spatially and temporally variable rainfall-runoff from the grid system. An example of the application of NEXRAD rainfall on an alluvial fan and watershed near Tucson, Arizona is shown in Figure 40. You can accomplish the same result with gridded network data from a system of rain gages. After the GDS interpolation, each FLO-2D grid element will have a rainfall hyetograph to represent the storm. This is the ultimate temporal and spatial discretization of a storm event and the resulting flood replication has proven to be very accurate.

As previously discussed, runoff from building roofs is another rainfall feature. Setting IRAINBUILDING = 1 in RAIN.DAT will enable the rainfall on the surface area reduced portion of the grid element identified as a building (area reduction factor - ARF value) to be contributed to the surface water on a grid element (Figure 40). The roof runoff in dense urban areas can constitute a significant percentage of the total storm volume when it is added directly to the ground surface volume. The building ARF values are in addition to the RTIMP impervious surface infiltration assignment.

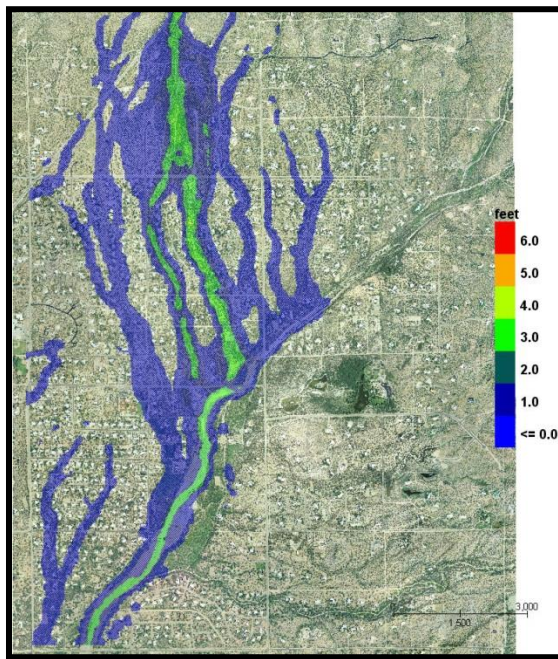


Figure 40. Flooding Replicated from NEXRAD Data near Tucson, Arizona.

## 4.12 Infiltration and Abstraction

Precipitation losses, abstraction (interception) and infiltration are simulated in the FLO-2D model. Infiltration is simulated using either the Green-Ampt infiltration model, the SCS curve number method, or the Horton model. The infiltration parameters can be globally assigned or have grid system spatial variation. Typically, unique hydraulic conductivity and soil suction values for each grid element define the spatial variation. No infiltration is calculated for assigned streets, buildings or impervious surfaces in the grid elements. Channel infiltration can be also be simulated. Although channel bed and bank seepage are usually only minor portion of the total infiltration losses in the system, it can affect the floodwave progression in an ephemeral channel. The surface area of a natural channel is used to approximate the wetted perimeter to compute the infiltration volume.

### Abstraction

Precipitation losses, initial abstraction (interception and depression storage) and infiltration, are simulated in the FLO-2D model. The initial abstraction is filled prior to simulating infiltration and typical initial abstraction values are presented in **Table 5**. Surface depression storage (TOL parameter in TOLER.DAT) is an initial loss (a portion of the initial abstraction) from the potential surface flow. This is the volume of water stored in small surface depressions (puddles) that does not become part of the overland runoff or infiltration. The assignment of initial abstraction should consider the depression storage represented by the TOL value and be appropriately reduced. The TOL parameter can be spatially variable with a unique value assigned to each grid element.

Table 5. Initial Abstraction.	
Surface Cover	Abstraction (inches)
Natural <sup>1</sup>	
Desert and rangeland	0.35
Hillslopes Sonoran desert	0.15
Mountain with vegetation	0.25
Developed – Residential <sup>1</sup>	
Lawns	0.20
Desert landscape	0.10
Pavement	0.05
Agricultural fields and pasture	0.50
Conifers <sup>2</sup>	0.01 - 0.36
Hardwoods <sup>2</sup>	0.001 - 0.08
Shrubs <sup>2</sup>	0.01 - 0.08
Grass <sup>2</sup>	0.04 - 0.06
Forest floor <sup>2</sup>	0.02 - 0.44

<sup>1</sup>Maricopa County Drainage Design Manual, 1992.  
<sup>2</sup>W. T. Fullerton, Masters Thesis, CSU, 1983.

### Green-Ampt Infiltration

The Green-Ampt (1911) equation was selected to compute infiltration losses in the FLO-2D model because it is sensitive to rainfall intensity. When the rainfall exceeds the potential infiltration, then

runoff is generated. The infiltration continues after the rainfall has ceased until all the available water has runoff or has been infiltrated. The Green-Ampt equation is based on the following assumptions:

- Air displacement from the soil has a negligible effect on the infiltration process;
- Infiltration is a vertical process represented by a distinct piston wetting front;
- Soil compaction due to raindrop impact is insignificant;
- Hysteresis effects of the saturation and desaturation process are negligible;
- Flow depth has limited effect on the infiltration processes.

A derivation of the Green-Ampt infiltration method can be found in Fullerton (1983). To utilize the Green-Ampt model, hydraulic conductivity, soil suction, volumetric moisture deficiency, soil storage depth and the percent impervious area must be specified. Typical hydraulic conductivity, porosity and soil suction parameters are presented in Table 6 and Table 7.

**Table 6. Green-Ampt Infiltration - Hydraulic Conductivity and Porosity.**

Classification	(in/hr) <sup>1</sup>	(in/hr) <sup>2</sup>	(in/hr) <sup>3</sup>	Porosity <sup>4</sup>
sand and loamy sand	1.20	1.21 - 4.14	2.41 - 8.27	0.437
sandy loam	0.40	0.51	1.02	0.437
loam	0.25	0.26	0.52	0.463
silty loam	0.15	0.14	0.27	0.501
silt	0.10			
sandy clay loam	0.06	0.09	0.17	0.398
clay loam	0.04	0.05	0.09	0.464
silty clay loam	0.04	0.03	0.06	0.471
sandy clay	0.02	0.03	0.05	0.430
silty clay	0.02	0.02	0.04	0.479
clay	0.01	0.01	0.02	0.475
very slow			< 0.06 <sup>3</sup>	
slow			0.06-.20 <sup>3</sup>	
moderately slow			0.20-0.63 <sup>3</sup>	
moderate			0.63-2.0 <sup>3</sup>	
rapid			2.0-6.3 <sup>3</sup>	
very rapid			> 6.3 <sup>3</sup>	

<sup>1</sup>Maricopa County Drainage Design Manual, 1992.  
<sup>2</sup>James, et. al., Water Resources Bulletin Vol. 28, 1992.  
<sup>3</sup>W. T. Fullerton, Masters Thesis, CSU, 1983.  
<sup>4</sup>COE Technical Engineering and Design Guide, No. 19, 1997

**Table 7. Green-Ampt Infiltration - Soil Suction.**

Classification	(in) <sup>1</sup>	(in) <sup>2</sup>	(in) <sup>3</sup>
sand and loamy sand	2.4	1.9-2.4	
sandy loam	4.3	4.3	

Loam	3.5	3.5	
silty loam	6.6	6.6	
Silt	7.5		
sandy clay loam	8.6	8.6	
clay loam	8.2	8.2	
silty clay loam	10.8	10.8	
sandy clay	9.4	9.4	
silty clay	11.5	11.5	
Clay	12.4	12.5	
Nickel gravel-sand loam			2.0 - 4.5
Ida silt loam			2.0 - 3.5
Poudre fine sand			2.0 - 4.5
Plainfield sand			3.5 - 5.0
Yolo light clay			5.5 - 10.0
Columbia sandy loam			8.0 - 9.5
Guelph loam			8.0 - 13.0
Muren fine clay			15.0 - 20.0

<sup>1</sup>Maricopa County Drainage Design Manual, 1992.

<sup>2</sup>James, W.P., Warinner, J., Reedy, M., Water Resources Bulletin Vol. 28, 1992.

<sup>3</sup>W. T. Fullerton, Masters Thesis, CSU, 1983.

The volumetric moisture deficiency is evaluated as the difference between the initial and final soil saturation conditions (See Table 8). Depression storage is an initial loss from the surface flow (TOL value). This is the amount of water stored in small surface depressions that does not become part of the overland runoff or infiltration.

Table 8. Green-Ampt Infiltration Volumetric Moisture Deficiency.		
Classification	Dry (% Diff)	Normal (% Diff)
sand and loamy sand <sup>1</sup>	35	30
sandy loam	35	25
loam	35	25
silty loam	40	25
silt	35	15
sandy clay loam	25	15
clay loam	25	15
silty clay loam	30	15

sandy clay	20	10
silty clay	20	10
Clay	15	5

<sup>1</sup>Maricopa County Drainage Design Manual, 1992.

### ***Infiltration Depth Limitation***

An optional infiltration soil depth storage limit can be assigned globally (last parameter in line 1 of the INFIL.DAT file) or as a spatially variable parameter for each grid element. When the wetting front reaches the storage depth limitation for a floodplain grid element, the infiltration is ceased. This infiltration volume limit can be quickly filled in an alluvial fan distributary channel or in other areas of concentrated flow resulting in increased runoff. It can also affect the time to peak discharge. For channels, the infiltration is not stopped, but when the water front reaches the infiltration storage depth, the hydraulic conductivity is reduced exponentially. In this case, the infiltration is assumed to continue under a saturated condition that feeds the groundwater system. The limiting soil depth is assigned as the soil depth below the ground surface. The actual available storage is the soil depth times the porosity times the soil moisture deficit. In other words, a portion of available pore space is occupied by the moisture in the soil at the start of the simulation. As an example, the user may define a storage depth limit of 10 ft with a porosity of 40 percent (or 0.40) and a soil moisture deficient of 30% (0.30). The available volumetric storage in the soil for this case is 1.2 ft per square foot of surface area ( $10 \times 0.4 \times 0.3$ ). If instead the volumetric soil moisture deficit (12% or 0.12) is given, the result is the same 1.2 ft. This represents a solid depth of water that can be infiltrated. Once this accumulated water depth (1.2 ft) is infiltrated, the infiltration stops for that grid element. The spatially variable soil depth limit by grid element is assigned as the last parameter in line F of INFIL.DAT.

### ***Channel Infiltration***

For channel infiltration, the surface area of a natural channel is used to approximate the wetted perimeter to compute the infiltration volume. In addition to the depth limit for saturated hydraulic conductivity, an exponential decrement of the hydraulic conductivity can be applied for long duration flow losses such as irrigation releases from dams. Instead of stopping the infiltration when the wetting front reaches the limiting 2 infiltration depth, the hydraulic conductivity is reduced exponentially using the same form as the Horton equation described below. The time is referenced to when the wetting front reaches the assigned limiting depth and the decay coefficient is hardwired to a value of 0.00005 which enables the final hydraulic conductivity to be reached in about 16 hours after the wetting front reaches the limiting soil depth. The global limiting depth in line 1 of INFIL.DAT must be assigned and Line R for each channel reach must have the initial and final hydraulic conductivity and the limiting soil depth.

### ***SCS Curve Number Infiltration***

The SCS runoff curve number (CN) loss method is a function of the total rainfall depth and the empirical curve number parameter which ranges from 1 to 100. The SCS rainfall loss is a function of hydrologic

soil type, land use and treatment, surface condition and antecedent moisture condition. The method was developed on 24-hour hydrograph data on mild slope eastern rural watersheds in the United States. Runoff curve numbers have been calibrated or estimated for a wide range of urban areas, agricultural lands and semi-arid range lands. The SCS CN method does not account for variation in rainfall intensity. It was developed for predicting rainfall runoff from ungaged watersheds and its attractiveness lies in its simplicity. For large basins (especially semi-arid basins) which have unique or variable infiltration characteristics such as channels, the CN method tends to over-predict runoff (Ponce, 1989).

The SCS curve number parameters can be assigned graphically in the GDS to allow for spatially variable rainfall runoff. Shape files can be used to interpolate SCS-CNs from ground cover and soil attributes. The SCS-CN method can be combined with the Green-Ampt infiltration method to compute both rainfall-runoff and overland flow transmission losses. For this case, the SCS-CN method will be applied to grid elements with rainfall occurring and the Green-Ampt method will compute infiltration for grid elements that do not have rainfall during the timestep. This will enable transmission losses to be computed with Green-Ampt on alluvial fans and floodplains while the SCS-CN method is used to compute the rainfall loss in the watershed basin.

### Horton Infiltration

The Horton infiltration method is promoted by several agencies including the Urban Drainage and Flood Control District (UDFCD) in Denver, Colorado. The UDFCD Drainage Criteria Manual (2008) suggests that the model represents a reasonable balance between simplicity and infiltration processes in urban watersheds where the runoff is not sensitive to soil parameters. This Horton equation is defined by:

$$f = f_o + (f_i - f_o) e^{-at}$$

where:

$f$  = infiltration rate at any time  $t$  after the rainfall begins (in/hr)

$f_i$  = initial infiltration rate (in/hr)

$f_o$  = final infiltration rate (in/hr)

$a$  = decay coefficient (1/seconds)

$t$  = time from the rainfall initiation (seconds)

This equation simulates initial high infiltration early in the storm and decays to a steady rate with soil saturation. The parameters depend on soil conditions and vegetative cover. The UDFCD (2008) has recommended Horton parameters based on the NRCS hydrologic soil groups (**Table 9**).

**Table 9. Horton Infiltration Parameters.**

NRCS Soil Group	Infiltration (in/hr)		Decay Coeff. ( $a$ )
	Initial ( $f_i$ )	Final ( $f_o$ )	
A	5.0	1.0	0.0007
B	4.5	0.6	0.0018
C	3.0	0.5	0.0018
D	3.0	0.5	0.0018

#### **4.13 Evaporation**

Open water surface evaporation losses for long duration floods in large river systems can be simulated. This component was implemented for the 173-mile Middle Rio Grande model from Cochiti Dam to Elephant Butte Reservoir in New Mexico. The open water surface evaporation computation is based on a total monthly evaporation that is prorated for the number of flood days in the given month. The user must input the total monthly evaporation in inches or mm for each month along with the presumed diurnal hourly percentage of the daily evaporation and the clock time at the start of the flood simulation. The total evaporation is then computed by summing the wetted surface area on both the floodplain and channel grid elements for each timestep. The floodplain wetted surface area excludes the area defined by ARF area reduction factors. The evaporation loss does not include evapotranspiration from floodplain vegetation. The total evaporation loss is reported in the SUMMARY.OUT file and should be compared with the infiltration loss for reasonableness.

#### **4.14 Overland Multiple Channel Flow**

The purpose of the multiple channel flow component is to simulate the overland flow in rills and gullies rather than as overland sheet flow for floodplain routing (Figure 41). Surface water is often conveyed in small channels and simulating rill and gully flow concentrates the discharge with higher depths and velocities to improve the model runoff timing. This may be especially important in urban areas where small drainage channels and swales exist. In the multiple channel routine, overland sheet flow within the grid element is routed to the multiple channel and then the flow between the grid elements is computed as rill and gully flow. No overland sheet flow is exchanged between grid elements if both elements have assigned multiple channels. The gully geometry is defined by a maximum depth, width and flow roughness. The multiple channel attributes can be spatially variable on the grid system and can be assigned or edited graphically with the GDS or QGIS programs.



*Figure 41. Gully on an Alluvial Fan where Overland Sheet Flow is Minimal.*

If the gully flow exceeds the specified gully depth, the multiple channels can be expanded by a user specified incremental width. This channel widening process assumes these gullies are alluvial channels and will widen to accept more flow as the flow reaches bankfull discharge. There is no gully overbank discharge to the overland surface area within the grid element. The gully will continue to widen until the gully width exceeds the width of the grid element, then the flow routing between grid elements will revert to sheet flow. This enables the grid element to be overwhelmed by large flood flows. If no incremental width is assigned, the flow depth just continues to increase vertically in the channel because there is no overbank out of channel flow exchange with the floodplain. During the falling limb of the hydrograph when the flow depth is less than 1 ft (0.3 m), the gully width will decrease to confine the discharge until the original width is again attained. The user can assign the range of slope where the multiple channel widening is computed. There is also a channel avulsion routine that will force the multiple channel to take a new path when the flow exceeds the bankfull depth. The primary features of the multiple channel routine are:

- Improves the runoff timing compare to overland sheet flow;
- Shallow rectangular channels;
- Channel bed slope is based on grid element topography;
- Multiple channel widths can expand to accept more discharge to simulate alluvial fan channels.

To assign multiple channels in the graphic editor programs, simply draw a polyline and select width, depth and n-values. There is no required order of the channels or grid elements in the MULT.DAT file, but it simplifies editing if the multiple channel elements are listed in order in downstream direction. The maximum flow depth results of a rainfall watershed model with

multiple channels. Typically, multiple channels are assigned when observed in aerial photography at the outfalls of subbasins as shown in Figure 42.

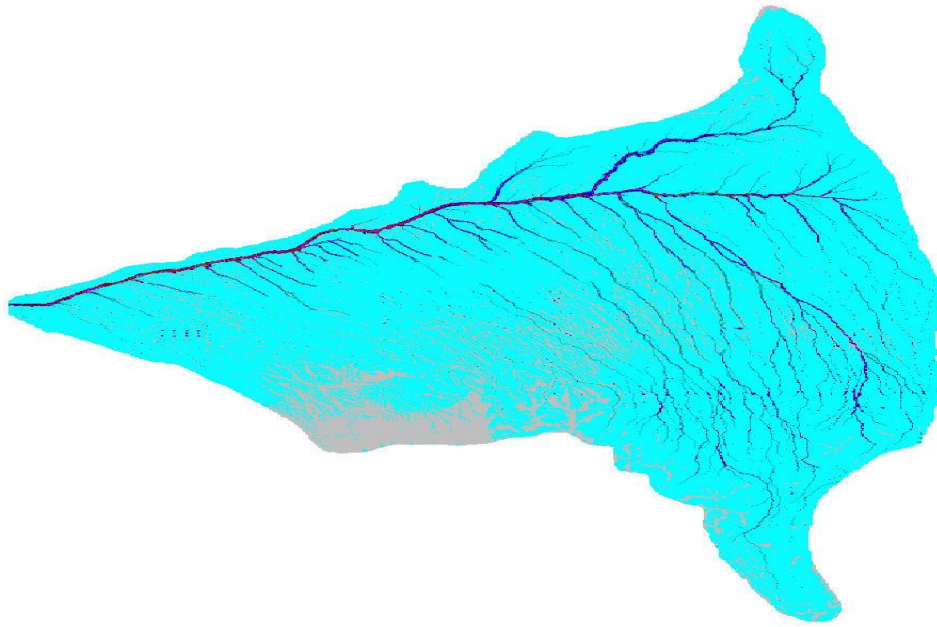


*Figure 42. Maximum Flow Depth with Multiple Channel Flow Shown as Dark Blue and Red.*

If multiple channels convey the flow to 1-D channels or rivers, then the multiple channel should terminate before the channel bank element and have the multiple channel bed elevation in the terminating node (cell elevation – multiple channel depth) be higher than the cell elevation and the bank elevation in the channel bank element. If necessary, use an adjust to the width and depth as the multiple channel approaches the 1-D channel over several multiple channel elements to simulate the multiple channel becoming wider and shallower on the flat river floodplain.

#### **4.15 Sediment Transport – Total Load**

When a channel rigid bed analysis is performed, any potential cross section changes associated with sediment transport are assumed to have a negligible effect on the predicted water surface. The volume of storage in the channel associated with scour or deposition is relatively small compared to the entire flood volume. This is a reasonable assumption for large river floods on the order of a 100-year flood. For large rivers, the change in flow area associated with scour or deposition will have negligible effect on the water surface elevation for flows exceeding the bankfull discharge. On steep alluvial fans, several feet of scour or deposition will usually have a minimal effect on the flow paths of large flood events. For fan small flood events, the potential effects of channel incision, avulsion, blockage, bank or levee failure and sediment deposition on the flow path should be considered.

To address mobile bed issues, FLO-2D has a sediment transport component that can compute sediment scour or deposition. Within a grid element, sediment transport capacity is computed for either channel, street or overland flow based on the flow hydraulics. The sediment transport capacity is then compared

with the sediment supply and the resulting sediment excess or deficit is uniformly distributed over the grid element potential flow surface using the bed porosity based on the dry weight of sediment. For surveyed channel cross sections, a non-uniform sediment distribution relationship is used. There are eleven sediment transport capacity equations that can be applied in the FLO-2D. Each sediment transport formula was derived from unique river or flume conditions and the user is encouraged to research the applicability of a selected equation for a particular project. Sediment routing by size fraction and armoring are also options. Sediment continuity is tracked on a grid element basis.

During a FLO-2D flood simulation, the sediment transport capacity is based on the predicted flow hydraulics between floodplain or channel elements, but the sediment transport computation is uncoupled from the flow hydraulics. Initially the flow hydraulics are computed for all the floodplain and channel elements for the given time step and then the sediment transport is computed based on the flow hydraulics for that timestep. This assumes that the change in channel geometry resulting from deposition or scour will not have a significant effect on the average flow hydraulics for that timestep. If the scour or deposition is less than 0.10 ft (0.3 m), the sediment storage volume is not distributed on the bed but is accumulated. Generally, it takes several timesteps (~1 to 10 seconds) to accumulate enough sediment so that the resulting deposition or scour will exceed 0.10 ft (0.03 m). This justifies the uncoupled sediment transport approach used in FLO-2D.

Sediment routing by size fraction requires a sediment size distribution. A geometric mean sediment diameter is estimated for each sediment interval represented as a percentage of the total sediment sample. Generally, a six or more sediment sizes and the corresponding percentages are determined from a sieve analysis. Each size fraction is routed in the model and the volumes in the bed (floodplain, channel or street) are tracked. Initial sediment size fractions can be specified on a grid element basis for an alluvial fan or watershed surface to compute spatially variable sediment transport. Different areas of the grid system can be assigned different bed sediment size distributions by groups. The variation in size fraction distribution is then tracked over the floodplain or fan surface. The sediment supply to a river reach can also be entered in sediment size fractions. An example of sediment data for routing by size fraction is presented below:

Sediment Diameter (mm)	Percent Finer
0.074	0.058
0.149	0.099
0.297	0.156
0.59	0.230
1.19	0.336
2.38	0.492
4.76	0.693
9.53	0.808
19.05	0.913
38.10	1.000

Bed armoring is automatically computed for sediment routing by size fraction. There are no switches to initiate armoring. The armoring process occurs when the upper bed layers of sediment become coarser as the finer sediment is transported out of the bed. An armor layer is complete when the coarse bed material covers the bed and protects the fine sediment below it. To assess armoring, the FLO-2D model tracks the sediment size distribution and volumes in an exchange layer defined by three times the  $D_{90}$  grain size of the bed material (Yang, 1996; O'Brien, 1984). The potential armor layer is evaluated for each timestep by grid element when the volume of each size fraction in the exchange layer is assessed (Figure 43).

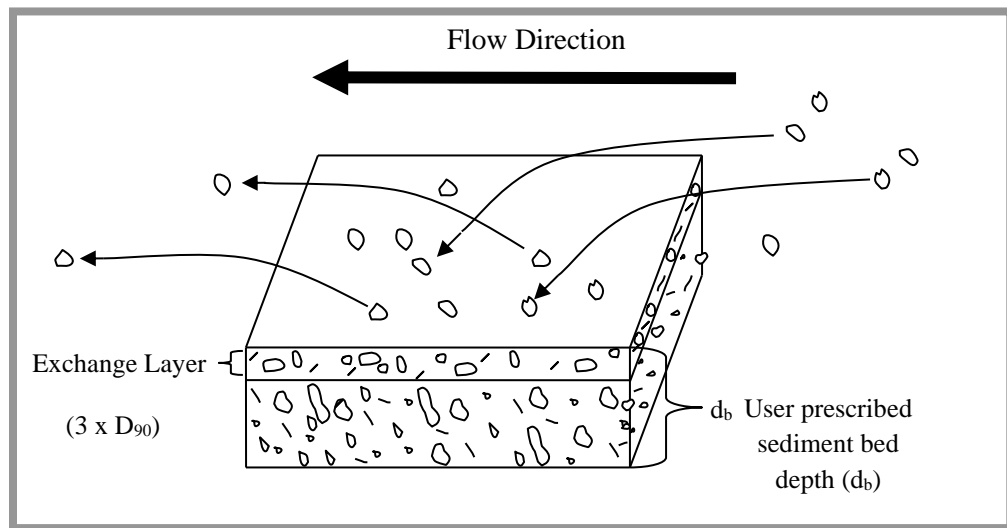


*Figure 43. Sediment Transport Bed Exchange Layer.*

### Sediment Supply

There are two options for computing the sediment supply to a given project. The first option is to calculate a sediment supply discharge  $Q_s$  rating curve in the form of:

$$Q_s = a Q_w^b$$

where

$Q_w$  is the water discharge,

a is a coefficient and

b is an exponent.

This equation is typically derived from a known stream gaging station that is recording suspended sediment load. This data sediment load base is usually limited to large rivers and is not available for alluvial fan or watershed overland flow.

The second method is to compute the sediment supply at a FLO-2D model inflow node using one of the applicable sediment transport capacity equations (out of the 11 available equations in the FLO-2D

model). In this case the sediment transport capacity out of the inflow node constitutes the sediment supply to the contiguous downstream channel or floodplain node. When the channel or floodplain inflow node sediment transport capacity represents the sediment supply to the model, the FLO-2D model does not permit scour or deposition in the inflow node (Figure 44). The inflow node will have an assigned water inflow hydrograph. To avoid excessive scour downstream of the inflow node additional rigid grid elements can be assigned (R-lines in the SED.DAT file). These may be positioned for an alluvial fan simulation so that sediment transport equilibrium is achieved at or near the apex.

Rigid bed inflow node with hydrograph

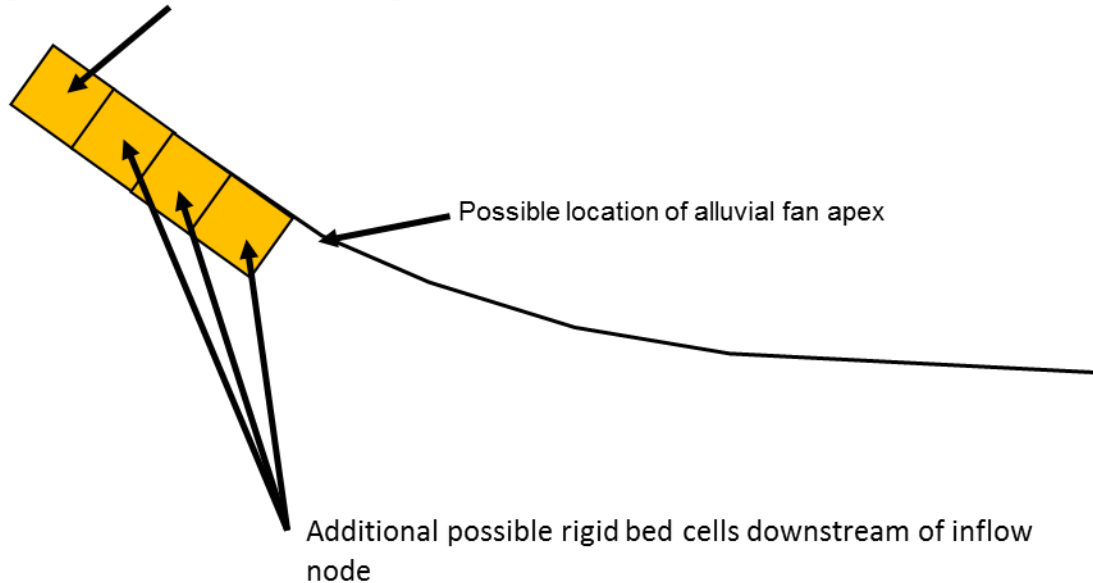


*Figure 44. Inflow Node Locations.*

The size fraction percentage is tracked separately in the exchange layer and the rest of the channel bed. When the exchange layer has less than 33% of the original exchange layer volume, the exchange layer is replenished with sediment from the rest of the floodplain or channel bed using the initial bed material size distribution. This effectively creates an armor layer that is 2 times the  $D_{90}$  size of the bed material. As sediment is removed from the exchange layer, the bed coarsens, and the size fraction percentage is recomputed. If all smaller sediment size fractions in the exchange layer are removed leaving only the coarse size fraction that the flow cannot transport and the exchange layer thickness is greater than 33% of the original exchange layer thickness, then the bed is armored and no sediment is removed from the bed for that timestep. Sediment deposition can still occur on an armored bed if the supply of a given size fraction to the element exceeds the sediment transport capacity out of the element. The user can specify the total depth of the channel bed available for sediment transport. Sediment scour is limited for adverse slopes to essentially the average reach slope.

FLO-2D calculates the sediment transport capacity using each equation for each grid element and timestep. The user selects only one equation for use in the flood simulation but can designate one

floodplain or channel element to view the sediment transport capacity results for all the equations based on the output interval. The computed sediment transport capacity for each of the eleven equations can then be compared by output interval in the SEDTRAN.OUT file. Using this file, the range of sediment transport capacity and those equations that appear to be overestimating or underestimating the sediment load can be determined.

Each sediment transport equation is briefly described in the following paragraphs. The user is encouraged to further research which equation is most appropriate for the channel morphology or hydraulics or a specific project. When reviewing the SEDTRANS.OUT file, it might be observed that generally the Ackers-White and Engelund-Hansen equations compute the highest sediment transport capacity; Yang and Zeller-Fullerton result in a moderate sediment transport quantity; and Laursen and Toffaleti calculate the lowest sediment transport capacity. This correlation however varies according to project conditions. A brief discussion of each sediment transport equation in the FLO-2D model follows:

**Ackers-White Method.** Ackers and White (1973) expressed sediment transport in terms of dimensionless parameters, based on Bagnold's stream power concept. They proposed that only a portion of the bed shear stress is effective in moving coarse sediment. Conversely for fine sediment, the total bed shear stress contributes to the suspended sediment transport. The series of dimensionless parameters are required include a mobility number, representative sediment number and sediment transport function. The various coefficients were determined by best-fit curves of laboratory data involving sediment size greater than 0.04 mm and Froude numbers less than 0.8. The condition for coarse sediment incipient motion agrees well with Sheild's criteria. The Ackers-White approach tends to overestimate the fine sand transport (Julien, 1995).

**Engelund-Hansen Method.** Bagnold's stream power concept was applied with the similarity principle to derive a sediment transport function. The method involves the energy slope, velocity, bed shear stress, median particle diameter, specific weight of sediment and water, and gravitational acceleration. In accordance with the similarity principle, the method should be applied only to flow over dune bed forms, but Engelund and Hansen (1967) determined that it could be effectively used in both dune bed forms and upper regime sediment transport (plane bed) for particle sizes greater than 0.15 mm.

**Karim-Kennedy Equation.** The simplified Karim-Kennedy equation (F. Karim, 1998) is used in the FLO-2D model. It is a nonlinear multiple regression equation based on velocity, bed form, sediment size and friction factor using a large number of river flume data sets. The data includes sediment sizes ranging from 0.08 mm to 0.40 mm (river) and 0.18 mm to 29 mm (flume), slope ranging from 0.0008 to 0.0017 (river) and 0.00032 to 0.0243 (flume) and sediment concentrations by volume up to 50,000 ppm. This equation is suggested for non-uniform riverbed conditions for typical large sand and gravel bed rivers. It will yield results similar to Laursen's and Toffaleti's equations.

**Laursen's Transport Function.** The Laursen (1958) formula was developed for sediments with a specific gravity of 2.65 and had good agreement with field data from small rivers such as the Niobrara River near Cody, Nebraska. For larger rivers the correlation between measured data and predicted sediment transport was poor (Graf, 1971). This set of equations involved a functional relationship between the

flow hydraulics and sediment discharge. The bed shear stress arises from the application of the Manning-Strickler formula. The relationship between shear velocity and sediment particle fall velocity was based on flume data for sediment sizes less than 0.2 mm. The shear velocity and fall velocity ratio expresses the effectiveness of the turbulence in mixing suspended sediments. The critical tractive force in the sediment concentration equation is given by the Shields diagram.

**MPM-Smart Equation.** This is a modified Meyer-Peter-Mueller (MPM) sediment transport equation (Smart, 1984) for steep channels ranging from 3% to 20%. The original MPM equation underestimated sediment transport capacity because of deficiencies in the roughness values. This equation can be used for sediment sizes greater than 0.4 mm. It was modified to incorporate the effects of nonuniform sediment distributions. It will generate sediment transport rates approaching Englund-Hansen on steep slopes.

**MPM-Woo Relationship.** For computing the bed material load in steep sloped, sand bed channels such as arroyos, washes and alluvial fans, Mussetter, et al. (1994) linked Woo's relationship for computing the suspended sediment concentration with the Meyer-Peter-Mueller bedload equation. Woo et al. (1988) developed an equation to account for the variation in fluid properties associated with high sediment concentration. By estimating the bed material transport capacity for a range of hydraulic and bed conditions typical of the Albuquerque, New Mexico area, Mussetter et al. (1994) derived a multiple regression relationship to compute the bed material load as a function of velocity, depth, slope, sediment size and concentration of fine sediment. The equation requires estimates of exponents and a coefficient and is applicable for velocities up to 20 fps (6 mps), a bed slope  $< 0.04$ , a  $D_{50} < 4.0$  mm, and a sediment concentration of less than 60,000 ppm. This equation provides a method for estimating high bed material load in steep, sand bed channels that are beyond the hydraulic conditions for which the other sediment transport equations may be applicable.

**Parker, Klingeman and McLean (1982).** This equation was derived primarily for gravel or sandy bed material load. It was based on Milhous (1973, 1982) sediment transport measurements at Oak Creek, Oregon. At low flows the equation generates sediment load that is entirely bedload. For higher flows approaching bankfull discharge, the predicted bed material load is presumed to be mixed suspended and bedload for the smaller sediment size fractions. The substrate based equation predicts individual size fraction transport rates for channel width average conditions which are then summed to get a total bed load.

**Toffaleti Approach.** Toffaleti (1969) develop a procedure to calculate the total sediment load by estimating the unmeasured load. Following the Einstein approach, the bed material load is given by the sum of the bedload discharge and the suspended load in three separate zones. Toffaleti computed the bedload concentration from his empirical equation for the lower-zone suspended load discharge and then computed the bedload. The Toffaleti approach requires the average velocity in the water column, hydraulic radius, water temperature, stream width,  $D_{65}$  sediment size, energy slope and settling velocity. Simons and Senturk (1976) reported that Toffaleti's total load estimated compared well with 339 river and 282 laboratory data sets. This equation has a number of empirical and poorly defined coefficients that may give poor results for highly variable conditions.

**Van Rijn.** This equation predicts the total sediment discharge assuming a parabolic distribution of suspended sediment in the lower half of the flow and a uniform distribution in the upper half of the flow. The uniform sediment distribution in upper flow portion is based on the maximum value of the parabolic in the from the lower flow. The bedload discharge and suspended load is computed separately and added together to derive the total sediment load. For a discussion between measured and predicted data for the equation using laboratory and field tests revealing see T.W. Strum (2001).

**Yang Method.** Yang (1973) determined that the total sediment concentration was a function of the potential energy dissipation per unit weight of water (stream power) and the stream power was expressed as a function of velocity and slope. In this equation, the total sediment concentration is expressed as a series of dimensionless regression relationships. The equations were based on measured field and flume data with sediment particles ranging from 0.137 mm to 1.71 mm and flows depths from 0.037 ft to 49.9 ft. Most of the data was limited to medium to coarse sands and flow depths less than 3 ft (Julien, 1995). Yang's equations in the FLO-2D model can be applied to sand and gravel.

**Zeller-Fullerton Equation.** Zeller-Fullerton is a multiple regression sediment transport equation for a range of channel bed and alluvial floodplain conditions. This empirical equation is a computer-generated solution of the Meyer-Peter, Muller bed-load equation combined with Einstein's suspended load to generate a bed material load (Zeller and Fullerton, 1983). For a range of bed material from 0.1 mm to 5.0 mm and a gradation coefficient from 1.0 to 4.0, Julien (1995) reported that this equation should be accurate with 10% of the combined Meyer-Peter Muller and Einstein equations. The Zeller-Fullerton equation assumes that all sediment sizes are available for transport (no armoring). The original Einstein method is assumed to work best when the bedload constitutes a significant portion of the total load (Yang, 1996).

In summary, Yang (1996) made several recommendations for the application of total load sediment transport formulas in the absence of measured data. These recommendations for natural rivers are slightly edited and presented below:

- Use Zeller and Fullerton equation when the bedload is a significant portion of the total load.
- Use Toffaleti's method or the Karim-Kennedy equation for large sand-bed rivers.
- Use Yang's equation for sand and gravel transport in natural rivers.
- Use Ackers-White or Engelund-Hansen for subcritical flow in lower sediment transport regime.
- Use Laursen's formula for shallow rivers with silt and fine sand.
- Use MPM-Woo's or MPM-Smart for steep slope, arroyo sand bed channels and alluvial fans.

Yang (1996) reported that ASCE ranked the equations (not including Toffaleti, MPM-Woo, Karin-Kennedy) in 1982 based on 40 field tests and 165 flume measurements in terms of the best overall predictions as follows with Yang ranking the highest: Yang, Laursen, Ackers-White, Engelund-Hansen, and combined Meyer-Peter, Muller and Einstein.

It is important to note that in applying these equations, the wash load is not included in the computations. The wash load should be subtracted from any field data before comparing the field

measurements with the predicted sediment transport results from the equations. It is also important to recognize if the field measurements are sediment supply limited. If this is the case, any comparison with the sediment transport capacity equations would be inappropriate.

There are two other sediment transport options available in the FLO-2D model; assignment of rigid bed element and a limitation on the scour depth. Rigid bed element can be used would simulate a concrete apron in a channel below a culvert outlet, channel bed rock or a concrete lined channel reach. The scour depth limitation is a control that can be invoked for sediment routing.

#### **4.16 Mud and Debris Flow Simulation**

Very viscous, hyperconcentrated sediment flows are generally referred to as either mud or debris flows. Mudflows are non-homogeneous, nonNewtonian, transient flood events whose fluid properties change significantly as they flow down steep watershed channels or across alluvial fans. Mudflow behavior is a function of the fluid matrix properties, channel geometry, slope and roughness. The fluid matrix consists of water and fine sediments. At sufficiently high concentrations, the fine sediments alter the properties of the fluid including density, viscosity and yield stress.

There are several important sediment concentration relationships that help to define the nature of hyperconcentrated sediment flows. These relationships relate the sediment concentration by volume, sediment concentration by weight, the sediment density, the mudflow mixture density and the bulking factor. When examining parameters related to mudflows, it is important to identify the sediment concentration as a measure of weight or volume. The sediment concentration by volume  $C_v$  is given by:

$$C_v = \text{volume of the sediment}/(\text{volume of water plus sediment})$$

$C_v$  is related to the sediment concentration by weight  $C_w$  by:

$$C_v = C_w \gamma / \{\gamma_s - C_w(\gamma_s - \gamma)\}$$

where  $\gamma$  = specific weight of the water and  $\gamma_s$  = specific weight of the sediment. The sediment concentration can also be expressed in parts per million (ppm) by multiplying the concentration by weight  $C_w$  by  $10^6$ . The specific weight of the mudflow mixture  $\gamma_m$  is a function of the sediment concentration by volume:

$$\gamma_m = \gamma + C_v(\gamma_s - \gamma)$$

Similarly the density of the mudflow mixture  $\rho_m$  is given by:

$$\rho_m = \rho + C_v (\rho_s - \rho)$$

and

$$\rho_m = \gamma_m / g$$

where  $g$  is gravitational acceleration. Finally, the total mixture volume of water and sediment can be determined by multiplying the water volume by the bulking factor. The bulking factor is simply:

$$BF = 1/(1 - C_v)$$

The bulking factor is 2.0 for a sediment concentration by volume of 50%. A sediment concentration of 7% by volume for a conventional river bedload and suspended results in a bulking factor of 1.075 indicating that the flood volume is 7.5% greater than if the flood was considered to be only water.

These basic relationships will be valuable when analyzing mudflow simulations. Most mudflow studies require estimates of the sediment concentration by volume and the bulking factor to describe the magnitude of the event. Average and peak sediment concentrations for the flood hydrograph are important variables for mitigation design.

The full range of sediment flows span from water flooding to mud floods, mudflows and landslides. The distinction between these flood events depends on sediment concentration measured either by weight or volume (Figure 45). Sediment concentration by volume expressed as a percentage is the most commonly used measure. Table 10 lists the four different categories of hyperconcentrated sediment flows and their dominant flow characteristics. This Table 10 was developed from the laboratory data using actual mudflow deposits. Some variation in the delineation of the different flow classifications should be expected based on the sample geology.

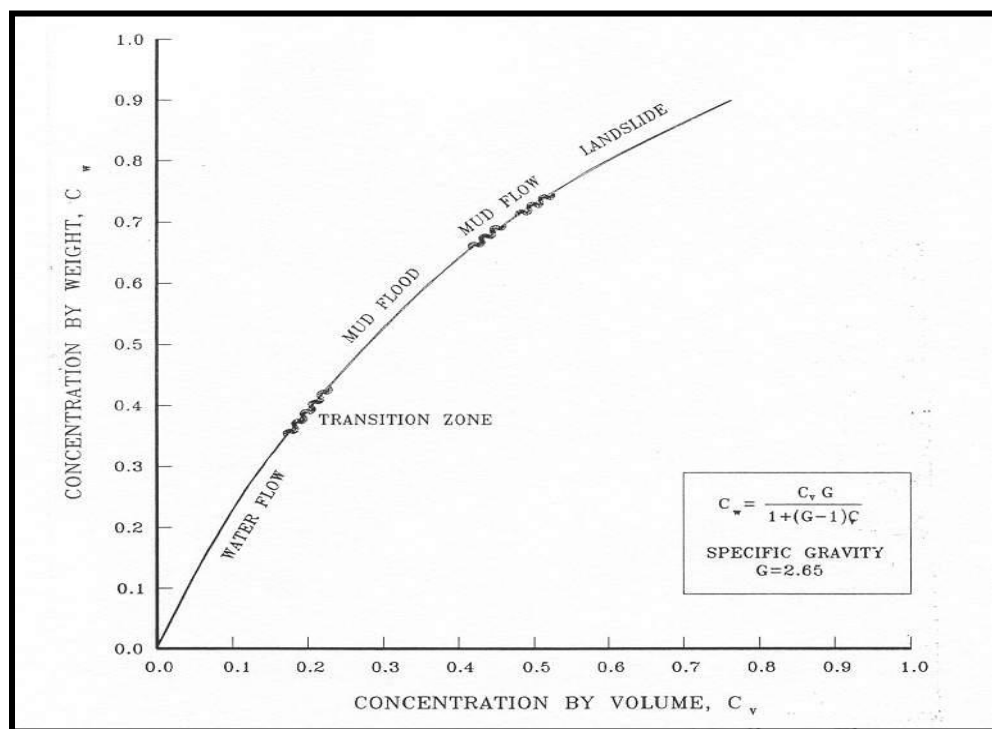


*Figure 45. Classification of Hyperconcentrated Sediment Flows.*

Initial attempts to simulate debris flows were accomplished with one-dimensional flow routing models. DeLeon and Jeppson (1982) modeled laminar water flows with enhanced friction factors. Spatially varied, steady-state Newtonian flow was assumed, and flow cessation could not be simulated. Schamber and MacArthur (1985) created a one-dimensional finite element model for mudflows using the Bingham rheological model to evaluate the shear stresses of a nonNewtonian fluid. O'Brien (1986)

designed a one-dimensional mudflow model for watershed channels that also utilized the Bingham model. In 1986, MacArthur and Schamber presented a two-dimensional finite element model for application to simplified overland topography (Corps, 1988). The fluid properties were modeled as a Bingham fluid whose shear stress is a function of the fluid viscosity and yield strength.

Table 10. Mudflow Behavior as a Function of Sediment Concentration.			
	Sediment Concentration		Flow Characteristics
	by Volume	by Weight	
Landslide	0.65 - 0.80	0.83 - 0.91	Will not flow; failure by block sliding
	0.55 - 0.65	0.76 - 0.83	Block sliding failure with internal deformation during the slide; slow creep prior to failure
Mudflow	0.48 - 0.55	0.72 - 0.76	Flow evident; slow creep sustained mudflow; plastic deformation under its own weight; cohesive; will not spread on level surface
	0.45 - 0.48	0.69 - 0.72	Flow spreading on level surface; cohesive flow; some mixing
Mud Flood	0.40 - 0.45	0.65 - 0.69	Flow mixes easily; shows fluid properties in deformation; spreads on horizontal surface but maintains an inclined fluid surface; large particle (boulder) setting; waves appear but dissipate rapidly
	0.35 - 0.40	0.59 - 0.65	Marked settling of gravels and cobbles; spreading nearly complete on horizontal surface; liquid surface with two fluid phases appears; waves travel on surface
	0.30 - 0.35	0.54 - 0.59	Separation of water on surface; waves travel easily; most sand and gravel has settled out and moves as bedload
	0.20 - 0.30	0.41 - 0.54	Distinct wave action; fluid surface; all particles resting on bed in quiescent fluid condition
Water Flood	< 0.20	< 0.41	Water flood with conventional suspended load and bedload

Takahashi and Tsujimoto (1985) proposed a two-dimensional finite difference model for debris flows based a dilatant fluid model coupled with Coulomb flow resistance. The dilatant fluid model was derived from Bagnold's dispersive stress theory (1954) that describes the stress resulting from the collision of sediment particles. Later, Takahashi and Nakagawa (1989) modified the debris flow model to include turbulence.

O'Brien and Julien (1988), Julien and Lan (1991), and Major and Pierson (1992) investigated mudflows with high concentrations of fine sediment in the fluid matrix. These studies showed that mudflows

behave as Bingham fluids with low shear rates ( $<10\text{ s}^{-1}$ ). In fluid matrices with low sediment concentrations, turbulent stresses dominate in the core flow. High concentrations of non-cohesive particles combined with low concentrations of fine particles are required to generate dispersive stress. The quadratic shear stress model proposed by O'Brien and Julien (1985) describes the continuum of flow regimes from viscous to turbulent/dispersive flow.

Hyperconcentrated sediment flows involve the complex interaction of fluid and sediment processes including turbulence, viscous shear, fluid-sediment particle momentum exchange, and sediment particle collision. Sediment particles can collide, grind, and rotate in their movement past each other. Fine sediment cohesion controls the nonNewtonian behavior of the fluid matrix. This cohesion contributes to the yield stress  $\tau_y$  which must be exceeded by an applied stress in order to initiate fluid motion. By combining the yield stress and viscous stress components, the well-known Bingham rheological model is prescribed.

For large rates of shear such as might occur on steep alluvial fans ( $10\text{ s}^{-1}$  to  $50\text{ s}^{-1}$ ), turbulent stresses may be generated. In turbulent flow an additional shear stress component, the dispersive stress, can arise from the collision of sediment particles. Dispersive stress occurs when non-cohesive sediment particles dominate the flow and the percentage of cohesive fine sediment (silts and clays) is small. With increasing high concentrations of fine sediment, fluid turbulence and particle impact will be suppressed, and viscous flow will occur. Sediment concentration in a given flood event can vary dramatically and as a result viscous and turbulent stresses may alternately dominate, producing flow surges.

FLO-2D routes mudflows as a fluid continuum by predicting viscous fluid motion as function of sediment concentration. A quadratic rheologic model for predicting viscous and yield stresses as function of sediment concentration is employed and sediment continuity is observed. As sediment concentration changes for a given grid element, dilution effects, mudflow cessation and the remobilization of deposits are simulated. Mudflows are dominated by viscous and dispersive stresses and constitute a very different phenomenon than those processes of suspended sediment load and bedload in conventional sediment transport. It should be noted that the sediment transport and mudflow components **cannot** be used together in a FLO-2D simulation.

The shear stress in hyperconcentrated sediment flows, including those described as debris flows, mudflows and mud floods, can be calculated from the summation of five shear stress components. The total shear stress  $\tau$  depends on the cohesive yield stress  $\tau_c$ , the Mohr-Coulomb shear  $\tau_{mc}$ , the viscous shear stress  $\tau_v$  ( $\eta \frac{dv}{dy}$ ), the turbulent shear stress  $\tau_t$ , and the dispersive shear stress  $\tau_d$ .

$$\tau = \tau_c + \tau_{mc} + \tau_v + \tau_t + \tau_d$$

When written in terms of shear rates ( $dv/dy$ ), the following quadratic rheological model can be defined (O'Brien and Julien, 1985):

$$\tau = \tau_y + \eta \left( \frac{dv}{dy} \right) + C \left( \frac{dv}{dy} \right)^2$$

where

$$C = \rho_m l^2 + f(\rho_m, C_v) d_s^2$$

and

$$\tau_y = \tau_c + \tau_{mc}$$

In these equations  $\eta$  is the dynamic viscosity;  $\tau_c$  is the cohesive yield strength; the Mohr Coulomb stress  $\tau_{mc} = p_s \tan \phi$  depends on the intergranular pressure  $p_s$  and the angle of repose  $\phi$  of the material;  $C$  denotes the inertial shear stress coefficient, which depends on the mass density of the mixture  $\rho_m$ , the Prandtl mixing length  $l$ , the sediment size  $d_s$  and a function of the volumetric sediment concentration  $C_v$ . Bagnold (1954) defined the functional relationship  $f(\rho_m, C_v)$  in the above equation as:

$$f(\rho_m, C_v) = a_i \rho_m \left[ \left( \frac{C_*}{C_v} \right)^{1/3} - 1 \right]$$

where  $a_i$  ( $\sim 0.01$ ) is an empirical coefficient and  $C_*$  is the maximum static volume concentration for the sediment particles. It should be noted that Takahashi (1979) found that the coefficient  $a_i$  may vary over several orders of magnitude. Egashira et al. (1989) revised this relationship and suggested the following:

$$f(\rho_s, C_v) = \frac{\pi}{12} \left( \frac{6}{\pi} \right)^{1/3} \sin^2 \alpha_I \rho_s (1 - e_n^2) C_v^{1/3}$$

where the energy restitution coefficient  $e_n$  after impact ranges  $0.70 < e_n < 0.85$  for sands,  $\alpha_I$  is the average particle impact angle and  $\rho_s$  is the mass density of sediment particles.

The first two stress terms in the above quadratic rheological model are referred to as the Bingham shear stresses (Figure 46). The sum of the yield stress and viscous stress define the total shear stress of a cohesive mudflow in a viscous flow regime. The last term is the sum of the dispersive and turbulent shear stresses and defines an inertial flow regime for a mud flood. This term is a function of the square of the velocity gradient. A discussion of these stresses and their role in hyperconcentrated sediment flows can be found in Julien and O'Brien (1987, 1993).

A mudflow model that incorporates only the Bingham stresses and ignores the inertial stresses assumes that the simulated flow is dominated by viscous stresses. This assumption is not universally appropriate because all mud floods and some mudflows are very turbulent with velocities as high as 25 fps (8 m/s). Even mudflows with concentrations up to 40% by volume can be highly turbulent (O'Brien, 1986). Depending on the fluid matrix properties, the viscosity and yield stresses for high sediment concentrations can still be relatively small compared to the turbulent stresses. If the flow is controlled primarily by the viscous stress, it will result in lower velocities. Conversely, if the viscosity and yield stresses are small, the turbulent stress will dominate, and the velocities will be higher.

To delineate the role of turbulent and dispersive forces in sand and water mixtures, Hashimoto (1997) developed simplified criteria involving only flow depth  $d$  and sediment size  $D_i$ . When  $d/D_i < 30$ , the intergranular forces are dominant. If  $d/D_i > 100$ , inertial forces dominate. In the range  $30 < d/D_i < 100$  both forces play an important role in the momentum exchange. It should be noted, that sediment concentration is a critical factor that is not accounted for in this criterion.

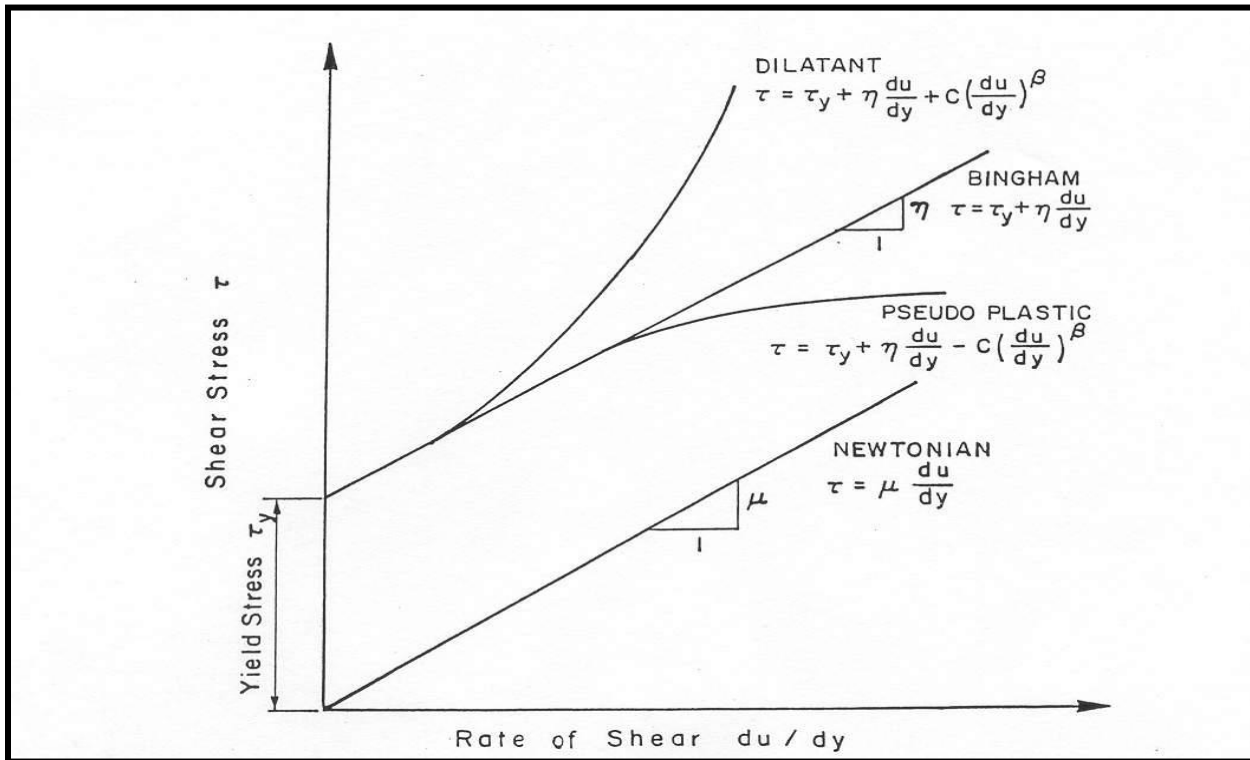


*Figure 46. Shear Stress as a Function of Shear Rate for Fluid Deformation Models.*

To define all the shear stress terms for use in the FLO-2D model, the following approach was taken. By analogy, from the work of Meyer-Peter and Müller (1948) and Einstein (1950), the shear stress relationship is depth integrated and rewritten in the following form as a dimensionless slope:

$$S_f = S_y + S_v + S_{td}$$

where the total friction slope  $S_f$  is the sum of the yield slope  $S_y$ , the viscous slope  $S_v$ , and the turbulent-dispersive slope  $S_{td}$ . The viscous and turbulent-dispersive slope terms are written in terms of depth-averaged velocity  $V$ . The viscous slope can be written as:

$$S_v = \frac{K}{8} \frac{\eta}{\gamma_m} \frac{V}{h^2}$$

where  $\gamma_m$  is the specific weight of the sediment mixture. The resistance parameter  $K$  for laminar flow equals 24 for smooth wide rectangular channels but increases significantly ( $\sim 50,000$ ) with roughness and irregular cross section geometry.

In Table 11 for Kentucky Blue Grass with a slope of 0.01, K was estimated at 10,000 (Chen, 1976). A value of K = 2,285 was calibrated on the Rudd Creek, Utah mudflow for a residential area and has been used effectively for most urban studies. For laminar and transitional flows, turbulence is suppressed and the laminar flow resistance parameter K becomes important. In the FLO-2D model if K = 0 in the SED.DAT file, the value of K is automatically computed from the Manning's n-value.

Table 11. Resistance Parameters for Laminar Flow. <sup>1</sup>	
Surface	Range of K
Concrete/asphalt	24 - 108
Bare sand	30 - 120
Graded surface	90 - 400
Bare clay - loam soil, eroded	100 - 500
Sparse vegetation	1,000 - 4,000
Short prairie grass	3,000 - 10,000
Bluegrass sod	7,000 - 50,000

<sup>1</sup> Woolhiser (1975)

The flow resistance  $n_{td}$  of the turbulent and dispersive shear stress components are combined into an equivalent Manning's n-value for the flow:

$$S_{td} = \frac{n_{td}^2 V^2}{h^{4/3}}$$

At very high concentrations, the dispersive stress arising from sediment particle contact increases the flow resistance  $n_{td}$  by transferring more momentum flux to the boundary. To estimate this increase in flow resistance, the conventional turbulent flow resistance n-value  $n_t$  is increased by an exponential function of the sediment concentration  $C_v$ :

$$n_{td} = n_t b e^{mCv}$$

where:  $n_t$  is the turbulent n-value and  $b$  is a coefficient (0.0538) and  $m$  is an exponent (6.0896). This equation was based on unpublished paper by Julien and O'Brien (1998) that relates the dispersive and turbulent resistance in hyperconcentrated sediment flows as function of the ratio of the flow depth to the sediment grain size. The friction slope components can then be combined in the following form:

$$S_f = \frac{\tau_y}{\gamma_m h} + \frac{K \eta V}{8 \gamma_m h^2} + \frac{n_{td}^2 V^2}{h^{4/3}}$$

A quadratic equation solution to the friction slope equation has been formulated in the FLO-2D model to estimate the velocity for use in the momentum equation. The estimated velocity represents the flow velocity computed across the floodplain or channel element boundary using the average flow depth between the elements. Reasonable values of K and Manning's n-value can be assumed for the channel and overland flow resistance. The specific weight of the fluid matrix  $\gamma_m$ , yield stress  $\tau_y$  and viscosity  $\eta$

vary principally with sediment concentration. Unless a rheological analysis of the mudflow site material is available, the following empirical relationships can be used to compute viscosity and yield stress:

$$\tau_y = \alpha_2 e^{\beta_2 C_v}$$

and

$$\eta = \alpha_1 e^{\beta_1 C_v}$$

where  $\alpha_i$  and  $\beta_i$  are empirical coefficients defined by laboratory experiment (O'Brien and Julien, 1988). The viscosity (poises) and yield stress ( $\text{dynes}/\text{cm}^2$ ) are shown to be exponential functions of the volumetric sediment concentration  $C_v$  of silts and clays (and in some cases, fine sands) and do not include larger clastic material rafted along with the flow (Table 12 and Figure 47 and Figure 48).

**Table 12. Yield Stress and Viscosity as a Function of Sediment Concentration.**

Source	$\tau_y = \alpha e^{\beta C_v}$ ( $\text{dynes}/\text{cm}^2$ )		$\eta = \alpha e^{\beta C_v}$ (poises)	
	$\alpha$	$\beta$	$\alpha$	$\beta$
<b>Field Data</b>				
Aspen Pit 1	0.181	25.7	0.0360	22.1
Aspen Pit 2	2.72	10.4	0.0538	14.5
Aspen Natural Soil	0.152	18.7	0.00136	28.4
Aspen Mine Fill	0.0473	21.1	0.128	12.0
Aspen Watershed	0.0383	19.6	0.000495	27.1
Aspen Mine Source Area	0.291	14.3	0.000201	33.1
Glenwood 1	0.0345	20.1	0.00283	23.0
Glenwood 2	0.0765	16.9	0.0648	6.20
Glenwood 3	0.000707	29.8	0.00632	19.9
Glenwood 4	0.00172	29.5	0.000602	33.1
<b>Relationships Available from the Literature</b>				
Iida (1938)*	-	-	0.0000373	36.6
Dai et al. (1980)	2.60	17.48	0.00750	14.39
Kang and Zhang (1980)	1.75	7.82	0.0405	8.29
Qian et al. (1980)	0.00136	21.2	-	-
	0.050	15.48	-	-
Chien and Ma (1958)	0.0588	19.1-32.7	-	-
Fei (1981)	0.166	25.6	-	-
	0.00470	22.2	-	-

\*See O'Brien (1986) for the references.

Conversion: Shear Stress: 1 Pascal (PA) = 10  $\text{dynes}/\text{cm}^2$

Viscosity: 1 PAs = 10  $\text{dynes}\cdot\text{sec}/\text{cm}^2$  = 10 poises

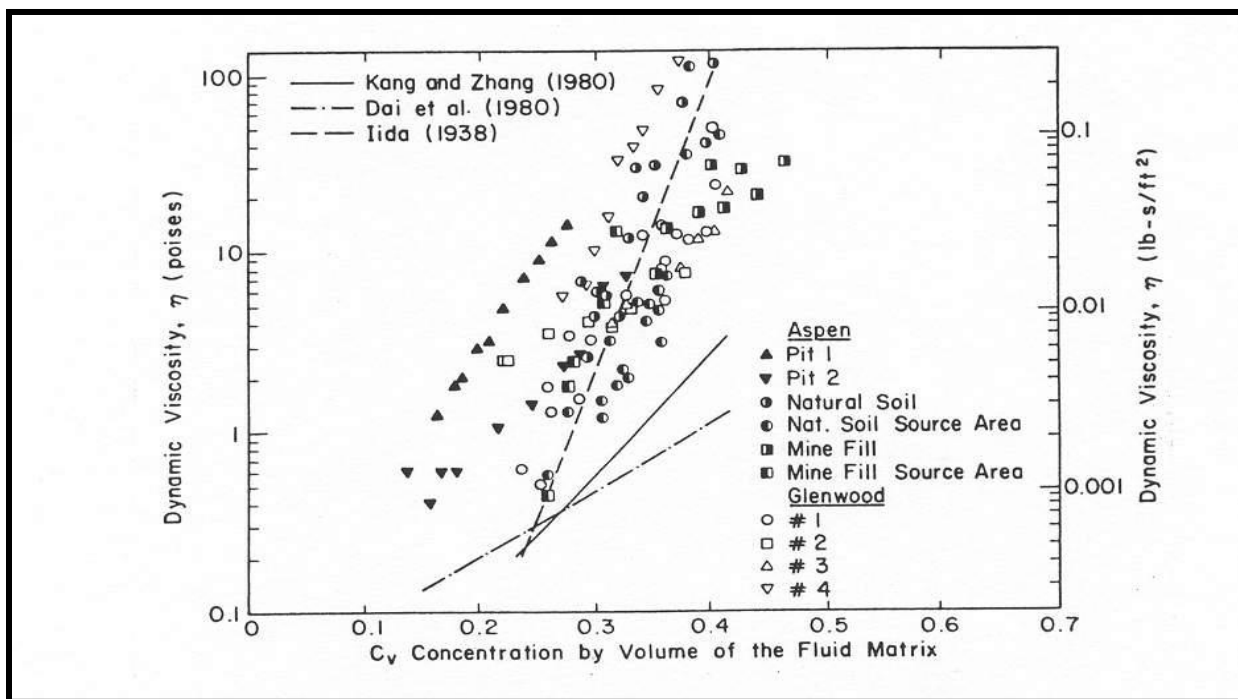


Figure 47. Dynamic Viscosity of Mudflow Samples versus Volumetric Concentration.

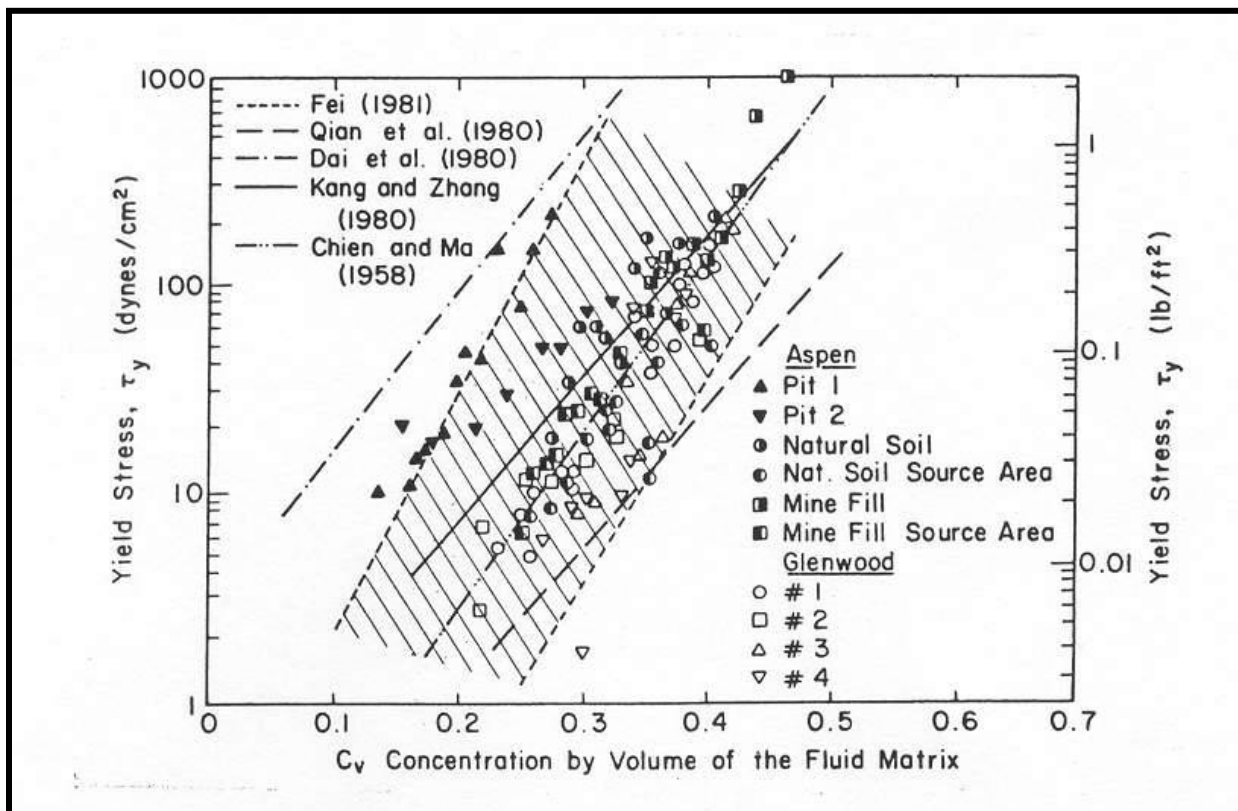


Figure 48. Yield Stress of Mudflow Samples versus Volumetric Concentration.

The viscosity of the fluid matrix is also a function of the type and percentage of silts and clays and the fluid temperature. Very viscous mudflows have high sediment concentrations and correspondingly high yield stresses and may result in laminar flow although laminar flows in nature are extremely rare. Less viscous flows (mud floods) are always turbulent.

For a mudflow event, the average sediment concentration generally ranges between 20% and 35% by volume with peak concentrations approaching 50% (Table 12 and Figure 47 and Figure 48). Large flood events such as the 100-year flood may contain too much water to produce a viscous mudflow event. Smaller rainfall events such as the 10-year or 25-year return period storm may have a greater propensity to create viscous mudflows. Most watersheds with a history of mudflow events will gradually develop a sediment supply in the channel bed such that small storms may generate mudflow surges. Most rainfall induced mudflows follow a pattern of flood response. Initially clear water flows from the basin rainfall-runoff may arrive at the fan apex. This may be followed by a surge or frontal wave of mud and debris (40 to 50% concentration by volume). When the peak arrives, the average sediment concentration generally decreases to the range of 30 to 40% by volume. On the falling limb of the hydrograph, surges of higher sediment concentration may occur.

To simulate mudflows with the FLO-2D model, the MUD switch in the CONT.DAT must be turned on (MUD = 1) and the viscosity and yield stress variables in SED.DAT file must be specified (Line M). It is recommended that the viscosity and yield stress exponents and coefficients from Table 9 be selected for inclusion in the SED.DAT file. The field sample Glenwood 4, for example, creates a very viscous mudflow. A volumetric sediment concentration or a sediment volume must then be assigned to the water discharge for a timestep in the discretized inflow hydrograph in the INFLOW.DAT file. The inflow sediment volume may represent channel scour, bank erosion or hillslope failure. The incremental sediment volume is tracked through the routing simulation and reported as a total sediment volume in the summary volume conservation tables. This total sediment volume should be reviewed to determine if it is a reasonable sediment supply or yield from the watershed.

When routing the mud flood or mudflow over an alluvial fan or floodplain, the FLO-2D model preserves continuity for both the water and sediment. For every grid element and timestep, the change in the water and sediment volumes and the corresponding change in sediment concentration are computed. At the end of the simulation, the model reports on the amount of water and sediment removed from the study area (outflow) and the amount and location of the water and sediment remaining on the fan or in the channel (storage). The areal extent of mudflow inundation and the maximum flow depths and velocities are a function of the available sediment volume and concentration which can be varied in the FLO-2D simulations. For further discussion on model hyperconcentrated sediment flows, refer to the FLO-2D white paper document *“Simulating Mudflows Guidelines”*.

#### **4.17 Specific Energy, Impact and Static Pressure**

For overland flow, the specific energy, impact pressure and static pressure are computed and reported to a file on an output interval basis. MAPPER Pro and MAXPLOT can graphically display these parameters with spatial variability.

The specific energy is computed by adding the flow depth velocity head ( $V^2/2g$ ) to the flow depth. The maximum specific energy is reported to the file SPECENERGY.OUT by grid element.

The impact pressure  $P_i$  for a floodplain grid element is reported as a force per unit length (impact pressure  $\times$  flow depth). The user can then multiply the impact pressure by the structure length within the grid element to get a maximum impact force on the structure. Impact force is a function of fluid density, structure materials, angle of impact, and a number of other variables. To conservatively estimate the impact pressure, the equation for water taken from Deng (1996):

$$P_i = k \rho_f V^2$$

where  $P_i$  is the impact pressure, coefficient  $k$  is 1.28 for both English and SI units,  $\rho_f$  = water density and  $V$  is the maximum velocity regardless of direction. For hyperconcentrated sediment flows such as mud floods and mudflows, the fluid density  $\rho_f$  and coefficient  $k$  is a function of sediment concentration by volume. The coefficient  $k$  is based on a regressed relationship as a function of sediment concentration from the data presented in Deng (1996). This relationship is given by,

$$k = 1.261 e^{Cw}$$

where  $Cw$  = sediment concentration by weight. The impact pressure is reported in the file IMPACT.OUT.

The static pressure  $P_s$  for each grid element is also expressed as a force per unit length. It is given by the maximum flow depth to the center of gravity  $\hat{h}$  times the specific weight of the fluid. The static pressure is then multiplied by the flow depth to compute the static force per unit length of structure (assumes surface area  $A = l \times d$ ). The maximum static pressure is written to the STATICPRESS.OUT file.

$$P_s = \gamma \hat{h}$$

#### **4.18 Floodway Delineation**

The floodplain management concept of the floodway delineation is to reserve an unobstructed area of flood conveyance passage while allowing for potential utilization of the floodplain. In the United States FEMA procedures outline a method for designating a floodway using the Corps of Engineers HEC-RAS model. Floodway boundaries are designed to accommodate a 100-yr flood within acceptable limits. The floodplain areas that can be eliminated from potential flood storage without violating the floodway criteria can be considered for potential development. The general guidelines for floodway delineation are:

- The floodway is based on the 100-yr flood.

- The floodplain is divided into floodway and floodway fringe zones. It is generally assumed that all the flood conveyance in the floodway fringe is eliminated.
- The floodway will pass the 100-yr flood without raising the water surface elevation more than 1 ft (0.3 m) above the maximum floodplain water surface.
- The floodway is determined by means of equal reduction of conveyance on both sides of the channel.

The above guidelines are convenient artifacts of the single discharge, steady flow HEC-RAS model but do not reflect reality. Flooding in the floodway fringe is never eliminated. If development is allowed in the floodway or along the floodway fringe, flood volume will be forced into other areas of the floodway fringe or downstream even if the water surface is raised less than 1 ft. Furthermore, the assumption that equal reduction of conveyance on both sides of the channels is also not true because floodplain water surface elevations are always different on each side of the river. Equal conveyance reduction is an oversimplification related to steady flow, uniform water surface in HEC-RAS results. In the Rio Grande floodplain for example, the measured water surface may be several feet higher on one side of the river than the other and even several feet higher at the riverbank than near the levee over a 1,000 ft (300 m) from the river.

The HEC-RAS procedure to delineate a floodway to apply encroachment criteria using one or more options and make reasonable adjustments until acceptable results are obtained both from a flood hydraulics standpoint and from a floodplain management perspective. Floodway determination is difficult for a number of flooding conditions including streams with a mild slope and large floodplain; rivers with split flow or levee overflow; alluvial fans with unconfined flooding and mobile boundaries; high velocity channels; and developed floodplain areas with ineffective flow areas. One of primary concerns is that the floodway encroachment procedure using HEC-RAS ignores the effects of floodwave attenuation and potential increase in water surface elevation in the downstream floodway fringe zone. Physically constricting the conveyance flow area with a floodway would have the effect of forcing more flood volume downstream. Using a single discharge model to delineate a floodway can underestimate the potential impacts of increased downstream flooding as development encroaches on the upstream floodplain fringe. The application of an encroachment depth will also increase the channel conveyance and storage. This may offset some of the volume getting forced downstream by the floodway encroachment.

The floodway routine in the FLO-2D model is automated. Since FLO-2D is a flood routing model, the floodway component can address all the physical process issues associated with the HEC-RAS floodway encroachment scheme. To delineate a floodway for a FLO-2D flood simulation, first it is necessary to complete a base flood simulation to define the water surface for the existing conditions. An output file (FLOODWAY.OUT) is generated that lists the maximum water surface elevations for each floodplain grid element. The user then sets the floodway switch in the CONT.DAT to “on” and assigns the encroachment depth (ENCROACH in CONT.DAT). Typically, one foot (0.3 m) is assigned as the encroachment depth. The FLO-2D floodway simulation is then run. At runtime, the model will add the encroachment depth to the maximum water surface elevation in the FLOODWAY.OUT file to compute

an encroachment water surface elevation for a given grid element that must be exceeded in order for the model to exchange the discharge with other grid elements. As the overbank flooding ensues, the model confines the flood to those floodplain grid elements whose encroachment water surface elevation is not exceeded. This forces more water volume downstream increasing the floodplain inundation in response to the upstream confined floodway conveyance. The result is a mapped area of the floodway and floodway fringe that reflects the redistribution of the flood volume in the system. The procedure for performing the floodway simulation is as follows:

- Complete a base run FLO-2D floodwall simulation.
- Set IFLOODWAY = 1 or “on” and ENCROACH = ~ 1 ft (0.3 m) in CONT.DAT.
- Run the floodway simulation with FLO-2D.

The FLO-2D floodway rules for sharing discharge are:

1. The FLO-2D Model defines floodway elements as floodplain elements with flow depth > ENCROACH value in the base run. Channel bank elements are automatically assigned as floodway elements.
2. If the two floodplain elements sharing discharge are non-floodway elements, flow is shared between the elements (allows for rainfall runoff).
3. If both floodplain elements are floodway elements, then flow is shared between them.
4. If one floodplain element is a floodway element and the other is not, flow is not shared until the predicted water surface exceeds the base flood simulation maximum water surface elevation plus the ENCROACH value. When this occurs, the non-floodway element is re-assigned to be a floodway element.

In this manner, the flow first fills the floodway element until the maximum water surface plus the encroachment depth is exceeded. Then the flow spills over into other floodplain grid elements. The floodway is expanded automatically away from the channel banks or the center of the unconfined conveyance area as the floodway elements are filled. The floodway schematic flow chart is shown in Figure 49 and an example of a floodway delineation for overland flow without a channel is shown in Figure 50 and 51. Figure 52 shows a floodway delineation for a flooding from a small channel. Using MAPPER Pro, the floodway can be displayed a shaded contour, a contour line plot, or as a single contour outline only the floodway area.

The primary objective in creating the FLO-2D floodway routine was to automate the floodway routine and remove the subjectivity that is necessary with the HEC-RAS floodway delineation. Nevertheless, some judgment may still be required when delineating the final floodway boundary.

## FLO-2D Floodway Scheme

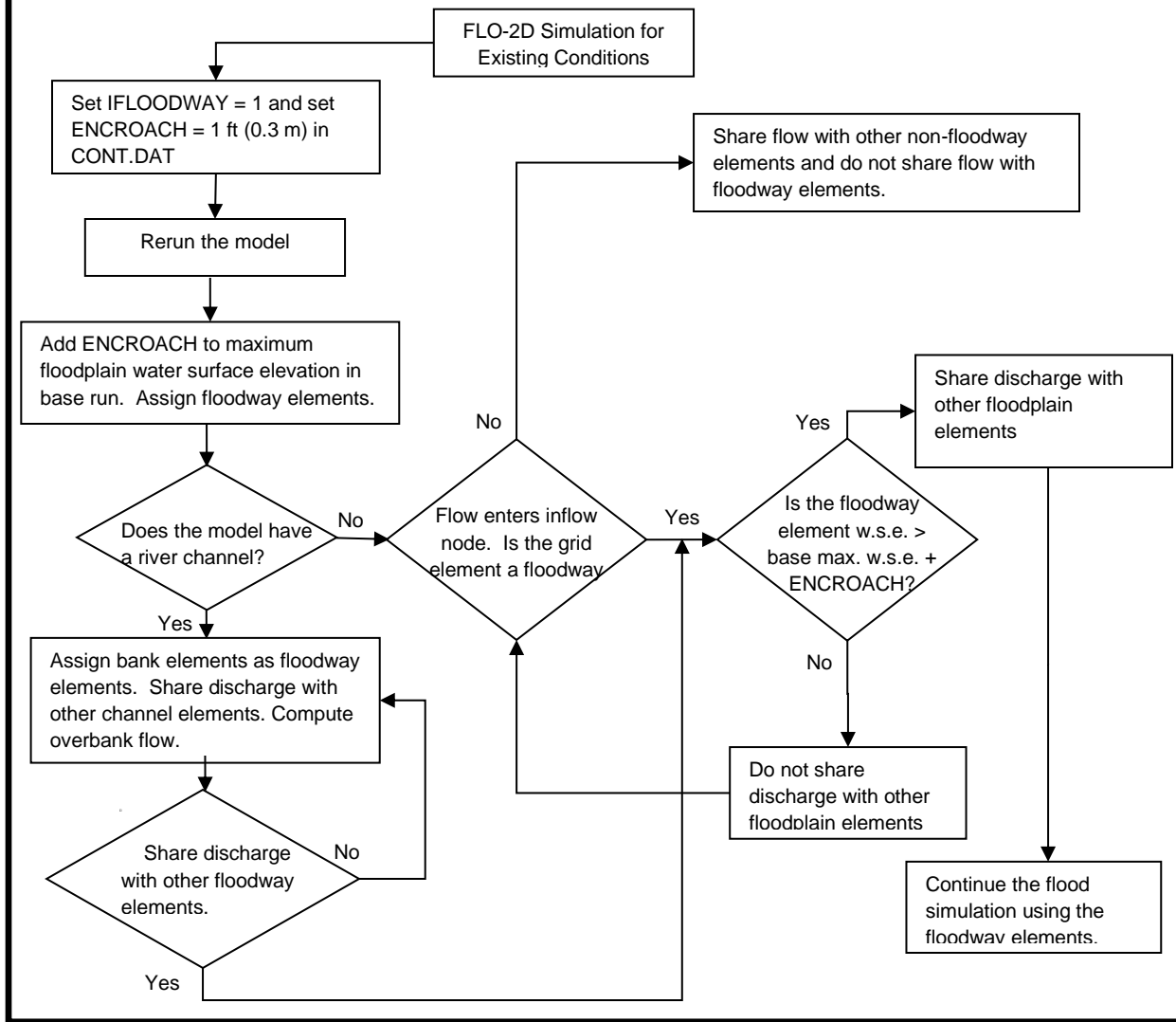
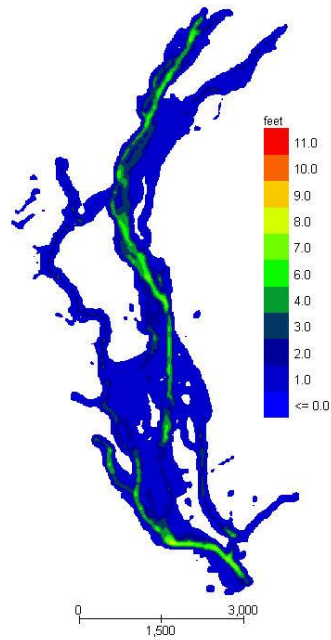


Figure 49. Floodway Schematic Flow Chart.

Grid Element Maximum Flow Depth



*Figure 50. Base Flood.*

Grid Element Maximum Flow Depth

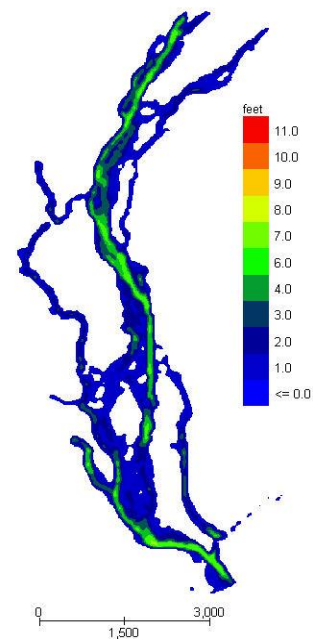


*Figure 51. Floodway Delineation No Floodway.*

Grid Element Maximum Flow Depth

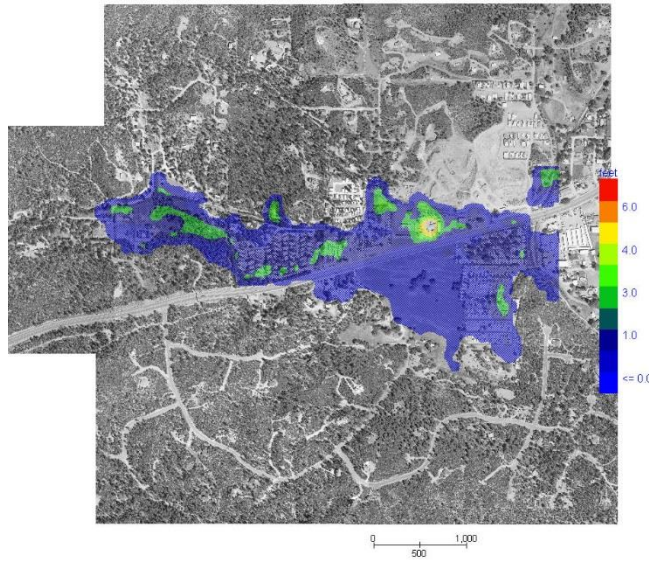
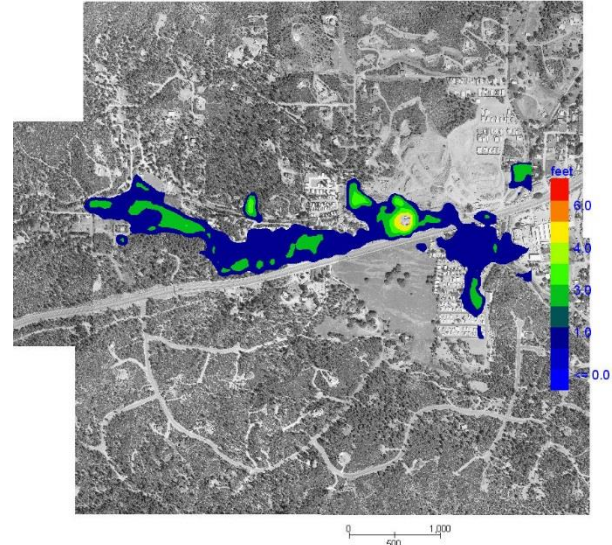


*Figure 52. Floodway Delineation.*

Grid Element Maximum Flow Depth



Base Flood Delineation (Left)

Floodway Delineation (Right)

## 4.19 Groundwater – Surface Water Modeling

The FLO-2D flood routing model is linked with the USGS MODFLOW-2005 Groundwater Flow Process (GWF) package to simulate integrated surface – subsurface water exchange which can occur in any direction, as unsteady and spatially distributed flow. The models are fully coupled allowing groundwater recharge and river recharge from groundwater simultaneously. At any particular time in the simulation, water may be infiltrating from the surface water to the groundwater on one portion of the project while on other areas the opposite may occur. The model timesteps are synchronized as follows:

- The MODFLOW simulation is divided into a series of stress periods during which specific parameters (e.g. variable heads) are constant.
- Each stress period, in turn, is divided into a series of computational timesteps.
- FLO-2D model timesteps are smaller than the MODFLOW model timesteps, so a number of FLO-2D computational sweeps are performed to match the MODFLOW model simulation time.

Infiltrated floodplain water predicted by FLO-2D is exchanged to the groundwater cells below. If the groundwater is lower than the channel bed elevation, the infiltration volume is passed to the corresponding MODFLOW grid element. If the groundwater is higher than the channel water surface elevation, the exchange flow will enter the river.

The GDS creates the data for the integration of the models. It will generate a subset of the required variables for groundwater simulation (Figure 53). Refer the MODFLO-2D manual for more details.

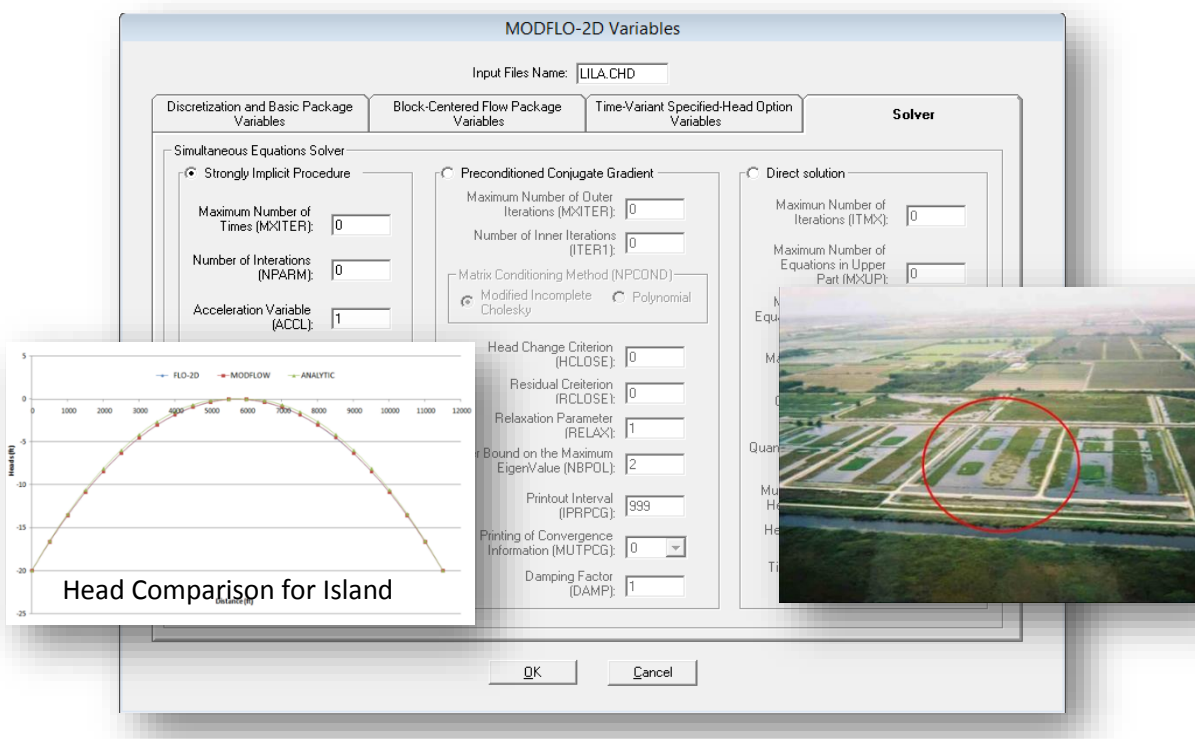


Figure 53. GDS Data Entry for a MODFLOW Groundwater Simulation.

#### 4.20 Building Collapse

In the FLO-2D model, the loss of flood storage due to buildings is simulated with area reduction factors (ARF values) that reduce the surface area of a grid element (percentage). A grid element may be totally blocked ( $ARF = 1$ ) or partially blocked ( $ARF < 1$ ). A group of grid elements together may constitute a large building such as a school or mall (Figure 54 a and b). In Figure 54 the grey grid elements represent total blockage while the yellow elements are partially blocked. The flood flow will go around a totally blocked building.



*Figure 54. Buildings with a FLO-2D Grid System and ARF Values Representing Buildings.*

During a flood event or a mud/debris flow, it is possible that a building could collapse and be removed. There are number of ways for this to happen. The flood dynamic forces or static pressure could simply knock the structure over, push it off the foundation, or rip it apart. Scour and erosion could undermine the structure resulting a collapse into the flow. Large rocks could impact the structure. The integrity of the building structure could be compromised by getting wet. In any case, the flooding could destroy the building and allow the flow to go through the previously occupied grid element(s).

To predict the collapse of the building during flooding vulnerability curves can be applied. An approach to predicting building collapse was undertaken by Pilotti, et al. (2016) that is like the Bureau of Reclamation (BOR, 1988) application of vulnerability curves for people, vehicles and structures. Pilotti (2016) considered a masonry building constructed with materials such as brick or stone bound together by mortar. These types of building walls have low tensile strength and support the roof or upper story load. During a flood the collapse of a wall can result in the entire destruction of the building.

#### Building Vulnerability

Pilotti et al. (2016) provides a rigorous mathematical formulation of the approach which includes the computation of the dynamic forces and pressures on a building cell, the axial loading, the maximum bending moment and the resistive forces. His final product is a set of vulnerability curves based on a maximum depth for a given velocity above which the building will fail (Figure 55). This method is similar to BOR (1988) vulnerability curves for mobile homes and buildings with a foundation (Figure 56 and Figure 57). Other building types and potential failure mechanisms could be considered to generate a series of vulnerability curves.

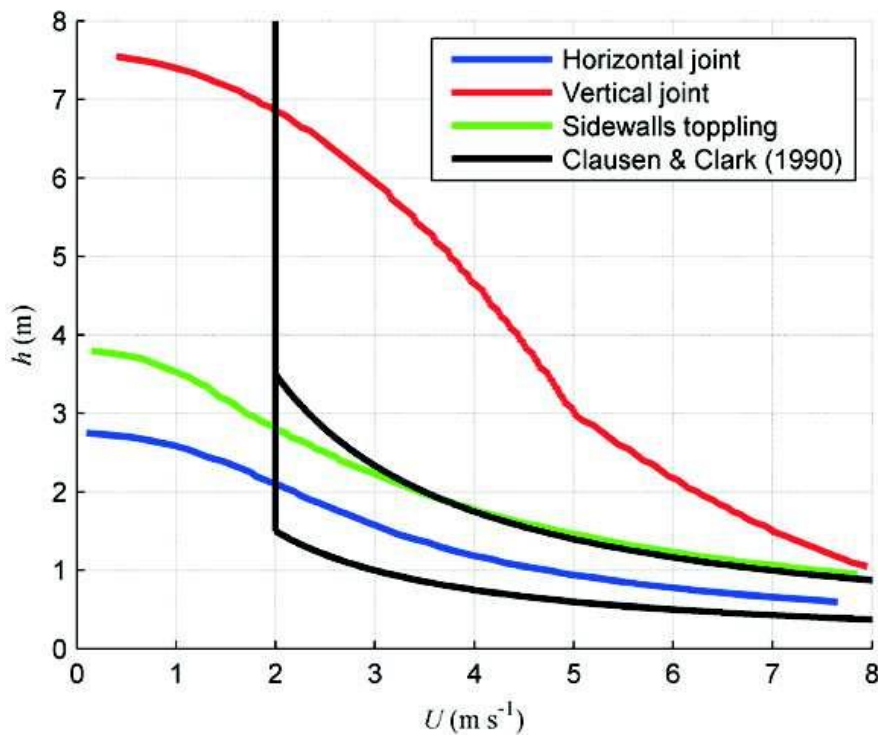


Figure 55. Vulnerability Curves. (Pilotti et al., 2016).

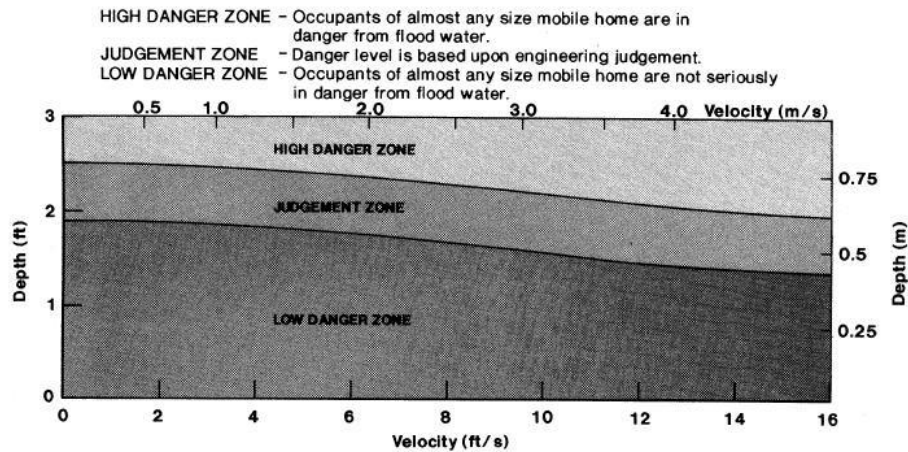


Figure 56. Vulnerability Curve for Mobile Homes (BOR, 1988).

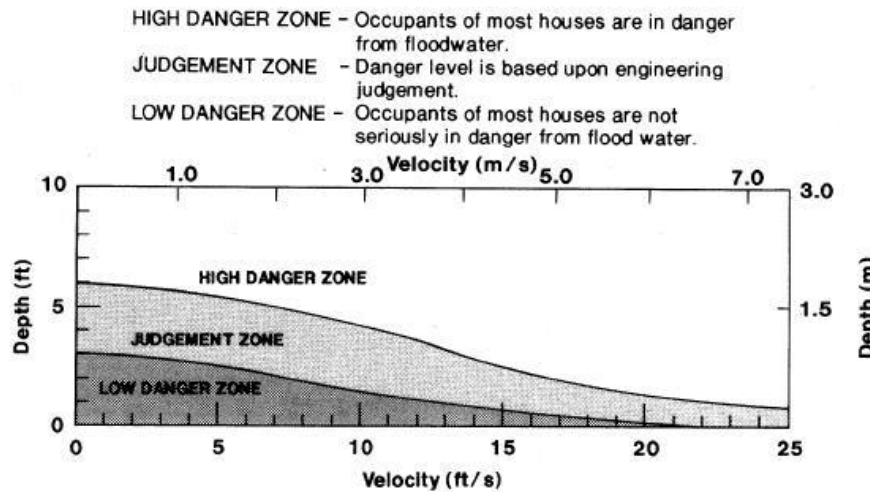


Figure 57. Vulnerability Curves for Buildings with a Foundation (BOR, 1988).

In the work of Pilotti et al (2016), a conservative approach was taken to generate the depth for a given flood velocity that would cause the building to collapse. This line is expressed as a polynomial equation with depth as a function of velocity which predicts the maximum flow depth (threshold depth) above which the building is presumed to fail (Figure 58).

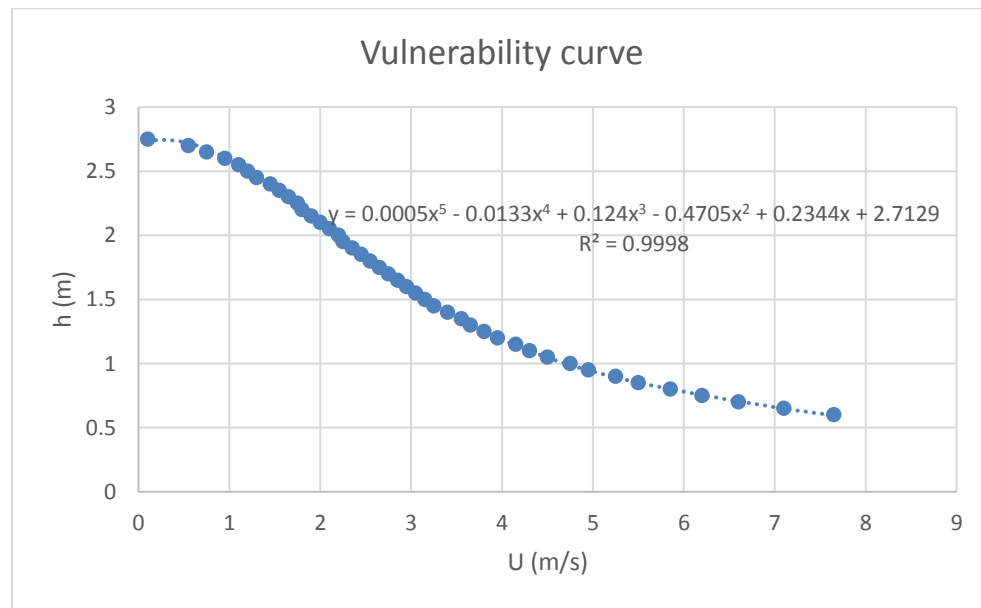


Figure 58. Vulnerability Curve for a Masonry Building (Pilotti et al., 2016).

Plotting all three vulnerability curves (including the 2 BOR curves) on the same graph reveals that a masonry building is predicted to be less susceptible to collapse (Figure 59). The three vulnerability curves have been interpreted as poor or highly susceptible to flood collapse (mobile homes), moderate for buildings with foundations, and good for building with more substantial construction. A fourth curve (Clausen & Clark, 1990) was recommended by Pilotti et al. (2016) (Figure 59 black lines). According to Clausen & Clark (1990) building collapse is not predicted for a velocity less than 6 fps. The Clausen & Clark black lines in Figure 59 constitute a range of hydraulic values depending on construction materials and methods, but only the lower curve is applied in the FLO-2D model.

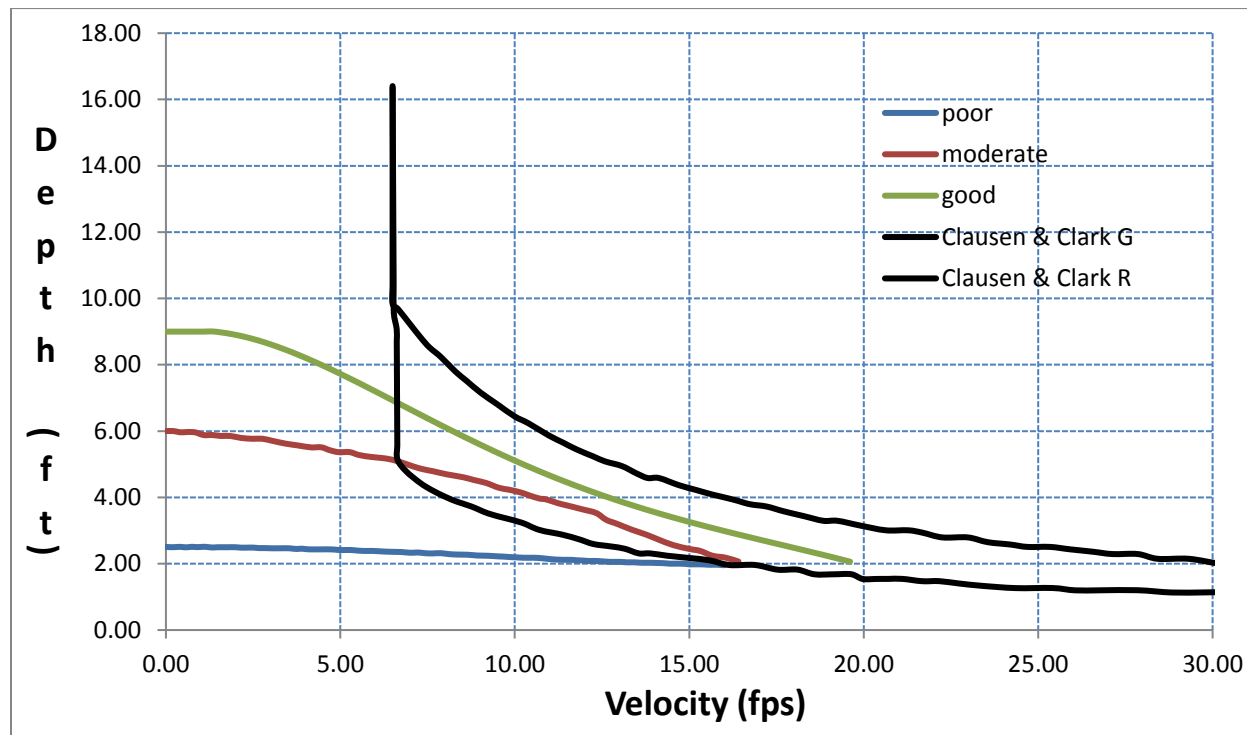


Figure 59. Vulnerability Curves for Building Subject to Collapse.

The vulnerability curves for the BOR mobile homes and buildings with foundations were regressed by digitizing Figure 56 for the delineation between the High Danger and the Judgment Zones. These curves should be considered as general guidelines for the potential for a building to collapse during a flood event. More research could define a series of vulnerability curves for different types of construction.

### Implementation of the Building Collapse in the FLO-2D Model

The polynomial equations relating the threshold depth for a building collapse as function of velocity for the four vulnerability curves shown in Figure 57 has been implemented in the FLO-2D model. There are two methods for initiating the building collapse routine: 1) Create the BUILDING\_COLLAPSE.DAT file consisting of the grid element; and 2) Assigning negative ARF values. In the first method, the vulnerability curves (1-poor, 2-moderate, 3-good and 4-Clausen & Clark upper curve) from Figure 57 includes a global curve and spatial variable curve assignments. In the file, Line 1 is a global vulnerability

curve assignment which is superseded by the individual grid element vulnerability curves. If a building consists of multiple grid elements, each element must have a vulnerability curve assignment to collapse the entire building. The global vulnerability curve value could be zero. A portion of a typical BUILDING\_COLLAPSE.DAT file is follows:

```

0 Global Vulnerability Curve
2
6756      1
1 Grid element, grid element curve (poor)
2 Grid element, grid element curve (moderate)
3 Grid element, grid element curve (good)
4
1
...

```

Assigning a nonzero value to the global vulnerability curve would initiate potential building failure for any of the buildings in the model.

The building collapse routine can also be activated by assigning a negative value to a completely blocked ARF value or to partially blocked ARF values as shown in the list below from an ARF.DAT file. The grid elements in red are assigned a negative value to assess the potential for collapse. This can be done in the FLO-2D graphical editor GDS. For this case, the upper Clausen & Clark (1990) is applied.

```

T 1450
T 1451
T -1452
T -1453
T 1454
T 2502
T 3818
T -3861
T -4435
T 4766
46 0.10 0.00 0.50 0.00 0.00 0.00 0.50 0.00 0.00
68 0.00 0.00 0.00 0.00 0.00 0.00 0.00 0.50
69 0.30 0.00 0.00 0.00 0.50 0.00 0.00 0.00 0.00
119 0.40 0.50 0.70 0.00 0.00 1.00 0.00 0.00 0.00
120 0.00 0.00 0.00 0.50 0.00 0.00 1.00 0.00 0.00
142 0.20 0.20 0.00 0.00 0.70 0.00 0.00 0.00 1.00
143 0.00 0.00 0.00 0.20 0.00 0.00 0.00 1.00 0.00
161 -0.50 0.00 0.00 0.00 0.00 0.00 0.00 0.00 0.00
162 -0.50 0.70 0.20 0.00 0.00 1.00 0.00 0.00 0.00
163 -0.10 0.00 0.00 0.70 0.00 0.00 1.00 0.00 0.00
182 0.30 0.00 0.00 0.00 0.00 0.00 0.00 0.00 0.00
185 0.00 0.00 0.00 0.00 0.20 0.00 0.00 0.00 1.00

```

A portion of building or the entire building can be assigned the collapse trigger (negative ARF value). For a complete collapse of the building that encompasses several elements, all of the designated building cells have to be assigned a negative ARF value. When the flow depth exceeds the tolerance value (TOL), the predicted flow velocity upstream of the building is used in the building collapse equation to predict the threshold collapse depth. In Figure 60, the building (shown in red) encompasses the entire grid element and the flooding is coming from the North direction (top of the page). The velocity used to compute the building collapse threshold depth is shown by the red arrow as the velocity from grid element 222 to grid element 221. If the flood flow depth exceeds the threshold depth for grid element 221, the ARF value in the building element is reset to zero (ARF = 0.0) for the next computational timestep and the flow can go through the building element. The negative ARF values in the ARF.DAT file can be combined during the same simulation with those in the BUILDING\_COLLAPSE.DAT file.

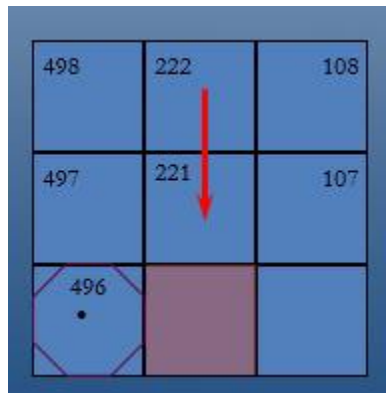


*Figure 60. Building (red square) is Flooded from the North Direction.*

A conservative approach is taken to predict the potential collapse of buildings. Based on vulnerability curves of depth versus velocity, when the computed threshold depth is exceeded by flood flow depth associated with a predicted velocity, the building area reduction factor ARF value is reset to zero enabling the flow to go through the grid element and fill it with flood storage. The building collapse routine is triggered by assigning grid element building vulnerability curves in BUILDING\_COLLAPSE.DAT or by assigning a negative ARF values for either a totally blocked or partially blocked grid element. In the future other building vulnerability curves to cover an expanded matrix of building types can be considered.

#### **4.21 Predicting Alluvial Fan Channel Avulsion**

Avulsion of alluvial fan channels depicts the rapid abandonment of one channel and the formation of a new channel with a steeper slope. Fuller (2012) defines avulsion as the process by which flow is diverted from an existing channel to a new water course. Channel avulsion is generally in response to two factors: 1) Sediment deposition or channel aggradation; and 2) Availability of a steeper slope in an alternative downslope direction (Schumm, 1977). Channel avulsion can also occur with the headcutting of an incised channel (sometimes referred to as channel piracy). A more extensive discussion of alluvial channel avulsion is presented in Fuller (2012).

Channel avulsion involves complex sediment transport processes that are difficult to predict with a flood routing model. The physical process of sediment scour and deposition by size fraction is impossible to predict with any accuracy on a channel reach basis, in part, because of the unknown volumes of different sediment sizes in the upstream watershed. Alluvial fan channel avulsion is often associated with hyperconcentrated sediment flows (mud and debris flow) frontal waves and surges. These frontal waves, surges or just high concentrations of coarse sediment deposit in channel at constrictions, break-in-slopes, or other channel variations and partially fill or plug the channel, forcing the flow overbank and initiating the scour or incision of a new channel down a steeper slope.

The area of inundation for alluvial fan flooding has been predicted by the FEMA FAN probabilistic model (FEMA, 2003) using an avulsion method modification. This is a simplistic model that has several limitations and is not recommended for studies or mapping where a realistic evaluation of the potential area of inundation or fan flood hydraulics is required. This model, however, has been used by FEMA to generate Flood Insurance Study (FIS) maps with alluvial fan flood hazard zones.

The Flood Control District of Maricopa County (FCDMC) requested a simplified avulsion routine be implemented in the FLO-2D model. Several FLO-2D model enhancements have been supported by the FCDMC. It was proposed that alluvial fan avulsion routine be developed for the FLO-2D model to assess the channel conveyance capacity on the area of inundation. The FCDMC outlined a methodology to guide the channel avulsion development.

### **FCDMC Simplified Channel Avulsion Approach**

The FCDMC proposed simplified channel avulsion analysis was presented as having three parts. Part 1 was the channel overtopping assessment; Part 2 was the channel avulsion assessment and Part 3 was to delineate the flood hazard associated with the channel avulsion. To summarize the District's channel avulsion concept, the focus is to simulate channels from a fan apex area that have the potential to overtop and avulse at predicted locations resulting an altered area of inundation. The District provide the following brief outline to accomplish this.

The District delineated different distributary channels starting with the primary or feeder channel at an alluvial fan apex (Figure 61). The first part of the analysis is to identify the locations for channel overtopping along the feeder channel and the first-level branch channels for 100-year flood where the point of avulsion is the first-level bifurcation point. The FLO-2D model will be used to estimate the channel overtopping locations.

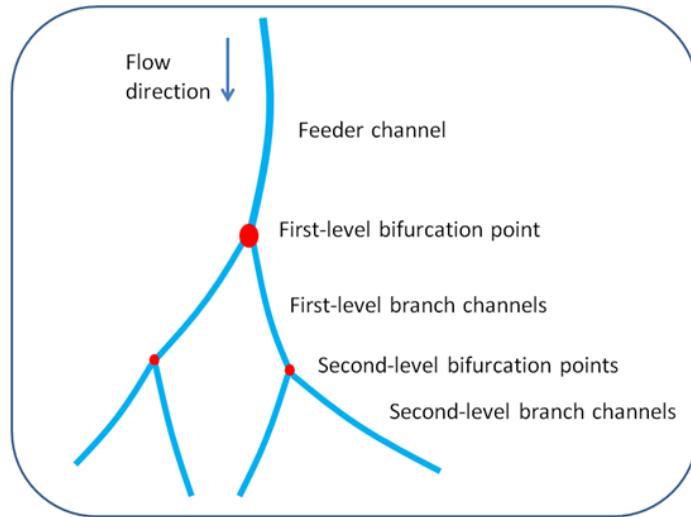


*Figure 61. Alluvial Fan Distributary Channel Definition for Avulsion Analysis (from FCDMC, 2014).*

In the conceptual outline, the District acknowledges the dependency of channel avulsion on sediment deposition indicating major channel avulsion usually occurs during a large flood after previous small floods fill the channel with sediment deposits on the order of 1 to 2 ft. Often sediment deposition has propensity to occur in bends, upstream of constrictions or break-in-slope, or in the presence of obstructions or increased roughness. While the role of sediment transport in channel avulsion is understood and could be simulated with the FLO-2D model, the District proposed to undertake a simpler approach to avoid the complexity associated with predicting sediment deposition. The District avulsion model concept was to:

- a. Build a 25-ft or smaller grid system for the 100-year flood and run the model where the grid element size would essentially constitute the channel cross section.
- b. Modify the channel topography (cross section) to account for the sediment deposition.
- c. Run the FLO-2D model and identify the channel overtopping locations.
- d. Predict the peak discharge at each overtopping location. This would provide the basis for the secondary channel.

To estimate the channel width and depth based on the peak discharge, the District propose to apply channel width and depth estimates based on empirical regime theory shown in Figure 62 and Figure 63 (USACE, 1994). The District indicates that if the channel depth is greater than or equal to 2 feet, then the newly formed channel is a major channel avulsion and the area of inundation is an active alluvial fan area. By assigning a representative sediment size fraction for the alluvial fan and the estimated peak discharge, Figure 62 and Figure 63 (provided by the District), can be used to estimate the channel width and depth.

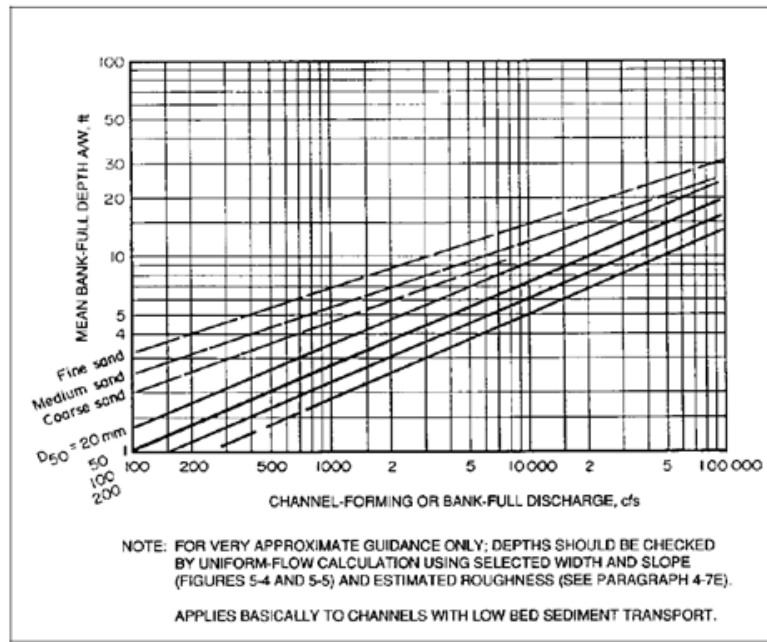


Figure 62. Channel Forming Depth versus Channel Forming Discharge (from USACE, 1994).

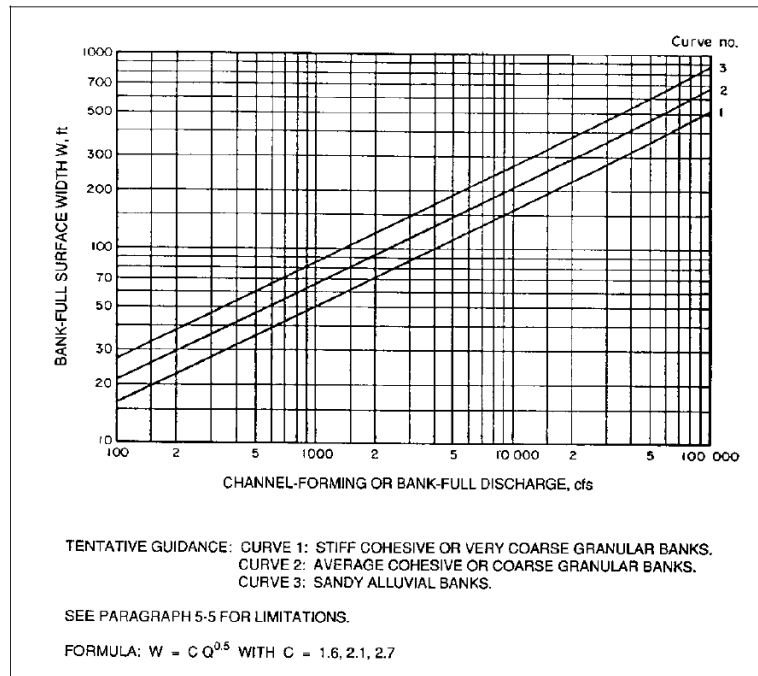


Figure 63. Channel Forming or Bank Full Discharge (from USACE, 1994).

The final task is to assess the area of inundation. It was observed by the District that since the newly formed channel caused by avulsion will impact a new area of the fan, further channel avulsion downstream may occur downstream and this may require several model iterations to delineate the entire fan area of inundation.

## **Implementing the FCDMC Channel Avulsion Approach into FLO-2D**

### ***Concepts and Assumptions***

The District original recommendation was to use small FLO-2D grid elements to represent the channel. This approach has several limitations:

- The premise of channel avulsions is based on a loss of channel conveyance capacity.
- The channel will have unique width to depth ratios and roughness which would be obscured by the uniform floodplain elements.
- Overbank flooding cannot be simply assessed using depressed floodplain elements because of the multi-directional flow.

The District's proposed avulsion method is based on computed widths and depths from Figure 62 and Figure 63 or the avulsed channels that cannot be simply represented by the floodplain element geometry. Using the floodplain elements on steep slopes does not limit the unconfined flow in the FLO-2D model to a singular direction because the upstream element water surface elevation may exceed the downstream cell elevations allowing the flow to distribute to all the downstream contiguous elements. It was apparent that to mimic channel avulsion, it is necessary to simulate channel flow in the FLO-2D model. It is fortunate, however, that the FLO-2D model has a distributary channel component referred to as "multiple channels".

The purpose of the multiple channel flow component is to simulate the overland flow in small channels rather than as overland sheet flow. Overland flow is often conveyed in small channels, even though they occupy only a fraction of the potential flow area. In the FLO-2D Pro Model Reference Manual (2013), the multiple channel flow is referred to as rill and gully flow. Schumm, et al. 1984, distinguish between rills and gullies as follows. Rills are an ephemeral small (smallest) channel formed by runoff and may be seasonal in nature and the result of overland flow. A gully is relatively deep channel formed by recent erosion where no previously defined channel existed. On alluvial fans, these two types of channels typically form the distributary system downstream of the fan apex and can have the same physical processes associated with avulsion, albeit to different scales. These channels should be distinguished from the entrenched or incised primary channel near the fan apex leading out of the watershed canyon mouth.

Simulating rill and gully distribute flow concentrates the discharge and may improve the timing of the runoff routing. The multiple channel routine calculates overland flow as sheet flow within the grid element and flow between the grid elements is computed as rill and gully flow. No overland sheet flow is exchanged between grid elements if both elements have assigned multiple channels. The gully

geometry is defined by a maximum depth, width and flow roughness. The multiple channel attributes can be spatially variable on the grid system and can be edited with the GDS program.

If the gully flow exceeds the specified gully depth, the multiple channel can be expanded by a specified incremental width. This channel widening process assumes these gullies are alluvial channels and will widen to accept more flow as the flow reaches bankfull discharge. There is no gully overbank discharge to the overland surface area within the grid element. The gully will continue to widen until the gully width exceeds the width of the grid element, then the flow routing between grid elements will revert to sheet flow. This enables the grid element to be overwhelmed by flood flows. During the falling limb of the hydrograph when the flow depth is less than 1 ft (0.3 m), the gully width will decrease to confine the discharge until the original width is again attained. The user can assign the range of slope where the multiple channel widening is computed.

#### ***4.22 Low Impact Development (LID) Modeling***

Low impact development (LID) can be assessed with the FLO-2D model using a spatially variable tolerance value TOL on individual grid elements. The TOL parameter was originally designed to represent a flow depth below which no discharge is shared between two grid elements. Typically for a large flood event a TOL value of 0.1 ft (0.03 m) is assigned in the TOLER.DAT file so that the model does not exchange discharge for negligible depths approaching zero. The intent is to reduce the number of computations required for large grid systems. For hydrology models, a lower TOL parameter represents the important physical process of depression storage. Depression storage remains on the grid system after the rainfall had ceased and is a portion of the initial abstraction (depression storage + interception) that must be filled for runoff to initiate. The initial abstraction cannot be more than the TOL value.

The concept of the LID is that each new residential or commercial construction would be required to design flood retention storage into the site development. This may include bioretention, green roofs, rain gardens, permeable pavement, drainage disconnection, swales, and on-site storage (Figure 64). Spatially variable TOL values would be assigned on a grid element basis to represent the composite LID techniques on a given grid element (Figure 65). Depending on size multiple grid elements may represent an individual lot or development. Different grid elements may represent different LID techniques. The volume of on-site retention storage can be assessed by multiplying the lot surface area by the retained flow depth (TOL value). This would provide flood hazard mitigation on a lot by lot basis. The LID storage would be displayed as a final flow depth in the Mapper program.

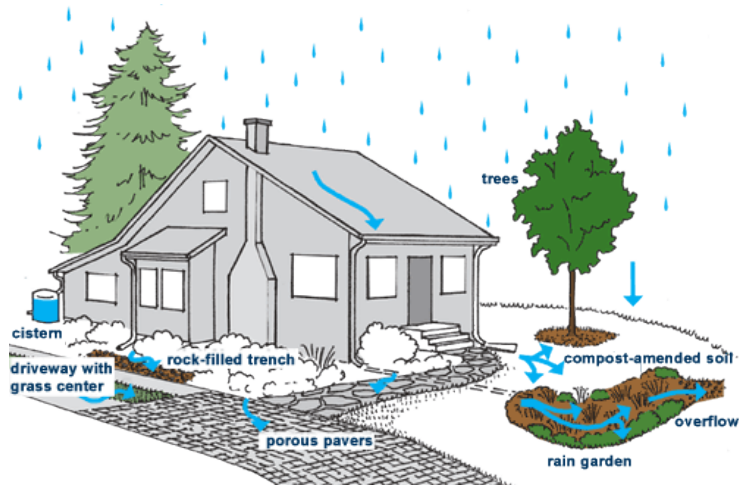


*Figure 64. Low Impact Development Water Retention.*

(Seattle Public Utilities, Rainwise Program,  
<http://www.seattle.gov/util/MyServices/DrainageSewer/Projects/GreenStormwaterInfrastructure/RainWise>)

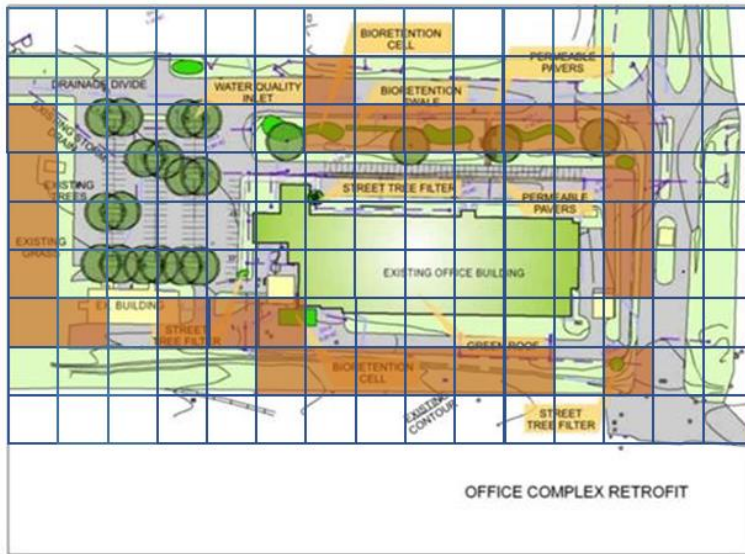


Figure 65. FLO-2D Grid Element LID Concept – Spatially Variable TOL Elements (brown).

(<http://www.lowimpactdevelopment.org>)

## FLO-2D Model Revisions for the LID Tool

The global assignment of the TOL value is still required in the first line (first parameter) in the TOLER.DAT but the name has been revised to TOLGLOBAL. When a FLO-2D model is initiated the TOLGLOBAL value

would be assigned to all the grid elements. This value would then be superseded by the spatially variable TOL(i) assignment for each grid element (Figure 3) listed in the file TOLSPATIAL.DAT.

There has been no change in how the TOL value is applied in the model code. The TOL depression storage must be filled before flow is exchanged with a neighbor grid element (Figure 66). Flow depth less than or equal to the TOL value will remain on the grid element after the simulation is complete. The typical range for Global TOL when used for depression storage only is:

$$0.004 < \text{TOL} \leq 0.1$$

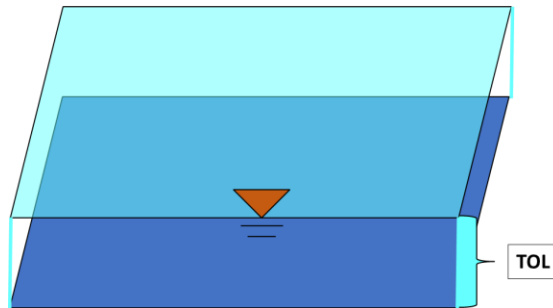


*Figure 66. Global TOL.*

The range for spatially variable TOL assignment when LID is added to depression storage is from:

$$0.001 \text{ to } 5.0 \text{ ft.}$$

5299	0.25
5111	0.25
4923	0.25
4735	0.25
4547	0.25
4359	0.25
5300	0.25
5112	0.25
4924	0.25
4736	0.25
4548	0.25
4360	0.25
5301	0.25
5113	0.25
4925	0.25

*Figure 67. Spatially Variable TOL Value Format in TOLSPATIAL.DAT.*

### **Using the LID Tool Results**

After a FLO-2D simulation with the spatially variable TOL grid element assignment, the primary effect will be greater water retention on those grid elements with TOL values that are higher than TOLGLOBAL. The results can be viewed in Mapper or MAXPLOT as higher final flows depths. It should be noted that final flow depths may also include residual flow that has not yet drained from the surface water. A difference plot can be generated in MAXPLOT to demonstrate the effect of the spatially variable TOL values by comparing the FINALDEP.OUT files for a base run with no spatially variable TOL values to a FLO-2D simulation where the spatially TOL values are assigned. Figure 68 is MAXPLOT graphic of the difference between the spatially variable and global TOL values and shows that the assignment of spatially variable TOL values results in higher depths. The global TOL value was 0.004 ft and the spatial variation in the TOL value ranged from 0.25 to 0.67 ft covering roughly 45% of the grid system. In this project the amount of storage on the floodplain after the storm has ended is higher (almost double) with the spatially variable TOL values.

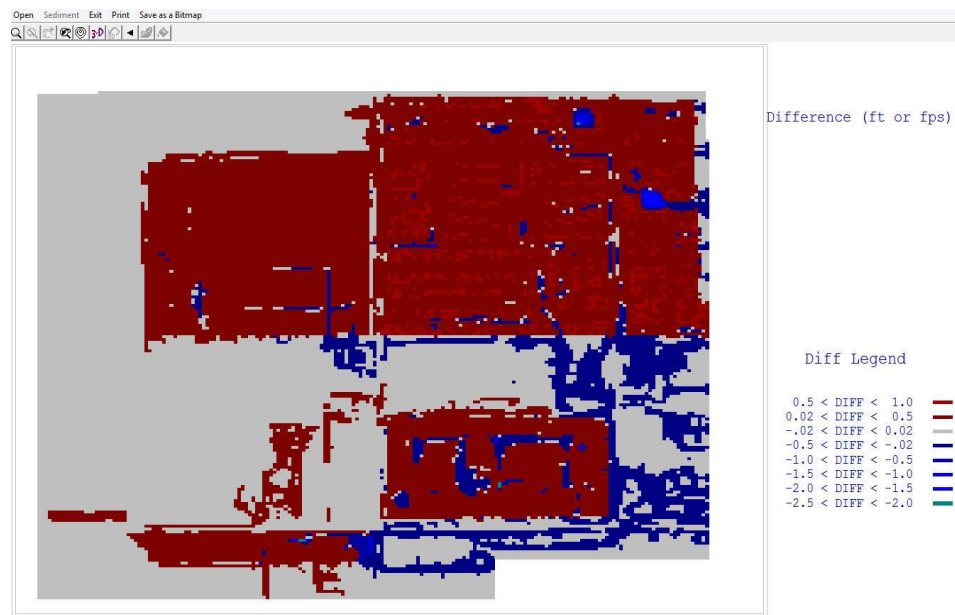


*Figure 68. MAXPLOT Difference Analysis of the FINALDEP.OUT Files (Spatially Variable – Base Run).*

In the SUMMARY.OUT File, the runoff from the grid system and the volume of water in the storm drain is lower (Figure 69). Clearly there is a more water retained on the floodplain surface that does not flow off the grid system or enter the storm drain because higher spatially variable TOL values are assigned. The spatially variable TOL values representing LID retention storage can have significant impact on the flood hazard or storm drain system downstream of where the LID techniques would be implemented.

OVERLAND FLOW	WATER	OVERLAND FLOW	WATER
WATER LOST TO INTERCEPTION	0.00	WATER LOST TO INTERCEPTION	0.00
FLOODPLAIN STORAGE	45.13	FLOODPLAIN STORAGE	24.29
FLOODPLAIN OUTFLOW HYDROGRAPH	11.56	FLOODPLAIN OUTFLOW HYDROGRAPH	23.02
-----	-----	-----	-----
FLOODPLAIN OUTFLOW, INTERCEPTION & STORAGE	56.68	FLOODPLAIN OUTFLOW, INTERCEPTION & STORAGE	47.31
=====	=====	=====	=====
*** STORM DRAIN TOTALS ***		*** STORM DRAIN TOTALS ***	
FLO-2D TO SWMM	15.53	FLO-2D TO SWMM	25.20
SWMM TO FLO-2D FROM RETURNING FLOW	0.29	SWMM TO FLO-2D FROM RETURNING FLOW	0.59
SWMM TO FLO-2D FROM OUTFALL	0.00	SWMM TO FLO-2D FROM OUTFALL	0.00
FLO-2D TO SWMM FROM OUTFALL	0.00	FLO-2D TO SWMM FROM OUTFALL	0.00
-----	-----	-----	-----
NET VOLUME	15.24	NET VOLUME	24.62

Figure 69. SUMMARY.OUT Comparison.

For comparison purposes, a simulation was run on the same project in Figure 69 that included infiltration. Figure 70 represents the difference between the ‘with infiltration’ and ‘without infiltration’ simulations (spatial TOL – spatial TOL with infiltration). The final depth is higher without the infiltration being removed from the floodplain surface. The primary final depth differences shown in Figure are for the areas with the LID TOL value assignments.

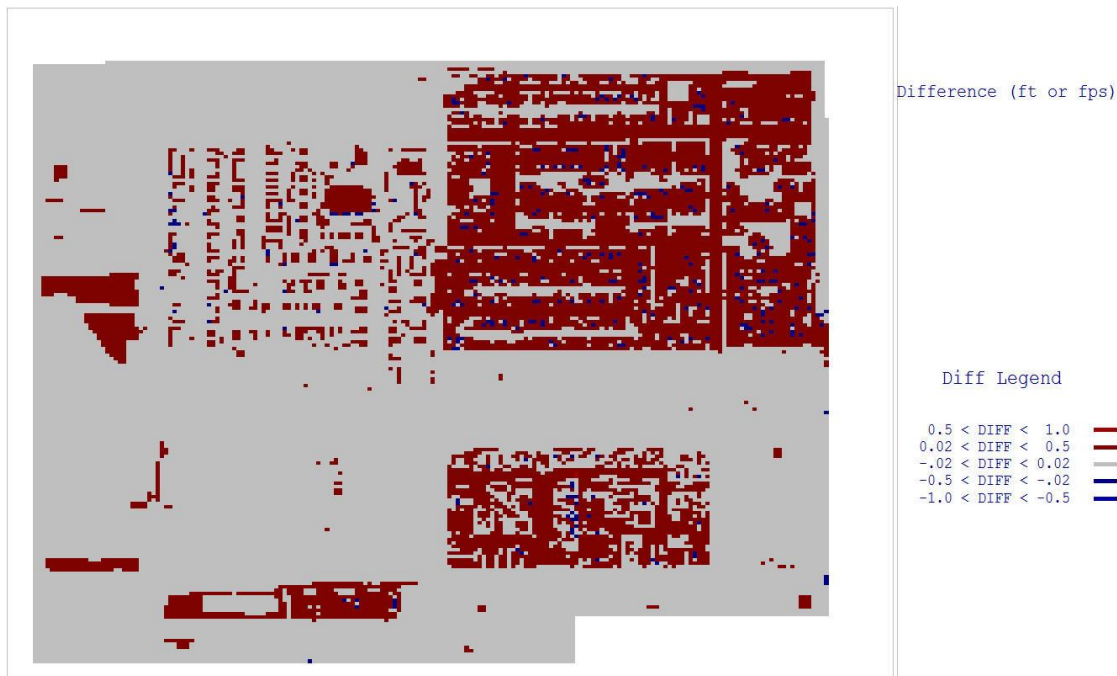


Figure 70. MAXPLOT Difference Analysis of the FINALDEP.OUT Files (Spatially Variable – Infiltration).

The infiltration losses remove water from the final floodplain storage reducing the water retention from 45 af to 40 af. The volume of water that reaches the floodplain outfall elements is reduced from 11.5 af to 8 af (30% reduction) for water that is infiltrated. The volume entering the storm drain system is reduced from 12.5 af to 11 af due to the infiltration (Figure 71).

OVERLAND INFILTRATED AND INTERCEPTED WATER	0.72 INCHES
OVERLAND FLOW	WATER
WATER LOST TO INFILTRATION & INTERCEPTION	13.45
FLOODPLAIN STORAGE	39.73
FLOODPLAIN OUTFLOW HYDROGRAPH	7.93
=====	=====
FLOODPLAIN OUTFLOW, INFILTRATION & STORAGE	61.11
=====	=====
*** STORM DRAIN TOTALS ***	
FLO-2D TO SWMM	10.83
SWMM TO FLO-2D FROM RETURNING FLOW	0.02
SWMM TO FLO-2D FROM OUTFALL	0.00
FLO-2D TO SWMM FROM OUTFALL	0.00
-----	-----
NET VOLUME	10.81

Figure 71. SUMMARY.OUT File for the Spatially Variable TOL Value and Infiltration.

#### 4.23 Building Rainfall Runoff

##### Building Runoff

It is a FLO-2D model option to simulate rainfall runoff from buildings. Buildings are represented by Area Reduction Factors (ARFs) and Width Reduction Factors (WRFs) in the FLO-2D model. ARF values remove surface area from potential water storage on a grid element. WRF values block flow directions between contiguous grid elements. The WRF values are not utilized in estimating rainfall runoff from buildings.

Figure 72 displays buildings on a FLO-2D model with 25 ft grid elements. In this figure, the buildings may occupy a portion of a grid element, the entire grid element, or multiple grid elements. The ARF and WRF values can be assigned automatically using shape file interpolation in the Grid Developer System (GDS) or manually by selecting one or more cells and assigning the ARF and WRF values to them (see the FLO-2D GDS Manual).

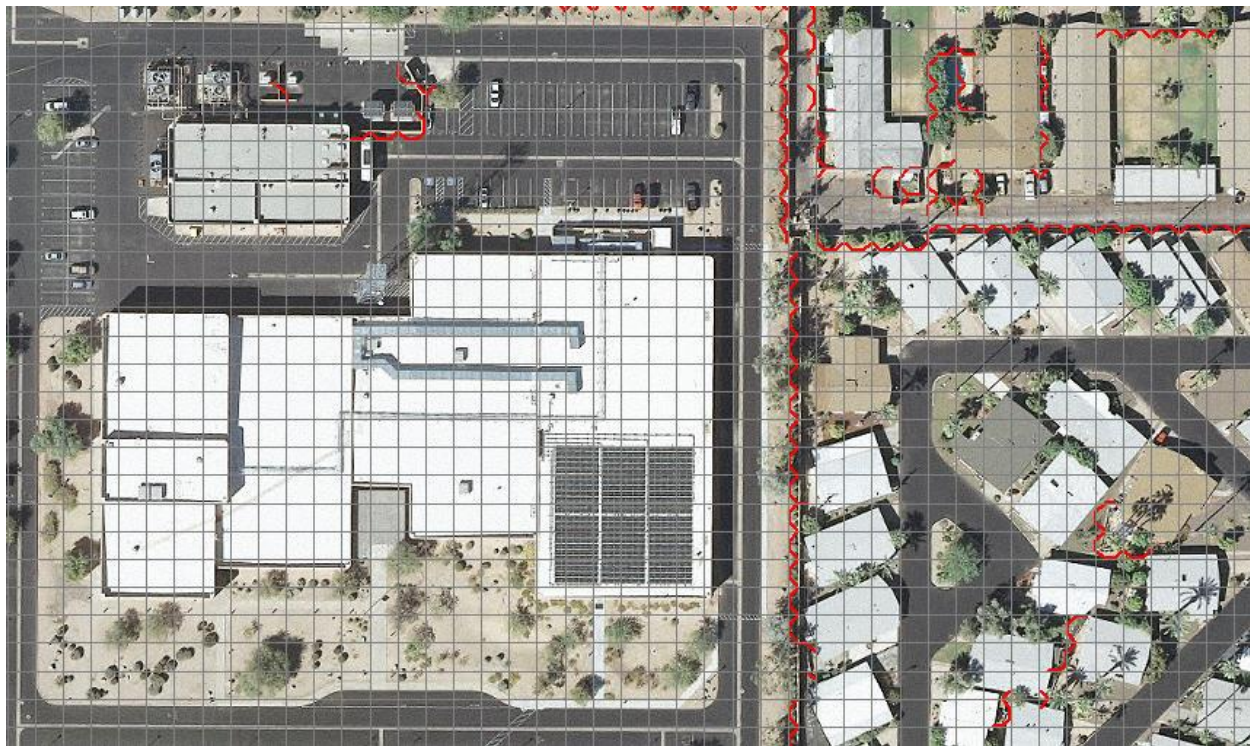


*Figure 72. Buildings on a 25 ft Grid System (red lines indicate walls represented as levees).*

There are two options to simulating rainfall runoff from buildings. For the first option, the user assigns the building ARF values. The building may be completely blocked ( $ARF = 1.$ ) or partially blocked ( $ARF < 1.$ ). When the rainfall occurs on a grid element with a partial ARF value, the rainfall on the entire grid element (including the portion with the assigned building ARF value) is accumulated on the remaining grid element surface area not covered by the building. The building portion of grid element surface area is considered impervious and sheds rainfall but does not store water. This accumulated rainfall depth ( $> TOL$  value) is then available for routing to contiguous grid elements. If the grid element surface area is totally blocked and has no storage ( $ARF = 1.$ ), then there is no rainfall runoff from this grid element. In this case, it is assumed that the rainfall goes to the building downspout, into the storm drain system and off the model. For this option: `IRAINBUILDING = 0` (RAIN.DAT file, line 1, second variable).

For the second option, the rainfall on completely blocked cells constitutes runoff from the building to the surface area. Rainfall on the totally blocked grid elements ( $ARF = 1$ ) is assumed to be routed through the building drain system to the surface area. The rainfall is accumulated on the grid element surface area and is passed to contiguous grid elements within the building and is then exchanged with cells outside the building as runoff. Figure 73 shows the same buildings in Figure 72 represented by the ARF values. The gray grid elements are completely blocked ( $ARF = 1$ ) and the yellow elements are partially blocked ( $ARF < 1$ ). The rainfall on an interior grid element (e.g. green element in Figure 73), is routed to the building boundary based on grid element elevation (ground topography) and roughness (Manning's n-value). This option is assumed to be representative of the shallow flow on a building roof being routed through the building's drainage system to the downspout. The user can control the

drainage direction by adjusting the grid element elevations inside the building. This option requires that IRAINBUILDING = 1 in the RAIN.DAT file (line 1, second variable) be assigned. Totally blocked elements are gray (ARF = 1) and Partially Blocked elements are in varying shades of yellow.



*Figure 73. Assigned ARF Values to the Buildings.*

There are several assumptions for the rainfall runoff from the buildings:

- When IRAINBUILDING = 1, the rainfall runoff will only be routed between completely blocked elements within the building.
- The routing is based on the internal building topography (grid element elevation).
- The flow roughness (Manning's n-value) for the completely blocked buildings is 0.03 (hard coded in the model).
- Based on the eight potential flow directions, the flow width for a blocked element (ARF = 1) is  $0.41412 * \text{grid element side}$  (i.e. WRF = 0.).
- The flow from inside the building to outside of the building is based on a hard-coded head difference in the water surface elevation of 0.5 ft (0.15 m). The actual water surface and ground elevations across the building walls are ignored in the flow computation.
- The flow can only be exchanged from inside to outside the building. No flow is permitted from outside to inside the building.
- The flow depth must exceed a TOL = 0.0042 for flow to be exchanged between interior building elements. This represents ponded water storage and is hard coded in the model.

The following example project (Figure 74) has a large building on a steep alluvial fan slope to the north (top of the page). To simulate runoff from the building to the fan surface IRAINBUILDING = 1.

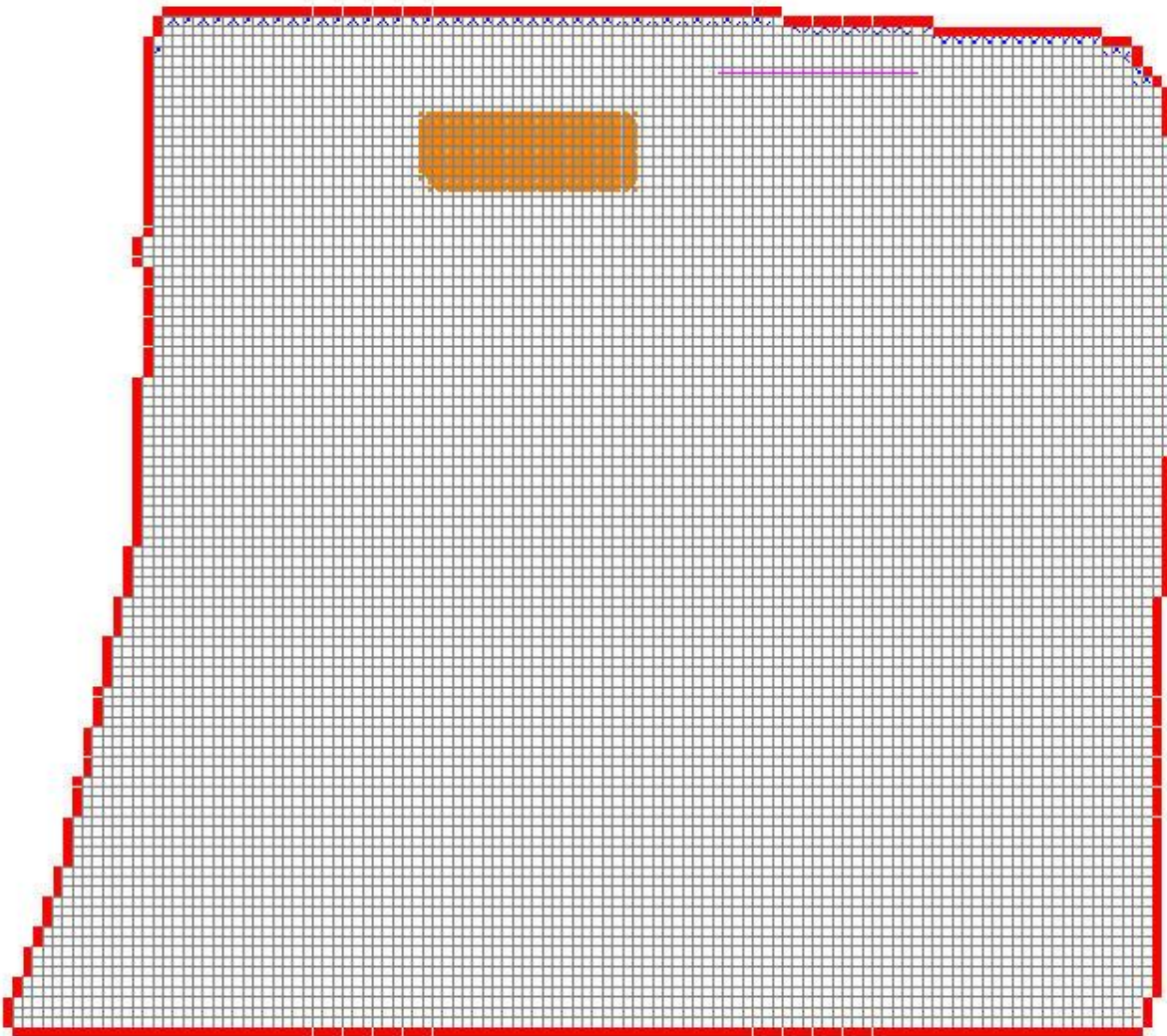


Figure 74. Location of a Large Building.

The rainfall results in flooding on the alluvial fan with the floodwave moving from south to north (towards the top of the page). The building is in a swale and takes a direct hit from the flooding. Figure 75 shows the flooding (maximum depths - dark blue grid elements) piling up on the upstream side of the building (south side of the building) and flowing to the west to get around the building. Along the building south wall, the predicted interior maximum depths are less than the tolerance value (gray cells).

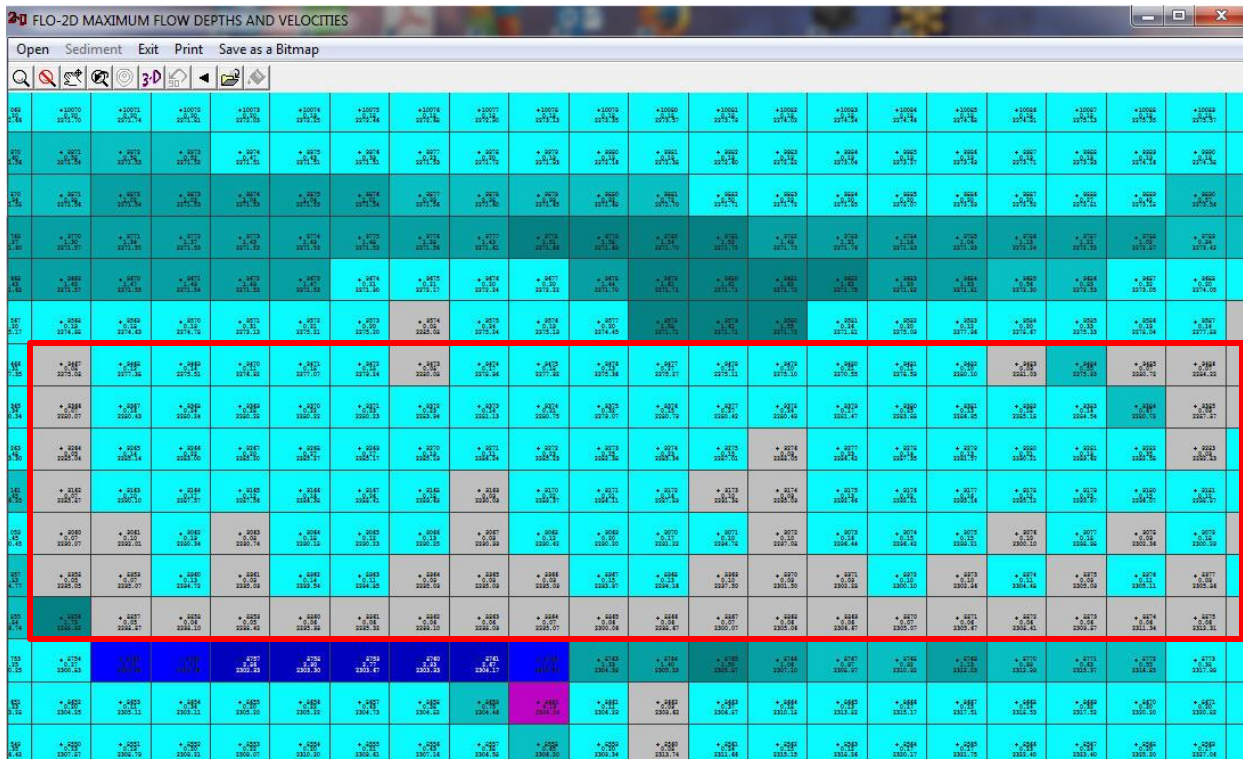
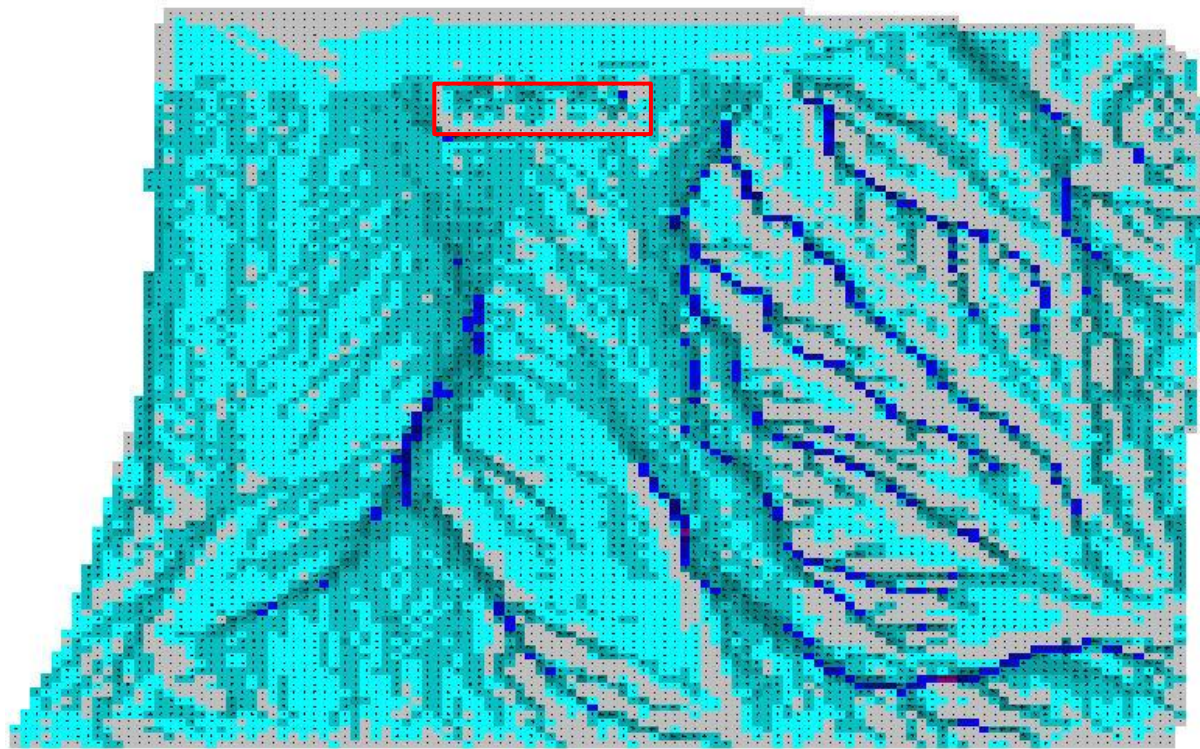
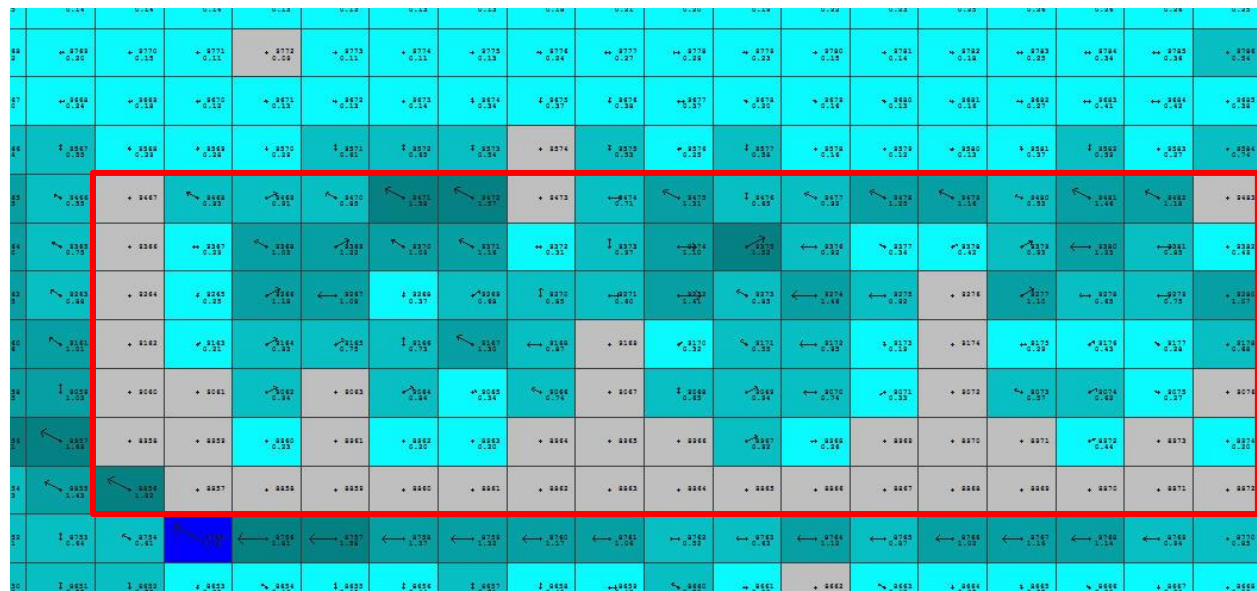


Figure 75. Maximum Flow Depths Inside the Building.

The rainfall runoff flows inside the building to reach the north wall and is debouched from the building. The building is outlined in red. Figure 76 shows the maximum velocities on the alluvial fan and indicates that the flow is moving inside the building. The flow is routed in the building interior based on the topography and roughness until it reaches the north side and then crosses to the outside of the building (Figure 77). This example illustrates that the flooding outside the building will progress around the building and the rainfall runoff on the building roof leaves the building. It is possible for the flow to leave the building in any direction. The building is outlined in red.



*Figure 76. Maximum Flow Velocities on the Alluvial Fan.*



*Figure 77. Maximum Flow Velocities.*

## Downspout

The building location selected for this project is shown in Figure 78. The red lines in these figures are levees and represent a parapet wall surrounding the entire building roof. On the project building, the levee elements encompass the blocked building (ARF = 1) elements. The completely blocked elements represent the building roof. The roof grid element elevations are usually assigned a ground elevation. These building elevations can be edited to represent the roof. The roof elements can be selected together and assigned a uniform elevation representing a flat roof (Figure 78). The parapet wall is simulated by selecting the appropriate grid elements and assigning the levee grid element direction and crest (wall elevation) as shown in the Figure 80 levee edit dialog box. Attention must be paid to the selection all the potential levee obstruction flow directions to completely contain the rainfall storage on the building roof. The parapet wall is shown as the red levee in Figure 78 representing the roof boundary. The roof elevation was assigned as approximately 20 ft higher than the ground elevation. This data base is enough to simulate rainfall storage on a flat roof. This is one of the test simulations.

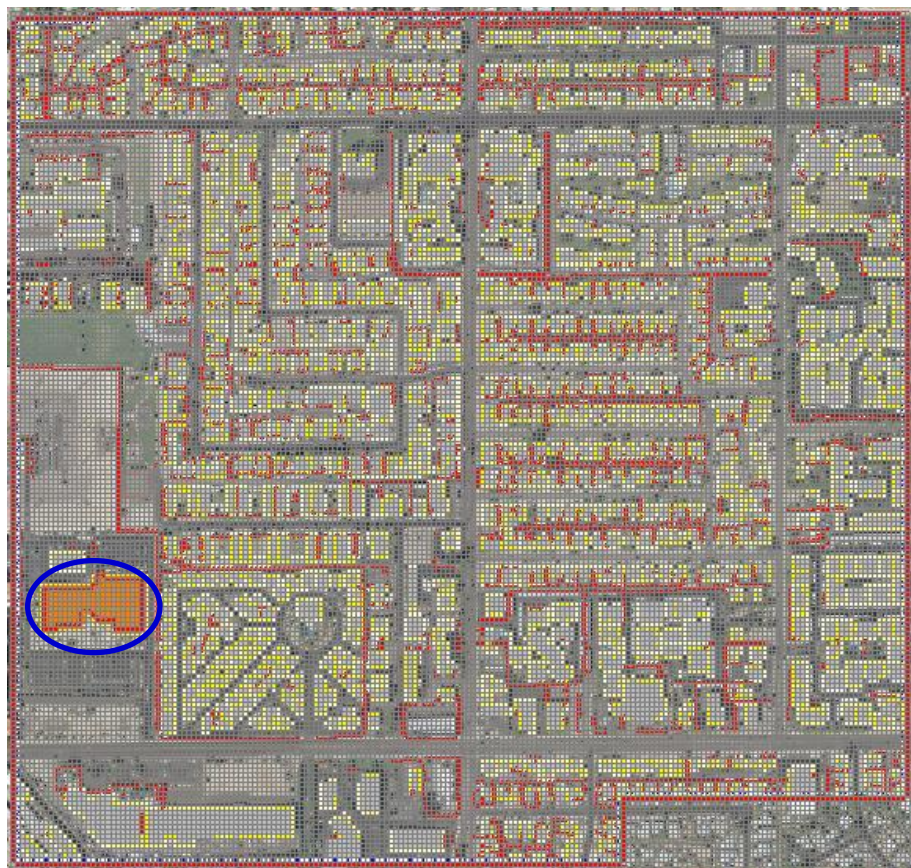
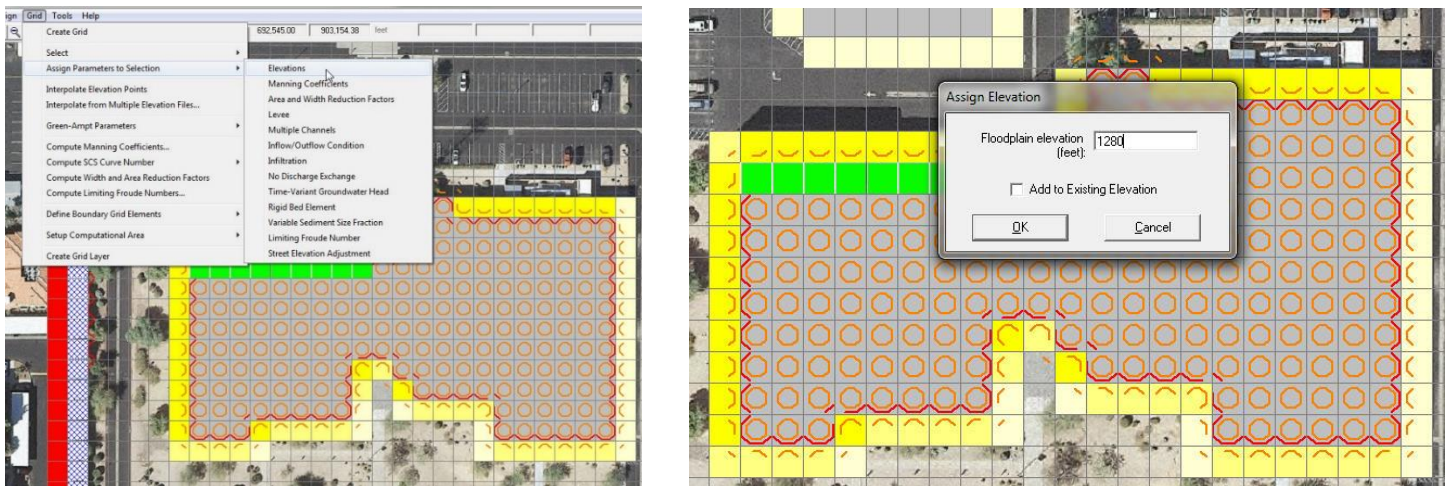
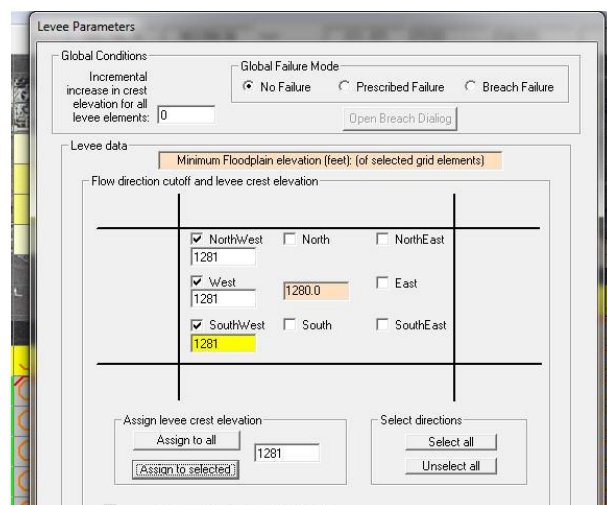


Figure 78. Project Building Location (in blue oval).



*Figure 79. Building Roof Element Elevation Editing.*



*Figure 80. Grid Element Levee Crest Elevation Editing.*

### ***Adjust Roof Slope***

A sloped roof can be established by modifying the roof elevations. Individual grid element elevations can be edited by double clicking a given cell and using the elevation field (Figure 81). Grid element elevations can be reset in corners and along the roof borders to establish some cornerstone elevations for further editing.

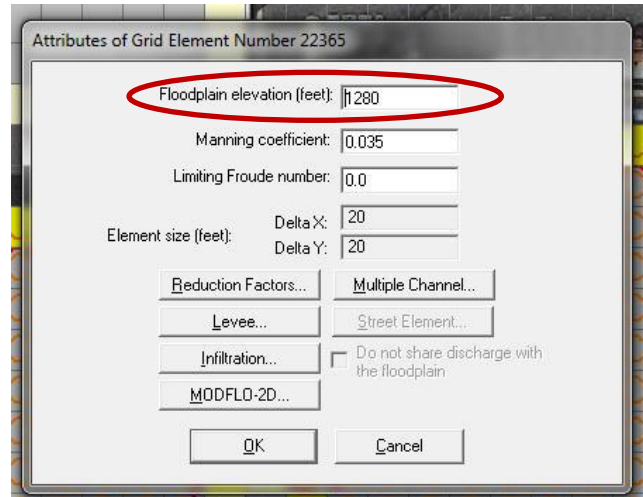


Figure 81. Grid Element Elevation Editing.

To establish a sloped roof, select a line of grid elements between two cornerstone elements with known roof elevations, then choose the street elevation editor (Figure 82).

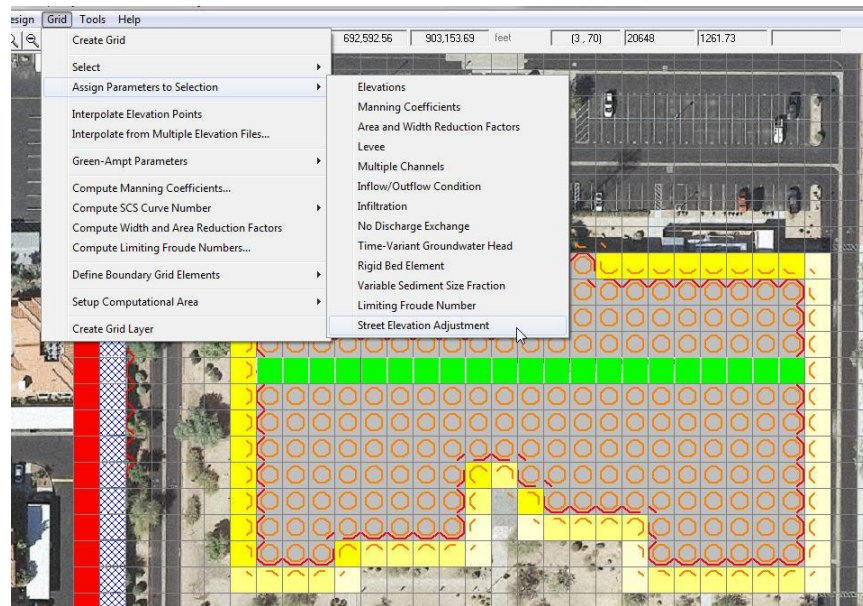


Figure 82. Roof Element Elevation Editing Command.

Select the *Elevation Adjustments Tab* shown in Figure 83 below. This will activate a dialog box window which will enable a linear slope interpolation between the two selected cornerstone elements (Figure 84). Figure 85 displays the roof element elevations prior to interpolation.

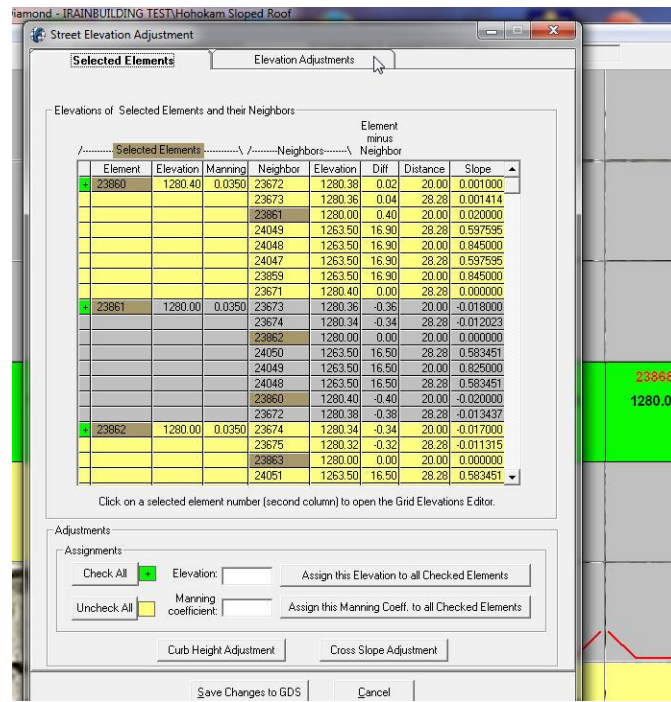


Figure 83. Roof Element Elevation Editing Tab.

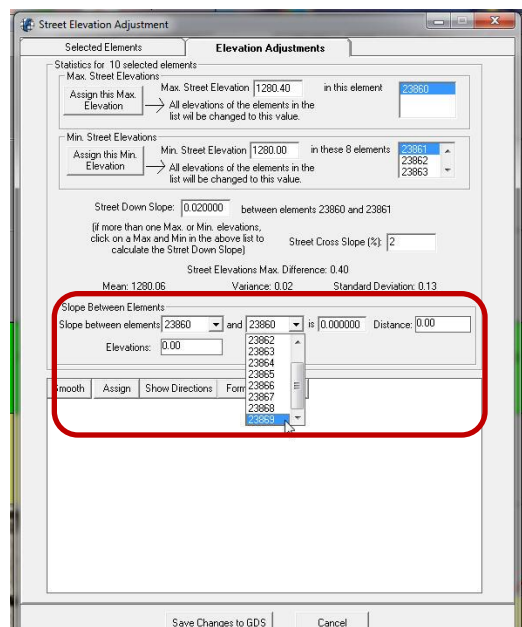
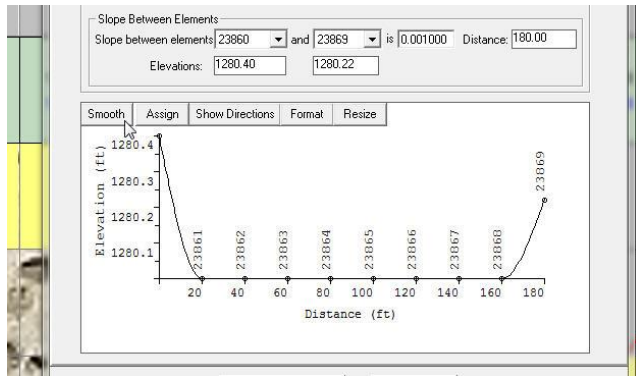
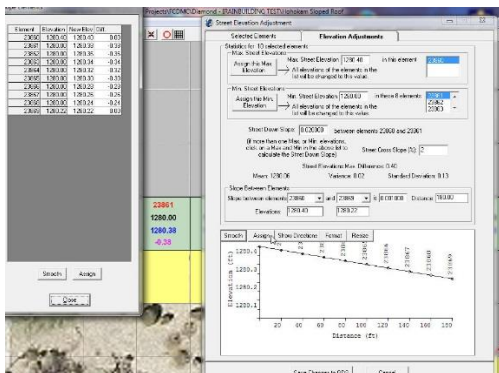


Figure 84. Selecting the Two Cornerstone Grid Elements to Interpolate the Roof Slope.



*Figure 85. Graphic Display of the Roof Element Elevations Between the Two Cornerstone Cells.*

The **Assign** button will complete the interpolation of the roof cell elevations between the cornerstone elements and save the results as shown in Figure 86.



*Figure 86. Completed Roof Element Elevation Slope Interpolation.*

### Downspout Hydraulics

The downspout discharge can be simulated as a hydraulic structure identifying the inlet node on the roof and the outlet node on the ground and assigning an inlet control rating table. The inlet control rating table can be based on orifice flow using the equation:

$$Q = C * A * (2.*g*DEPTH)^{0.5}$$

where:

C = coefficient that ranges from 0.62 to 0.72

A = flow area of the opening

g = acceleration due to gravity (32.2 fps or 9.81 m/s)

DEPTH = flow depth on orifice (cell flow depth)

The hydraulic structure data file is organized as follows:

```
S Downspoutname 0 1 22365 21991 0 0 0 0
T      0        0
T      0.25     1.0
T      0.5      2.0
T      1        3.5
T      5        5.5
```

In the S-line above, the data includes a downspout name, floodplain or channel element (floodplain = 0), rating curve or table (rating table = 1), inlet and outlet cell number, and 4 additional controls that not required. The rating table assignment should begin with zero depth and zero discharge and the remaining T-lines are depth and discharge can be based on the above orifice equation. This data can be entered graphically in the GDS.



*Figure 87. Downspout Hydraulic Structure as Brown Elements in the Upper Right Corner.*

The hydraulic structure editor dialog window for the downspout inlet and outlets shown in Figure 87 is displayed in Figure 88. Note that the downspout inlet and outlet elements do not have to be contiguous. Any number of downspouts can be simulated in any location on the building roof.

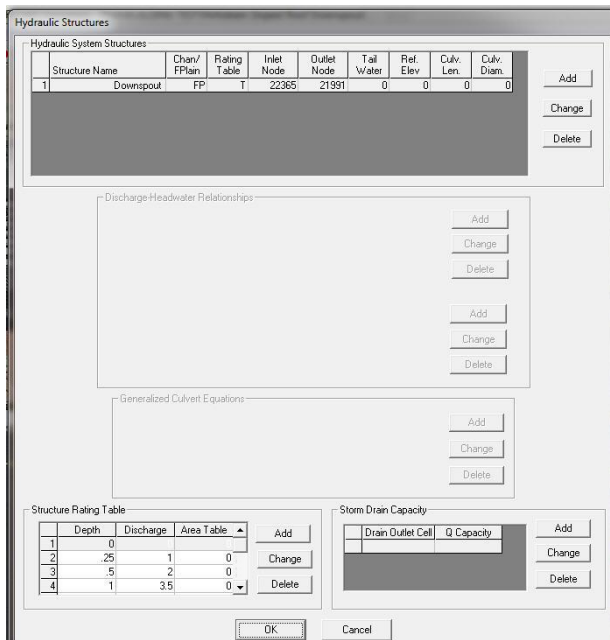


*Figure 88. Hydraulic Structure Dialog Box with Entered Downspout Data.*

#### **Verification Testing of the Building Roof Runoff Enhancements**

The building runoff enhancements were tested in two projects. Since both projects showed an identical response on different scales, only the results of the small scale, more detailed project will be presented. Several tests were developed to verify the roof runoff computations. These include:

- Rainfall accumulation on a flat roof
- Rainfall runoff movement on sloped roof
- Parapet wall overtopping
- Downspout discharge to the ground

In the first test, three inches of rain is applied to the project in two hours. The project has buildings, walls, infiltration and storm drains. To focus on the building with the assigned downspout, the storm drain component was turned off. Only the building discussed in this document will be reviewed. The simulation was terminated after the rainfall ended after two hours. The flat roof elevation was 1280.00 and after 2 hours, the computed final roof flow depths results in a uniform water surface elevation of 1280.25 on all the elements since there is no outlet (Figure 89) using the FLO-2D Maxplot map program).

The sloped roof test is designed to predict the rainfall runoff flow to the downspout. The downspout is in grid element 22365 (upper right corner of the building NE) and the entire roof slopes to this location. Most of the roof has a slope of 0.001 or 0.02 ft per 20 ft grid element. The slope in the final few grid elements in the NE corner of the roof are a little steeper. In this case, the parapet walls are one foot high and since the maximum water surface elevation does not exceed 1281, there is no flow overtopping the parapet walls. The maximum water surface elevation is shown in Figure 90. Note that

all the roof maximum water surface elevations are equal, but the maximum flow depths vary with the roof elevation and the deepest depth is predicted at the downspout element. The downspout outlet element 21990 has the same water surface elevation and small depth in both simulations.

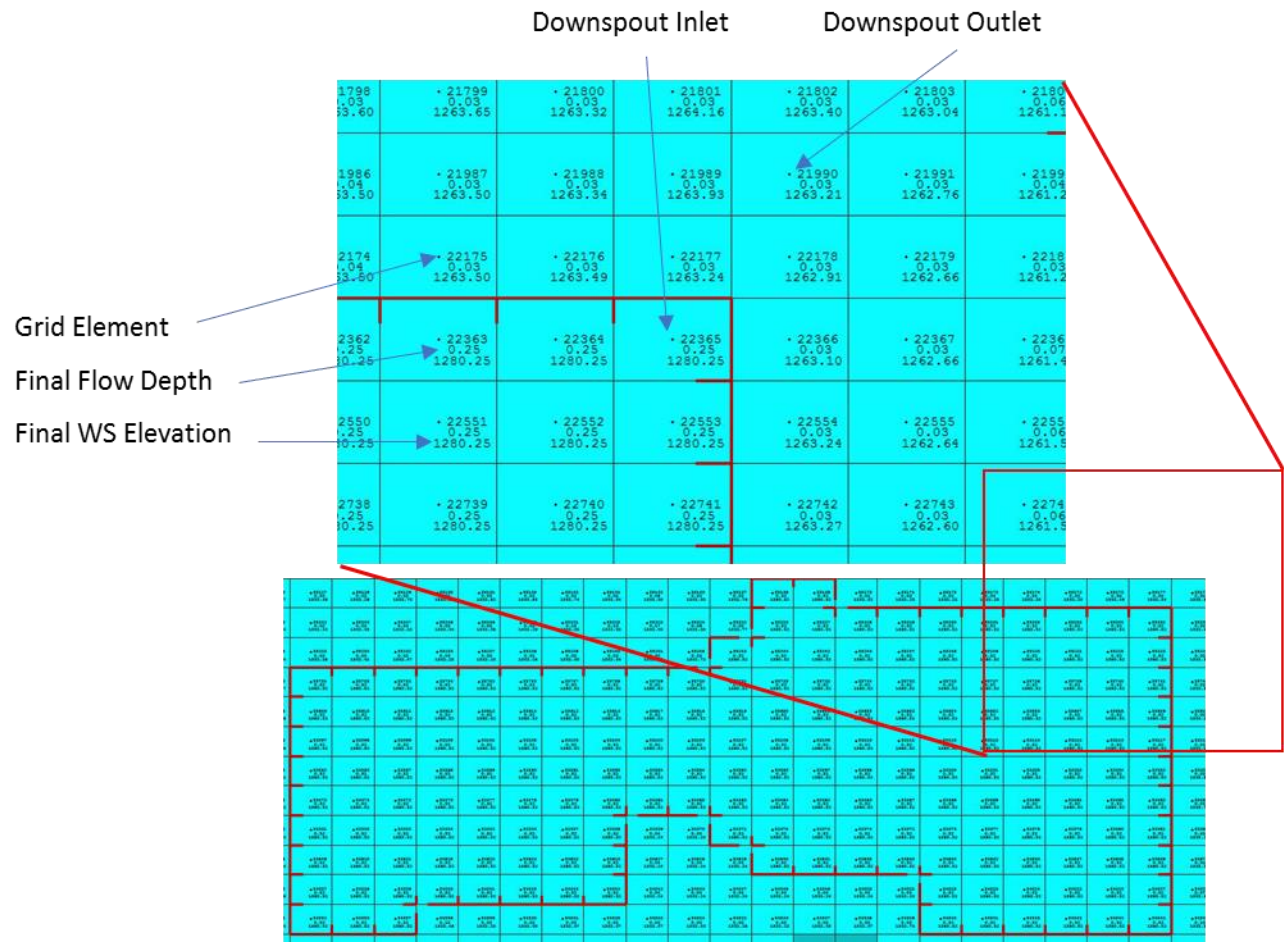


Figure 89. Total Rainfall (3 inches) Accumulated on a Flat Roof.

**Cells 22365 and 21990 will be the downspout inlet and outlet respectively**

• 21985 0.15 1263.61	• 21986 0.14 1263.60	• 21987 0.10 1263.57	• 21988 0.16 1263.47	• 21989 0.03 1263.93	• 21990 0.03 1263.21	
• 22173 0.15 1263.61	• 22174 0.14 1263.60	• 22175 0.10 1263.57	• 22176 0.07 1263.53	• 22177 0.10 1263.31	• 22178 0.15 1262.99	
• 22361 0.39 1280.59	• 22362 0.44 1280.59	• 22363 0.49 1280.59	• 22364 0.54 1280.59	• 22365 0.59 1280.55	• 22366 0.03 1263.10	
• 22549 0.34 1280.59	• 22550 0.39 1280.59	• 22551 0.44 1280.59	• 22552 0.49 1280.59	• 22553 0.54 1280.59	• 22554 0.03 1263.24	
• 22737 0.41 1280.59	• 22738 0.43 1280.59	• 22739 0.45 1280.59	• 22740 0.47 1280.59	• 22741 0.49 1280.59	• 22742 0.03 1263.27	
• 22925 0.39 1280.59	• 22926 0.43 1280.59	• 22927 0.43 1280.59	• 22928 0.45 1280.59	• 22929 0.47 1280.59	• 22930 0.03 1263.18	
• 23113 0.37 1280.59	• 23114 0.39 1280.59	• 23115 0.41 1280.59	• 23116 0.43 1280.59	• 23117 0.45 1280.59	• 23118 0.03 1263.05	

Figure 90. Maximum Flow Depth and Water Surface Elevation on a Sloped Roof.

#### (Compare the Inlet and Outlet Maximum WS Elevations)

In the third simulation, the parapet wall was lowered by 0.75 ft to 1280.25 in the LEVEE.DAT file for the downspout inlet grid element 22365. During the simulation the maximum water surface elevation exceeds the parapet wall elevation for the downspout inlet element (22365 NE flow direction 5) and overtops the wall (Figure 91). Compare this grid element maximum water surface elevation and flow depth in Figure 90 and note that they are lower because the parapet wall is overtopped and some rainfall storage is discharged to the ground. Any number of parapet wall cells (levee elements and the blocked direction) can be overtopped.

• 21798 0.04 1263.61	• 21799 0.03 1263.65	• 21800 0.14 1263.43	• 21801 0.03 1264.16	• 21802 0.03 1263.40	• 21803 0.04 1263.05	• 21 0 1261
• 21986 1263.60	• 21987 0.09 1263.66	• 21988 0.09 1263.46	• 21989 0.09 1263.33	• 21990 0.03 1263.21	• 21991 0.05 1262.78	• 21 0 1261
• 22174 0.15 1263.60	• 22175 0.10 1263.60	• 22176 0.10 1263.53	• 22177 0.10 1263.31	• 22178 0.15 1263.07	• 22179 0.15 1262.69	• 22 0 1261
• 22362 0.37 1280.46	• 22363 0.34 1280.44	• 22364 0.38 1280.41	• 22365 0.38 1280.35	• 22366 0.03 1263.10	• 22367 0.05 1262.68	• 22 0 1261
• 22550 0.26 1280.46	• 22551 0.30 1280.45	• 22552 0.32 1280.42	• 22553 0.36 1280.41	• 22554 0.03 1263.24	• 22555 0.03 1262.64	• 22 0 1261
• 22738 0.37 1280.47	• 22739 0.36 1280.46	• 22740 0.36 1280.44	• 22741 0.36 1280.44	• 22742 0.03 1263.27	• 22743 0.03 1262.60	• 22 0 1261
• 22956 0.30 1280.48	• 22957 0.30 1280.47	• 22958 0.30 1280.46	• 22959 0.30 1280.46	• 22960 0.03 1263.18	• 22961 0.03 1262.57	• 22 0 1261

Figure 91. Maximum Flow Depth (Sloped Roof with Parapet wall Being Overtopped).

The overtopping discharge is reported below from the file LEVOVERTOP.OUT. The discharge is reported as negative representing flow out of the grid element.

LEVEE OVERTOPPING DISCHARGE (CFS OR CMS): POSITIVE DISCHARGE REPRESENTS INFLOW TO NODE  
 LEVEE ELEMENTS WITH NO OVERTOP DISCHARGE ARE NOT REPORTED  
 DISCHARGE IS REPORTED BY DIRECTION

GRID ELEMENT	TIME	TOTAL DISCHARGE	N	E	S	W	NE	SE	SW	NW
22365	3.30	-0.02	0.00	0.00	0.00	0.00	-0.02	0.00	0.00	0.00
	3.40	-0.06	0.00	0.00	0.00	0.00	-0.06	0.00	0.00	0.00
	3.50	-0.09	0.00	0.00	0.00	0.00	-0.09	0.00	0.00	0.00
	3.60	-0.17	0.00	0.00	0.00	0.00	-0.17	0.00	0.00	0.00
	3.70	-0.23	0.00	0.00	0.00	0.00	-0.23	0.00	0.00	0.00
	3.80	-0.36	0.00	0.00	0.00	0.00	-0.36	0.00	0.00	0.00
	3.90	-0.54	0.00	0.00	0.00	0.00	-0.54	0.00	0.00	0.00
	4.00	-0.70	0.00	0.00	0.00	0.00	-0.70	0.00	0.00	0.00
	4.10	-0.69	0.00	0.00	0.00	0.00	-0.69	0.00	0.00	0.00
	4.20	-0.72	0.00	0.00	0.00	0.00	-0.72	0.00	0.00	0.00
	4.30	-0.74	0.00	0.00	0.00	0.00	-0.74	0.00	0.00	0.00
	4.40	-0.75	0.00	0.00	0.00	0.00	-0.75	0.00	0.00	0.00
	4.50	-0.75	0.00	0.00	0.00	0.00	-0.75	0.00	0.00	0.00
	4.60	-0.75	0.00	0.00	0.00	0.00	-0.75	0.00	0.00	0.00
	4.70	-0.76	0.00	0.00	0.00	0.00	-0.76	0.00	0.00	0.00
	4.80	-0.78	0.00	0.00	0.00	0.00	-0.78	0.00	0.00	0.00
	4.90	-0.78	0.00	0.00	0.00	0.00	-0.78	0.00	0.00	0.00
PEAK Q	4.92	-0.79								
	5.00	-0.78	0.00	0.00	0.00	0.00	-0.78	0.00	0.00	0.00
	5.10	-0.77	0.00	0.00	0.00	0.00	-0.77	0.00	0.00	0.00
	5.20	-0.74	0.00	0.00	0.00	0.00	-0.74	0.00	0.00	0.00
	5.30	-0.72	0.00	0.00	0.00	0.00	-0.72	0.00	0.00	0.00
	5.40	-0.72	0.00	0.00	0.00	0.00	-0.72	0.00	0.00	0.00
	5.50	-0.72	0.00	0.00	0.00	0.00	-0.72	0.00	0.00	0.00
	5.60	-0.70	0.00	0.00	0.00	0.00	-0.70	0.00	0.00	0.00
	5.70	-0.72	0.00	0.00	0.00	0.00	-0.72	0.00	0.00	0.00
	5.80	-0.68	0.00	0.00	0.00	0.00	-0.68	0.00	0.00	0.00
	5.90	-0.66	0.00	0.00	0.00	0.00	-0.66	0.00	0.00	0.00
	6.00	-0.65	0.00	0.00	0.00	0.00	-0.65	0.00	0.00	0.00

The final test simulation combines the sloped roof with a downspout in grid element 22365. The inlet (red oval) maximum water surface is lowered by the downspout water discharge as shown in Figure 92. The downspout outlet element 21990 (blue oval) has an increased maximum water surface when compared with Figure 90 and Figure 91.

+ 21798 0.10 1263.61	+ 21799 0.09 1263.65	+ 21800 0.11 1263.43	+ 21801 0.11 1264.16	+ 21802 0.10 1263.40	+ 21803 0.10 1263.05
+ 21986 0.14 1263.60	+ 21987 0.09 1263.56	+ 21988 0.15 1263.46	+ 21989 0.08 1263.98	+ 21990 0.12 1263.30	+ 21991 0.05 1262.78
+ 22174 0.14 1263.80	+ 22175 0.10 1263.57	+ 22176 0.07 1263.53	+ 22177 0.10 1263.31	+ 22178 0.14 1263.02	+ 22179 0.06 1262.69
+ 22362 0.10 1280.41	+ 22363 0.10 1280.38	+ 22364 0.10 1280.33	+ 22365 0.10 1280.28	+ 22366 0.10 1263.10	+ 22367 0.10 1262.67
+ 22550 0.22 1280.42	+ 22551 0.24 1280.39	+ 22552 0.26 1280.36	+ 22553 0.28 1280.33	+ 22554 0.08 1263.24	+ 22555 0.08 1262.64
+ 22738 0.25 1280.43	+ 22739 0.25 1280.40	+ 22740 0.27 1280.39	+ 22741 0.28 1280.38	+ 22742 0.27 1263.27	+ 22743 0.26 1262.60
+ 22926 0.25 1280.44	+ 22927 0.25 1280.42	+ 22928 0.27 1280.41	+ 22929 0.28 1280.40	+ 22930 0.08 1263.18	+ 22931 0.08 1262.57
+ 23114 0.25 1280.45	+ 23115 0.25 1280.45	+ 23116 0.27 1280.43	+ 23117 0.28 1280.42	+ 23118 0.08 1263.05	+ 23119 0.08 1262.54

Figure 92. Maximum Flow Depth and Water Surface Elevation. (Sloped Roof with a Downspout).

The discharge out of the downspout is reported below from the HYDROSTRUCT.OUT file.

#### STRUCTURE OUTFLOW DISCHARGE

INFLOW AND OUTFLOW DISCHARGE MAY BE DIFFERENT IF STRUCTURE IS A LONG CULVERT OR IF OUTFLOW COMBINES MULTIPLE CULVERTS

OUTFLOW DISCHARGE IS REPORTED AS NEGATIVE

FLOODPLAIN GRID ELEMENTS	TIME (HRS)	DISCHARGE (CFS OR CMS)
--------------------------	------------	------------------------

THE MAXIMUM DISCHARGE FOR: Downspout	STRUCTURE NO.	1 IS:	0.94 AT TIME: 4.91
INFLOW NODE: 22365	OUTFLOW NODE: 21990		
0.10	0.00	0.00	
0.20	0.00	0.00	
0.30	0.00	0.00	
0.40	0.00	0.00	
0.50	0.00	0.00	
0.60	0.00	0.00	
0.70	0.00	0.00	
0.80	0.00	0.00	
0.90	0.00	0.00	
1.00	0.00	0.00	
1.10	0.00	0.00	
1.20	0.00	0.00	
1.30	0.00	0.00	
1.40	0.00	0.00	
1.50	0.00	0.00	
1.60	0.00	0.00	
1.70	0.04	-0.04	
1.80	0.07	-0.07	
1.90	0.08	-0.08	
2.00	0.10	-0.10	
2.10	0.13	-0.13	

2.20	0.14	-0.14
2.30	0.14	-0.14
2.40	0.15	-0.15
2.50	0.15	-0.15
2.60	0.16	-0.16
2.70	0.16	-0.16
2.80	0.17	-0.17
2.90	0.16	-0.16
3.00	0.16	-0.16
3.10	0.16	-0.16
3.20	0.17	-0.17
3.30	0.17	-0.17
3.40	0.22	-0.22
3.50	0.27	-0.27
3.60	0.34	-0.34
3.70	0.46	-0.46
3.80	0.51	-0.51
3.90	0.64	-0.64
4.00	0.76	-0.76
4.10	0.83	-0.83
4.20	0.86	-0.86
4.30	0.89	-0.89
4.40	0.91	-0.91
4.50	0.91	-0.91
4.60	0.91	-0.91
4.70	0.92	-0.92
4.80	0.93	-0.93
4.90	0.94	-0.94
5.00	0.94	-0.94
5.10	0.93	-0.93
5.20	0.91	-0.91
5.30	0.88	-0.88
5.40	0.87	-0.87
5.50	0.86	-0.86
5.60	0.86	-0.86
5.70	0.85	-0.85
5.80	0.85	-0.85
5.90	0.82	-0.82
6.00	0.79	-0.79

The FLO-2D model simulation of rainfall runoff from building roofs has been modified to allow parapet walls (levees) to store rainfall water, enable the parapet walls to be overtopped and discharge storm off the roof through a downspout. The FLO-2D code was edited to create these enhancements and a new executable program was compiled. The primary revisions involved allowing component interaction with the completely blocked grid elements representing the buildings (ARF = 1). The three new tools were tested extensively with a flat and sloped roof to validate that:

- Rainfall was accurately predicted to accumulate on a flat roof;
- Rainfall runoff was predicted to flow to the lowest cell on a slope roof;

- Rainfall runoff flowed to the lowest roof cell and overtopped a low parapet wall;
- Roof storage was discharged through a downspout located at the lowest roof cell.

There are no required data file revisions to use these new building rainfall tools.

#### **4.24 Gutter Tool**

The street gutters are designed to convey shallow flow during storm runoff less than or equal to the design discharge without traffic interruption. Typical curb and gutter cross sections have a triangular shape created by the cross slope associated with the street or road crown. Gutter cross slopes can range from flat to 8%. For the FLO-2D street routing, the triangular shape is assumed to have a 2 percent straight cross slope. The gutter flow will be exchanged with other upstream and downstream street gutter elements, the sidewalk (which is part of street gutter element), and other street elements (not having a gutter). Floodplain flow is exchange with the gutter elements through the sidewalk. The Dept. of Transportation Urban Drainage Design Manual (revised 2013) presents a gutter flow capacity equation that is used for computing flow in triangular channels. DOT Equation 4.2 is given as:

$$Q = (K_u/n) S_x^{1.67} S_L^{0.5} T^{2.67}$$

where:

$K_u$  = 0.56 in English units

$n$  = Manning's roughness

$Q$  = discharge (cfs)

$T$  = flow top width (ft) =  $d/S_x$  where  $d$  = flow depth at the curb

$S_x$  = cross slope (ft/ft)

$S_L$  = street longitudinal slope (ft/ft)

This DOT equation is Mannings equation for normal flow depth (steady, uniform flow) with an additional coefficient of 0.188:

$$Q = VA = (1.486/n) d^{0.67} S_L^{0.5} A (0.188)$$

where:

$A$  = flow area =  $0.5 d T$  ( $\text{ft}^2$ ) area of a triangle

The 0.188 coefficient accounts for the hydraulic radius of a wide channel where the top width is more than 40 times the flow depth. This coefficient ( $\sim 5 \times n$ -value) is analogous to the shallow flow  $n$ -value in FLO-2D for flow depths less than 0.5 ft. For a street  $n$ -value of 0.02, the (0.188) coefficient would be equivalent to applying a 0.1 shallow flow  $n$ -value (SHALLOW).

## Gutter Flow

Street gutter flow is defined in the Figure 93 where  $h$  = curb height.

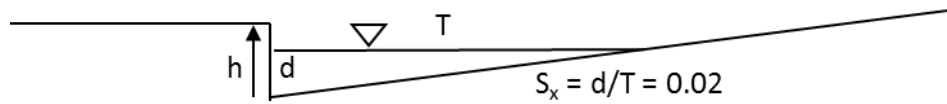


Figure 93. Gutter Diagram.

The gutter flow can be shared in all eight flow directions (Figure 94):

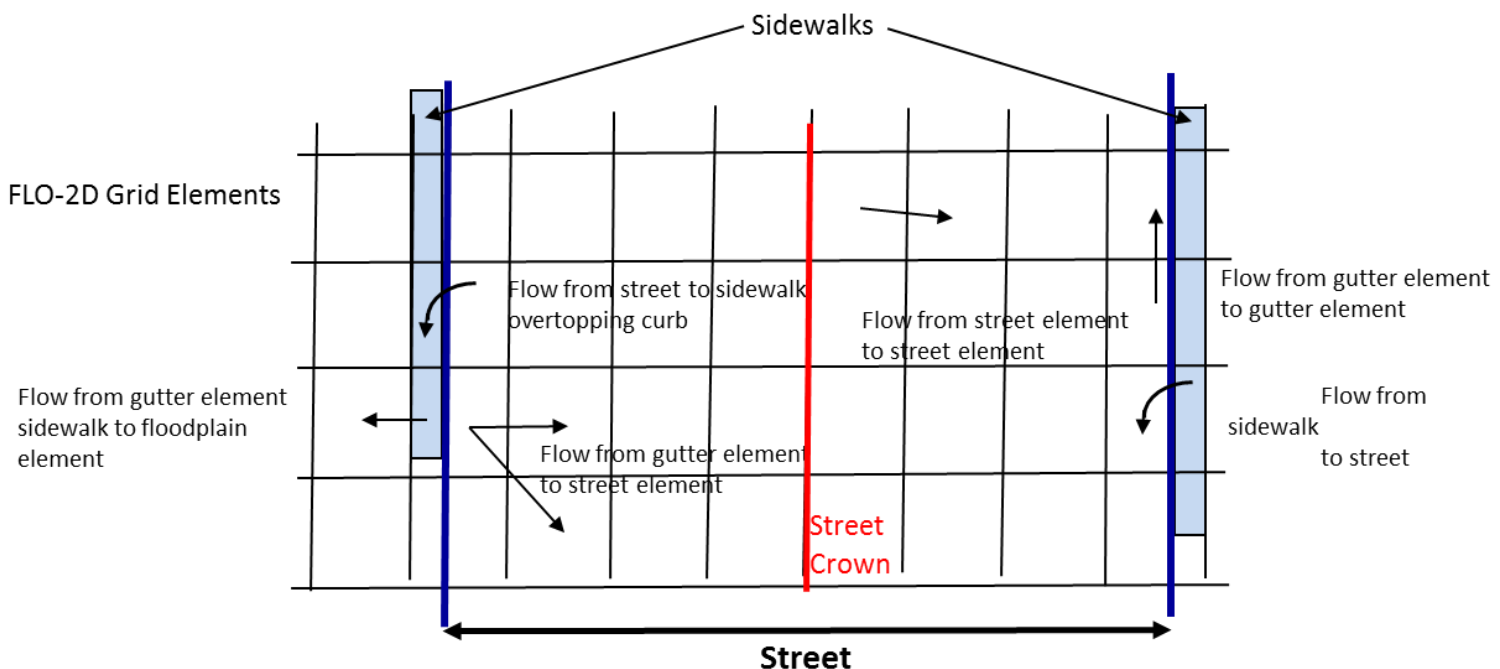


Figure 94. Street and Gutter Flow Diagram.

The street elements are floodplain elements with appropriate elevations and n-values to represent street flow. The discharge exchange can occur between street elements, between street and floodplain elements (outside the street), between gutter elements and street elements or between gutter elements and floodplain elements. To share flow between gutter elements and floodplain elements, the flow must first overtop the curb and be exchanged with the sidewalk. The sidewalk is at least 10% of the side of the grid element. If the assigned street width is greater than 0.9 times the grid element side, then the width is limited to 0.9 times the side. When the flow depth exceeds the curb height and the water surface elevation on the sidewalk, the flow is shared from the gutter element to the sidewalk. If the water surface elevation on the sidewalk exceeds the TOL value and is higher than the gutter water surface elevation, then the flow is shared from the sidewalk to the gutter. The flow is shared between

the gutter element and the contiguous floodplain elements using the floodplain flow depth and the gutter element sidewalk flow depth.

Flow from the gutter to the sidewalk inside the gutter element is depicted in Figure 95.

$$\text{Gutter WSE} = \text{FPE} + d;$$

$$\text{Sidewalk elevation} = \text{FPE} + H$$

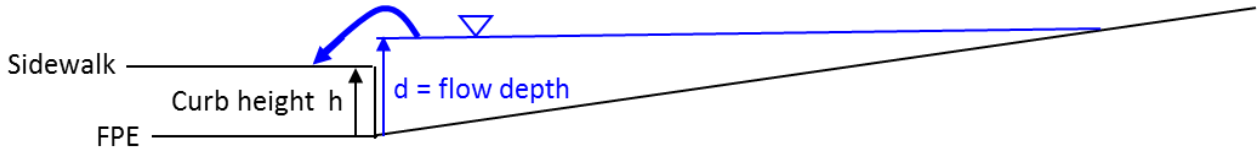


*Figure 95. Flow Distribution Street to Sidewalk.*

Flow from the sidewalk to the gutter inside the gutter element Sidewalk is depicted in Figure 96.

$$\text{WSE} = \text{FPE} + h + \text{FPD}; \quad \text{Gutter WSE} = \text{FPE} + d$$

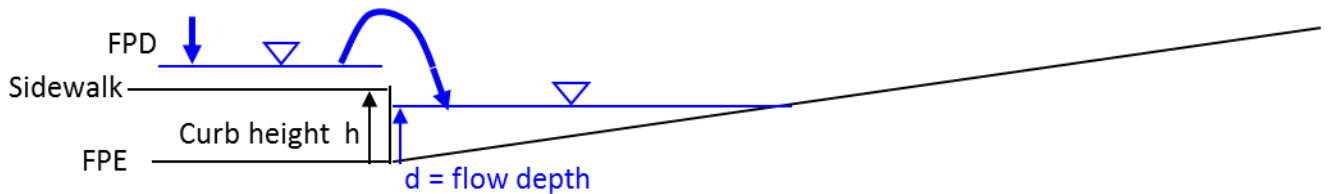


*Figure 96. Flow Distribution Sidewalk to Street.*

### Results:

In the following example (Figure 97) the gutter elements are displayed in brown. The gutter elements are only assigned to the north side of the street in a single line along one street running east to west. Approximately two-thirds of the length of the street, the street is shift one row to the north. The inflow element is at the start of the street on the left side (green element). The inflow discharge is initial zero cfs, increases to 10 cfs in 0.1 hrs and steady at 10 cfs for the 1 hr flow simulation. No rainfall or infiltration are simulated. Buildings and walls are simulated.



*Figure 97. Gutter Elements with Storm Drain.*

The gutter flow maximum depth results shown below indicate that with the gutter the flow is confined to the street elements and the volume is further distributed downstream. The flow has less spreading between the street and floodplain elements along the street with the gutter flow.

The results without the gutter are shown Figure 98:



*Figure 98. Flow Depth without Gutter*

The gutter flow results are displayed in the Figure 99.



Figure 99. Flow Depth with Gutter.

#### 4.25 Bridge Routine

Many bridge hydraulic analyses are conducted using steady state peak flow conditions where the objective is to predict the maximum water surface elevation profile upstream of the bridge and through the bridge. Typically, most bridge design and flood conveyance analyses have been performed with HEC-2 or HEC-RAS where a prescribed discharge (peak Q) is presumed and the water surface elevation is computed. In a two-dimensional flood routing model, the opposite is required; the upstream and downstream flow depths and water surface elevations are known and the discharge through the bridge is computed. In a FLO-2D flood simulation, the focus is to predict the discharge between two grid elements and to spatially distribute the flood volume. As such, the bridge component is a link between two grid elements (channel or floodplain) and the discharge through the bridge is computed by representing the various physical features of the bridge that constrict the flow (see Figure 100).



Figure 100. Constricted Flow through a Bridge (Tom Imbrigotti, USGS).

The head loss or energy loss through a bridge (referred to as the afflux) is generated from three primary sources:

- Flow expansion from the bridge downstream;
- Flow resistance associated with surface friction (piers, abutments and soffit when submerged) and other roughness conditions included, but not limited to, bed forms, vegetation, non-uniform flow (scour holes and piers);
- Flow contraction by the bridge configuration.

The energy loss attributed to flow expansion is presumed to be about twice the contraction energy loss (Hamill, 1999). It should be noted, however, that uniform flow in the river reach upstream of the bridge is the exception rather than the conventionally assumed condition which complicates the prediction of the water surface profile that is associated with the head loss.

The objective in applying the bridge routine in FLO-2D is not to provide a detailed flow field through the bridge and predict scour around piers, but rather to accurately assess the relationship between upstream/downstream water surface elevations of the two grid elements linked by the bridge, and to compute the discharge passing between them. In this manner, the flow can be assessed as one-dimensional with no variation in water surface elevation in the bridge cross section. The average flow velocity through the bridge is depth integrated. The FLO-2D model does not support a grid system draped over the bridge cross section and the flow field around bridge piers is not computed. Scour holes are not predicted since the water volume stored in the scour holes is negligible compared to the volume of water passing through bridge. The primary result of the FLO-2D bridge routine for unsteady flow is to assess the deviation from the approximate normal depth flow condition through the bridge that results in an upstream backwater effect. This will enable the accurate analysis of bridge constricted floodplain and river reaches that exhibit non-uniform and unsteady flow conditions (Figure 101).

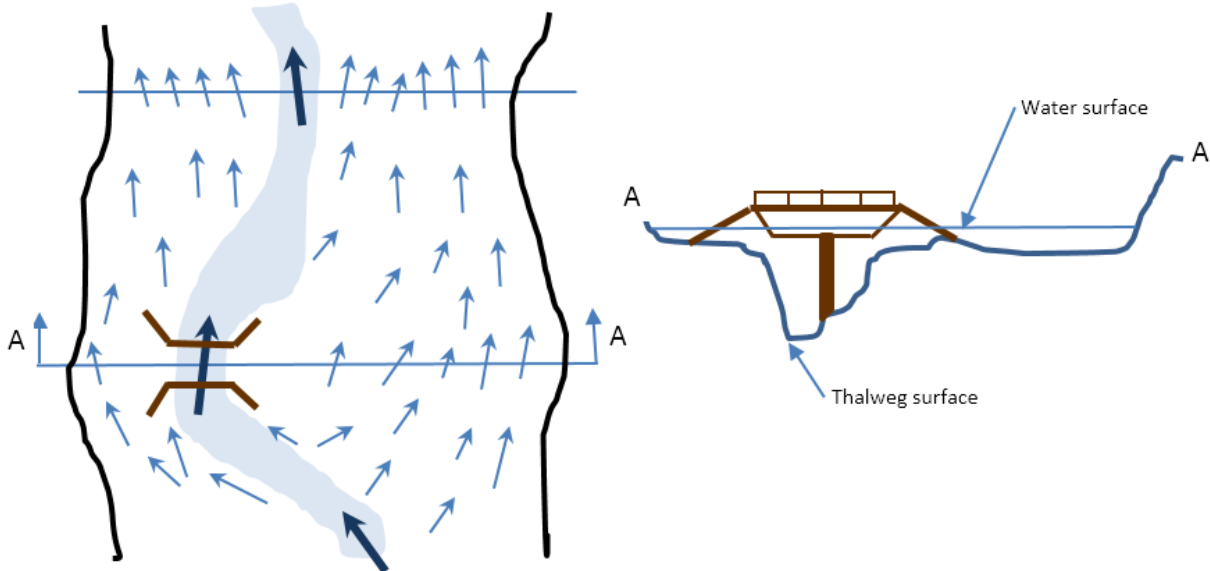


*Figure 101. Unsteady Non-Uniform Flow through a Bridge Constriction.*

## Bridge Flow

There are three basic flow conditions through a bridge: free surface flow, pressure flow and pressure flow plus deck overtopping flow. Pressure flow, which occurs when the deck or superstructure is submerged, is defined as either sluice gate or orifice flow. Flow through a bridge constriction is a function of the upstream headwater and downstream tailwater elevations (water surface slope), the extent of the constriction (cross section variation), the bridge geometry (flow area, wetted perimeter, low chord, etc.) and various site factors such as vegetation encroachment, bed scour, and riprap. Similar bridges at different locations experience different flow conditions for the same discharge. The flow may be subcritical or supercritical, although supercritical flow may be limited to a bridge with a concrete apron or bedrock substrate. Subcritical flow is the most prevalent flow regime as bridge constrictions typically reduce upstream velocities and cause backwater effects as opposed to flow acceleration through the bridge. Five types of subcritical bridge flow are shown in Figure 102 though Figure 106 where the flow depth at the bridge  $Y_z$  required to submerge the bridge opening is greater than about 1.1 \* Z (distance from the bed to the bridge low chord) (Chow, 1959 and Hamill, 1999).

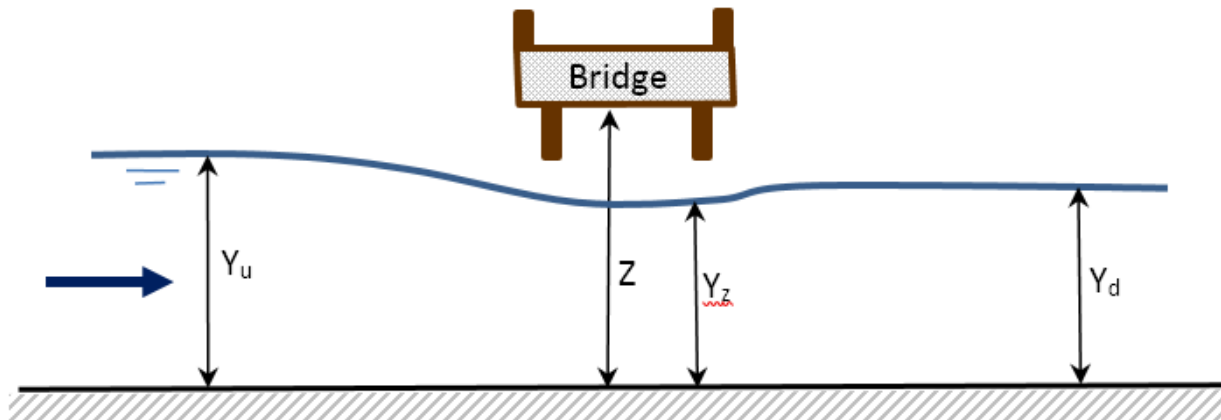


Figure 102. Type 1 Flow: Free surface, subcritical flow ( $Z > Y_u > Y_d$ ).

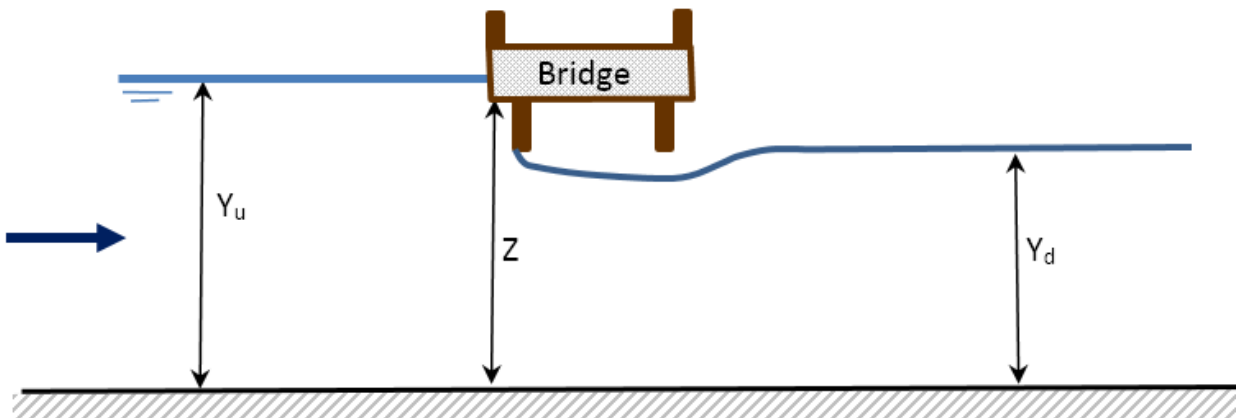


Figure 103. Type 2 Flow: Inlet submerged, outlet free surface, partially full, sluice gate flow ( $Y_u > Z > Y_d$ ).

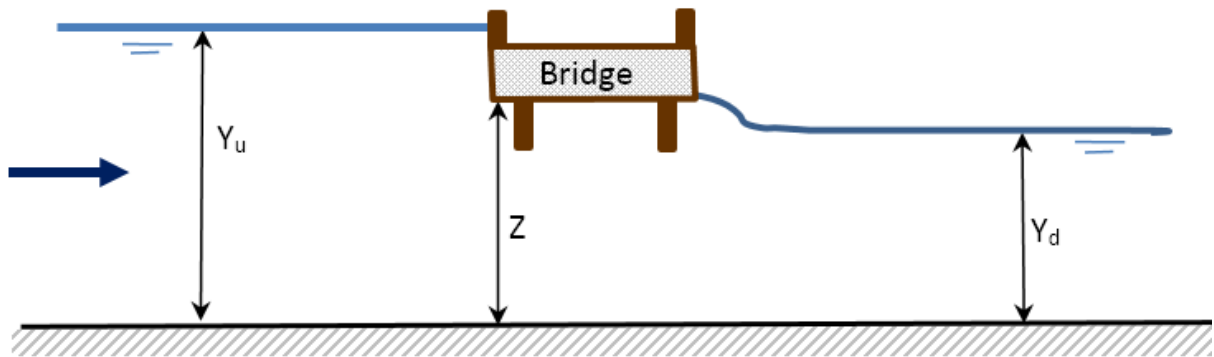


Figure 104. Type 3 Flow: Inlet submerged, outlet submerged, opening full, sluice gate-orifice transition flow ( $Y_u > Z > Y_d$ ).

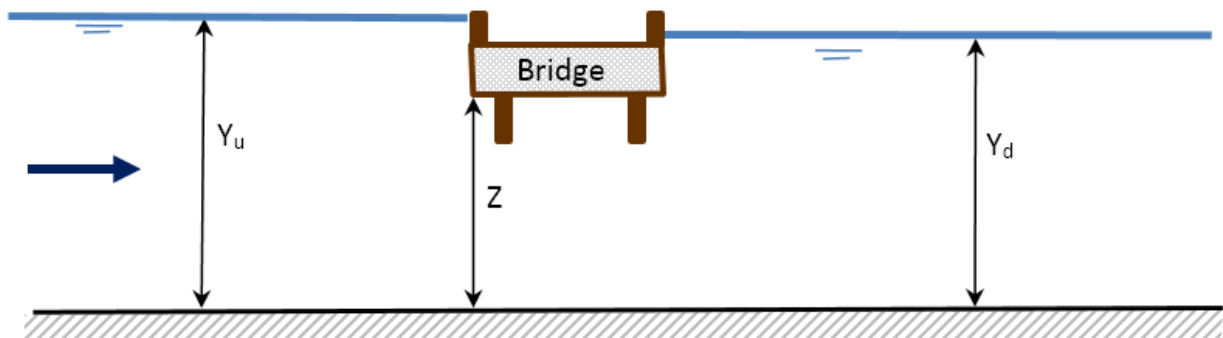
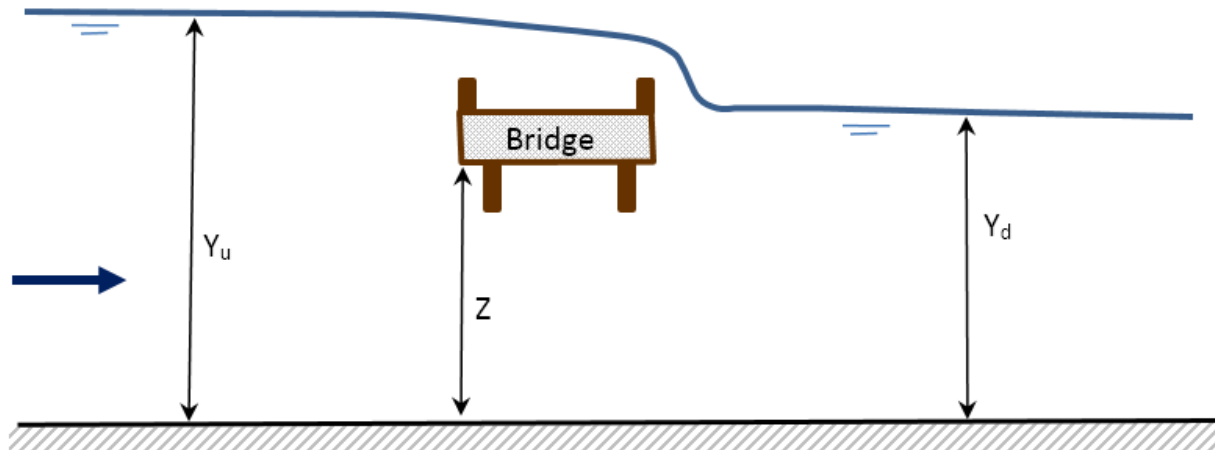


Figure 105. Type 4 Flow: Inlet submerged, outlet submerged, orifice flow ( $Y_u > Y_d > Z$ ).



*Figure 106. Type 5 Flow: Inlet submerged, outlet submerged, deck overflow ( $Y_u > Y_d > Z$ ).*

Type 1 flow is the most common flow in terms of frequency since the bridge is designed to pass a selected design flood event. The design flood may have a backwater condition extending some distance upstream. Sluice gate flow (Type 2) occurs when the upstream opening is submerged, but the downstream water surface elevation is below the bridge soffit. For this case, the discharge through the bridge depends on the upstream water surface elevation and the bridge geometry and the downstream water surface elevation is irrelevant. The submergence of the upstream opening may be sporadic until the upstream flow depth ( $Y_u$ ) is ten percent greater than the bridge low chord elevation. As the water surface level approaches the low chord, the discharge becomes highly turbulent and fluctuates rapidly, alternating between free surface flow and pressure flow (Type 3 flow as shown in Figure 107). The transition between sluice gate flow and orifice flow is unique to the bridge and may be temporally variable with scour, deposition or debris blockage. Based on project applications, sluice gate flow may persist until the upstream flow depth is 1.5 times or greater than the depth to the low chord.



Figure 107. Pressure Flow with the Water Surface above the Low Chord Elevation (M. Huard, USGS).

Once the bridge inlet has been permanently submerged, a rapid increase in upstream water surface may occur resulting in submergence of both the upstream and downstream openings and the bridge cross section flowing full. This is defined as drowned orifice flow (Type 4) and can only happen when both upstream and downstream water surface elevations exceed the 1.1 times Z (height of the bridge opening). Since the downstream water prevents the efficient flow through the bridge, upstream flooding can quickly ensue. In this case, the discharge control is a combination of the bridge structure and the channel characteristics.

When the flow begins to overtop the bridge, the discharge is the sum of the pressure flow plus the deck overflow (Type 5 flow, Figure 5). This is typically modeled as broadcrested weir flow with a coefficient in the range of 2.65 to 3.21. If the bridge has guard rails or debris, the selected weir coefficient should be conservatively low. Typically, overtopping flow is shallow, but for a long bridge the overflow discharge can be significant. An assumption of weir flow to represent overdeck discharge can only be an approximation because of several factors that are not limited to:

- Tailwater submergence;
- Variable deck elevation;
- Unsteady flow conditions;
- Guardrail supports causing blockage and spatially variable flow;
- Debris blockage.



Figure 108. Bridge Deck Overflow with Guardrail (Llano River Bridge Collapse, CBS Austin).

### Bridge Flow Modeling

The FLO-2D modeling approach and equations for the different types of bridge flow are discussed in this section. The objective is to compute the bridge discharge that will consist of either:

- Free surface flow
- Pressure flow
- Weir flow (overtopping) plus pressure flow

The effect of submergence from rising downstream tailwater is also determined by the FLO-2D model.

The bridge discharge computations will be performed inside the FLO-2D routing algorithm for the floodplain and 1-D channel components in conjunction with the existing hydraulic structure routine. The full dynamic wave momentum equation is applied to route flow between any two contiguous floodplain or channel grid elements. The velocity (and hence the discharge) is computed at one of eight floodplain flow directional boundaries between two cells. Prior to the bridge routine, the discharge for the bridge (or any hydraulic structure) located between two cells was computed only with a rating curve or table. The hydraulic structure inflow and outflow elements do not have to be contiguous (Figure 109). In the bridge flow modeling component, the free surface flow, pressure flow and deck overflow will replace the rating curve or table. The model will identify the flow condition, compute the appropriate discharge and exchange the discharge volume between the inflow and outflow nodes. As previously discussed, the flow discharge is controlled by the upstream headwater in the inflow node, the channel and bridge geometry and roughness, and tailwater water elevation in the outflow node. In the case where a bridge is located on the floodplain (such as a wash) spanning several elements, an inflow and outflow node (or multiple nodes) are still assigned and the two bridge cross sections are required.

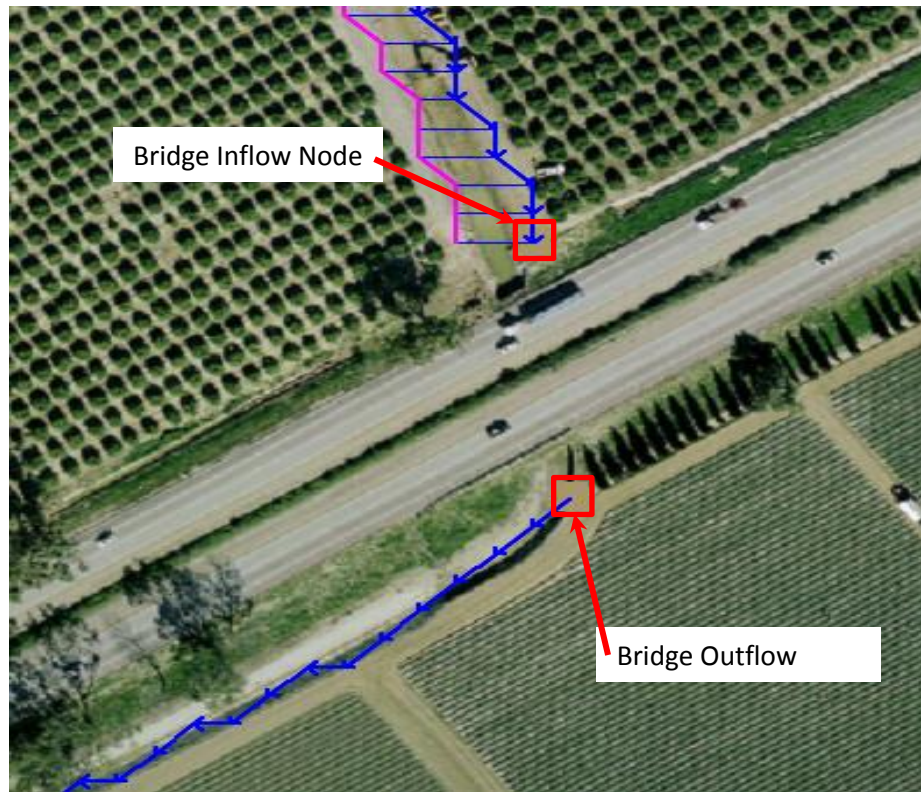


Figure 109. FLO-2D Model Bridge Inflow and Outflow Elements Separated by a Number of Grid Elements.

#### **Free Surface Flow**

The most frequent discharge through a bridge is subcritical low flow or free surface flow. Typically, the bridge constricts the channel with abutments and piers, has higher flow resistance, and increases the wetted perimeter resulting in a departure from upstream normal flow depth condition (backwater effect). The method to evaluate the discharge is referred to as the 1950's USGS method based on extensive laboratory and field tests as presented in Chow (1959) and Hamill (1999). This procedure was originally documented in Chow (1959) and is widely applied for subcritical flow in a solution of the energy and continuity equations. Various bridge configurations are considered in the method which includes piers, wingwalls, flow skew, entrance effects, submergence and two cross sections. The upstream cross section should be located beyond the influence of the bridge (Xsec 1 in Figure 7). Cross section 2 should be located at the bridge minimum cross section flow area (Xsec 2 in Figure 7). The USGS method assumes that the bridge constriction is a discharge-stage control given by an equation in which the discharge is expressed as a function of the flow area, head loss across the bridge ( $\Delta h$  in Figure 7), and a coefficient of contraction as discussed below. The complete derivation of the free surface (flow below the low chord) equation can be reviewed in either Hamill (1999) or Chow (1959).

The subcritical discharge  $Q$  through constrictions equation is given in Chow's (1959) book [Open Channel Flow](#) (p. 479, Eqn 17-15) as:

$$Q = C A_2 \{2g (\Delta h - h_f + \alpha_1 V_1^2/2g)\}^{0.5}$$

where:

$A_2$  = flow area at cross section 2 (Figure 7 downstream end of bridge)

$\Delta h = y_1 - y_2$   $y_1$  depth upstream of bridge –  $y_2$  depth at downstream end of bridge

$h_f$  = frictional loss

$\alpha_1$  = energy coefficient at cross section 1

$V_1$  = depth averaged velocity at cross section 1

$g$  = gravitational acceleration

$C = C_c / (\alpha_2 + k_e + k_p)^{0.5}$ ;  $C_c$  = coefficient of contraction,  $\alpha_2$  = energy coefficient at cross section 2,

$k_e$  = eddy loss coefficient,  $k_p$  = non-hydrostatic pressure coefficient

The terms can be combined and expanded to yield Eqn 17-20 in Chow (1959, p. 490) in English units:

$$Q = 8.02 C A_2 (\Delta h/\beta)^{0.5} \quad (1)$$

where:

$$\beta = 1 - \alpha_1 C^2 (A_2 - A_1)^2 + 2gC^2 (A_2/K_2)^2 (L_B + L_{1-2} K_2/K_1);$$

$L_B$  = length of contracted reach

$L_{1-2}$  = length of the reach from cross section 1 to cross section 2 (Figure 7)

$K_1$  and  $K_2$  = conveyance at cross sections 1 and 2;  $K_1 = 1.486/n A_1 R_1^{0.67}$ ,  $K_2 = 1.486/n A_2 R_2^{0.67}$

$n$  = Manning's n-value through the contracted reach

$A_1$ ,  $R_1$  and  $A_2$ ,  $R_2$  are the cross section flow areas and hydraulic radii respectively (Figure 110).

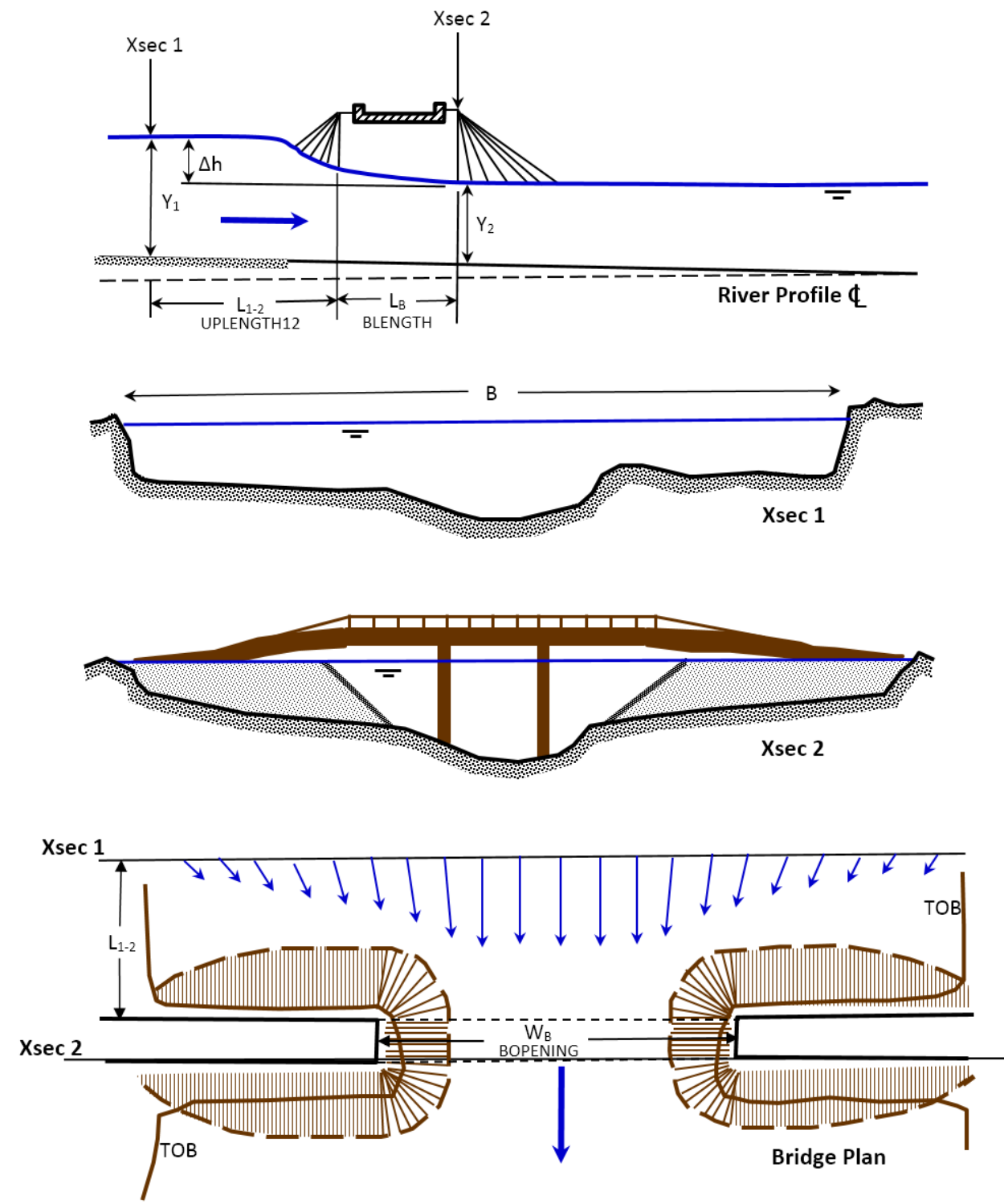


Figure 110. Conceptual Bridge Plan and Profile with River Cross Sections.



To apply this free surface flow equation, the type of bridge opening (one of four) must be selected and the bridge parameters and coefficients must be determined. The USGS figures for the four bridge types used to determine the coefficients are presented in the Appendix as reproduced from Hamill (1999). The relationships between the bridge parameters in Appendix figures that are used to evaluate the coefficients are hardcoded into the FLO-2D model in tabular form for linear interpolation. Conceptually, the role of the bridge coefficients is to represent a resistance to flow that will decrease the discharge similar to the Manning's n roughness coefficient with the exception that a decrease in the bridge coefficients will have the same effect as an increase in the Manning's n-value.

The USGS bridge discharge method embodies a number of assumptions both theoretically and practically to simplify the required data. The following assumptions have been acknowledged as potentially limiting the accuracy of the modeling approach.

- i. Two cross sections will be used to represent the bridge. If there is no 1-D FLO-2D channel, the cross sections are still required data (BRIDGE\_XSEC.DAT file). For a 1-D channel, the bridge cross sections can be represented by existing channel cross sections with the first cross section being the bridge inflow node channel cross section. This cross section should represent essentially normal depth upstream of the bridge (beyond backwater effects). The length between the two cross sections (UPLENGTH12 – L<sub>1-2</sub> in Figure 7) can be adjusted and can be longer than a grid element side length if the cell size is too short to extend to the normal flow depth conditions.
- ii. The bridge flow will be exchanged between the upstream inflow and downstream outflow elements (INFLONOD or OUTFLONOD in HYSTRU.C.DAT file) for either the channel or floodplain. Conceptually the bridge will be located between these two elements and share discharge between them. The inflow and outflow nodes don't have to be contiguous. The bridge cross section will constitute the boundary between these elements.
- iii. If there is widespread floodplain flooding, the upstream cross section should be limited to the 1-D channel top of banks. For a bridge on the floodplain with no channel, the cross section should be limited to a perceived channel width or the bridge opening width. The cross section should not encompass the entire valley floodplain.
- iv. The flow depth at the bridge is defined by the upstream inflow element water surface elevation and the bridge cross section thalweg in cross section 2 (Figure 7). This is not entirely accurate, since the water surface will vary from the upstream cross section to the bridge cross section, but water surface elevation at the bridge is not computed directly by the model. Given the potential of backwater effects, however, the impact of the variable water surface elevation on the flow depth will not be significant.
- v. The water surface head difference will be assessed from the upstream inflow node headwater and the downstream outflow node tailwater.
- vi. The bridge will assume to have the same constriction coefficients and losses regardless of whether the flow is upstream or downstream.

- vii. A velocity coefficient of  $\alpha_1 = 1.3$  is assumed and hardcoded for natural streams from Chow (1959, p. 28) representing an average of lower values ( $\alpha_1 \sim 1.1$ ) for large uniform prismatic and higher values for small nonuniform natural channels (ranging up to 1.5).

### ***Sluice Gate Flow***

Once the water surface level reaches the low chord or soffit of the bridge, the water surface control switches from the channel to the bridge and the discharge mimics a sluice gate flow (Figure 3b). In general, sluice gate flow applies only when the water level is on the upstream bridge face, but the highly turbulent transition to orifice flow is obscure with potential for drowning the downstream opening (Figure 3c). In a stage-discharge plot, the free surface channel flow and the bridge flow rapidly diverge as the water surface approaches the soffit (Figure 8). The difference between the two water surfaces is the afflux. The bridge flow in this figure is concave upwards above the soffit. Sluice gate discharge  $Q_p$  (pressure flow) is described by the equation:

$$Q_p = CA_b (2g \Delta H)^{0.5} \quad (2)$$

where:

$C$  = coefficient of discharge (0.3 to 0.6 dimensionless, Figure 111)

$A_b$  = cross section flow area through the bridge opening

$g$  = gravitational acceleration

$\Delta H$  = energy gradient from upstream to tailwater elevation  $Y_c$  given by (see Figure 103):

$$Y_u - Y + V_u^2 / 2g$$

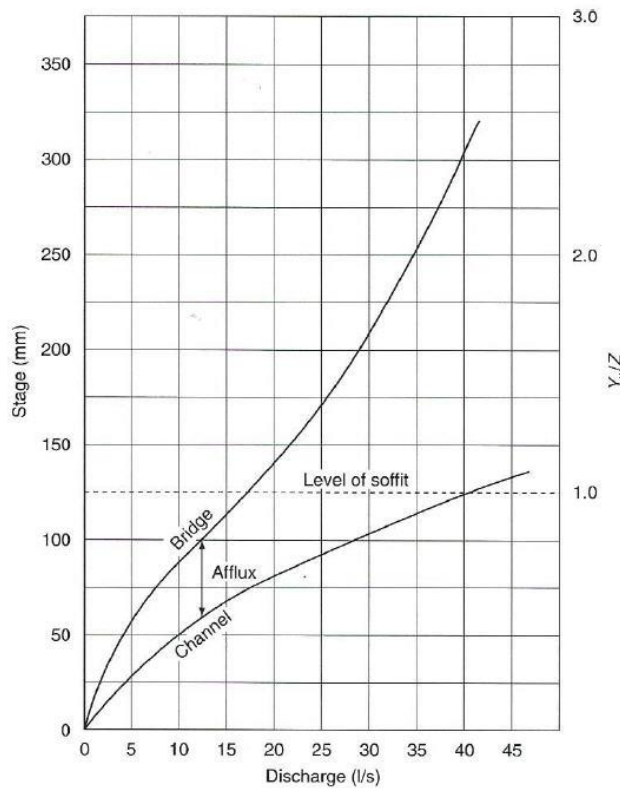


Figure 111. Stage-Discharge Variation between Free Surface Flow and Bridge Flow (Hamill, 1999; p. 53).

For subcritical flow the velocity head term  $V_u^2/2g$  (including the velocity coefficient) can be ignored and lowest flow depth  $Y$  through the bridge will vary from approximately  $Z/2$  to the downstream tailwater elevation (Figure 103 and Figure 104). Figure 112 indicates a range of 0.27 to 0.50 for the sluice gate coefficient as a function of the low chord submergence, however, Hamill (1999, Figure 2.11, p. 55) indicates that the coefficient can approach 0.6 depending on the bridge configuration.

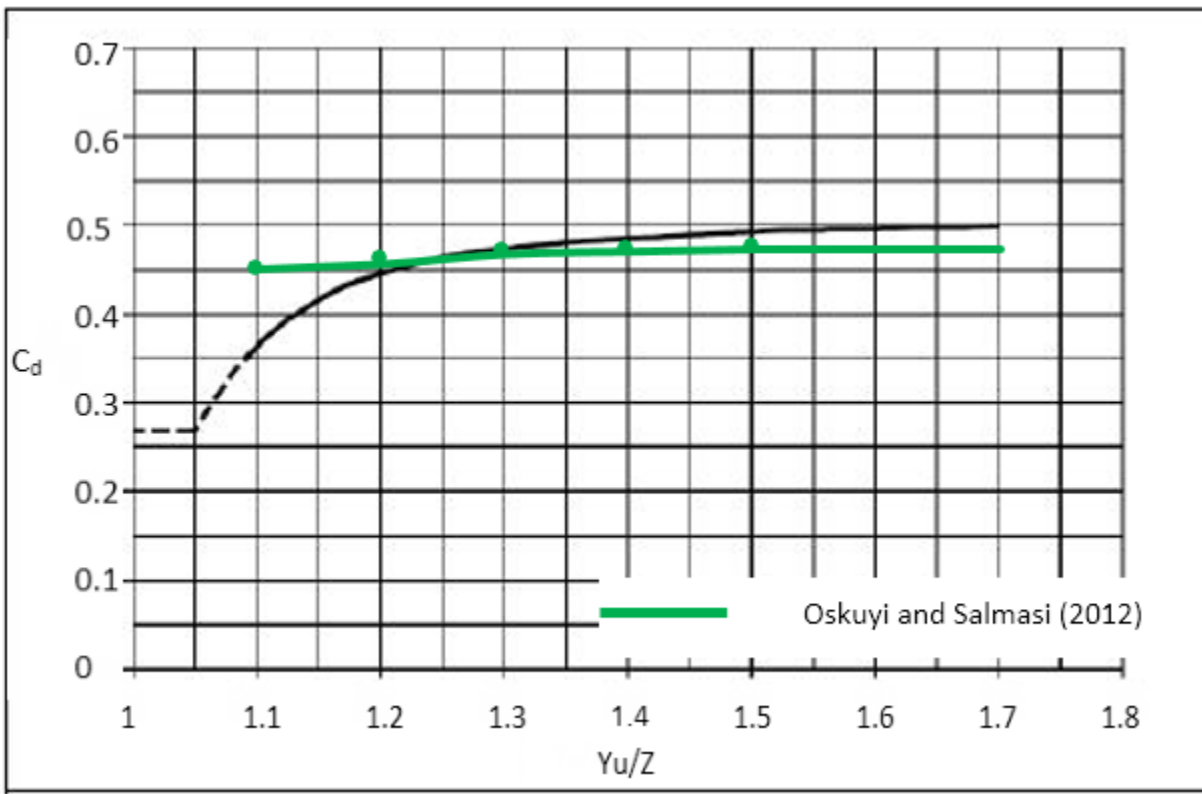


Figure 112. Sluice Gate Discharge Coefficient as Function of the Low Chord Submergence (FHA, 2012).

An important aspect of sluice gate flow is that there is a transition between sluice gate flow and free surface flow and again between sluice gate flow and drowned orifice flow (discussed below). These transitions are unique for each channel and bridge site. There may also be a hysteresis effect between the rising and recession limbs of the hydrograph. Factors that contribute to the variability in the transition flow zone (establishment of submergence) are numerous but can include an inclined bridge low chord. Ideally, the transition from free surface flow to sluice gate flow as noted in the literature, extends to a submergence level of  $Y_u/Z = 1.1$ , but practically it may be as high as  $Y_u/Z = 1.5$  depending on the bridge configuration and its hydraulic performance.

It should be mentioned that the above sluice gate equation (Hamill, 1999), differs from the vertical sluice gate discharge equation which is also occasionally applied to bridge flow. For the vertical sluice gate case, the assumed discharge is a function of the square root of the difference between upstream uniform flow depth and some percentage of the gate opening. Oskuyi and Salmasi (2012) presented a vertical sluice gate coefficient relationship with limited variability over a range of flows:

$$C = 0.445 (Y_u/Z)^{0.122}$$

which is plotted as the green line in Figure 9. The FHA curve in Figure 9 has a regressed relationship of:

$$C = 0.341 (Y_u/Z)^{0.931}$$

with a correlation coefficient  $R^2 = 0.61$ . This equation is used in the FLO-2D model.

### Orifice Flow

Orifice flow is defined by a pressure flow condition through the bridge where both the upstream and downstream water surface elevations are above the low chord ( $Y_u > Z$ ,  $Y_d > Z$ ) indicating a drowned opening (Figure 3d). The orifice equation for discharge is:

$$Q_p = CA_b (2g \Delta H)^{0.5} \quad (3)$$

where:

$C$  = Coefficient of discharge

$A_b$  = Bridge opening cross section flow area

$\Delta H$  = difference between the energy gradient elevation upstream and tailwater downstream

In this equation, which is similar to the sluice gate equation,  $\Delta H$  is given by the difference in the headwater  $Y_u$  and tailwater  $Y_d$  plus the velocity head  $V_u^2/2g$ , which again is assumed to be negligible for subcritical flow (at least when considering the variability of the coefficient). The orifice coefficient of discharge  $C$ , as determined by experiment, ranges from 0.7 to 0.9 (USCOE HEC, 1995). A value of 0.8 is recommended for a typical two- to four-lane concrete girder bridge coefficient (Hoggan, 1989; p. 401). Hamill (1999) plots data from actual bridge flow and other sources to demonstrate the variation of the coefficient of discharge with submergence (Figure 10).

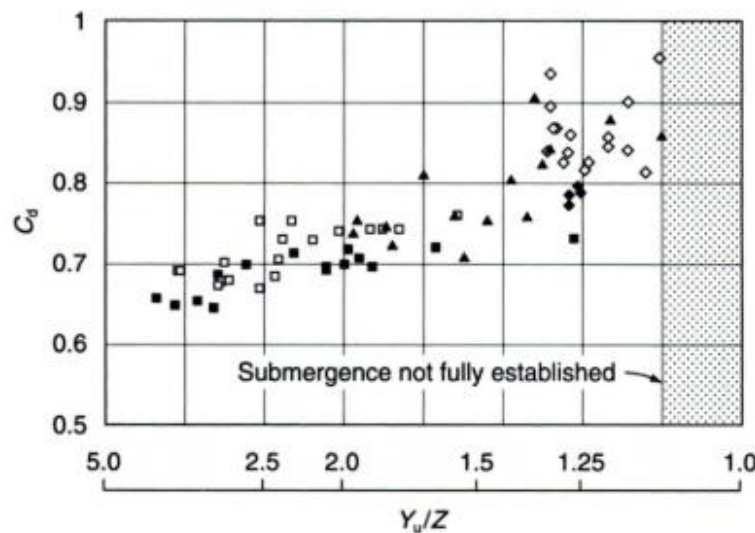


Figure 113. Orifice Coefficient of Discharge as Function of Low Chord Submergence (Hamill, 1999).

The regressed relationship of the data in Figure 10 for  $Y_u/Z > 1.25$  is given by:

$$C = 0.80 (Y_u/Z)^{-0.184}$$

This equation is used in the FLO-2D model and results in a coefficient variability in the range of 0.7 to 0.8. This is compared with the sluice gate flow discharge coefficient, which ranges from about 0.4 to 0.5 as shown in Figure 9.

### **Pressure Flow Plus Weir Flow**

Once the flow is above the deck, then the total discharge through bridge  $Q_T$  is the sum of the pressure flow (sluice gate or orifice flow) plus the weir flow over the bridge deck:

$$Q_T = Q_p + Q_w$$

Broadcrested weir flow is generally used to represent flow over a bridge deck as given by:

$$Q_w = C L_c \Delta H^{1.5}$$

where:

$C$  = Broadcrested weir discharge coefficient which varies from 2.6 to 3.1

$\Delta H$  = energy grade line between headwater and roadway crest elevation (or railing) or tailwater

$L_c$  = crest length

Broadcrested weir flow representing bridge overflow is usually justified because flow across the crest (roadway) is considered broad and the flow depth on the bridge is shallow. When combined with the pressure flow, the overtopping flow will result in equal energy loss. If the tailwater drowns out the weir control, then a submergence factor in the FLO-2D hydraulic structure routine will be applied to the discharge. Submergence generally becomes an issue when the tailwater depth divided by the headwater depth approaches 0.80. Since a bridge deck is not an ideal smooth broadcrested weir, a lower coefficient of discharge in the range of 2.6 to 2.8 is suggested (FHA, 2012). Some consideration should be given to the deck railing configuration. Is the deck railing segmented and spanning the entire bridge? Does it have multiple rails or is it solid? Are there walkways that are elevated above the road bed? Is the bridge deck inclined, sloping from one side to the other? Can debris collect on the deck railing? All these possible flow conditions will decrease the broadcrested weir coefficient.

It is important to note the difference between the weir coefficient  $C$  and a discharge coefficient  $C_q$ . The weir coefficient is a lumped parameter that is based on the weir's characteristics and includes the discharge coefficient.

$$C = 2/3 C_q (2g)^{0.5}$$

The discharge coefficient  $C_q$  is same in both English and SI (metric) units and is dimensionless. The weir coefficient, however, is not dimensionless since it is a function of the gravitational acceleration  $g$  ( $\text{ft}/\text{s}^2$  or  $\text{m}/\text{s}^2$ ). To convert from English to metric, multiply the weir coefficient  $C$  by 0.552.



## Modeling Bridge Flow with FLO-2D

The bridge flow routine in FLO-2D is called by the hydraulic structures component which establishes the inflow and outflow nodes, the headwater, tailwater and submergence conditions, and the components for discharge exchange (floodplain to floodplain, channel to channel, floodplain to channel, or channel to floodplain). The rating curve and table data that is normally assigned for FLO-2D bridge flow is not required. As previously mentioned, the bridge inflow and outflow nodes do not have to be contiguous in the grid system. They can be separated by several grid elements to represent a four-lane highway bridge. In the FLO-2D model, the discharge is routed to the inflow node to determine the headwater and flow depth conditions. Then the free surface, pressure flow or weir flow equations compute the bridge discharge to the outflow node, which is then routed to the downstream elements by the model's routing algorithm.

### ***Data Requirements and Parameter Definition***

Two lines of data in the HYSTRUC.DAT file (B-lines) and two cross sections are required for each bridge being simulated. The original S-Line in HYSTRUC.DAT identifies the bridge inflow and outflow nodes and its association with the either the channel or the floodplain. The rating curve or table switch in the S-Line is set to 3 (ICURVTABLE(i) =3) to define a bridge analysis for that structure. The S-Line is then followed by two B-lines where (i) is the bridge number in HYSTRUC.DAT.

The first B-line of data in the HYSTRUC.DAT file provides the user with the opportunity to directly assign the free surface low flow discharge coefficients. The second B-line includes the various bridge parameters such as low chord, deck length, pier width, etc.

- 1) B IBTYPE(i), COEFFP(i), C\_PRIME\_USER(i), KF\_COEF(i), KWW\_COEF(i), KPHI\_COEF(i), KY\_COEF(i), KX\_COEF(i), KJ\_COEF(i)
- 2) B BOPENING(i), BLENGTH(i), BN\_VALUE(i), UPLENGTH12(i), LOWCHORD(i), DECKHT(i), DECKLENGTH(i), PIERWIDTH(i), SLUICECOEFADJ(i), ORIFICECOEFADJ(i), COEFFWEIRB(i), WINGWALL\_ANGLE(i), PHI\_ANGLE(i), LBTOEABUT(i), RBTOEABUT(i)

A typical HYSTRUCT.DAT file for a bridge would be as follows:

```

S Name   0   3   631   625   1   0.0   0   0
B 1  0. 0. 0. 0. 1. 1. 1. 1.
B 15. 40. 0.05 40. 1378.00 1380.00 22.00 0. 0. 0.50 3.05 0. 0. 1376.5 1377.2

```

These parameters are defined in Table 13 and are used to compute the coefficients for free surface flow presented in the Appendix. The Appendix figure showing the relationships with the bridge configuration are used to interpolate the free surface coefficients from the data entered in Line B-2. All the Appendix figures were digitized and are hardcoded into the model.

**Table 13. Bridge Parameters (B-Lines in HYSTRU.C.DAT)**

VARIABLE	FMT	RANGE	DESCRIPTION
STRUCHAR	c	B	Character identifier for the bridge routine
IBTYPE	i	1 – 4	Type of bridge configuration (see Appendix figures)
COEFF*	r	0.1 - 1.0	Overall bridge discharge coefficient – assigned or computed (default = 0.)
C_PRIME_USER*	r	0.5 - 1.0	Baseline bridge discharge coefficient to be adjusted with detail coefficients
KF_COEF*	r	0.9 - 1.1	Froude number coefficient – assigned or computed (= 0.)
KWW_COEF*	r	1.0 - 1.13	Wingwall coefficient – assigned or computed (= 0.)
KPHI_COEF*	r	0.7 - 1.0	Flow angle with bridge coefficient – assigned or computed (= 0.)
KY_COEF*	r	0.85 - 1.0	Coefficient associated with sloping embankments and vertical abutments (= 0.)
KX_COEF*	r	1.0 - 1.13	Coefficient associated with sloping abutments – assigned or computed (= 0.)
KJ_COEF*	r	0.6 - 1.0	Coefficient associated with pier and piles – assigned or computer (= 0.)
BOPENING	r	0.0 - $\infty$	Bridge opening width (ft or m). See Figure 7.
BLENGTH	r	0.0 - $\infty$	Bridge length from upstream edge to downstream abutment (ft or m)
BN_VALUE	r	0.030 - 0.200	Bridge reach n-value (typical channel n-value for the bridge cross section)
UPLENGTH12	r	0.0 - $\infty$	Distance to upstream cross section unaffected by bridge backwater (ft or m)
LOWCHORD	r	0.0 - $\infty$	Average elevation of the low chord (ft or m).
DECKHT	r	0.0 - $\infty$	Average elevation of the top of the deck railing for overtop flow (ft or m)
DECKLENGTH	r	0.0 - $\infty$	Deck weir length (ft or m).
PIERWIDTH	r	0.0 - $\infty$	Combined pier or pile cross section width (flow blockage width in ft or m)
SUICECOEFADJ	r	0.0 - 2.0	Adjustment factor to raise or lower the sluice gate coefficient which is 0.33 for $Y_u/Z = 1.0$
ORIFICECOEFADJ	r	0.0 - 2.0	Adjustment factor to raise or lower the orifice flow coefficient which is 0.80 for $Y_u/Z = 1.0$
COEFFWEIRB	r	2.65 - 3.21	Weir coefficient for flow over the bridge deck. For metric: COEFFWIERB x 0.552
WINGWALL_ANGLE	r	30° - 60°	Angle the wingwall makes with the abutment perpendicular to the flow
PHI_ANGLE	r	0° - 45°	Angle the flow makes with the bridge alignment perpendicular to the flow
LBTOEABUT	r	ELEVATION	Toe elevation of the left abutment (ft or m)
RBTOEABUT	r	ELEVATION	Toe elevation of the right abutment (ft or m)

\* If the coefficient is assigned 1.0, that bridge coefficient is either not important or has no effect.

The two cross sections are located: 1) Upstream of the bridge where essentially normal depth occurs (upstream of the bridge backwater effects); and 2) At the bridge to reflect the channel contraction and low chord. The cross section data is listed in the BRIDGE\_XSEC.DAT file. The two required bridge cross sections are shown in Figure 7. This data is necessary regardless of whether there are 1-D channel cross sections or no surveyed cross sections associated with a bridge on the floodplain. The bridge cross section can be located anywhere in the bridge that defines the bridge contraction. The upstream cross section is located by the distance  $L_{1-2}$  (Figure 7). The pier or pile widths are not entered in the cross section data. The sum of all the pier or pile widths (PIERWIDTH) is entered in the B-line data in HYSTRU.C.DAT (Table 1). The cross section data is entered in the BRIDGE\_XSEC.DAT file in the ASCII format below (data separated by spaces). In line 1, X indicates the start of a new bridge cross section and the number 631 is bridge inflow node grid element number. The remaining lines are station from the left top of bank, upstream bed elevation at the given station, and the bridge station bed elevation.

```
X 631
0.00 1380.00 1385.00
0.60 1378.70 1378.46
5.00 1377.00 1376.96
5.50 1376.85 1376.68
6.00 1376.75 1376.46
12.65 1376.70 1376.46
15.85 1376.78 1376.51
```

18.95	1377.20	1377.00
20.65	1378.15	1377.26
22.00	1378.70	1378.44
22.10	1380.00	1385.00

The bridge cross section is referenced to the upstream cross section stations. The bridge cross section contraction corresponds to the abutments or channel bank elevations under the bridge deck. The low chord data (LOWCHORD) represents the average low elevation of the deck structure and the deck elevation (DECKHT) represents the average elevation of deck (typically the railing). The bridge deck may be inclined from one side of the channel to the other (not level) and judgment may be necessary to select low chord or deck elevations to represent the initiation of full pressure flow under the bridge or full weir flow over the bridge.

To get started, use bridge as-builts or design drawings and survey the bridge cross sections or digitally extract them from topographic data in a GIS or CADD program. The FLO-2D QGIS Plug-In can be used. Enter the bridge configuration data using an ASCII file editor or using the QGIS graphical interface. The older GDS will not have a bridge editor function.

To assist in understanding the free surface bridge flow routine, some specific detailed comments are provided:

Notes on the bridge configuration data:

- i. ITYPE = 1-4 bridge configurations representing the type of constriction I through IV depending on abutment type shown in the Appendix figures. The bridge type will be used to assign the various coefficients. Refer also to Figures 17-16 through 17-23 beginning on page 480 of Chow (1959) or Figure 4.4 through 4.13 beginning on page 113 of Hamill (1999). These two sets of figures are essentially the same but Hamill (1999) has a little more detail in some of the figures and for that reason, Hamill's (1999) figures has been reproduced in the Appendix.
- ii. The various coefficients are estimated from a linear interpolation between two points on the lines representing the bridge parameters and coefficient data in the Appendix plots. Typically, the lines in Appendix figures were divided into 8 to 12 segments to generate the digital data base.
- iii. The bridge opening (BOPENING) is the width of the contracted cross section between the top of banks.
- iv. L<sub>1-2</sub> = distance upstream of the surveyed constricted cross section (UPLENGTH12). This cross section should be located upstream of the backwater effects of the bridge (up to several lengths of the bridge opening width).
- v. Refer to the Appendix figures for parameter definition such as the radius of the leading edge of the Type I abutment, length of the wingwall chamfer for various three chamfer angles (30°, 45° and 60°), angle of bridge with respect to the flow, and angle of wingwall.

Comments on the bridge coefficients:

The general discharge coefficient for bridge contraction C (COEF) is proposed to account for eddy loss associated with contraction, nonuniform distribution of the velocity, and nonhydrostatic pressure distribution all contributed to the afflux. The discharge coefficient is defined as:

$$C = C' K_i$$

where:

C' (C\_PRIME\_USER) is the standard value of the coefficient of discharge for given bridge type of constriction;

K<sub>i</sub> are various multiplicative coefficients used to adjust the value of C' to account for nonstandard conditions involving the Froude number, entrance rounding, abutment chamfer, flow angularity, side depths, side slopes, bridge submergence, and piers.

Most of the coefficients represent a loss of energy or increase flow resistance through the bridge, but a couple of the coefficients for a particular stage or bridge configuration can result in more efficient flow and the coefficient can be greater than 1.0 such as for the Froude number and angle of the wingwall.

To derive the various discharge coefficients, the bridge opening ratio m must be determined where  $m = W_b/B$  and  $W_b$  is the contracted cross section width and B is the upstream channel cross section width for a prismatic channel. For a non-prismatic channel, the bridge opening ratio represents the percentage of the flow that can be conveyed through the bridge cross section without contraction. In this case, the opening ratio represents a ratio of the discharge conveyance through the two cross sections and the FLO-2D model performs this computation.

Some notes on the various bridge coefficients for free surface flow are listed below. The user has an option to assign the coefficients ( $K_i > 0.01$ ) or have the model compute the coefficients ( $K_i = 0.0$ ). If  $K_i = 1.0$ , then this bridge feature and its coefficient has no effect on the bridge flow.

$K_F$  (KF-COEF) = coefficient based on the effect of Froude number  $K_F = f(F_b)$ . The Froude number at the bridge is computed for Type 1 or Type IV bridges (see Appendix Figures) using the discharge, flow area and depth,  $F_b = Q/A_b (g y_b)^{0.5}$ . No additional data is required.

$K_r$  = coefficient of entrance rounding for Type I only. Percent of contraction m and r/b are required where r = radius of the corner and b = contracted bridge width, Appendix Figure A.1c.

$K_w$  (KWW\_COEF)= coefficient of wingwall chamfer for Type 1 only. Contraction percentage m and w/b for three possible chamfer angles are required where w is the chamfer length and b = contracted bridge opening. Appendix Figure A.2.

$K_\phi$  (KPHI\_COEF)= coefficient of bridge angle of attack to flow  $\Phi$  based on the bridge contraction m for all types of bridge configurations shown in the Appendix Figures.

$K_y$  (KY\_COEF)= coefficient of side flow depths on each vertical abutment (a and b) for  $(y_a + y_b)/2b$ , where  $y_a$  and  $y_b$  are the flow depths above the toe of each abutment (at different elevations) only for Type II bridge configurations Appendix Figure A.3.

$K_x$  (KX\_COEF)= coefficient of the abutment upstream slope as a function of the ratio of the distance to upstream water surface  $x$  from bridge deck to the bridge contraction width  $b$ . The  $K_x$  coefficient for different values  $x/b$  and deck widths ( $L$ ) for Type III abutments are shown in Appendix Figures A.5, A.6 and A.7.

$K_\theta$  = coefficient for wingwall angle  $\theta$  to the approach flow as a function of the bridge opening ratio  $m$  for Type IV bridges. Appendix Figures A.8 and A.9.

$K_j$  (KJ\_COEF)= coefficient for reduced flow area associated with bridge piers and piles for all Types of bridge configurations as a function of the bridge opening ratio  $m$  and the ratio of the contracted flow area due to the piers and piles (Appendix Figure A.10).

Two coefficients proposed by Chow (1959) and Hamill (1999) are not used in the bridge analysis.

$K_e$  = coefficient for eccentricity ratio (different abutment extension lengths into the flow). As recommended by Hamill (1999), the effect of the eccentricity on the discharge is generally small and can be ignored.

$K_t$  = coefficient of submergence. Tailwater submergence is already accounted for in the existing hydraulic structure routine and will be automatically applied with the bridge routine.

The coefficients have minimum and maximum limits based the Appendix figures.

### Discharge Computations

The free surface flow routine appears to be minutely detailed and overly complicated. The free surface flow is not as important as the pressure and weir flow, especially if the free surface flow is not overbank. If the flow is less than bankfull then a poor estimate of the bridge hydraulics would only result in 0.5 ft (0.16 m) error or so in the channel water surface elevation and the actual discharge would be about the same as the upstream flow. Even though Manning's equation only applies to steady, uniform flow conditions (which are not generally encountered at a bridge contraction), adjusting the Manning's n-value to represent the bridge hydraulics would undoubtedly provide a reasonably accurate bridge discharge up to the low chord. If the bridge discharge coefficients could be correlated with appropriate increases in the Manning's n-value, the free surface flow data requirements could be greatly simplified.

To perform the free surface flow, pressure flow and weir flow discharge calculations, the water surface elevations upstream and downstream predicted by the FLO-2D model routing algorithms are used. This data enables the upstream, bridge and downstream flow depths to be computed. Some adjustments to the flow depth and head across the bridge are made for certain conditions:

- The head at the bridge is interpolated based on the distance between the upstream cross sections and bridge.
- If the head exceeds the flow depth, the head is set to the flow depth.

- If the tailwater is higher than the headwater and the upstream water surface elevation is higher than the low chord, the head is computed as the difference between the upstream water surface elevation and the low chord.

Based on the respective flow depths, the upstream and bridge cross section channel geometry is computed including flow area, top width, wetted perimeter and hydraulic radius. Using the bridge configuration, channel geometry, and bridge opening ratio, the various free surface flow discharge coefficient adjustments (displayed in the Appendix) are computed resulting in an overall bridge discharge coefficient. Manning's n-values are adjusted for flow depth using the FLO-2D n-value modification method expressed as an exponential relationship of bankfull depth. The discharge through the bridge as free surface flow is then computed using Eqn (1).

Once the bridge flow water surface exceeds the low chord elevation, the discharges from the sluice gate flow equation (2) and the orifice flow equation (3) are computed. If both the upstream and downstream water surface elevations are greater than the low chord and if the depth to low chord height ratio exceeds 1.125, then the orifice discharge is used to represent the pressure flow. For the same upstream and downstream flow depth, if the bridge flow depth divided by low chord height is less than 1.125, the minimum of the sluice gate flow or the orifice flow discharge is applied to represent the pressure flow. For any other condition where the upstream water surface elevation exceeds the low chord, orifice flow is computed. Finally, when the upstream water surface elevation exceeds the deck height, the orifice pressure flow and deck weir flow is combined to represent the discharge past the bridge. The objective is to have a smooth transition between the applications of the three discharge equations. For all conditions, it is assumed that the flow will not accelerate through the bridge (in other words, there will be some backwater effects). If the bridge discharge is greater than the upstream grid element discharge, the bridge discharge is set equal to the upstream discharge. If it is possible that the flow will accelerate through the bridge as in the case of a concrete apron, then the bridge should be simulated as a closed culvert using the FLO-2D generalized culvert equations routine.

## **Summary**

The objective of the FLO-2D bridge routine is to compute the discharge through the bridge based on the physical configuration and features of the bridge. The bridge discharge is shared between two grid elements (channel or floodplain) that do not have to be contiguous and whose flow hydraulics (depth and water surface) are computed by the FLO-2D routing algorithm. Bridge discharge is defined by 1-D flow in the cross sections upstream and through the bridge. No two-dimensional flow field velocities in the bridge cross section are predicted by the model, so no flow patterns around the piers or scour hole depths can be simulated. The focus of the bridge routine is to relate the bridge discharge to the flow volume in the upstream and downstream channel elements or to the floodplain overbank flow.

The FLO-2D bridge routine enables the user to compute the discharge through bridges without using an external program to generate a stage-discharge rating curve or table. The routine will compute the discharge for three classes of flow regime, free surface flow for discharge below the bridge low chord, pressure flow when the discharge is above the low chord but below the bridge deck and combined pressure and weir flow as the discharge goes over the bridge. The pressure flow and weir flow

computations are relatively straight forward. The free surface flow is more complex with a number of multiplicative coefficients that represent various features of the bridge and their effects on the flow. The pressure flow will be either sluice gate flow or orifice flow, whichever is smaller. There may not be a smooth transition between the two types of flow representation and some adjustment of the coefficients may be necessary. An adjustment factor to raise or lower the computed sluice gate or orifice coefficient is available as a data input parameter. The user has complete control of all the coefficients utilized in the bridge routine for all flow regimes.

Matching HEC-RAS or other models with bridge components may not be exact because of the computational approach (e.g. solution to the 1-D energy equation vs flood routing with the full-dynamic wave momentum equation) and because the FLO-2D bridge routine has more detail for both free surface flow and pressure flow. Ultimately, the bridge flow control with coefficient adjustments, however, should provide a suitable correlation between the models. Unless there is an opportunity to calibrate the bridge coefficients to a field data set, it should not be assumed that the HEC-RAS or other bridge routines are necessarily more accurate. A primary focus of the bridge routine application should be to achieve numerical stability for the bridge flow over a wide range of unsteady, non-uniform discharges.



## Chapter 5. FLO-2D PROJECT APPLICATIONS

The FLO-2D website ([www.flo-2d.com](http://www.flo-2d.com)) has numerous webinars, video animations of predicted flooding, PowerPoint presentations and various documents that highlight FLO-2D model project applications. The five primary projects applications of the FLO-2D model are river projects, unconfined floodplain and alluvial fans models, watershed and rainfall/runoff analyses, urban and storm drain simulations, and coastal flooding.

### 5.1 *River Applications*

Simulating river flow is one of the more common applications of the FLO-2D model (Figure 114). The key to simulating river flooding is correctly assessing the relationship between the flood volume in the channel and the volume distributed on the floodplain. There are several key factors that help to define an accurate relationship between channel volume and geometry. The surveyed channel cross sections should be appropriately spaced to facilitate transitions between wide and narrow cross sections in the model. The channel volume is dependent on a good estimate of the total channel length (sum of the channel element lengths). This length should be compared to channel centerline distance of model project reach. Finally, predicted water surface elevations are based on the channel roughness values and calibrating the model roughness with known discharges and surveyed water surfaces will finalize the channel flood routing accuracy.

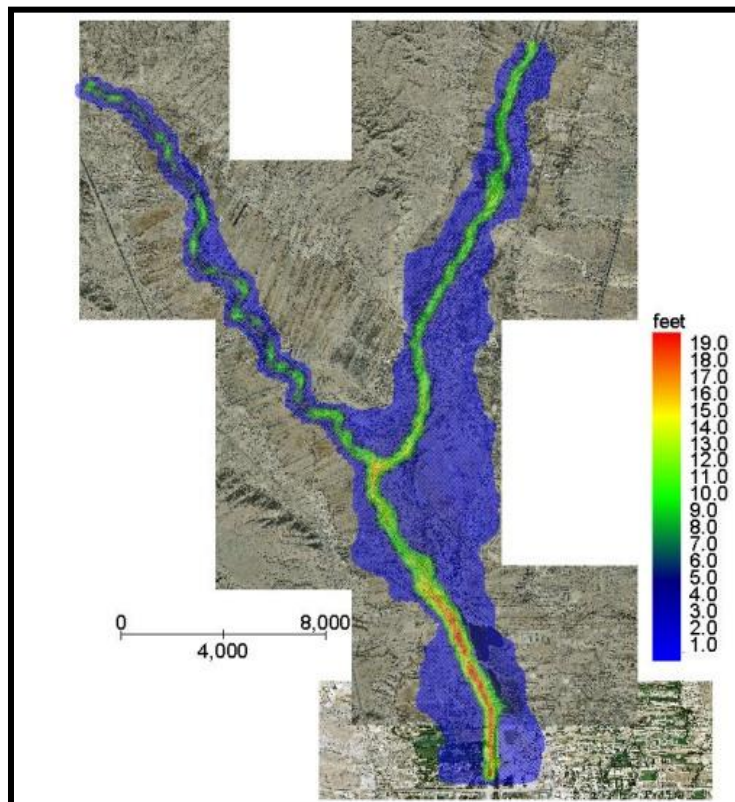


*Figure 114. Middle Rio Grande and Rio Chama Confluence Model.*

When preparing a channel simulation, the available cross sections are distributed to the various channel elements based on reaches with similar geomorphic features. The bed elevation is then adjusted between channel elements with surveyed cross sections. The n-values are estimated from knowledge of the bed material, bed forms, vegetation or channel planform. The n-values may also serve to correct any mismatched channel flow area and slope. Roughness values can also be adjusted by specifying a maximum Froude number. Using this approach, the relationship between the channel flow area, bed slope and n-value can be adjusted to better represent the physical system, calibrate the water surface elevations, eliminate any numerical surging, and speed-up the simulation.

The two most important FLO-2D results are the channel hydrograph at a downstream location and the floodplain area of inundation. Typically, if the area of inundation is correct, then the channel flow depths and water surface elevations will be relatively accurate. Replicating the channel hydrograph and the floodplain inundation while conserving volume is a good indication that the volume distribution between the channel and the floodplain is reasonable.

Flood routing details related to channel flow include simulating hydraulic structures, levees, infiltration, and sediment transport. Hydraulic structures may include bridges, culverts, weirs, diversions or any other channel hydraulic control. Levees are usually setback from the river on the floodplain but can control the water surface in the channel if the flood is confined. Channel infiltration is based solely on the hydraulic conductivity and represents average bed and bank seepage conditions. Bed scour or deposition associated with a mobile analysis is non-uniformly distributed on the channel cross section. Mudflows can also be routed in channels.

## **5.2 Unconfined Floodplain and Alluvial Fan Flooding**

The primary focus of an unconfined flood simulation is how the volume is distributed over the floodplain surface. The flood volume controls the area of inundation (Figure 115). FLO-2D can simulate an unconfined floodwave progression over a dry flow domain without specifying any boundary criteria. No hot starts or prescribed water surface elevations are required.

Important flood routing details include topography, rainfall spatial variation in infiltration and roughness, flow obstructions, levees, hydraulic structures, streets. The timing of the floodwave progression over the floodplain can be improved with rills and gullies. Street flow may control shallow flooding distribution in urban areas. Buildings and walls that obstruct flow paths and or eliminate floodplain storage. The levee routine can be used to simulate berms, elevated roadway or railroad embankments or other topographic features to confine the flow on the floodplain. Hydraulic conveyance facilities such as culverts may control local water surface elevations. Spatially variable rainfall may inundate areas outside the primary flood path. It is possible to model detention basins using either the grid element elevation or levees to define the basin storage area. An appropriate grid element size should be selected to generate enough interior elements to adequately simulate the basin.

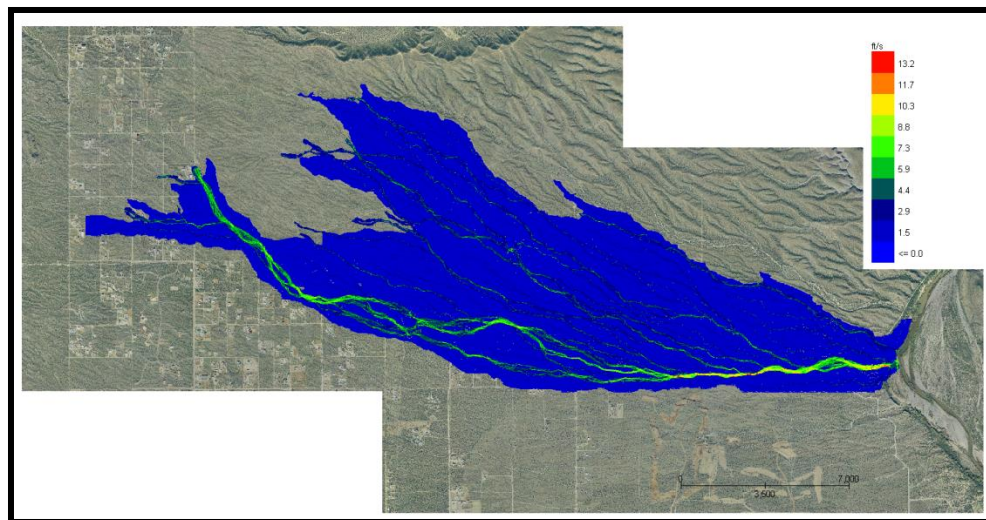


*Figure 115. Unconfined Alluvial Fan Flooding*

### **5.3 Watershed Rainfall Runoff Simulation**

FLO-2D can be used as a watershed model to predict rainfall runoff using one of three infiltration loss methods. The model can generate a flood hydrograph at a point of concentration as inflow to a downstream flood model. Rainfall runoff can result in sheet flow or concentrated in rills and gullies using the multiple channel component which will reduce the travel time associated with sheet flow. It is possible to simulate rainfall while routing a flood overland and have the rainfall occur directly off the water surface without abstraction. Spatially variable rainfall distribution using real time rain gage or NEXRAD data can also be modeled. The GDS will reformat the rain gage data for real time storm runoff and flood simulation. Basin water course depressions created in the data base because of the lack of DTM data on the channel bed can be smoothed out with the GDS smoothing tool. This will eliminate potential flood storage associated with the artificial depressions.

Using the FLO-2D model to cover the watershed and urban areas avoids the need to create separate models with generated hydrographs from the upper basin constitute the inflow to the urban model. The watershed-urban interface will be more accurate as a single model since the inflow will not all be concentrated at a few points. Runoff will occur as sheet flow all along the interface.

The watershed can also be a source of sediment supply for the urban project area for either sediment transport modeling or mud and debris flows. Sediment supply for conventional bedload and suspended analysis can be generated in the upper basin by simply applying one of the eleven sediment transport formulas. For mudflows there are two methods for loading the hydrograph with sediment. A sediment concentration by volume is assigned to a discretized time interval of the inflow hydrograph. A second method is to load the inflow hydrograph with a volume of sediment. In this manner, spatially

differential sediment loading in a watershed channel can be simulated. Once the hydrograph is bulked with sediment, the mudflow is routed as a water and sediment continuum over the hydrograph. The bulked sediment hydrograph is tracked through system conserving volume for both water and sediment. Flow cessation and flow dilution are possible outcomes of the mudflow routing.

#### 5.4 Urban Flooding

One of the primary applications of the FLO-2D model is urban flood hazard delineation. It is the most robust and detailed urban flood model available with the capability to model buildings, street flow, walls and berms, storm drains, hydraulic structures (culverts, bridges and weirs), rainfall, infiltration, building roof runoff, building collapses and LID components. Area drainage master plans in the Phoenix area are being completed with FLO-2D using grid systems on the order of 1.8 million elements. Urban grid element size is typically 20 ft, however, ten foot elements have been used with high resolution topographic data bases (Figure 116).

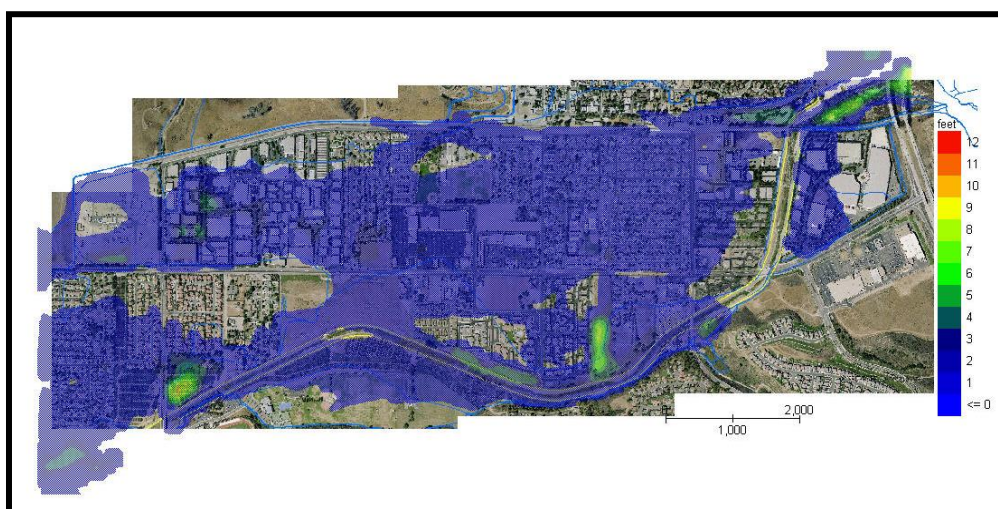


Figure 116. Urban flooding with Street Flow and Building Obstruction (1 million 10 ft elements)

A critical component of the urban flood model is the storm drain. The FLO-2D storm drain component is fully integrated with the surface water system including channels and detention basins (Figure 117). The detail in FLO-2D surface water and storm drain interface exceeds that of any other storm drain model. The FLO-2D model computes the storm drain inlet discharge based on the inlet geometry and the water surface elevation using weir and orifice control. The user can select from five types of storm drain inlets. The inlet and outfall exchange with the surface water (including return flow) are based on the water surface head not just the rim elevation. Figure 117 shows velocity vector and flow depth results in an urban area with the integrated storm drain system. Typically, the storm drain capacity is minor compared to the 100-year flood volume, the relations between return period flooding and the storm drain effectiveness can be tested for the more frequent events.

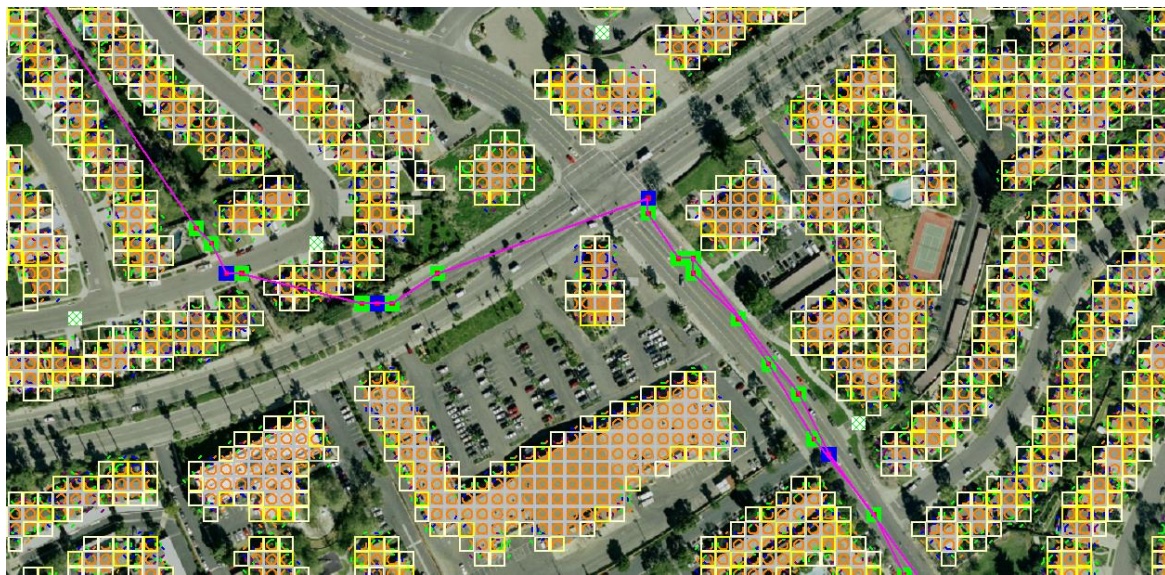


Figure 117. Urban Model with Streets, Buildings and Storm Drains

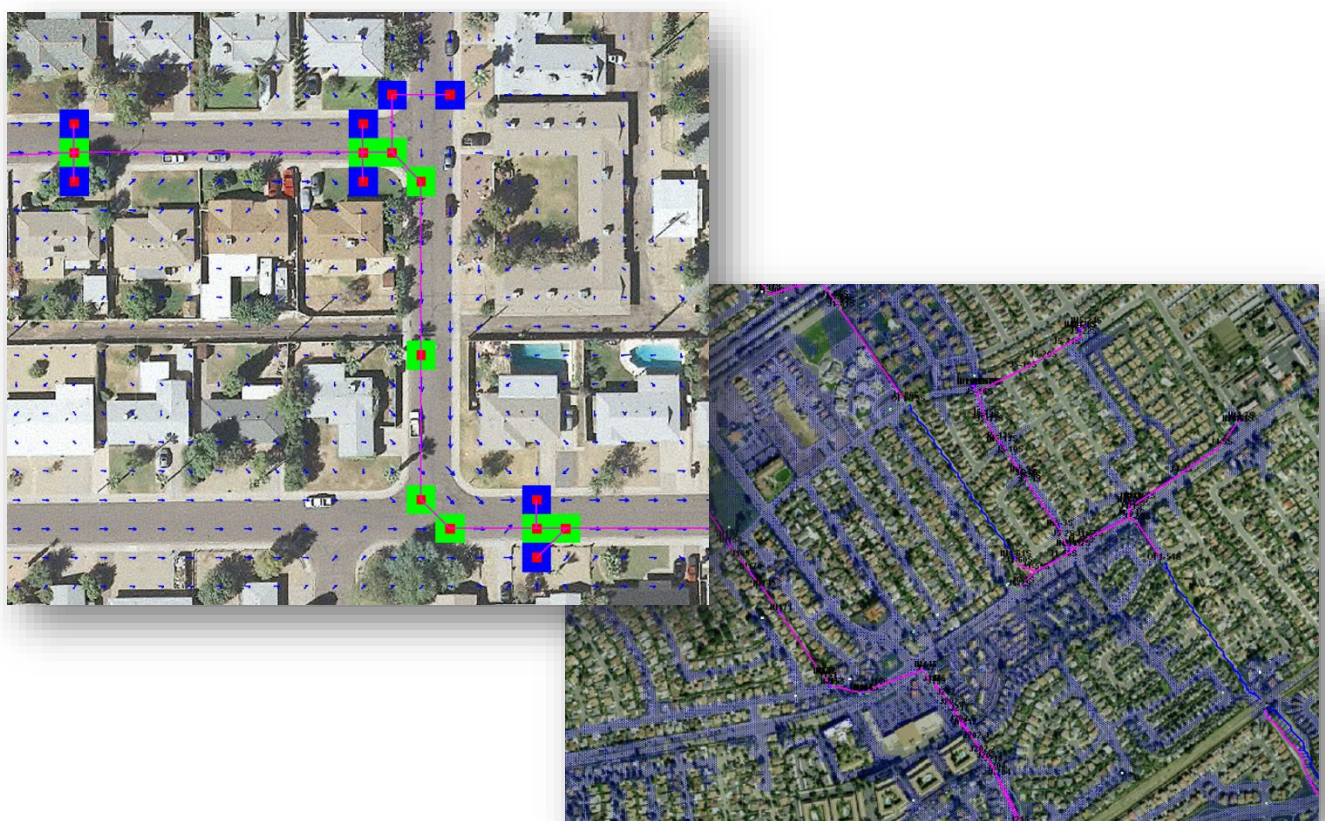


Figure 118. Urban Model Results with Storm Drains

## **5.5 Coastal Flooding**

FLO-2D can predict accurate ocean hurricane surge flooding for sea level scenarios including spatially variable hurricane rainfall. Storm surge inundation in urban areas requires detailed modeling of features coastal berms, walls, buildings, streets and channels. The impact on coastal urban storm drain systems with ocean outfalls from combined sea level rise and storm surge can be simulated with a FLO-2D model. Urban coastal flooding is controlled by:

- Volume of ocean water coming inland, flood volume and volume conservation
- Sediment bulking (add 20% volume)
- Flood mitigation – sea walls and levees
- Loss of storage due to buildings
- Street flow to urban outlying areas
- Channel flow and storage
- Loss of storm drain capacity with sea level rise

To simulate storm surges a time-stage relationship at the shoreline grid elements is required. This table can include high tides as well as multiple surge waves. A time-stage relationship (Table 14) can also be used to simulate a short duration tsunami event. A typical time-stage relationship is shown below.

**Table 14. Stage Time Relationship.**

Time (hrs)	Stage (ft)
0.0	0.43
5.0	0.75
11.0	1.29
16.0	6.63
24.0	0.38
36.0	0.62

In addition to the time-stage relationship, the model features that may define a coastal flood model are:

- Rainfall
- Streets
- Storm drain system
- Levees or flood walls
- Estuary channels and drainage canals
- Roughness
- Hydraulic structures (culverts and bridges)
- Buildings

A FLO-2D storm surge model was prepared for the Florida Keys using the ocean time-stage relationship associated with 2005 Hurricane Wilma (Figure 119). Using these area of inundation results, the products associated with coastal flood models include:

- Prediction of the overland progression of the hurricane surge through urban area.
- Risk/hazard assessment on urban development and infrastructure (storm drain system).
- Estimate groundwater level rise and its impact on drainage and utilities.
- Automatically estimate storm surge damage and mitigation costs.



*Figure 119. Hurricane Wilma 2005 Predicted Storm Surge in the Florida Keys*

## 5.6 Model Results – What Constitutes a Successful Flood Simulation?

When a FLO-2D simulation is completed, how do you know if the simulation was successful or accurate? There are three keys to a successful project application:

- Volume conservation
- Area of inundation
- Maximum velocities and numerical surging

Volume must be conserved for both the overland flow and channel flow. If the storage plus outflow volume was not conserved on the order of 0.0001 percent or better of the inflow volume, then it will be necessary to conduct a detailed review and determine where the volume conservation error occurred. If the volume was conserved, then the area of inundation can be quickly reviewed in either MAXPLOT or MAPPER Pro programs. If the area of inundation seems reasonable and the flood appears to have progressed completely through the system, then the maximum velocities in the channel, on the floodplain or in the streets should be reviewed for numerical surging. There are numerous webinars and Power Point presentations on project review and troubleshooting at the FLO-2D website. The Data

Input Manual has discussions on troubleshooting numerical surging and how to resolve it with applications of the limiting Froude number.

Once the FLO-2D flood simulation is providing reasonable results, you can fine tune the model and speed it up. Review the TIME.OUT file to determine which channel, floodplain or street elements are causing the most timestep reductions. Model speed may not be critical if the simulation is accurate with respect to volume conservation, discharge surging and area of inundation.

### **5.7    *FLO-2D Bridge Routine Comparison with HEC-RAS***

The objective of the FLO-2D bridge routine is to compute the discharge through the bridge based on the physical configuration and features of the bridge. The component enables the user to compute the bridge discharge without using an external program to generate a stage-discharge rating curve or table as required in the past for the FLO-2D model. Three classes of flow regime are computed: Free surface flow for discharge below the bridge low chord; Pressure flow when the discharge is above the low chord but below the bridge deck; and Combined pressure and weir flow as the discharge goes over the bridge. The pressure flow and weir flow computations are relatively straight forward. The pressure flow will be either sluice gate flow or orifice flow, whichever is smaller. The free surface flow is more complex with a number of multiplicative coefficients that represent the various bridge features and flow conditions. The bridge discharge is shared between two grid elements (channel or floodplain) that do not have to be contiguous.

Most bridge design and flood conveyance analysis have been performed with a 1-D HEC-RAS model where a discharge (peak Q) is prescribed and the water surface elevation is computed. In a two-dimensional flood routing model the opposite is required, the upstream and downstream flow depths and water surface elevations are known and the discharge through the bridge is computed. Matching HEC-RAS or other models with bridge components may not be exact because of the computational approach (e.g. solution to the 1-D energy equation vs flood routing with the full-dynamic wave momentum equation) and because the FLO-2D bridge routine has more detail for both free surface flow and pressure flow. Ultimately, the bridge flow control with coefficient adjustments, however, should be provide a suitable correlation between the models. In reality, unless there is an opportunity to calibrate the bridge coefficients to a field data set, it should not be assumed that the HEC-RAS or other bridge routines are necessarily more accurate.

The objective in applying the FLO-2D bridge routine is not to provide a detailed flow field through bridge and predict scour around piers but rather to accurately assess the relationship between upstream/downstream water surface elevations of the two grid elements linked by the bridge and compute the discharge passing between them. In this manner, the flow can be assessed as one-dimensional with no variation in water surface elevation in the bridge channel cross section. The average flow velocity through the bridge is depth integrated. The primary result of the FLO-2D bridge routine for unsteady flow is to assess the deviation from the approximate normal depth flow condition through the bridge that results in an upstream backwater effect. This will enable the accurate analysis of bridge constricted floodplain and river reaches that exhibit non-uniform and unsteady flow

conditions. For additional description and details of the FLO-2D bridge routine refer the White Paper ‘Bridge Hydraulics Component’.

### **Bridge Flow Modeling**

There are three basic flow conditions through a bridge: free surface flow, pressure flow and pressure flow plus deck overtopping flow. Pressure flow, which occurs when the deck or superstructure is submerged, is defined as either sluice gate or orifice flow. Flow through a bridge constriction is a function of the upstream headwater and downstream tailwater elevations (water surface slope), the extent of the constriction (cross section variation), the bridge geometry (flow area, wetted perimeter, low chord, etc.) and various site factors such as vegetation encroachment, bed scour, and riprap. The flow may be subcritical or supercritical although supercritical flow may limited to a bridge with a concrete apron or bedrock substrate. Subcritical flow is the most prevalent flow regime as bridge constrictions typically reduce upstream velocities and cause backwater effects as opposed to flow acceleration through the bridge.

Free surface flow is the most common flow since the bridge is designed to pass a selected design flood below the bridge soffit. Sluice gate flow occurs when the upstream opening is submerged but the downstream water surface elevation is below the low chord. For this case, the discharge thru the bridge depends on the upstream water surface elevation and the bridge geometry and the downstream water surface elevation is irrelevant. The transition between sluice gate flow and orifice flow is unique to the bridge and maybe temporally variable with scour, deposition or debris blockage. Sluice gate flow may persist until the upstream flow depth is 1.5 times or greater than the depth to the low chord.

Once the bridge inlet has been permanently submerged, a rapid increase in upstream water surface may occur resulting in submergence of both the upstream and downstream openings and the bridge cross section flowing full. This is defined as drowned orifice flow and can only happen when both upstream and downstream water surface elevations exceed the 1.1 times the height of the bridge opening. Since the downstream water prevents the efficient flow thru the bridge, upstream flooding can quickly ensue. In this case, the discharge control is a combination of the structure features and channel characteristics.

When the flow begins to overtop the bridge, the discharge is the sum of the pressure flow plus the deck overflow. This is typically modeled as broadcrested weir flow with a coefficient in the range of 2.65 to 3.21. If the bridge has guard rails or debris, the selected weir coefficient should be conservatively low. Typically, overtopping flow is shallow, but for a long bridge the overflow discharge can be significant. An assumption of weir flow to represent over deck discharge can only be an approximation because of a number of factors that are not limited to:

- Tailwater submergence;
- Variable deck elevation;
- Unsteady flow conditions;
- Guardrail supports causing blockage and spatially variable flow;

- Debris blockage.

The bridge discharge computations will be performed inside the FLO-2D routing algorithm for the floodplain and 1-D channel components in conjunction with the existing hydraulic structure routine. The model will identify the flow condition, compute the appropriate discharge and exchange the discharge volume between the inflow and outflow nodes. For details on the computation methods and equations for free surface, pressure flow and weir flow refer the companion White Paper on the FLO-2D ‘Bridge Hydraulics Component’.

## A Comparison of Bridge Flow Modeling between FLO-2D and HEC-RAS

### *Model Development*

A FLO-2D model of the Middle Rio Grande valley was prepared for the Corps of Engineers in the early 2000’s from Cochiti Dam to Elephant Butte Reservoir in New Mexico (~ 170 miles). This model was expanded and enhanced with smaller grid elements (250 ft), more spatial levee detail and was calibrated with field data during a 2005 prescribed release of the outlet works capacity. The data collection included discharge measurements, water surface elevation surveys, field reconnaissance of floodplain inundation, and flown aerial imagery. The model was then applied to 30 years of historical spring releases to support the application of the Corps’ Upper Rio Grande Water Operation Model. The Rio Grande FLO-2D model is still in use today. Riada Engineering and Wolf Engineering collaborated on developing this Rio Grande FLO-2D model for the Corps.

All the Middle Rio Grande bridges and diversions were modeled with rating tables. The rating tables were generated with HEC-RAS using 2 to 3 cross sections upstream and downstream of the bridge. The HEC-RAS bridge models were obtained and reviewed to locate a bridge that could be simulated for all three types of flow with the primary emphasis on the free surface and pressure flow. The original HEC-RAS model was applied for discharges up to 20,000 cfs. The maximum outlet discharge from Cochiti Dam is only 7,000 cfs without spillway release. The pre-history Rio Grande prior to management experienced flows in excess of 100,000 cfs, but since Cochiti Dam is a flood control facility, discharges over 7,000 cfs depend on tributary inflows. A discharge of 20,000 cfs will not overtop any of the bridges in the Middle Rio Grande. All the bridges were reviewed, and the Los Lunas Bridge was selected to review the computed discharge hydraulics with both HEC-RAS and FLO-2D models (Figure 120 and Figure 121).



Figure 120. Plan View of the Los Lunas Bridge.



Figure 121. View Downstream through Los Lunas Bridge (Wolf Engineering).

Figure 2

The Los Lunas Bridge spans a most of the Rio Grande active floodplain between the levees and has 16 sets of bridge pilings as shown in Figure 2. The HEC-RAS model of the bridge include 2 upstream cross sections and 3 downstream cross sections (Figure 122). The bridge deck is about 90 ft wide.

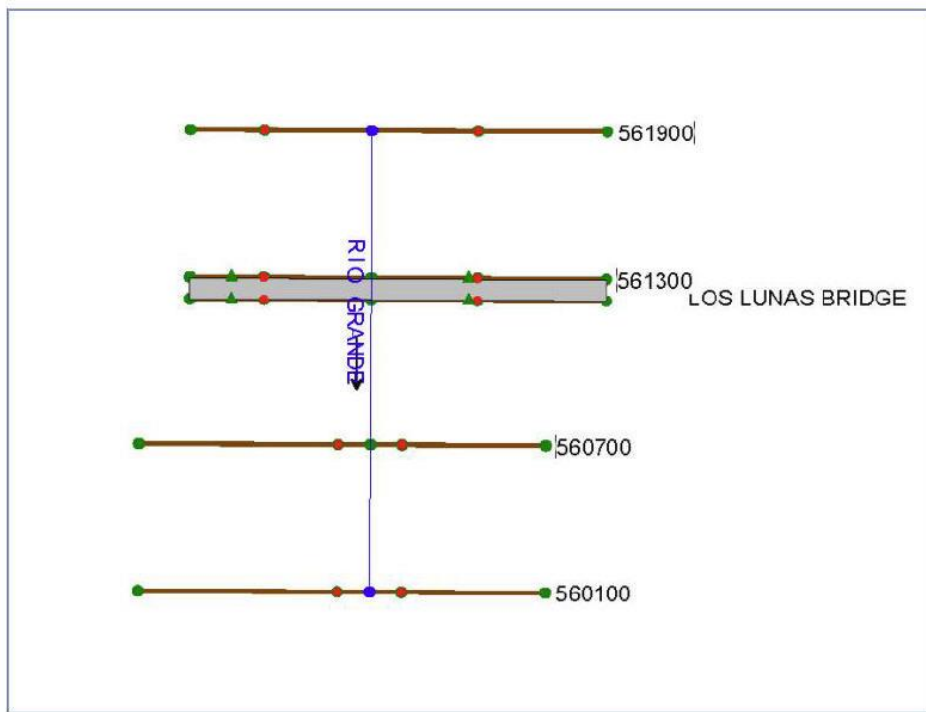


Figure 122. HEC-RAS Cross Sections and Stationing (Wolf Engineering).

The bridge geometry and cross section plots are shown in Figure 123 with the blocked areas due to the approach roadway and bridge decking. Both the deck soffit and roadway are curved with a difference of 1 ft between the minimum and maximum elevations. The low chord and weir were represented by an average elevation. The split channel with the island can be viewed in bridge cross section and in Figure 120.

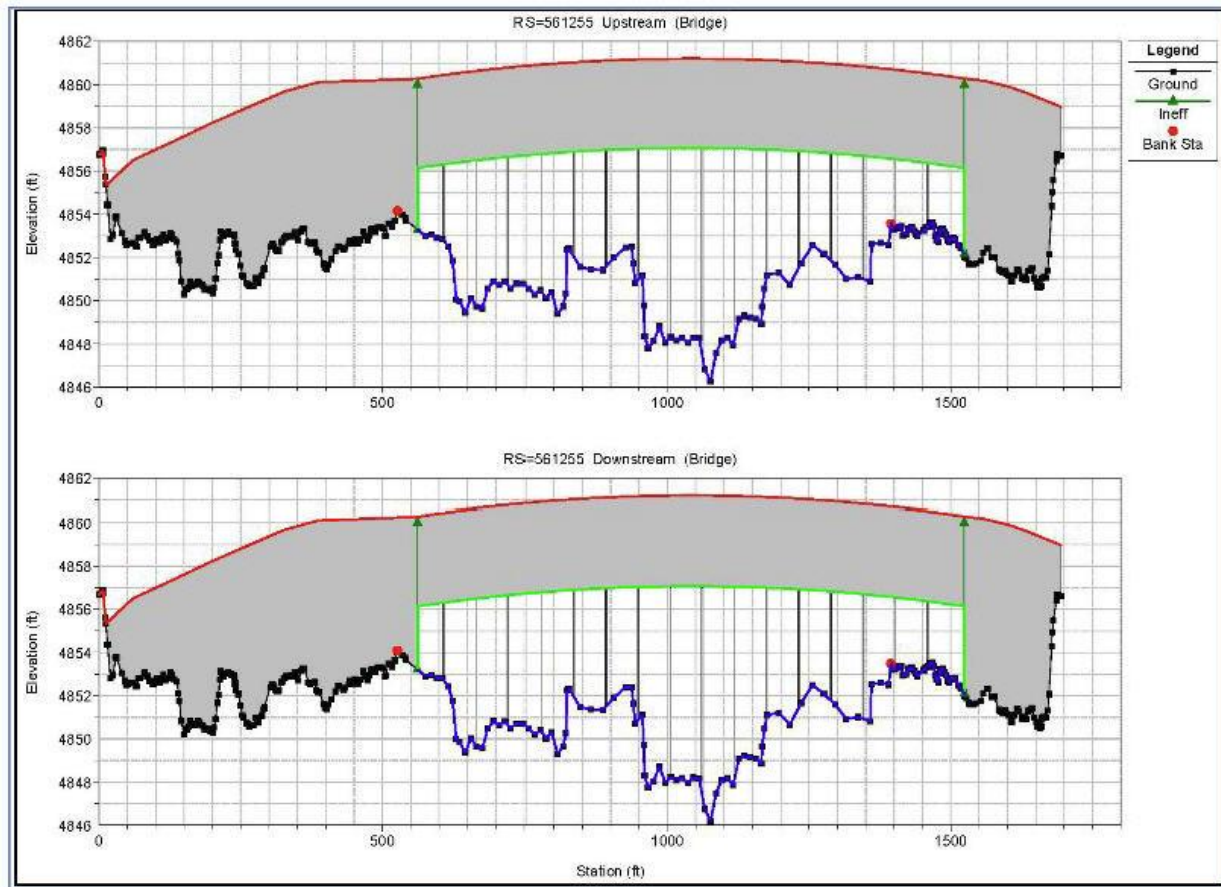
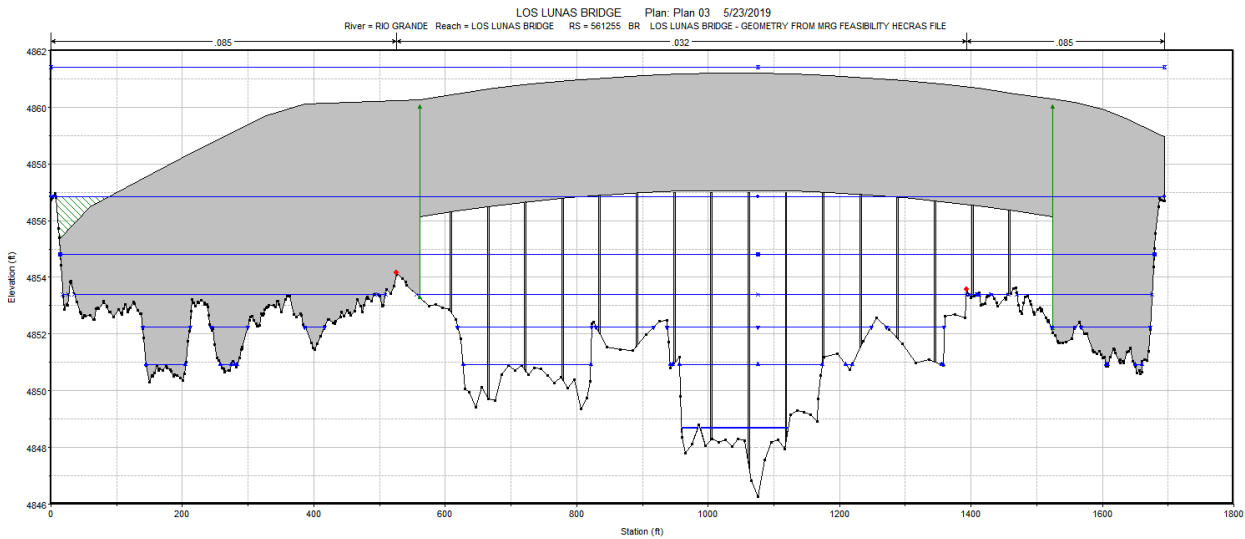


Figure 123. Los Lunas HEC-RAS Bridge

The original FLO-2D model rating table had 40 stage-discharge pairs ranging from 10 to 20,000 cfs. For this comparison, the HEC-RAS Los Lunas bridge model was run with only 7 discharges ranging from 100 cfs to 45,000 cfs (Figure 124). The vertical lines in the active channel area below the bridge soffit are the rows of piles. At 45,000 cfs the bridge deck was barely overtopped in the HEC-RAS model (blue horizontal lines in Figure 5). The seven steady flow discharges used in the two models were:

100 cfs 1,000 cfs 2,500 cfs 5,000 cfs, 10,000 cfs, 20,000 cfs, 45,000 cfs



*Figure 124. Los Lunas Bridge HEC-RAS Water Surface Elevations.*

The FLO-2D was run with the seven discharges assigned to an inflow channel element about 16 channel elements upstream of the bridge. Outflow nodes were assigned to a channel element about 9 channel elements downstream of the bridge and to the channel element just upstream of the inflow node. The inflow hydrograph to achieve steady was assigned as follows:

Time (hrs)	Q (cfs)
0.0	0.0
2.0	1,000
100.	1,000

The FLO-2D model was run for a simulation time of 6 hrs which was sufficient to achieve steady discharge at the bridge. The model was also setup with the following data and assumptions:

- Identical channel n-values (0.032);
- Spatially variable overbank FLO-2D n-values that did not match the HEC-RAS model;
- The upstream channel and bridge cross sections in the HEC-RAS model;
- The rest of the channel cross sections were the original ones in the FLO-2D model;
- Type 1 bridge configuration with no abutment or embankment slopes (vertical);
- Average low chord and deck elevations as determined from Figure 4;
- Deck length, bridge opening, and bridge width were determining from the HEC-RAS cross section;
- Pile width was the sum of the 16 sets of individual pile widths;
- No flow angle of attach with the bridge;
- No coefficient variation for Froude number which ranges from 0.2 to 0.3;
- No assignment for overall free surface flow discharge coefficient (to be computed).

## Model Comparison Results

The focus of comparing the HEC-RAS and FLO-2D models for the seven discharges is the predicted water surface elevations which, if equivalent, would indicate that the model hydraulics (depth, velocity, flow area) match well. The most important comparison are the model's predicted upstream backwater elevations. The HEC-RAS computed water surfaces elevations are shown in Figure 5. The FLO-2D predicted water surface elevations were extracted from the CHANMAX.OUT file but could also be read from the HYCHAN.OUT file. The BRIDGE\_DISCHARGE.OUT and HYDROSTRUCT.OUT files verified that the steady state discharges matched exactly for those flows which were less than the channel conveyance capacity of about 5,000 cfs. The only FLO-2D model revisions were:

- Adjustments were made to several channel element Mannings n-values. These n-value revisions were less than 0.005.
- Outflow nodes were added upstream and downstream of the bridge to having to use the entire Rio Grande model.

No attempt was made to accommodate the HEC-RAS model 1-D constraints with respect to the floodplain conditions including roadway approach, levee overtopping, or flow upstream or downstream past the outflow nodes. The following FLO-2D limitations were noted with respect to the overbank floodplain discharge:

- Floodplain storage was not filled to match the HEC-RAS 1-D steady flow inundation. No floodplain outflow nodes were assigned, and floodplain flow bypassed the channel outflow nodes both upstream and downstream.
- Overbank flow upstream re-entered the channel and flowed upstream in the channel.
- Downstream overbank flow bypassed the outflow node and re-entered the channel.

Of the three flow regimes, free surface flow, pressure flow and weir flow plus pressure flow, the most critical comparison is for the free surface flow regime water surface elevation because this computation is the most complex and detailed. It is also the most frequent flow through the bridge and should include the bridge design flow. Most bridges are not constructed to convey the design discharge as pressure or weir flow. It should be noted that the pressure flow and weir flow involve a single equation and calibration is relatively straight forward with only a coefficient adjustment. Conversely, predicting free surface flow requires a number of combined coefficients that represent various features of the bridge or specific flow conditions.

The comparison with the HEC-RAS stages for the discharges ranging from 100 cfs to 45,000 cfs for the five cross sections upstream and downstream of Los Lunas Bridge are shown in Figure 125. Pressure flow begins at about 18,000 cfs. Figure 126 and Figure 127 indicate that the FLO-2D predicted stage upstream of the bridge at and below the low chord matches the HEC-RAS stage exactly. This upstream reach with the backwater effect was the most critical aspect of the comparison. For flows greater than the low chord HEC-RAS predicts a higher stage because FLO-2D cannot fill the overbank floodplain storage area to HEC-RAS level because the discharge overtops the levees and flows beyond the cross

sections both upstream and downstream (Figure 130). The FLO-2D model could be manipulated to confine the 45,000 cfs with a longer duration inflow hydrograph and spatial constraints and floodplain outflow nodes, but the sole purpose of this effort would be to match the over deck flow stage. At this discharge, however, since the channel conveyance capacity is only about 5,000 cfs, most of the stage would reflect the floodplain conditions not the bridge.

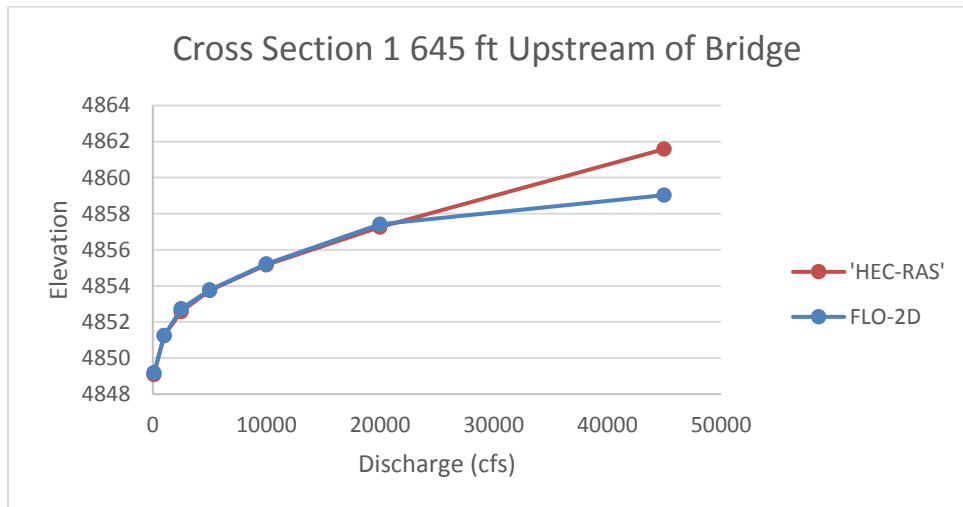


Figure 125. Los Lunas Bridge Stage-Discharge Relationship Cross Section 1.

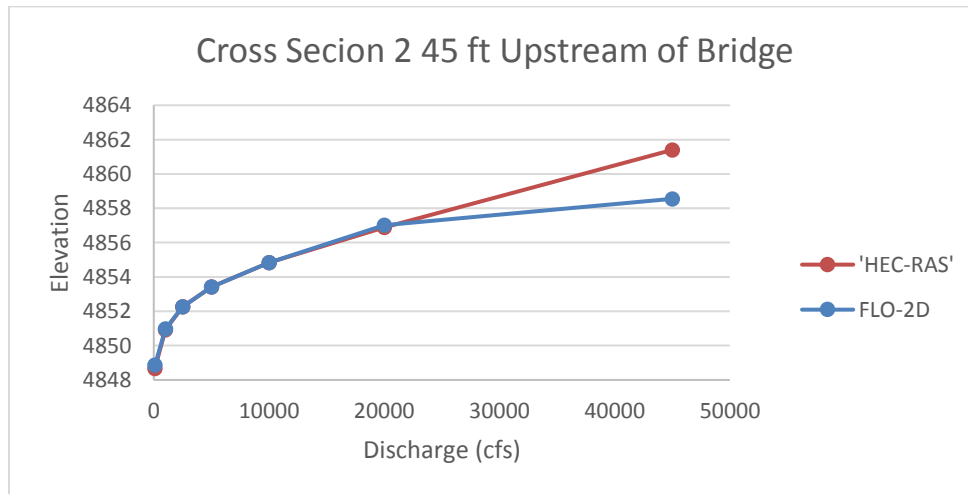


Figure 126. Los Lunas Bridge Stage-Discharge Relationship Cross Section 2.

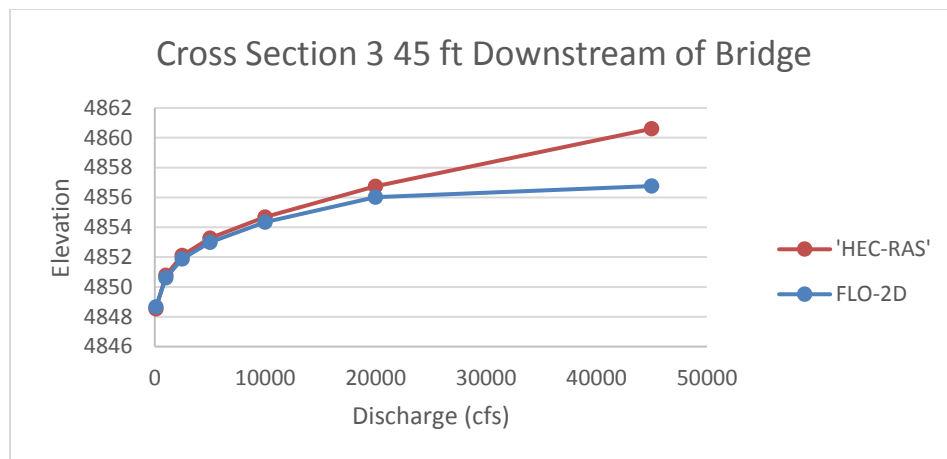


Figure 127. Los Lunas Bridge Stage-Discharge Relationship Cross Section 3.

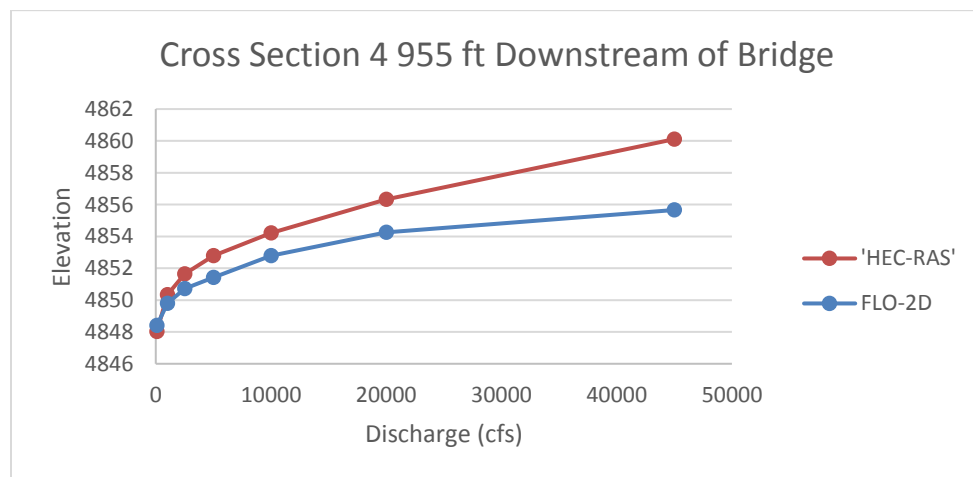
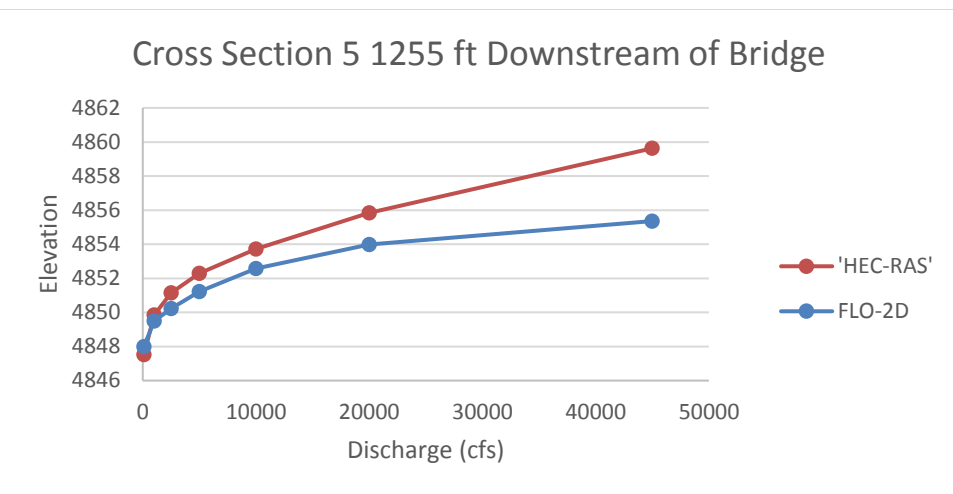


Figure 128. Los Lunas Bridge Stage-Discharge Relationship Cross Section 4.



*Figure 129. Los Lunas Bridge Stage-Discharge Relationship Cross Section 5.*

Downstream of the bridge, the FLO-2D and HEC-RAS stages do not match very well, particularly at the higher flows. This is because the FLO-2D model outflow node water surface elevation did not match the HEC-RAS water surface near cross section 5. The FLO-2D channel outflow node pulls down the in-channel water surface, but much of the water is also overbank on the floodplain at that location. Since the downstream water surface elevations were not important and did not affect the upstream stage-discharge, the additional effort required to match the model downstream stages was not considered.

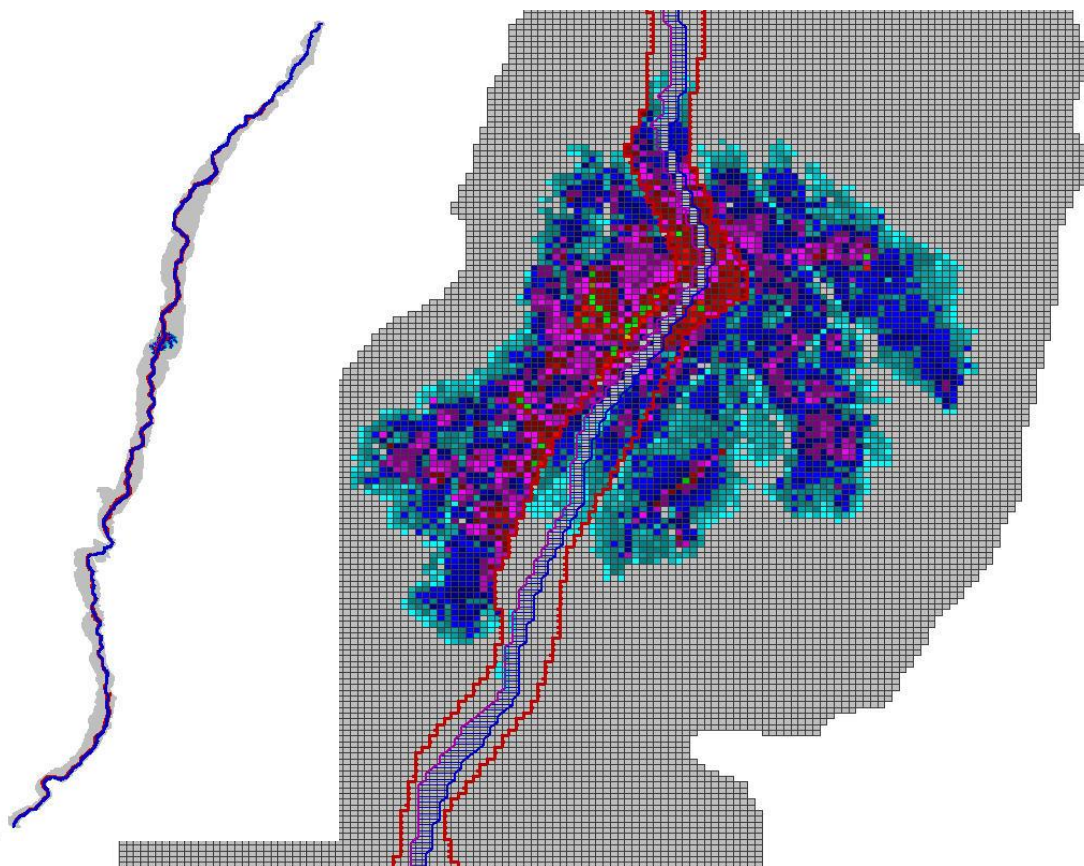


Figure 130. FLO-2D Maximum Depth for a Discharge of 45,000 cfs.

### Discussion

The objective of applying the FLO-2D and HEC-RAS bridge routines to the Los Lunas Bridge reach of the Rio Grande is to compare the prediction of the stage for various discharges. The HEC-RAS bridge routine involves an energy equation solution for a 1-D steady discharge step backwater condition and FLO-2D provides a 2-D full dynamic wave momentum equation model solution for routing flood flows. HEC-RAS presumes that the discharge covers the entire floodplain with a single water surface elevation and FLO-2D has a channel-floodplain interface to spatially distribute the flow in 2-dimensions on the floodplain. The focus of the comparison of the two models was on the bridge and upstream cross section water surface elevations due to the backwater effects.

The FLO-2D model matched the HEC-RAS predicted stages for all the upstream water surface elevations below the low chord of the bridge. For higher discharges, the FLO-2D model under predicted the HEC-RAS stages because the floodplain area of inundation was not filled. The FLO-2D duration was too short and the floodplain attributes in terms of the levee and spatial extent of the flooding were different from the 1-D HEC-RAS model. In the FLO-2D model, most of the discharge over 5,000 cfs was on the floodplain and the flow moved past the inflow and outflow nodes both upstream and downstream as

shown in Figure 7. It was also noted that the FLO-2D channel outflow conditions did not match the HEC-RAS model downstream boundary conditions, but this was less important than the floodplain flow bypassing the channel outflow node.

Matching HEC-RAS or other models with bridge components may not be exact because of the differences computational approach and because of the FLO-2D spatial variability of the floodplain flow distribution. Ultimately, the bridge free surface flow control with coefficient adjustments, however, provided a suitable correlation between the models.

The FLO-2D bridge routine enables the user to compute the discharge through bridges without using an external program to generate a stage-discharge rating curve or table. The routine will compute the discharge for three classes of flow regime, free surface flow for discharge below the bridge low chord, pressure flow when the discharge is above the low chord but below the bridge deck and combined pressure and weir flow as the discharge goes over the bridge. The pressure flow and weir flow computations are relatively straight forward. The free surface flow is more complex with a number of multiplicative coefficients that represent the various features of the bridge and their effects on the flow. The pressure flow will be either sluice gate flow or orifice flow, whichever is smaller. There may not be a smooth transition between the two types of flow representation and some adjustment of the coefficients may be necessary. An adjustment factor to raise or lower the computed sluice gate or orifice coefficient is available as data input parameter. The user has complete control of all the coefficients utilized in the bridge routine for all flow regimes.

## REFERENCES

- Ackers, P. and W.R. White, 1973. "Sediment Transport: New Approach and Analysis," J. of Hyd., ASCE, V. 99, no. HY11, pp. 2041-2060.
- Bagnold, R.A., 1954. "Experiments on a gravity-free dispersion of large solid spheres in a Newtonian fluid under shear," Proc. of the Royal Society of London, Series A, V. 249, 235-297.
- Bureau of Reclamation, 1988. "Downstream Hazard Classification Guidelines", ACER Technical Memorandum No. 11, Denver, Colorado.
- Chen, C.L., 1976. "Urban storm runoff inlet hydrograph study." Prepared for the Dept. of Transportation, PRWG 106-2, Utah State University, Logan Utah.
- Chow, V.T., 1959. Open-Channel Hydraulics, McGraw-Hill, NY.
- Clausen, L., P. Clark, 1990. "The development of criteria for predicting dam break flood damages using modeling of historical dam failures," Proc. Intl. Conf. on River Flood Hydraulics, W. White (ed.), Wiley U.K., 369-380.
- Cunge, J.A., F.M. Holly Jr., and A. Verwey, 1980. "Practical Aspects of Computational River Hydraulics," Pittman Advanced Publishing Program, London, UK.
- DeLeon, A.A. and R.W. Jeppson, 1982. "Hydraulic and numerical solutions of steady-state, but spatially varied debris flow," Hydraulics and Hydrology Series, UWRL/H-82/03, Utah State Univ. at Logan, Utah.
- Deng, Z., 1996. "Impact of Debris Flows and Its Mitigation," Ph.D. Dissertation submitted to the Dept. of Civil and Environmental Engineering, Univ. of Utah, Salt Lake City, Utah.
- DMA, 1985. "Alluvial fan flooding methodology and analysis," Prepared for FEMA by DMA Consulting Engineers, Rey, California, October.
- Egashira, S., K. Ashida, H. Yajima, and J. Takahama, 1989. "Constitutive equations of debris flow," Annals of the Disaster Prevention Research Institute, Kyoto Univ., No. 32B-2, 487-501.
- Einstein, H.A., 1950. "The Bed-load Function for Sediment Transportation in Open Channel Flows," USDA Tech. Bull. No. 1026.
- Engelund, F. and E. Hansen, 1967. "A Monograph on Sediment Transport in Alluvial Streams," Teknisk Forlag, Copenhagen.
- Federal Highway Administration, 2012. "Hydraulic Design of Safe Bridges," US Dept. of Transportation, Publication No. FHWA-HIF-12-018.
- Federal Emergency Management Agency, 2003, "Guidelines and Specifications for Flood Hazard Mapping Partners, Appendix G: Guidance for Alluvial Fan Flooding Analysis and Mapping."

- Fletcher, C.A.J., 1990. Computational Techniques for Fluid Dynamics, Volume I, 2<sup>nd</sup> ed., Springer-Velag, New York.
- FLO-2D, 2018. "Levee, Dam, and Wall Breach Guidelines." Build No 18. FLO-2D Software, Inc. Nutrioso, Arizona.
- Fread, D.L., 1998. "Breach: An Erosional Model for Earthen Dam Failures," National Weather Service, NOAA, Silver Spring, Maryland.
- Fuller, J.E., 2012. "Evaluation of Avulsion Potential on Active Alluvial Fans in Western and Central Arizona," Arizona Geological Survey, Contributed Report CR-12-D, JE Fuller Hydrology and Geomorphology, Inc.
- Fullerton, W.T., 1983. "Water and sediment routing from complex watersheds and example application to surface mining," Masters Thesis, Civil Engineering Dept., CSU, Fort Collins, CO.
- Graf, W.H., 1971. Hydraulics of Sediment Transport. McGraw-Hill, New York, N.Y.
- Grant, G.E., 1997. "Critical flow constrains flow hydraulics in mobile bed streams: A new hypothesis," Water Resources Research, V. 33, No. 2, pp. 349-358.
- Green, W.H. and G.A. Ampt, 1911. "Studies on soil physics, part I: The flow of air and water through soils," J. of Agriculture Science.
- Hamill, L., 1999. Bridge Hydraulics, E & FN Spon, NY.
- Hashimoto, H., 1997. "A comparison between gravity flows of dry sand and sand-water mixtures," Recent Developments on Debris Flows, Springer, A. Armanini and M. Michiue (eds.), NY, NY.
- Henderson, F. M., 1966. Open Channel Flow. MacMillan Publishing Co., Inc., NY, NY.
- Hoggan, D.H., 1989. Computer-Assisted Floodplain Hydrology & Hydraulics, McGraw-Hill, NY.
- Hromadka, T.V. and C.C. Yen, 1987. "Diffusive hydrodynamic model," U. S. Geological Survey, Water Resources Investigations Report 87-4137, Denver Federal Center, Colorado.
- James, W. P., J. Warinner, and M. Reedy, 1992. "Application of the Green-Ampt infiltration equation to watershed modeling," Water Resources Bulletin, AWRA, 28(3), pp. 623-634.
- Jia, Y., 1990. "Minimum Froude Number and the Equilibrium of Alluvial Sand Rivers," Earth Surface Processes and Landforms, John Wiley & Sons, London, Vol. 15, 199-200.
- Jin, M. and D.L. Fread, 1997. "Dynamic flood routing with explicit and implicit numerical solution schemes," J. of Hyd. Eng., ASCE, 123(3), 166-173.
- Julien, P.Y., 1995. Erosion and Sedimentation. Cambridge University Press, New York, N.Y.
- Julien, P.Y. and J.S. O'Brien, 1998. "Dispersive and turbulent stresses in hyperconcentrated sediment flows," Unpublished paper.

Julien, P.Y. and Y.Q. Lan, 1991. "On the rheology of hyperconcentrations", J. of Hyd. Eng., ASCE, 117(3), 346-353.

Karim, F., 1998. "Bed Material Discharge Prediction for Nonuniform Bed Sediments," J. of Hyd. Eng., ASCE, 124(6), 597-604.

Kusler, J., 1986. "Introduction: flooding in arid and semi-arid regions," Proc. of a Western State High Risk Flood Areas Symposium, 'Improving the Effectiveness of Floodplain Management in Arid and Semi-Arid Regions,' Association of State Floodplain Managers, Inc., Las Vegas, NV, March.

Laursen, E.M., 1958. "The total sediment load of streams," J. of the Hyd. Div., ASCE, V. 84, No HY1, 1530-1536.

MacArthur, R.C. and D.R. Schamber, 1986. "Numerical methods for simulating mudflows," Proc. of the 3rd Intl. Symp. on River Sedimentation, Univ. of Mississippi, 615-1623.

Major, J. and T.C. Pierson, 1992. "Debris flow rheology: experimental analysis of fine-grained slurries," Water Resources Research, 28(3), 841-857.

Meyer-Peter, E. and R. Muller, 1948. "Formulas for bedload transport," Proc. IAHR, 2<sup>nd</sup> Congress, Stockholm, 39-64.

Milhous, R.T., 1973. "Sediment transport in a gravel-bottomed stream," Ph.D. Dissertation, Dept. of Civil Engineering, Oregon State Univ., Corvallis, OR.

Milhous, R.T., 1982. "Effect of sediment transport and flow regulations of gravel-bed rivers," in Hay, R.D., J.C. Bathurst and C.R. Thorne (eds), Gravel-bed rivers: Fluvial processes, engineering and management. Wiley-Interscience, Toronto.

Mussetter, R.A., P.F. Lagasse, M.D. Harvey, and C.A. Anderson, 1994. "Sediment and Erosion Design Guide." Prepared for the Albuquerque Metropolitan Arroyo Flood Control Authority by Resource Consultants & Engineers, Inc., Fort Collins, CO.

O'Brien, J.S., 1984. "1983 Yampa River Cobble Reach Morphology Investigation," Submitted to the U.S. Fish & Wildlife Service, Salt Lake City, Utah, Prepared by: Civil Engineering Dept., Colorado State University, Fort Collins, Colorado.

O'Brien, J.S., 1986. "Physical processes, rheology and modeling of mudflows," Doctoral dissertation, Colorado State University, Fort Collins, Colorado.

O'Brien, J.S. and P.Y. Julien, 1985. "Physical processes of hyperconcentrated sediment flows," Proc. of the ASCE Specialty Conf. on the Delineation of Landslides, Floods, and Debris Flow Hazards in Utah, Utah Water Research Laboratory, Series UWRL/g-85/03, 260-279.

O'Brien, J.S. and P.Y. Julien, 1987. Discussion on "Mountain torrent erosion," By K. Ashida in Sediment Transport in Gravel-Bed Rivers, John Wiley & Sons, 537-539.

O'Brien, J.S. and P.Y. Julien, 1988. "Laboratory analysis of mudflow properties," J. of Hyd. Eng., ASCE, 114(8), 877-887.

- O'Brien, J.S., P.Y. Julien and W.T. Fullerton, 1993. "Two-dimensional water flood and mudflow simulation," *J. of Hyd. Eng.*, ASCE, 119(2), 244-259.
- O'Brien, J.S. and Simons, Li & Associates, Inc., 1989. "Flood hazard delineation for Cornet Creek, Telluride, Colorado," Submitted to Federal Emergency Management Agency, March.
- Oskuyi, N.N. and F. Salmasi, 2011. "Vertical Sluice Gate Discharge Coefficient," *Journal of Civil Engineering and Urbanism*, Sciencline Publication 2(3): 109-114.
- Parker, G., P.C. Klingeman and D.G. McLean, (1982). "Bedload and size distribution in paved gravel-bed streams," *J. of Hyd. Div.*, ASCE, 108(HY4), p. 544-571.
- Pilotti, M., Melanesi, L., Ransi, R., 2016. "People and buildings vulnerability to floods in Mountain Areas," 13<sup>th</sup> Congress, Interpraevent Conf. Proc., Lucerne, Switzerland, p. 791-8.
- Ponce, S.M., 1989. Engineering Hydrology, Prentice Hall, Englewood Cliffs, New Jersey.
- Ponce, V.M., R.M. Li and D.B. Simons, 1978. "Applicability of kinematic and diffusion models," *J. of Hyd. Div.*, ASCE, 104(1443), 353-60.
- Ponce, V.M. and F.D. Theurer, 1982. "Accuracy Criteria in Diffusion Routing," *J. of Hyd. Eng.*, ASCE, 108(6), 747-757.
- Schamber, D.R. and R.C. MacArthur, 1985. "One-dimensional model for mudflows," Proc. of the ASCE Spec. Conf. on Hydraulics and Hydrology in the Small Computer Age, V. 2, 1334-39.
- Schumm, S.A., 1977. The Fluvial System, John Wiley & Sons, Inc., New York, NY.
- Schumm, S.A., M.D. Harvey, and C.C. Watson, 1984. Incised Channels, Morphology, Dynamics and Control, Water Resources Publications, Littleton, CO.
- Simons, D.B. and F. Senturk, 1976. Sediment Transport Technology, Water Resource Publications, Fort Collins, CO.
- Shen, H.W. and J.Y. Lu, 1983. "Development of predictions of bed armoring," *J. of Hydraulic Engineering*, ASCE, 109(4), 611 - 629.
- Smart, G.M., 1984. "Sediment Transport Formula for Steep Channels," *J. of Hydraulic Engineering*, ASCE, 110(3), 267-275.
- Strum, T.W., 2001. "Open channel hydraulics," McGraw-Hill Education, NY, NY.
- Takahashi, T., 1979. "Debris flow on prismatic open channel flow," *J. of the Hyd. Div.*, ASCE, 106(3), 381 - 396.
- Takahashi, T. and H. Tsujimoto, 1985. "Delineation of the debris flow hazardous zone by a numerical simulation method," Proc. of the Intl. Symp. on Erosion, Debris Flow and Disaster Prevention, Tsukuba, Japan, 457-462.

- Takahashi, T. and H. Nakagawa, 1989. "Debris flow hazard zone mapping," Proc. of the Japan - China (Taipai) Joint Seminar on Natural Hazard Mitigation, Kyoto, Japan, 363-372.
- Toffaleti, F.B., 1969. "Definitive computations of sand discharge in rivers," J. of the Hyd. Div., ASCE, V. 95, no. HY1, pp. 225-246.
- Urban Drainage and Flood Control District (UDFCD), 2008. "Drainage Criteria Manual," Denver, Colorado.
- U.S. Army Corps of Engineers, 1994. "Channel Stability Assessment for Flood Control Projects," Engineer Manual. Department of the Army, Washington, DC 20314-1000. Manual No. 1110-2-1418
- US Army Corps of Engineers, 1995. "A Comparison of One-Dimensional Bridge Hydraulic Routines from: HEC-RAS, HEC-2 and WSPRO," Hydrologic Engineering Center, Research Document No. 41 (RD-41).
- U.S. Army Corps of Engineers, 1988. "Mud Flow Modeling, One- and Two-Dimensional, Davis County, Utah," Draft report for the Omaha District, Omaha, NE, October.
- U.S. Army Corps of Engineers, 1990. "HEC-1, Flood Hydrograph Package," User's Manual, Hydrologic Engineering Center, Davis, CA.
- U.S. Army Corps of Engineers, 1990. "HEC-2 Water Surface Profiles," Hydrologic Engineering Center, Davis, CA.
- U.S. Army Corps of Engineers, 1997. "Flood-Runoff Analysis," Technical Engineering and Design Guides, No. 19., ASCE Press, NY, NY.
- U.S. Department of Transportation, Federal Highway Administration, 2012. "Hydraulic Design of Highway Culverts," Pub. No. FHWA-HIF-12-026, National Technical Information Service, Springfield, VA.
- Woo, H.S. P.Y. Julien, and E.V. Richardson, 1988. "Suspension of large concentrations of sand," J. Hyd. Eng., ASCE, 114, no. 8, pp. 888-898.
- Woolhiser, D.A., 1975. "Simulation of Unsteady Overland Flow," in Unsteady Flow in Open Channels, Mahmood, K. and Yevjevich, V. eds., Water Resources Publications, Fort Collins, CO.
- Yang, C.T., 1973. "Incipient motion and sediment transport," J. of Hyd Div. ASCE, V. 99, no. HY10, pp. 1679-1704.
- Yang, C.T., 1996. Sediment Transport, Theory and Practice," McGraw-Hill, New York, N.Y.
- Zeller, M. E. and W. T. Fullerton, 1983. "A Theoretically Derived Sediment Transport Equation for Sand-Bed Channels in Arid Regions," Proceedings of the D. B. Simons Symposium on Erosion and Sedimentation, R. M. Li and P. F. Lagasse, eds., Colorado State University and ASCE.